Communications of the
# LUNAR AND PLANETARY
LABORATORY

Communications Nos. 173–183

Volume 9   Part 5

THE UNIVERSITY OF ARIZONA

Communications of the
LUNAR AND PLANETARY
LABORATORY

THE UNIVERSITY OF ARIZONA

1969-1973

/

COMMUNICATIONS OF THE LUNAR AND PLANETARY LABORATORY

These *Communications* contain the shorter publications and reports by the staff of the Lunar and Planetary Laboratory. They may be either original contributions, reprints of articles published in professional journals, preliminary reports, or announcements. Tabular material too bulky or specialized for regular journals is included if future use of such material appears to warrant it. The *Communications* are issued as separate numbers, but they are paged and indexed by volumes.

The *Communications* are mailed to observatories and to laboratories known to be engaged in planetary, interplanetary or geophysical research in exchange for their reports and publications. The University of Arizona Press can supply at cost copies to other libraries and interested persons.

VOLUME 9

TABLE OF CONTENTS

(continued)

VOLUME 9

AUTHOR INDEX

VOLUME 9

SUBJECT INDEX

Communications of the
LUNAR AND PLANETARY
LABORATORY

Viii

COMMUNICATIONS OF THE LUNAR AND PLANETARY LABORATORY

These *Communications* contain the shorter publications and reports by the staff of the Lunar and Planetary Laboratory. They may be either original contributions, reprints of articles published in professional journals, preliminary reports, or announcements. Tabular material too bulky or specialized for regular journals is included if future use of such material appears to warrant it. The *Communications* are issued as separate numbers, but they are paged and indexed by volumes.

The *Communications* are mailed to observatories and to laboratories known to be engaged in planetary, interplanetary or geophysical research in exchange for their reports and publications. The University of Arizona Press can supply at cost copies to other libraries and interested persons.

The University of Arizona   GERARD P. KUIPER, *Director*
Tucson, Arizona   *Lunar and Planetary Laboratory*

Editor, Gerard P. Kuiper
Assistant Editor, Micheline Wilson

ix
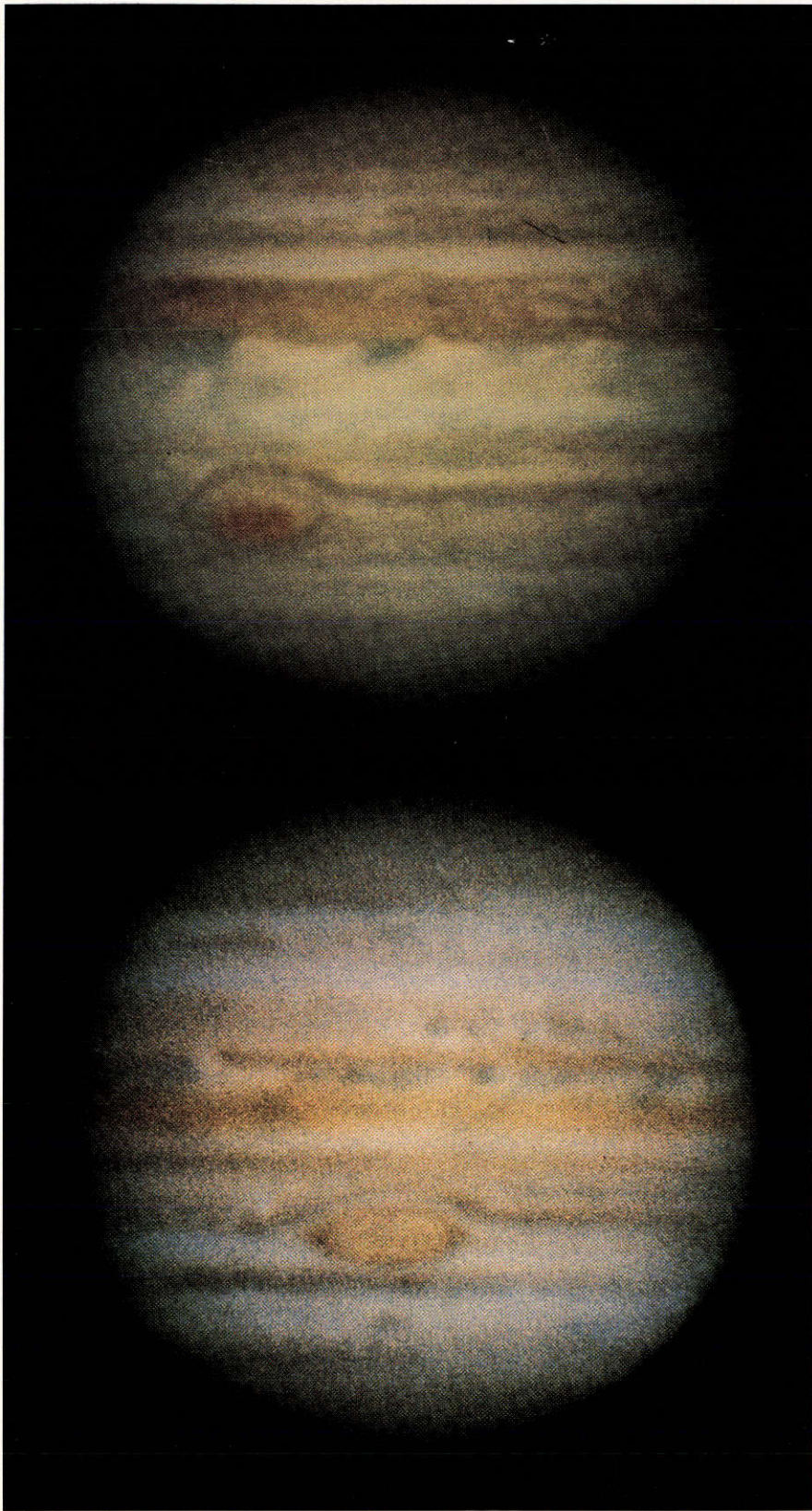
Dec 23, 1966   08:42:35 UT
May 18, 1968   03:03:00 UT

247
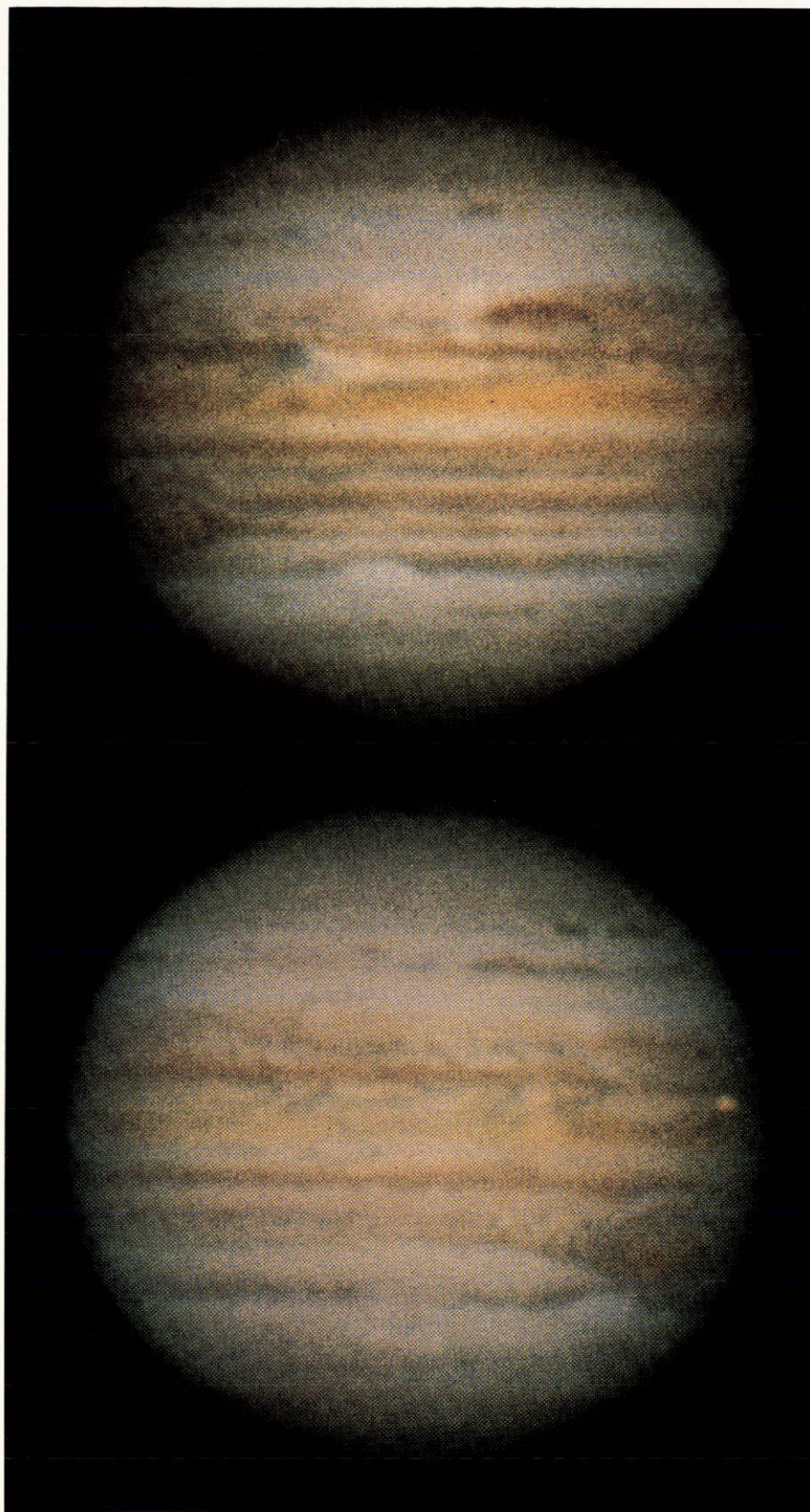
Apr 9, 1968   04:20:21 UT
Jan 25, 1968   10:13:40 UT

248

NO. 173   INTERPRETATION OF THE JUPITER RED SPOT, I.[*]

by   Gerard P. Kuiper

ABSTRACT

Sec. 2 briefly reviews the LPL research programs on Jupiter. They include
continuing photographic coverage of the planet in color and in several wave-
length bands; IR image scans especially around 5μ; medium and high-resolution
spectral studies in the photographic and the lead-sulfide regions, with labora-
tory comparisons; photometric and polarimetric studies; far-IR measurements at
high altitudes; chemical studies designed to match formation of Jovian cloud
particles; and participation in the NASA Pioneer missions. They are followed
in Sec. 3 with some preliminary interpretative remarks, in part suggested by
the remarkable IR spectra and IR images of the Earth and Mars obtained at NASA-
Goddard (Figs. 5 and 6). This leads to a discussion of the Red Spot and the
White Ovals in Sec. 4.

---

[*] This investigation was initiated by an invitation by *Sky and Telescope*, in
Sept. 1971, to summarize the large collection of LPL data on Jupiter which
I had examined during the summer months of 1971. The resulting new inter-
pretation of the Red Spot and the related data on the Jupiter clouds were
published in *Sky and Telescope*, Jan-Feb. 1972. The present text on the
Red Spot (Secs. 4 and 5) was completed as here presented Dec. 1971. Some
data about the Earth and Mars were later added in Secs. 2 and 3.

With the aid of $\lambda 8900$ CH_4 filter photographs it is shown that the Red Spot
is normally the highest cloud feature in the Jovian atmosphere, located squarely
on the South Tropical Zone at 22°S, itself high and prominent (Fig. 1). This
Zone and its Spot are compared with the highest (and most regular) cloud zone on
Earth, the North Tropical Convergence (Figs. 7-8), containing several moving
centers (Fig.10). A definite analogy is found to exist. The Red Spot is a ris-
ing column, obviously having its own energy source; it spreads outward at the top
level, in anti-cyclonic rotation. The cyclones of the terrestrial Tropical Con-
vergence behave likewise, the energy source being the latent heat of condensation.
It is concluded that the large and persistent Jovian cloud masses, of which the
Red Spot is the largest, are major organized storm arrays embedded in a near-
stagnant atmosphere, each probably possessing numerous short-lived rising "hot"
columns driven by released latent heat; and covered by a horizontally-expanding
gigantic cirrus cloud system, in anti-cyclonic rotation. The meteorological
theory of Organized Cumulus Convection is applied to the Red Spot and the White
Ovals. The theory allows for their dimensions. Evidence exists that the array
of hot towers under the Red Spot is eccentric (Fig. 14). The 90-day and the oc-
casional 5-8 year fluctuations in the motion of the Red Spot may be due to pro-
cesses analogous to those found in the Earth's Tropical Convergence. The 90-day
oscillation, discovered by Solberg in 1965, has been observed for 8 years now
(cf. Fig. 16); its trochoidal-type motion is typical for translating vortices
(Fig. 17).

The meteorology of the Jupiter atmosphere may lead to cyclic outbreaks due
to the restoration of the adiabatic gradient by the planetary heat flux after a
previous major "discharge"; the process resembles that attending terrestrial
cumulus formation. This cyclic process could contribute to the propagation of
the Red Spot through the STropZ with a period averaging about 5 years, correspond-
ing to an average daily rotation period of $9^h55^m38^s$. On this model the Red Spot
could indeed be unique in its Zone and of indefinite life. The long-term trends
in the Red Spot period, varying every 20-30 years (Sec. 4b), could be due also to
meteorological processes within the STropZ.

A recent rediscussion of the SEB outbreaks by Reese (1972) indicates that
three sources are responsible, which define a common and constant period of rota-
tion, in close agreement with that defined by the decametric radio observations.
This constant rotation period suggests that the Jupiter subsurface is solid and
strengthens the earlier discussion of the rotation of the surface layers of Jupi-
ter based on Figure 12. The gas eruptions probably interact with the incipient
atmospheric instability having its own relaxation time of roughly 5-10 years.
All three SEB sources are located 14° S and are reviewed in the context of other
NS asymmetries shown by the planet.

Plate I reproduces four LPL color records of Jupiter showing various ap-
pearances of the Red Spot, the White Ovals, the blue festoons, and other clouds.
Fuller discussions of these and of the intricate cloud belts will be published
separately. Appendix I gives comments on earlier views of the planetary heat
flux, the contraction time scale, and models of the Red Spot; Appendix II by
S. M. Larson gives a fuller interpretation of Figure 1.

1. Introduction

This paper is the first of a series summarizing the Laboratory's studies of the planet Jupiter directed toward a physico-chemical and meteorological understanding of its atmosphere and clouds. : Such a program draws on numerous data sources - often very inadequate. The complexity of the visible phenomena, and the explosive growth of terrestrial global meteorology, point to the necessity of considering all Jupiter observations in context, with the development of novel methods of observation always at a premium. The relative merits and costs of planetary research from a mountain observatory, an aircraft, a balloon, a satellite, and a deep-space probe, are important factors in reviewing the past decade and plans for the 1970's.

The planet Jupiter is somewhere intermediate between the Earth and the Sun. Therefore, even atmospheric studies must make some reference to the planet's interior. Hubbard's (1970, p. 693) models J8 and J9 make the hydrogen weight fractions 0.66 and 0.59, the central temperatures 7300° and 7500°K, the Helmholtz-Kelvin contraction time scale 4×10^9 years. "Thus the present model of Jupiter and the most recent determination of the net Jovian energy flux are consistent, but only marginally so" (*op. cit.* p. 696). The computed contraction of the surface is only 0.7 mm/year. The planet is assumed to be in convective equilibrium and to rotate as a solid body. This newly-derived hydrogen weight fraction, around 0.6, is more consistent with recent ideas on the origin of the solar system (via the formation of protoplanets that suffered subsequent mass losses) than the earlier fraction of 0.8 (de Marcus,1958) which nearly equalled that of the Sun. On the other hand, for the Jupiter atmosphere the He, C, and N ratios to H appear almost identical to those in the Sun (Owen, 1970, Table 1).

Smoluchowski (1971) adopts Hubbard's model and interprets his radial variation of temperature to imply that the planet is solid, at least from 0.55-0.8 R_J, where helium is immiscible with hydrogen (and might form small liquid inclusions in the metallic hydrogen). *Above 0.8 R_J solid molecular hydrogen is expected* and below about 0.45 R_J to the core, a liquid hydrogen-helium alloy containing also any heavier elements. The liquid part would be in convective equilibrium and produce the magnetic field. The derived pressure and temperature at the 0.8 R_J interface are 2.10^6 atm and 3600°K (Hubbard, *op. cit.*). A thin layer of liquid molecular hydrogen is assumed to exist "somewhere near 0.9 R_J and much less than 0.1 R_J thick", with p ~ 10^5 atm, T ~ 2000°K. This layer would be essentially an insulator if pure hydrogen; it cannot then generate a magnetic field of its own, and *cannot be responsible for the Red Spot by a magnetic process* (Smoluchowski, *op. cit.*).

The structure of the upper 1-2 percent of the planet (700-1400 km depth) is not well defined by the theoretical model studies and *will require improved empirical definition*. This type of information is likely to come from improved knowledge of the 120° < T < 320°K region, the deepest parts accessible through holes in the clouds with observations made around 5μ; from the radio wave emission at different wavelengths and its distribution over the disk; and radar echoes to probe for density discontinuities at depth. Opacity studies of the uppermost layers have been made by Trafton (1967). No reference is made here to radio observations or to the Jovian magnetosphere, since they do not appear to relate directly to the Jovian cloud layers. A review by Newburn and Gulkis (1971) considers all recent observations and theoretical deductions.

2. LPL Research Programs on Jupiter

a. Photographic Studies and Image Scans - Photography of the planet in
color and through filters (0.3-1.0μ) has been carried out with the 61-inch tele-
scope since its first night of operation, October 8, 1965. The optics were pro-
duced by Mr. Robert Waland. The primary is F/4, made good to λ/40. Two second-
aries are provided, F/13.5 and F/45, giving 10 and 3 arc sec/mm, respectively.
Enlarging cameras can produce images up to F/75 or larger, as desired. In recent
years we have added zero-deviation double prisms that *compensate for atmospheric
dispersion* (they can be moved and turned along the optical axis in front of the
focal plane, adjusted by visual inspection). Planetary resolutions down to 0.15
arc sec have been obtained. About one quarter of the telescope time has been
assigned to this program. This planetary photography program has been very de-
manding, requiring constant attention to detail: the nature of the dome con-
struction, dome paint, exhaust fans, their location and speeds, small exhausts
on rim of mirror, optimum use of wind screens and the dome's slit width; scale
of planetary images depending on brightness of sources; in-house color process-
ing to cut exposure times to 1/4; methods of compositing, etc. For the first year
this work was done by Messrs. D. Milon, A. Herring, and E. Whitaker, partly with
my participation; thereafter mostly by J. W. Fountain, S. M. Larson, R. B. Minton,
and J. Barrett. Messrs. J. Fountain and S. Larson describe in *LPL Communication
No. 174* the photographic techniques developed. One complex but thoroughly pro-
mising technique has not yet been used except experimentally: image reconstruction
for the instrumental and atmospheric blurring functions. This subject will be
treated in this Series.

Because of the planet's recent southerly declination,we have supplemented
our Jupiter photography at telescopes in the Southern Hemisphere: the 60-inch
reflector of the Cerro Tololo InterAmerican Observatory in February and May, 1969
(incidental to the Mars observations that year); and especially the 24-inch re-
fractor of the Bosscha Observatory, Lembang, Java, during May, July, August,
September, 1971. Mr. Steve Larson undertook the May 1971 run in Java; Mr. John
Fountain,all the others. We are much indebted especially to Dr. Bambang Hidajat
for his hospitality.

During the summer of 1971 I examined the entire LPL Jupiter collection,
then over 12,000 frames in color and 30,000 filter frames (UV to IR). The
impact was unforgettable and left me convinced that increased effort on this
planet was justified. Clearly, the use of color film and high image resoluton
were indispensable. After my examination I invited Mr. W. E. Fox, Director of
the Jupiter section of the Brit. Astr. Assoc., as a consultant for two months.
His remarkable visual memory of the everchanging details of the Jupiter cloud
patterns, much of it recorded in the *Journal* of the B. A. A., was a source of
much stimulation as we jointly re-examined the LPL collection. I had made a
provisional quality classification of the entire Jupiter collection in my ear-
lier examinations which was later refined by Mr. R. B. Minton and made the basis
for a log of the LPL data to be published later. The planet was found to be in
constant turmoil during the years 1965-71, especially in 1971, with everchanging
larger and smaller cloud masses seen in six main colors: orange, brown, dark
brown, yellow, cream, and light blue.

The study of Jupiter's zonal motions and of the clouds in each zone has been pursued for nearly a century, with Peek (1958) summarizing the results known up to that date. The first extensive photographic measures were made at the New Mexico State University by B. Smith and C. Tombaugh who in 1963 published a paper "Observations of the Red Spot On Jupiter". Chapman and Reese (1968) published another important study on Jupiter and included references to parallel investigations. Gordon Solberg, at LPL in 1971, had discovered at New Mexico a somewhat irregular 90-day oscillation in longitude of $0°.8$ average semi-amplitude that he traced back to at least 1964. A major irregular drift with some 1200° total amplitude between 1831 and 1970 has long been known and been the source of much speculation (Peek, 1958). The September 1974 and especially the October 1975 oppositions of Jupiter will be the most favorable in the next decade (planet near the equator and at perihelion). A maximum ground-based effort will be called for. In addition, two independent methods of image processing are being pursued on selected images of the entire LPL collection since 1965, promising resolution gains of 1.5-2.0.

In addition to the Jupiter photography in color and through filters, we have since 1968 taken photographs in the strong methane band at 8900Å, to show only the *uppermost cloud layers*. Figure 1 reproduces representative methane pictures for 1968-71. They are printed in two degrees of contrast to bring out their full range of intensities. The filter is 200Å wide, the methane band deep, and thus the exposures are roughly 100 times longer than normal near-infrared exposures. Either high-speed infrared film is used or an S1 image tube, with results comparable in quality. Figure 2 shows the alignment of Figure 1c with a red photograph taken nearly simultaneously. Fuller accounts of these studies are found in the *Communications* immediately following the current issue.

The proof that Figure 1 shows *real elevation differences* in the cloud cover and *not merely albedo differences* is given by Mr. S. Larson in Appendix II. Later an improved methane filter became available which transmitted less radiation from one of the wings of the broad CH_4 bands.

Whereas the methane records of Figure 1 show the *highest* cloud layers, the *deepest* penetration into the Jupiter atmosphere (at least for $\lambda < 35\mu$) is achieved between 4.5 and 5.5μ, where both methane and ammonia are very transparent. The penetration into the Jupiter atmosphere as a function of λ is the most powerful tool to explore empirically the vertical structure of the atmosphere, including the various cloud layers. This matter is reviewed more systematically in Sec. $3a$, below, on the basis of both the Jupiter emission spectrum and the known CH_4 and NH_3 absorptions.

   b. Jupiter's Spectral-energy Curve - This curve consists of the reflected and scattered sunlight, from 0.2-$3\mu\pm$; and the thermal emission beyond, with some overlap, 3-4μ.

The interests of the spectral-energy curve are manifold. The shortwave (solar) part contains numerous CH_4 and NH_3 bands of a great variety of strength - affording the opportunity to view the planetary atmosphere and its clouds from *a range of different depths* - the strongest bands merely showing the uppermost layers, etc. The study of vibrational and especially rotational temperatures (requiring high spectral resolution) adds specific *temperature data* to the different atmospheric layers so investigated. These data in turn must correlate with the local presence or absence of a *cloud layer*, the colors and composition of these clouds, etc., topics reviewed below.
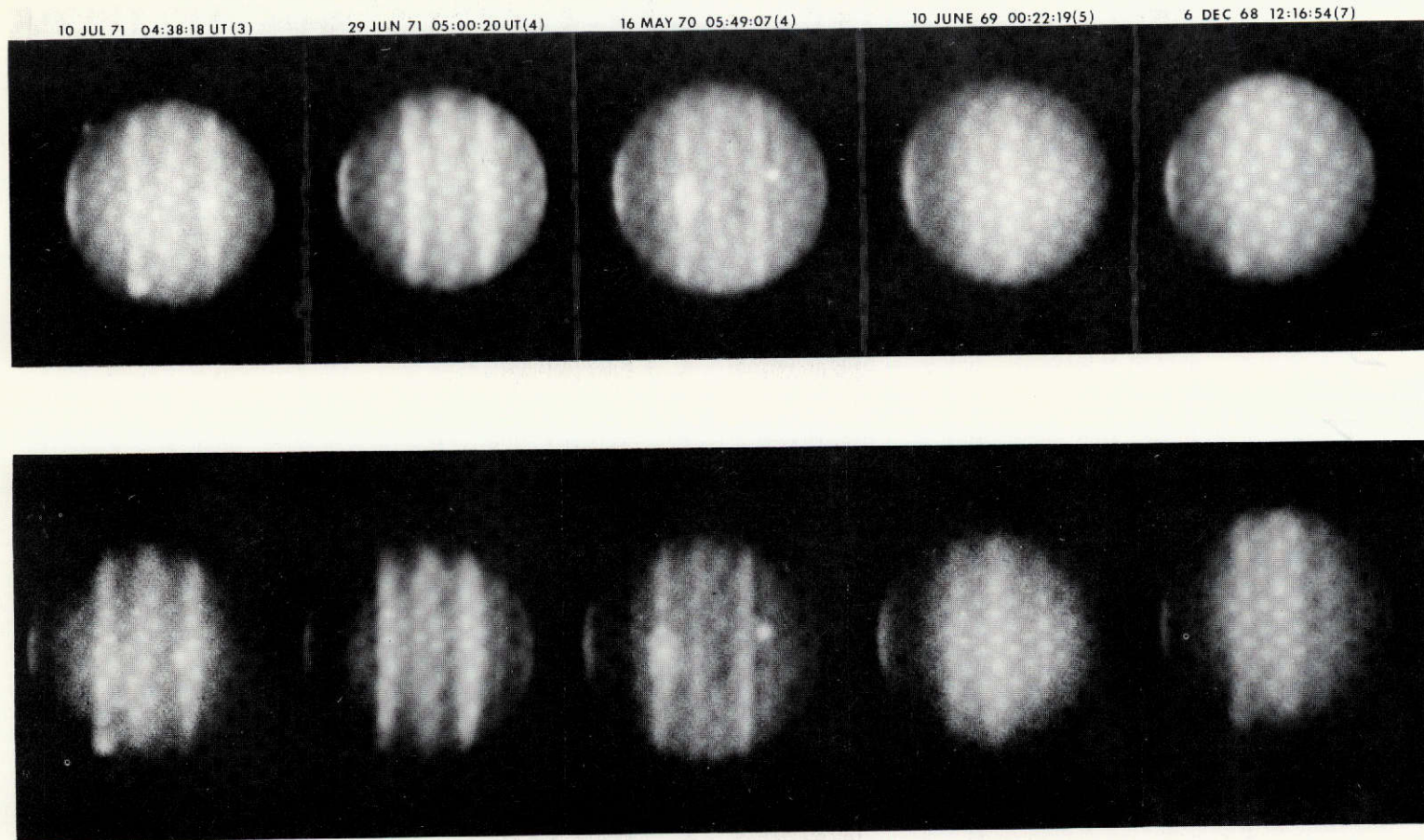
Fig. 1 61-inch photographs of Jupiter in the 8900Å methane band, 1968-1971. Composites, with times and numbers of frames shown in margin. Lower photograph shows two satellites and Red Spot as well as SEB disturbance. Middle photograph shows Red Spot and Io
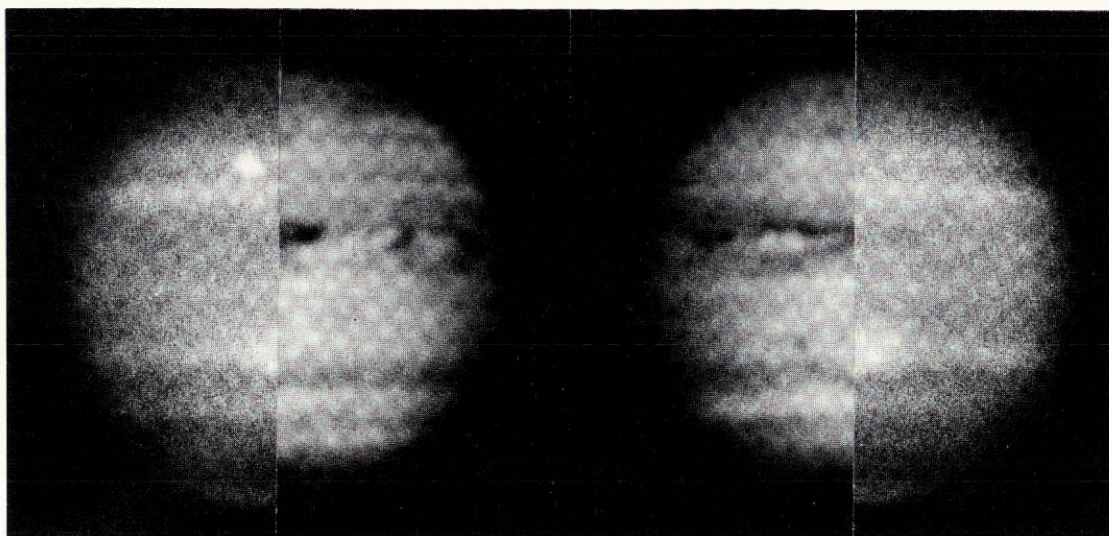
Fig. 2 Alignment of Fig. 1c with red photograph taken nearly simultaneously

The thermal-emission part supplies analogous data for the longer wavelengths. We are here dealing with some extremely strong fundamental vibrations; new effects due to H_2 and possibly other constituents, and H_2O at the deepest penetrations. The *radiation balance* of the planet is involved and all the complexities of a multi-layered atmosphere with an active meteorology, internally driven, unlike the Earth whose atmosphere is largely solar-driven.

A brief summary of the empirical data on the planet and on laboratory spectra must precede further comments.

The solar part of the reflection curve of Jupiter is shown, in outline, in Fig. 3a. It consists of a rather featureless blue and violet section, depressed toward the ultraviolet by the general color of the planet and attributed to scattering of sunlight by particles that are on the average somewhat yellowish. Rayleigh scattering by the overlying gas is not a major contribution though definitely present at the ultraviolet end, particularly for the poles of the planet, as was shown by Dr. Gehrels *et al*. (Fig. 4, below). The part $\lambda > 0.6\mu$ is cut up by absorption bands, generally increasing in strength toward longer wavelengths. The identifications are marked in the diagram. These identifications are based on laboratory comparisons, often made one at a time, ever since R. Wildt identified NH_3 in 1931 and in 1932 suspected some other photographically recorded bands were due to CH_4. T. Dunham pursued the matter with the much greater powers of the 100-inch Coudé spectrograph after 1932(cf. Dunham, Chapter XI, 1952). He confirmed the identification of NH_3 (approx. 5-10 meter atm.; *op. cit.* p. 303), though not all observed near-IR bands were yet matched by laboratory spectra.

Kuiper (1952) repeated the medium-resolution photographic spectral studies, 0.4-1μ, and obtained laboratory matching spectra throughout; and extended the spectral range with the newly developed PbS cell to about 2μ (*op. cit.* p. 364). Greatly improved spectra from 0.90-1.63μ, with sets of matching laboratory spectra of NH_3 and CH_4, were published later (Kuiper, 1963).

Systematic laboratory tests of numerous possible constituents in planetary atmospheres were published by Kuiper and Cruikshank in 1964 and 1967 (*LPL Comm. Nos. 34* and *79*). The gases examined were CH_4, NH_3, N_2O, CO, COS, C_2H_2, C_2H_4, C_2H_6, CH_3SH, CH_3NH_2, H_2S. A new study of the Jupiter spectrum for the region 0.95-1.62μ with 1.5 times the resolution of my 1963 study, also having detailed new laboratory comparisons, was published in 1968 by Cruikshank and Binder (*LPL Comm. No. 103*). They also derived new upper limits for C_2H_2, H_2S and HCN, and derived with great care composite spectra of CH_4 and NH_3 to match Jupiter. Important higher-resolution studies in the photographic infrared were made by Owen (1965) covering the region 0.77-1.12μ which led to upper limits of the abundances of 8 interesting compounds (C_2H_2, C_2H_4, C_2H_6, CH_3NH_2, CH_3D, HCN, SiH_4, HD). He clarified the identifications in the region of the 7900Å ammonia band which is indeed present in Jupiter, but not in Saturn; he found that the previous attribution of the Saturn absorptions to ammonia was mistaken; they were instead due to methane. Owen (1965) also reviewed the *temperatures* derived from different bands of NH_3 and H_2 (i.e., different levels in the atmosphere), finding a range from 128-200°K, indicating very considerable vertical thermal structure in the layers visible between 0.8μ and 3.75 cm, in accordance with temperature measurements quoted below. Moroz and Cruikshank (1969) studied from IR spectra, 1.3-1.6μ, the surface distribution of NH_3 and CH_4. They found a strong latitude effect on NH_3 as well as frequent time variations and a marked E-W inequality, all interpreted in terms of the effective cloud level.

IR spectroscopic investigations of much higher resolution were made by Connes *et al.* (1969) with the first Connes interferometer at the 1.8 meter Hautes Provence telescope; and later with the same interferometer at the 90-inch Steward Observatory telescope, by H. Larson and U. Fink. These results extend beyond this exploratory review of the solar part of the reflection curve of Jupiter.

The *thermal part* of the Jupiter energy curve, 3-1000μ, is known largely through the persistent research efforts, extending over several years, by Dr. Frank Low and associates. We shall refer to these investigations in order of increasing wavelength. The paper by Gillett, Low, and Stein (1969), based on 1967 observations with the 28-inch and 60-inch telescopes, deals with the Jupiter spectrum between 2.8 and 14μ. Because of its importance, we reproduce in Fig. 3*b* the plot of measures. The blackbody temperature from 9-14μ corresponds roughly to 125°K, in agreement with both earlier and later measures in that region (averaging about 128°K). This comparatively low temperature (in terms of the expected value for NH_3 cloud formation) had been interpreted by Kuiper (1952, p. 380) as due to the very strong double ammonia band covering the entire interval 9-14μ. This interpretation was confirmed by Gillett *et al.* who published the absorption spectrum of NH_3 for 10 cm path-length, 1 atm pressure, reproduced in Fig. 3*c*. The extraordinary new feature of the Gillett *et al.* contribution was the intensive emission between 4.4 and 5.5μ, equivalent to a blackbody temperature just under 230°K. These and subsequent studies *have shown this region to be the most extraordinary spectral band of the planet, allowing deep penetration into the Jupiter atmosphere* and an entirely novel set of investigations of the Jupiter clouds.

In April and May 1969 Westphal (1969) discovered *localized* thermal emission from Jupiter at 5μ, with peak brightness temperatures of at least 310°K, in narrow elongated regions between 5° and 20°N latitude. Low and Armstrong, independently, using the 61-inch telescope in June 1969, with 7 arc-sec resolution, found the North Equatorial Belt to have a higher temperature than the remainder of the disk. This work was later continued with higher resolution, with samples quoted on p. 221 of *LPL Communication No. 172*. These remarkably high temperatures prove that the Jupiter atmosphere is far from isothermal as had been assumed in some earlier model and opacity studies. Dr. Low's image scanner may be used also in the other atmospheric windows.

Fig. 3*a* Jupiter reflection curve (geometric albedo), 0.15-2.4μ. Sources: Anderson *et al.* (1969), Irvine *et al.* (1968), LPL spectral data and Johnson (1970). CH_4 circles, NH_3 crosses. (Ordinates 1-2μ somewhat uncertain)
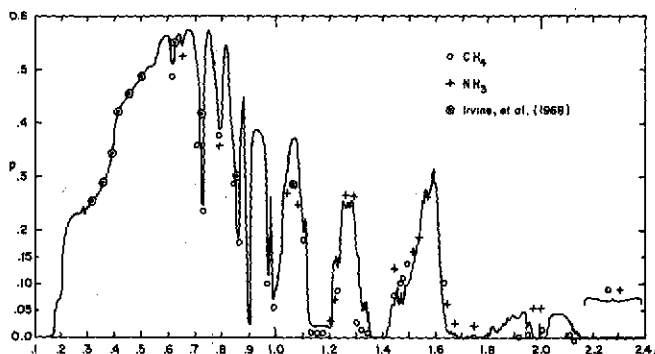
Fig. 3*b* Monochromatic surface brightness of Jupiter, 2.7-14μ (Gillett *et al.* 1969, Fig. 1). Arc at left, solar reflection if albedo is 1
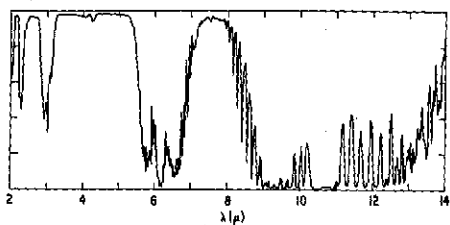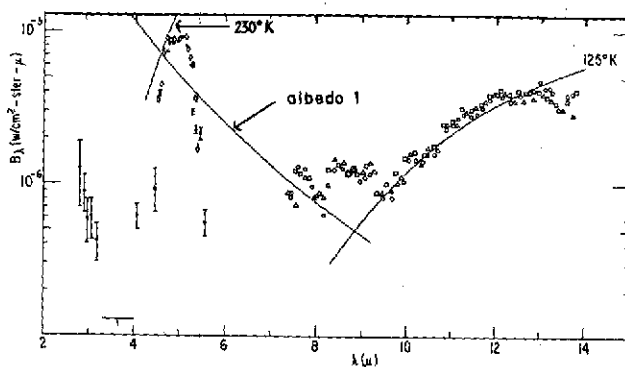
Fig. 3*c* NH_3 absorption spectrum of 10 cm at 1 atm, 2-14μ. (Gillett *et al.* 1969)
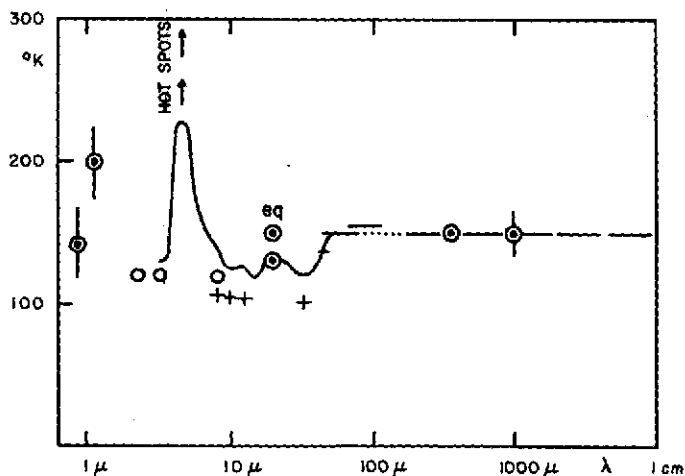
Fig. 3*d* Jupiter emission vs. wavelength, 3μ-1 cm, expressed as radiation temperature. Symbols as in 3*a*. Sources in text except values near 1μ based on H_2(.64, .82μ) and CH_4(1.1μ) (Owen 1965)

More extensive exploration of the Jupiter disk in the 5μ window was described in "High Resolution Measures of Jupiter at 5 Microns" by Keay, Low, Rieke and Minton (*Ap. J.* in press). The observations were made with the 61-inch telescope, mostly in May 1972.

The region around 20μ (approx. 17-24μ) was investigated (F. Low, 1966) at the Catalina Observatory. Low found an equatorial hot band on Jupiter, from approximately -10° to +10°, with a temperature of 150±5°K, with the rest of the planet at about 130°K.

Very recently Low, Rieke, and Armstrong succeeded in measuring the planet for the first time from Mt. Lemmon in the 28-40μ atmospheric window (*Ap. J. Letters,* in press). The wavelength band centered at 34μ is accessible only on very dry nights. The Jupiter temperature found was around 120°K.

Armstrong, Harper, and Low (1972) published results of the far-infrared brightness temperatures of Jupiter, measured in several bands from 30-300μ. The results are 136±1° for 30-45μ; 150±5° for 45-80μ; 153±7° for 65-110μ; and values close to 150°K for the intervals 125-300μ and around 350μ. The last re-sult (350μ) was in fact obtained from the Mt. Lemmon IR Observatory where obser-vations at that wavelength are possible under dry atmospheric conditions, with the results fully published by Harper, Low, Rieke, and Armstrong (1972). Currently the same authors are making further measures in the 1-1.4 mm range.

Low and Davidson (1965) measured the brightness temperature at 1 mm to be 155 ± 15°K. This level is maintained to about 3 cm beyond which the radiation temperature rises owing to increased penetration (Gulkis, personal communication). The entire set of data is summarized in Figure 3*d*. A portion of this energy curve (responsible for about 1/3 of the total planetary emission) lies between 20 and 35μ, an area specially studied by Owen and Walsh (1965).

c. Medium and High Resolution Spectroscopy - A new Laboratory effort in planetary spectroscopy began by using medium-resolution *interferometers*, with the initiation of the NASA Convair-990 flights out of NASA-Ames in April 1967. This program has been described in the *LPL Communications*, starting with *Nos. 93* and *94*, "Program of Astronomical Spectroscopy from Aircraft" and "Solar Comparison Spectra 1.0-2.5μ from Altitudes 1.5-12.5 km". Papers on the Venus spectrum follow-ed, describing the discovery of H_2O on that planet (previous announcements of 50-100 times the real amount were thereby superseded), based on the CV-990 observa-tions with a Block interferometer with resolution 8 (and later 5) wave-numbers; or resolution 1000 at 1.25μ and 500 at 2.5μ. Jupiter was also observed, both at the Catalina Observatory and on the CV-990, but no results were obtained distinct-ly better than with the grating (A) spectrometer. This was due to the smallness of the 12-inch telescope used on the CV-990, the low IR intensity of Jupiter, and to Jupiter's absorptions mostly coinciding with the water-vapor bands so that little was gained from high altitude at 1-3μ. Dr. H. L. Johnson (1970) investigated the spectrum of Jupiter from 1.2-4.2μ, with resolution 8 cm^{-1}, and derived ratio spectra in terms of the Moon.

Excellent results were obtained with the much higher-resolution original *Connes interferometer*, on indefinite loan from Dr. Pierre Connes of Paris, France, and placed at the Coudé focus of the 90-inch Steward Observatory telescope on Kitt Peak. Drs. Harold Larson, Uwe Fink, and Guy Michel (of Paris) have succeeded in
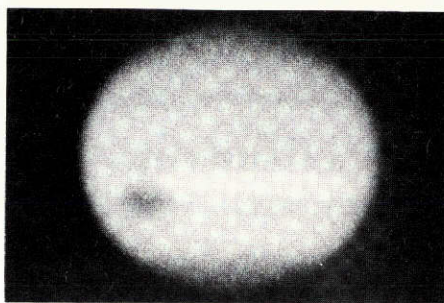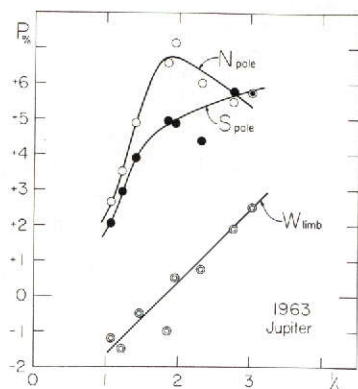
Fig. 4a Asymmetry between two hemispheres of Jupiter derived from polarization measurements (Gehrels *et al.*, 1969); *b*. Jupiter at $\lambda 3000$Å, 1971, April 8, 10:26:40 UT. (J. Fountain)

solving the numerous problems with the mounting and operation of this instrument. The interferometer is capable of a resolution of 180,000. Eight interferograms of Jupiter have been obtained so far, representing about 30 hours of net observing time. Five interferograms were obtained with resolution of 55,000; they have been Fourier-transformed and are being averaged and analyzed. These new spectra should give improved abundances, new isotope ratios, gas temperatures, and hopefully, new trace constituents.

A 500-channel spectrometer for the 0.35-1.0μ region using a cooled silicon-diode detector is being assembled for spectroscopy of small portions of the planetary disks, satellites, standard stars, and laboratory comparison sources. A later paper on the results will be issued.

d. Photometric and Polarimetric Studies - Dr. Tom Gehrels and his group have developed the measurement of polarization over a wide range of wavelengths, reaching a precision in the orthogonal ratios down to a few ten-thousandths. They found a systematic difference between the South and North Polar caps as well as the planet's limb (Gehrels *et al.*, 1969), as shown in Figure 4a. They interpreted the results as due to scattering by molecules plus aerosols; the North Pole shows a molecular optical depth in visible light of 0.6, the South Pole of 0.4, the equator of 0.05; the amounts of hydrogen deduced were 240, 160, 20 km atm., respectively. More recently, Mr. Lyn Doose (Ph. D. dissertation) systematically scanned the entire Jupiter disk with the 61-inch both *photometrically* for about 20 wavelength bands; and *polarimetrically* in 7 bands. The photometric scans included the 8890Å CH_4 band and a comparison band at 9200Å. They were used especially in the study of the Red Spot, both cloud level and scattering properties. Mr. Doose found the Red Spot to be about 5 km elevated above the surrounding cloud deck. It should be noted that the spectroscopically-determined H_2 content is about 4 times larger, 85 ± 15 km atm (Owen, 1969, p. 356). This difference can only partly be attributed to the wavelength difference of the two determinations 0.55 and 0.70μ.

What are the Jupiter *cloud colors*? LPL started a 40 narrow-band filter photometric program of the Jovian planets and satellites a year ago, covering 0.3 to 1.1μ, with spectral resolution $\lambda/\Delta\lambda$ about 30. The program was carried out by Mr. W.

Wamsteker. Data for the four Jovian satellites were published in *LPL Communication No. 167*; the four Jovian planets, the Saturn Ring, and Rhea of Saturn are still under observation. The results on the solid bodies (no atmospheres) have been less informative than hoped for. The region 1-4μ is much more informative (Kuiper, 1957; Fink *et al*., 1973).

e. Far-IR Measures at High Altitude - Low, Aumann, and Gillespie (1969) measured the total IR emission of both Jupiter and Saturn (5-100μ) on high-altitude flights with the NASA Lear Jet. They found the infrared emissions of the two planets 2.7 and 2.3 times the amount absorbed from the in-coming solar radiation. While qualitatively this result was not unexpected (see Appendix I), the actual amounts were unknown and are important empirical parameters in the recent model studies by Hubbard and others, referred to in Sec. 1.

f. Participation in NASA Pioneer Missions - Dr. Tom Gehrels is the principal investigator on the NASA Pioneer F (or 10) and G Missions for imagery and polarimetry. These are to operate in two colors at about 3-4 times present earth-based resolutions, for the limited periods of the encounters (Gehrels, Suomi, Krauss, 1972). The polarimetry will extend beyond the earth-based upper bound of 11° phase angle, and will therefore be far more informative than the available polarimetric data. Hopefully, distinct information will be derivable on particle sizes and the refractive index of the cloud material.

g. Laboratory Studies - A comparison program matching the spectral and broadband photometric observations is underway by Fr. Godfrey Sill, a chemist, using laboratory experiments and thermodynamic theory. He is preparing a report on his laboratory data for *LPL Communication No. 184*.

3. Interpretative Remarks

a. Comparisons with the Earth and Levels of Penetration - Since WWII the Earth has been observed as a planet, from above the atmosphere, on an ever increasing scale. What started as efforts to observe extended cloud systems and cyclones from rockets; temperature, pressure, and composition profiles of the atmosphere from rockets; circulation patterns and global weather systems; has developed, with the Tiros and Nimbus series, beginning in 1961, into an increasingly systematic global watch of the Earth. For instance, Nimbus III used (1969-70) five filter bands simultaneously:

(1) 0.2-4.8μ, to observe the integrated reflected sunlight;
(2) 6.3μ, to observe the upper tropospheric H_2O vapor;
(3) 10-12μ, to observe the thermal emission from the Earth's surface, where clear;
(4) 15μ, to observe the atmospheric CO_2; and
(5) 20-23μ, to observe the lower tropospheric H_2O and clouds.

These programs, mostly conducted at the Goddard Space Flight Center for the past decade, have fully succeeded after passing through the expected refinements in instrumentation and communication; and the necessary calibrations, often from specialized airborne equipment.

A simple transfer of these techniques to Jupiter is not feasible, but there are distinct parallels:

(1)   color and filter photography 0.3-1μ, as commonly practiced,
      with vidicon imaging techniques 1-2μ being improved;

(2)   the 0.89μ CH_4 photography observes the uppermost cloud layers;

(3)   the 5μ window provides the deepest penetration into the Jupiter
      atmosphere;

(4), (5) filter photography selected to cover intermediate depth and
      temperatures, e.g. may be selected on the basis of Figure 3.

The penetration into the Jupiter atmosphere may be roughly estimated from
Figure 3d with the aid of a model atmosphere based on available abundance ratios.
The intensities of the IR fundamentals v_2, v_3, and v_4 of CH_4 in mixtures with He,
A, and N_2 at pressures up to 3000 atm were derived by Armstrong and Welsh (1960).
The IR spectrum of NH_3 from 20-35μ was studied by Walsh (1969), both for pure NH_3
and mixtures with N_2, following the paper by Owen and Walsh (1965) dealing with
the Jupiter spectrum and the planetary heat balance. Walsh used path lengths up
to 196 meters, examined the pressure effects on the total absorptance, compared
his measures with theoretical line models (strong-line, weak-line) and found dis-
crepancies of importance to planetary spectral studies. Unfortunately, similar
laboratory data for NH_3 do not appear to exist beyond 35μ which would cover the
pure rotation spectrum. For this reason it is difficult to interpret Figure 3d
beyond 35μ, where, in fact, the temperature measures are only approximate in any
case. One would expect a temperature profile somewhat below 150°K, and possibly
as low as 135°K, in the region of the rotation spectrum of NH_3. It should be noted
that the effective temperature of the planet was found by Aumann *et al*. (1969) to
be 134±4°K, which would lead one to assume to be the weighted average for the region
of about 8-100μ. The remarkably high temperature observed in the 4.5-5.5μ window
averaged over the entire disk indicates that *gas absorptions* (mostly NH_3) rather
than clouds are responsible for the low temperatures measured at longer wavelengths.
The various windows at $\lambda < 6$μ should give supplementary information on particle sizes
and cloud layers vs. temperature or depth. The relative transparency of the 4.5-
5.5μ window suggests that the particles above 220°K are only micron size.

The window 0.74-0.76μ deserves special attention. The Uranus and Neptune
spectra show the CH_4 absorptions there to be extremely weak. Owen (1967), who
identified as CH_4 the weak lines I had observed here for Uranus and Neptune, de-
rived laboratory data implying that some 100 km atm of CH_4 would be needed to
give appreciable CH_4 absorption in this window. Since NH_3 also appears "absent",
one could assume that for Jupiter the penetration in this window might be limited
by Rayleigh scattering of H_2. Then the required amount of H_2 would be 500-600 km
atm, which, however, by Owen's (1969) temperature profile (assumed to be the adia-
bat) would make T>300°K. Some check on the reality of this deep penetration could
be made by setting an upper limit to the CH_4 content seen in this window from high
precision high-resolution spectral traces. About 1 km atm of CH_4 is expected if
indeed the limit is set by molecular Rayleigh scattering. Alternatively, the
penetration limit is set by atmospheric haze. This is probably true except for
the blue festoons, discussed later. These areas are probably too small for spec-
troscopic T determinations (0.82μ H_2, 1.1μ CH_4). Narrow pass-band filter studies
up to 1.6μ might assist here.

A filter selected to cover a given band (e.g. CH_4 6190Å or 8900Å) does not
show a *single* depth of penetration. A high-resolution spectrum is needed to show
the fraction of various degrees of absorption (each with their own penetration)
and possibly intervening stretches of continuum. The profiles of the photographic

CH_4 bands are smoother than the NH_3 bands (which show sharper, well-separated lines). The estimate of the effective *mean penetration* of the planetary image in the band must therefore be made with great care. The same problem has arisen for satellite spectral studies of the Earth.

The spectral curve between 0.2-0.3μ has been explained by Stecher, and in more detail by Greenspan and Owen (1967), as due to the scattering of H_2 and mild absorptions due to NH_3. The amount of H_2 so derived is 12 km atm, which is approximately the amount expected for the Jupiter stratosphere. This interpretation is consistent with the small but definite limb brightening at 0.30μ discovered by J. Fountain; and with the fact that the Red Spot and several cloud belts become visible around 3000Å (Fig. 4*b*). The amount of H_2 estimated from the intensity of the Red Spot in Figure 4*b* (assumed to be intrinsically dark) is some 20 km atm of H_2; this deeper penetration is roughly in accord with the lower Rayleigh scattering.

The interpretation of Figure 4*b* is considered by Mr. Fountain in a following *Communication*, in the context of his other narrow-band records of the planet. There is no close resemblance to Figure 1, clearly because of large brightness differences in the UV between the different high-level cloud belts, though all overlain with the common semi-transparent H_2 blanket (these differences cause the large range in color).

Comparison of the atmospheric *models* of Earth and Jupiter can be misleading since *Jupiter has an internally-driven meteorology.* Interesting computations, as have been made for the radiative balance within the Earth atmosphere, resulting from the various gaseous components (e.g. Dopplick, 1972, pp. 1278-1294), are therefore not readily transferable to Jupiter. Goody (1969) pointed out that in the upper atmosphere of Jupiter *the dynamics dominates radiative balance.*

The dynamical parallels between the Earth and Jupiter atmospheres are instructive. These are developed in Sec. 4 on a special topic: the terrestrial Tropical Convergence Zones are compared with the high-level cloud zones on Jupiter at 22° N and S, one of which contains the Red Spot. This leads to an interpretation of the Red Spot in terms of the theory of Organized Cumulus Convection (p. 288 ff).

Two introductory aspects are considered here: (a) the comparison of the Jupiter IR emission spectrum (Figs. 3*b* and 3*d*) with that of the Earth and Mars, all three showing variations in penetration with wavelength due to the gases present; and (b) near-monochromatic images of the Earth, both in the strong water-vapor band at 6.7μ and in a clear window, 10-12μ; to be compared with images of Jupiter taken in the very strong 0.9μ CH_4 band (Fig. 1) and in the clear 5μ window (cf. p. 221), respectively.

Hanel and Conrath (1970) published Earth spectra from 6.7-25μ for selected regions, the Sahara, the Mediterranean, and the Antarctic, which are reproduced in Figure 5*a*. The resolution is 2.8 cm^{-1}; the gases are identified. One notes the 15-20 fold change of intensity in the central atmospheric window, 10-12.5μ, depending on the surface temperature; and the nearly isothermal CO_2 band at 15μ which, because of its high absorptivity, shows the temperature of the atmosphere above 300 mb, which indeed is nearly constant over the Earth. The strong H_2O absorption at 24μ is similarly nearly isothermal over the globe, while the ozone, of medium strength only, shows an admixture with background radiation.

The relation to black-body curves is shown in Figures 5*b* and 5*c* (Hanel *et al.*
1972*a*), and is self-explantory. The effect of clouds in the atmospheric window of
8-14µ is shown in Figure 5*d*. It is seen that the depth of the strong CO_2 band is
not affected, because its level is *above* the clouds.

The Mars spectra are not unlike those of the Earth, except that CO_2 is stronger;
and H_2O and O_3 very weak or absent. Beautiful data were obtained by Hanel *et al.*
(1972*b*) on Mariner 9. The authors have consented to the reproduction here of two
of their published spectra. Figure 5*e* shows the spectrum after the atmospheric dust
had settled (normal condition). Figure 5*f* shows the spectrum under dusty conditions.
Reference is made to the original paper (Hanel *et al.*, 1972*b*, Figs. 7 and 10) for
most remarkable spectra of the two Martian polar caps.

The spectra of Mars (Figs. 5*e*, *f*), Earth (Fig. 5*a-d*), and Jupiter (Fig. 3) form
a sequence of both increasing gaseous absorptions and interference by clouds. While
the Mars continuum (due to its surface) is interrupted only by CO_2 and occasional
dust (and locally H_2O ice clouds: Curran *et al.*, 1973); the Earth continuum 8-14µ is
the only prominent one in the entire interval 2-1000µ, and even so is for about 50%
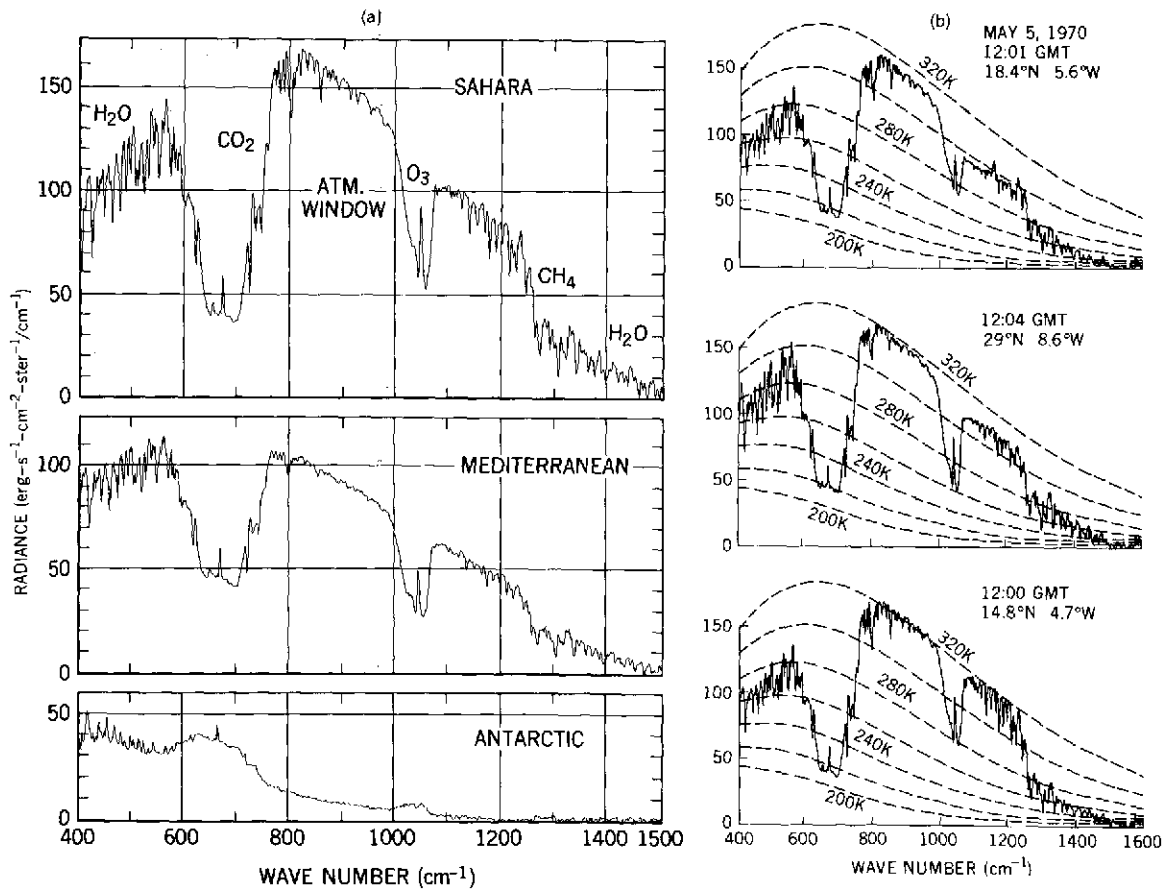
Fig. 5*a*. Thermal emission spectra of Earth, Nimbus IV, Orbit 29, 10 April 1970;
5*b*. Spectra on 5 May 1970, at times and coordinates given (courtesy Dr. Hanel)
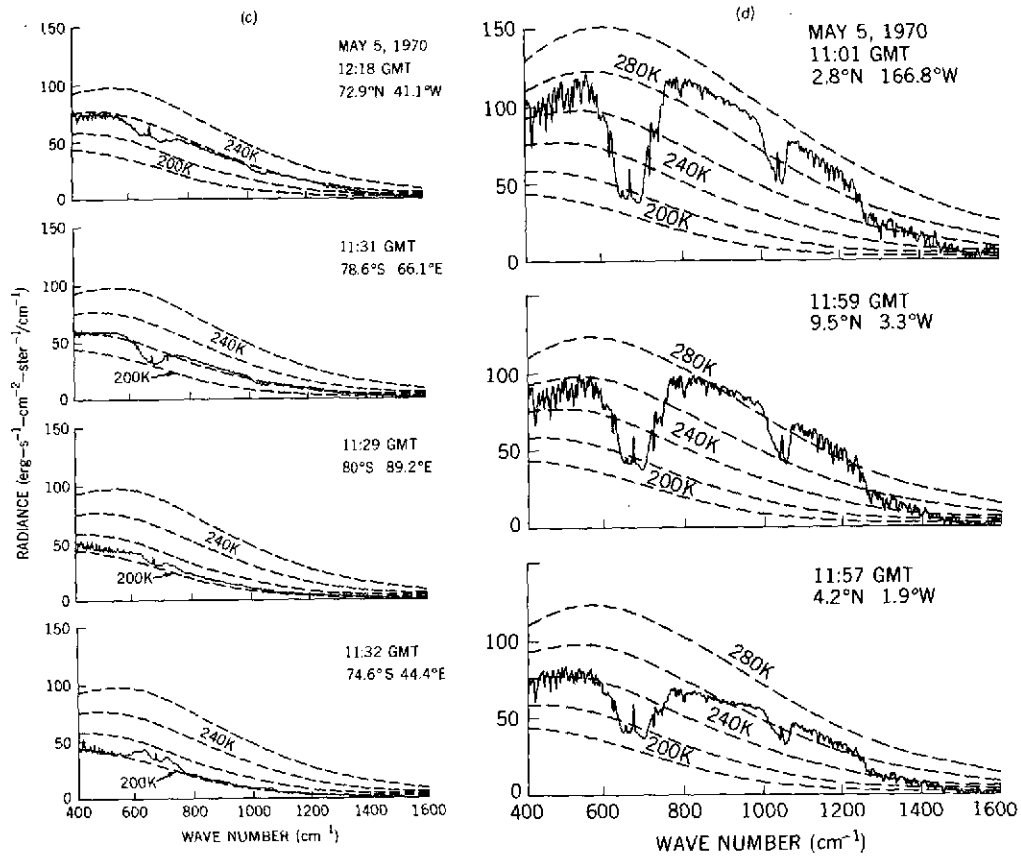
Fig. 5 (cont.) *c*. Spectra of areas of Greenland (upper frame) and Antarctica; *d*. Effects of clouds in atmospheric window, incl. departures from black-body curves (courtesy Dr. Hanel)
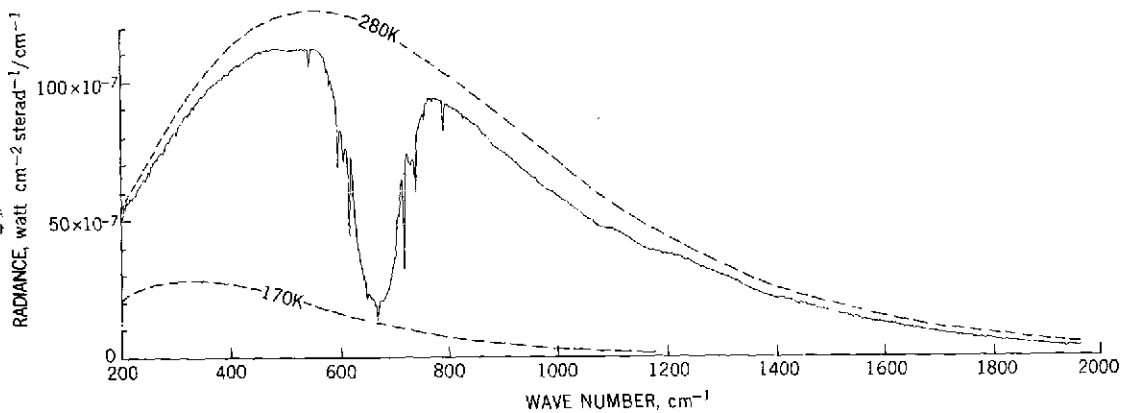
Fig. 5*e* Midlatitude spectrum of Mars, March 1972. Mariner 9 (Hanel *et al.* 1972*b*,Fig. 9), after atmospheric dust had settled
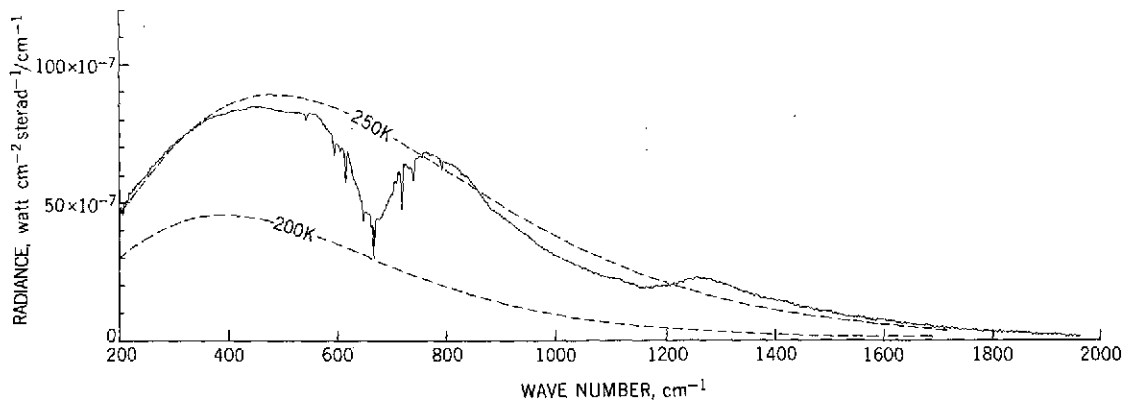
Fig. 5f Midlatitude spectrum of Mars, Dec. 1971, under dusty
conditions (Hanel *et al.*, 1972*b*, Fig. 8). Reduced atmospheric lapse
rate, hence shallow CO_2 band. SiO_2 bearing minerals in evidence
from 400-600 cm^{-1} and 850-1300 cm^{-1}

of the Earth's surface interrupted by clouds. Jupiter has only the 4.5-5.5µ major
window and its penetration is limited to small equatorial areas without clouds of
NH_3 and its compounds; and then stopped entirely by the deeper H_2O cloud zone, at
about 300°K.

Through the courtesy of Dr. W. Nordberg, NASA-Goddard, I am able to reproduce
in Figures 6*a* and *b* two composite images of the Earth in the 6.7µ H_2O band obtained
with the Temperature-Humidity Infrared Radiometer (THIR) aboard Nimbus V. These
montages cover most of the globe (with some Central Pacific and North of about 50°
missing) and were taken during the daylight orbits on 1 and 8 February 1973. The
11 or 12 strips each cover about 30° in longitude and thus are nearly adjacent near
the equator; but N and S of about 40° latitude they show increasing duplication
of features. The South Pole has been marked with white dots. Dr. Nordberg advised
me that the penetration at 6.7µ is on the average to about 300 mb. Dry, deeper and
thus hotter regions than average are shown darker; elevated (and colder) humid
regions are shown whiter. The two dry desert zones at ±30° are in evidence (dark)
as is the Tropical Convergence Zone (light colored). In the middle latitudes of
both hemispheres curious swirling patterns are seen containing several cyclonic
vortices. These broad patterns, made up of streamers 100-500 km wide, carry
finer-textured clouds (down to 10 km and probably finer) as is seen in the 10-
12µ frames taken simultaneously (Figs. 6*c*, *d*). These pictures also show the
continents (dark and hot) and thus fix the approximate coordinates.

Figures 6*a-d* are *negatives* of the observed radiation-intensity distribution,
printed thus to show the *highest* (coldest) structures as *white*. For this reason
they may be compared to Figure 1, though a more direct comparison is made in Fig-
ures 7-9, below, which, like Figure 1, were taken in reflected sunlight.

In the 5µ window nearly the entire Jupiter disk is seen to have radiation
temperatures above 210°K (Keay *et al.*, 1973; cf. p. 221 of this Volume). This
shows that the cloud deck seen visually is composed of small particles, 1µ or less
in diameter, a subject already commented on by Owen (1969). Along the central part
of the visible equator there is an elongated region, of variable size, above 230°K,
often containing one or more hot spots of temperatures 250-300°K. Owen (1969) finds
NH_3 in a convective Jupiter atmosphere of solar element-abundance ratios to be sat-
urated above the layer where T = 160°K, and unsaturated below. He thus concludes
that the NH_3 ice haze will extend *above* this level, and that the atmosphere should
be clear below (until other opacity sources become important). He thus accounts

707   706   705   704   703   702   701   700   699   698   697
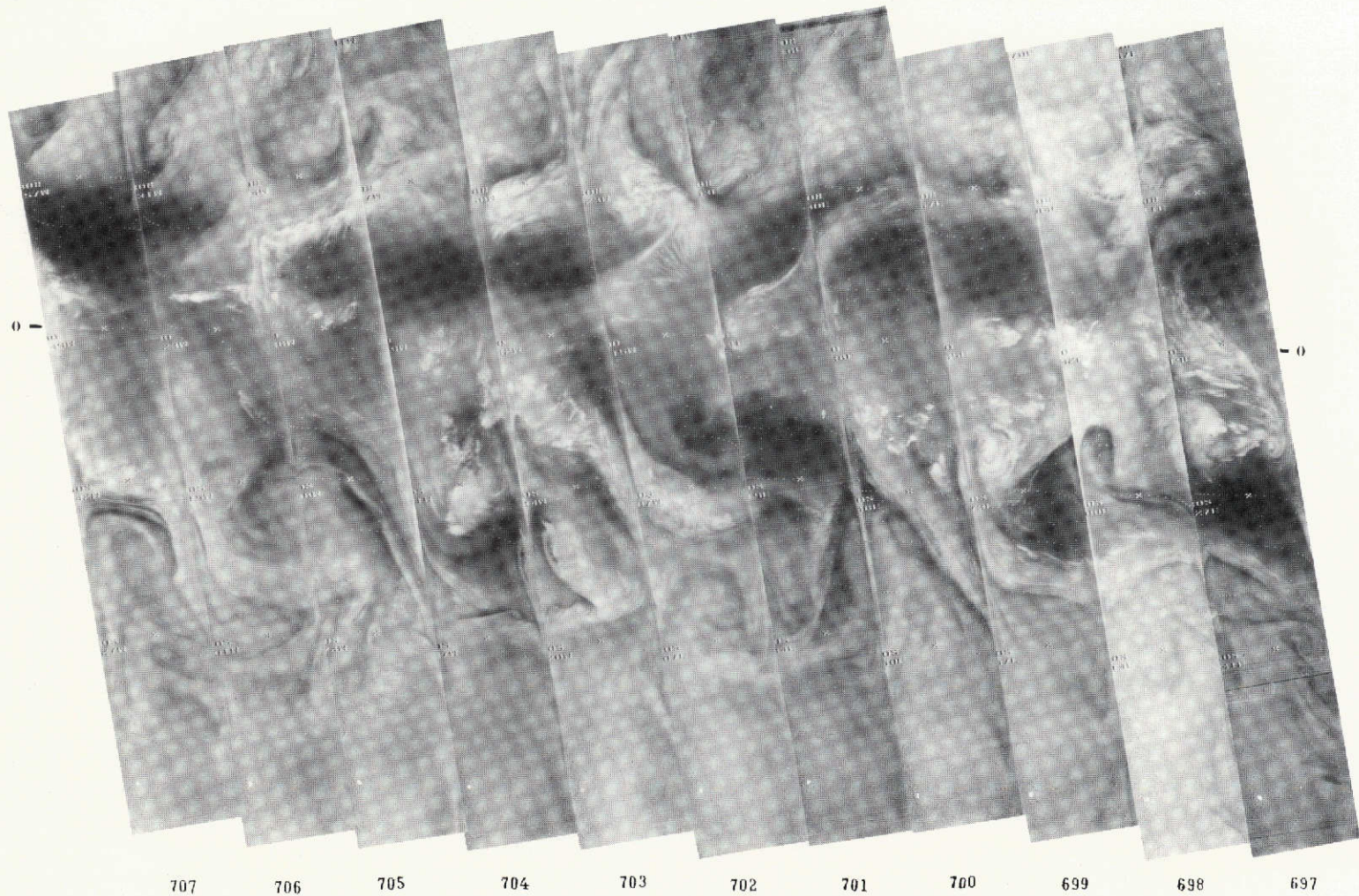
Fig. 6a Montage of 11 consecutive orbital strips of the Earth, each 30° wide at
the equator, observed in 6.7μ H$_2$O band, on Nimbus V; 1 Feb 1973. For identification
of longitudes cf. Fig. 6c. (Courtesy Dr. W. Nordberg, NASA)
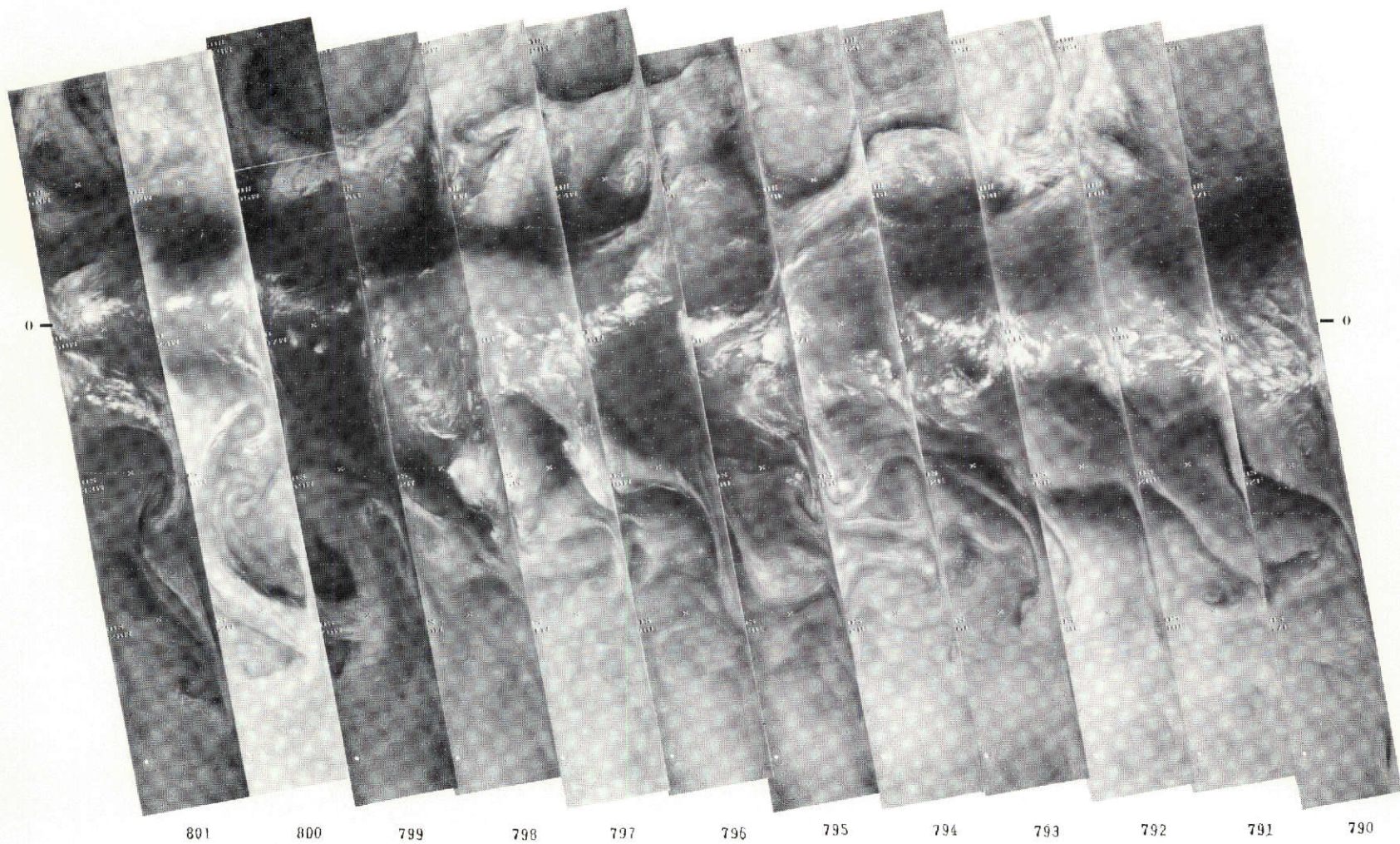
Fig. 6*b*   Montage of 12 consecutive strips, 8 Feb 1973; otherwise like Fig. 6*a*.
(Courtesy Dr. W. Nordberg, NASA)

707   706   705   704   703   702   701   700   699   698   697
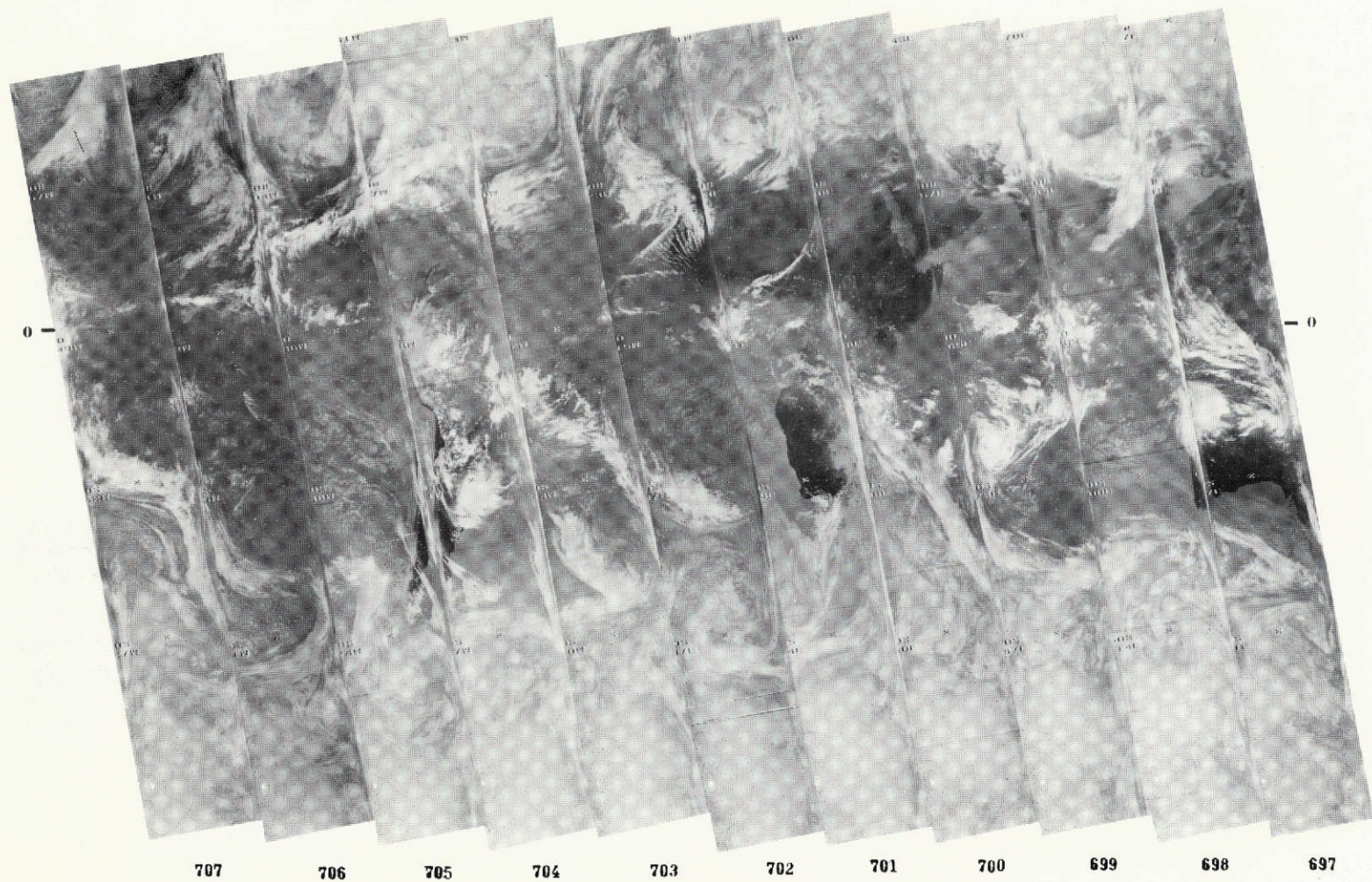
Fig. 6*c* Montage of 11 consecutive orbital strips taken in window 10–12.5μ
on Nimbus V, taken simultaneously with Fig. 6*a*. South America, Africa,
Arabia, India, and Australia well shown, with Pacific coastal outline of
North America. (Courtesy Dr. W. Nordberg, NASA)
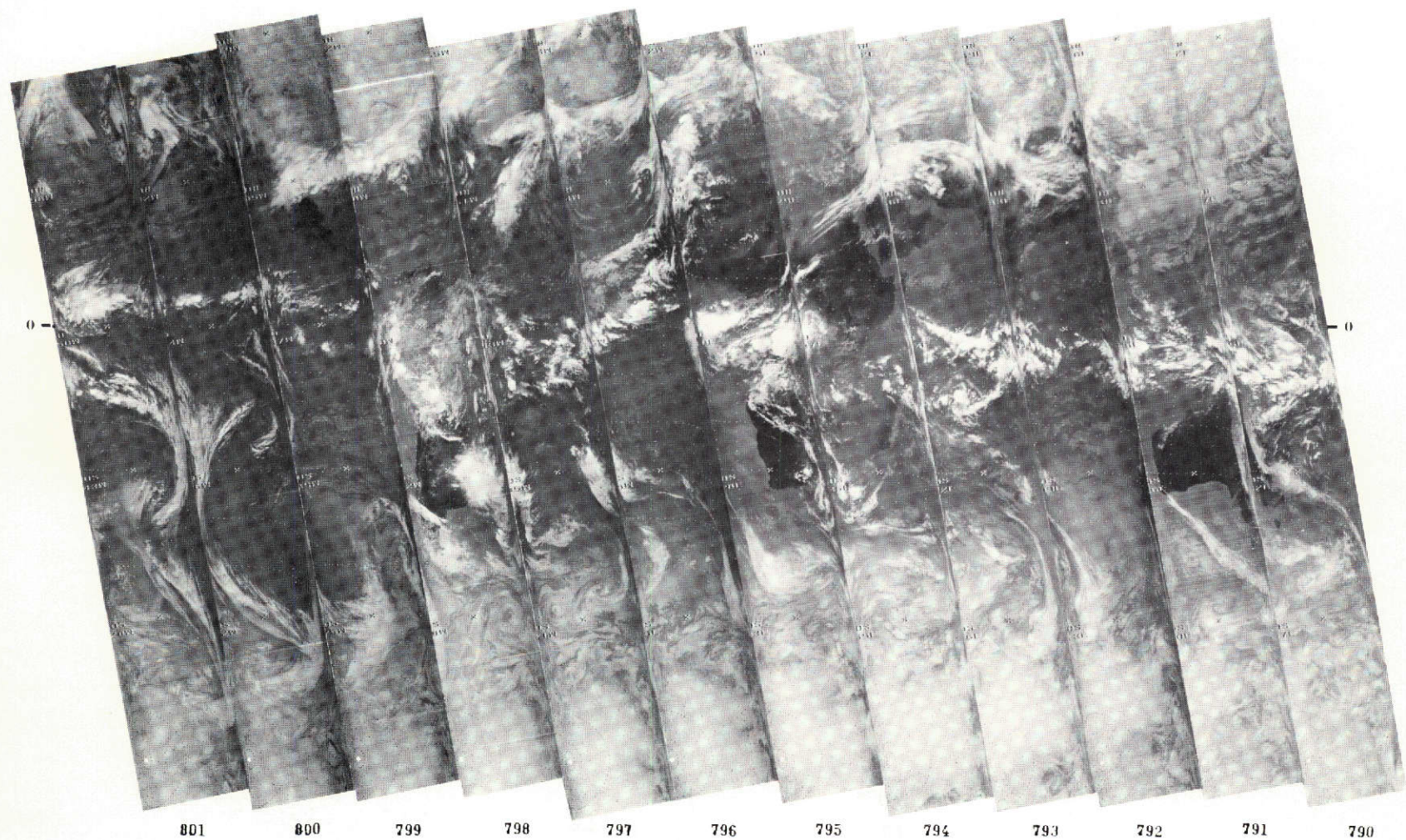
Fig. 6d Montage of 12 consecutive orbital strips taken in window 10-12.5µ, Nimbus V, taken simultaneously with Fig. 6b. South and Central America, Africa, Arabia, India, and Australia well shown. White dots at bottom indicate position of South Pole.
(Courtesy Dr. W. Nordberg, NASA)

for the rotational CH_4 temperature derived (cf. Fig. 3d) and possibly for the
temperature found for H_2 (0.82μ). This model is essentially consistent with
conclusions by Lewis (1969).

Lewis considers two composition models: A and B (differing in He content),
with model B probably more closely applicable to Jupiter. He further examines
the effects of H_2S interacting with NH_3, and concludes (p. 376) that solid NH_3
would be present above the layer at which T = 160°K (in agreement with Owen);
that NH_4SH would become increasingly abundant below the level at which T = 200°
up to T = 225°K; that H_2O ice would follow, T = 225°-270°, beneath which an
aqueous solution of NH_3 would exist to about 310°K. Lewis concludes "pure water
ice cannot be a major component of the clouds and pure liquid NH_3 is found to be
absent". Maximum opacities are expected around 160°K (solid NH_3), 225°K (NH_4SH)
and 300°K (aqueous NH_3 solution). What is clearly needed is a better definition
of the particle sizes and composition (see next section) of the 160°K cloud layer,
which can be done readily; and laboratory studies under simulated conditions on
the two other layers, both of which are accessible in the 5μ window.

It will be important to derive the precise dimensions and temperature of the
Red Spot at 5μ (so far found cooler) and relate the results to the interpretation
of the Red Spot proposed in Sec. 4. (If the size is comparable to the visible
size of the Red Spot, its T is probably low and the particle size >> 1μ; if the
size is much smaller, T is probably higher than its surroundings and refers to
the inner system of columns; see Sec. 4). Also, to determine the penetration in
the other spectral windows shown in Figure 3a, with the purpose of deriving fur-
ther data on the average cloud particle size.

It is a curious coincidence that the 6.7μ pictures of the Earth (Fig. 6a,b)
should penetrate to nearly the same temperature regions as the 5μ pictures of
Jupiter. The differences are important, however; the 5μ pictures of Jupiter show
clouds, probably composed of NH_4SH, the 6.7μ pictures of the Earth show the variable
elevations of moving air masses containing a given total amount of water vapor,
which, when high in the atmosphere, is accompanied by local H_2O cumulus formation.

b. *Cloud Colors* – The concept of the visible clouds as pure NH_3 ice crystals
is contradicted by the vivid colors observed, from white to cream, yellow, brown,
dark brown, and bluish-gray. Ammonia ice is white. Owen (1969) comments on the
apparent correlation of the colored regions with somewhat increased altitude. Owen
and Mason (1969), following the Lewis (1969) discussion, note that $(NH_4)_2S$ is yellow
and might be present on Jupiter.

An incisive study was published by Lewis and Prinn (1970). They point out that
the yellow color of $(NH_4)_2S$ is due to oxidation in our atmosphere and that the color-
ed substance is in fact the polysulfide $(NH_4)_2S_x$. They add that the oxidation could
not occur on Jupiter, but that *photolysis by solar UV* could produce the coloration.
They consider the transfer of 2200-2700Å solar radiation (2700Å is the cut-off limit
of H_2S absorption) and conclude that in areas of the planet where the NH_3 cirrus
cover is thin or absent the 210°-230°K level containing NH_4HS will be reached. The
result will be the production of H_2S_x, S_8, and $(NH_4)_2S_x$, all of which are yellow,
orange, or brown. No conclusion was reached for areas having a substantial NH_3 ice
cloud cover (which would cause absorption of UV); but they do point out that the
UV photolysis will act significantly in periods of about one week, contrary to an
earlier suggested explanation of the cloud colors by Sagan through the production
of colored organic matter, which would be some 10^5 times slower. The dynamics of
the Jupiter cloud masses requires the shorter time scale.

At this Laboratory, a parallel and independent investigation of the cloud colors was started in 1970 by Fr. G. Sill, on which he reported at the San Francisco meeting of the A. G. U., Dec. 8, 1970, Symposium on the Jovian Cloud Layers. Fr. Sill reproduced the processes in the laboratory and at temperatures appropriate for Jupiter, which led to the discovery that *many of these colors are temperature-dependent*. Sulfur is white at the Jupiter temperature; so is NH_4HS. Fr. Sill reports on his experiments in *LPL Communication No. 184*. Plate I shows the Jupiter colors.

Since cosmically S is less abundant than N by 5 or 6x, most of the ammonia will remain and produce clouds composed of ammonia cirrus (whitish). The dynamics of the cloud belts may bring the polysulfides to high altitudes where the photolysis would be enhanced. This would explain the fact that the Red Spot is both very high and orange in color. There is, however, evidence that a few days of solar exposure are needed. A sudden major outburst observed in July 1971 produced a *white* very high-level cloud.

In addition, there are blue areas concentrated in a narrow zone near the equator, often fan-shaped and called "festoons". Wildt's suggestion that the brown and blue colors of Jupiter may be due to alkali metals dissolved in liquid ammonia now appears unlikely because of the laboratory studies of Jolly (1964) and others. These showed the blue color to be due to the red wing of an enormous near-IR absorption strong at 0.6μ, but weaker at 1.0μ. We shall see later that the blue areas are probably essentially cloudless and allow deeper penetration into the atmosphere. The blue-grey festoons are well shown on Plate I.

Miller and Urey, and later Sagan, Ponnamperuma, and Woeller, have considered *non-equilibrium reactions* through electric discharges, and more recently by UV light. They all give rise to hydrogen as a byproduct and run therefore in the opposite sense from purely chemical reactions in the presence of an over-abundance of hydrogen. These reactions appear to depend on the products of interest being continually removed from the reaction site. In some of the experiments the polymers produced are trapped in a cold and colorless condition, with the colors appearing only upon subsequent heating of the product itself. These conditions would clearly not apply to Jupiter. In another experiment the precursors of the polymer are unrealistically concentrated in a small reaction vessel subjected to electric arcs for several days. It is assumed that the colors so produced stem from a conjugated system of bonding, with delocalized electrons. Such a system of multiple double bonds is very liable to attack by hydrogen. Under the comparatively high hydrogen pressure and moderate temperatures in the deeper Jovian atmosphere, it is difficult to see how any polymer could have anything but a fleeting existence. The laboratory reactions also gave rise to various unsaturated carbon compounds: benzene, ethylene, and acetylene. Since the latter two are gaseous, they should be detectable in the Jovian atmosphere, yet have not been found. Not until any carbon compound besides methane is discovered on Jupiter, can Jupiter cloud colors be so explained.

The Fischer-Tropsch synthesis has also been invoked to explain certain hydrocarbons and other more complex reactions in the solar system, particularly in meteorites (Studier *et al.*, 1968). The process involves reacting carbon monoxide and hydrogen:

$$nCO + (2n+1)H_2 \rightarrow C_nH_{2n+2} + nH_2O$$
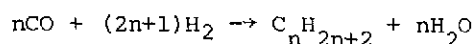
at temperatures of 450-650°K, over suitable catalysts of iron oxide, cobalt and nickel, to produce aliphatic hydrocarbons and water. Since the reaction will not

occur in the presence of a large abundance of hydrogen (methane is then produced),
and since metal and metal oxide catalysts are required, it is impossible to envi-
sage circumstances on Jupiter that would lead to the products of complex hydro-
carbons by the Fischer-Tropsch synthesis. The two preceding paragraphs were pre-
pared by Fr. Sill. It may be added that the photolysis of H_2 will favor an effec-
tive restoration of CH_4 and NH_3 from more complex compounds (Cadle, 1962).

c. *Periods of Rotation* - The observations of radio bursts in the 20-Mc fre-
quency range, now available for 20 years (1951-1971), give a *constant period of
rotation* for the radio sources, $9^h55^m29^s75 \pm 0.04^s$ (Carr, 1971; Duncan, 1971),
not counting an 11.9 year oscillation attributed to the variation of the Jovi-
centric declination of the Earth (Carr *et al.*, 1970). We may therefore reasonably
assume to know the *period of the solid Jupiter surface* (or stagnant liquid), at the
value just quoted; and that this period is *constant*, not wandering, e.g., as the
period of the Red Spot. Since the upper molecular layer of the planet cannot,
through magnetic forces, be responsible for 20-Mc radio bursts or the general
magnetic field (Smoluchowski, 1971),we assume tentatively that they are caused in
the Jupiter ionosphere (which explains their frequency range). In order that iono-
spheric bursts can be caused by events on the solid surface, a propagation mechanism
must be postulated. The problem has some similarity with the production of shock
waves near the solar photosphere (Ulmschneider, 1970, 1971), invoked as the heating
mechanism of the solar chromosphere and corona. The propagation of acoustic waves
over many scale heights presents problems; possibly turbulent energy is involved
instead. Gallet (1961) advocated this type of explanation, though he expressed
reservation about "volcanic activity" on Jupiter. If the gas vents are few in
number, they will not appreciably affect the total heat flux of the planet through
the solid surface.* We return to the reality of the gas vents in Sec. 5.

Satellite observations of the Earth (e.g., Cortright, 1968, Sec. I) show its
atmospheric circulation system to be very different from that of Jupiter, both
judged by the cloud-mass distribution. The enormous weather systems in the middle
latitudes are absent on Jupiter. Instead, a rather orderly system of belts and
zones is observed. The Earth receives its energy from the Sun; its axis is tilted
$23°5$; and there is a large transportation of heat in latitude by ocean currents.
Land, mountains, and water make for complex atmospheric circulation and precipi-
tation. The Jupiter atmosphere receives most of its energy from below; day-to-
night changes will be minor. The tilt of its axis on its orbit is 3°. The Jupiter
atmosphere is far deeper and denser than that of the Earth. The principal gases
producing clouds and "weather" will be water vapor and ammonia (interacting with
H_2S). Thus, the entire lower and denser atmosphere is likely to contain no "weather"
at all; only the upper 60-80 km or so, with the water condensation in the lower
parts, having ammonia in solution; and ammonia condensation in the upper parts.
Most likely, the near-adiabatic gradient caused by the weather zone will not con-
tinue downward, because radiative transport (through the 4.5-5.5μ window) probably

---

*
On the Earth the entire outward heat flow is 10^{13} cal/sec, the heat brought to
the surface by volcanism only 2×10^{10} cal/sec, or 0.2% (Coulomb and Jobert,
1963). The rest occurs by conduction at least through the outer layers. The
terrestrial flux thus amounts to 10^2 ergs/cm^2 sec, 1% of the Jupiter flux. Since
the Earth-like mass within Jupiter is probably about 10x Earth and since the sur-
face area of the planet is more than 10^2 times larger, the terrestrial processes
operating on Jupiter (radio-activity, etc.) can contribute only 10^{-3} of the Jupiter
heat flux. Thus, this flux is basically gravitational in origin. Cf. also Bishop
and de Marcus (1970).

suffices at the higher temperatures. The lower atmosphere may be nearly stagnant.
Solidification of hydrogen may then occur at moderate depths. A stagnant lower
atmosphere is favored by the periods of rotation of the surface layers, which appear
associated with that of the solid surface, 9^h55^m5. If a column near the equator
could rise vertically 120 km without friction, its period of rotation would in-
crease 60 sec.

Figures 1a-e show two high zones at 22°N and 22°S of variable width and in-
tensity, especially prominent in 1970 and 1971; and the Equatorial Zone, of
variable height and width. The 22° zones are identified as the *North and South
Tropical Zones* (cf. Fig. 2). The South Tropical Zone contains the *Red Spot* which
is even more prominent (i.e., higher) than the Zone itself (the high intensity is
not an albedo anomaly as was verified by photography at nearby wavelengths). The
22° Zones may heuristically be compared with the (double) Tropical Convergence on
the Earth, the only cloud belts that are systematically EW, at 6°-10°N. and S.,
and also the highest. The Trade Winds move toward the Tropical Convergence, from
the northeast and southeast in the two hemispheres. The moisture-laden air rises
in the Convergence, forms EW series of thunderstorms there, showing tremendous
anvils which break off and form cirrus in the upper troposphere, where the flow
returns poleward, in the opposite sense to the incoming Trade Winds at low level.
(As one who has observed Mars and Venus from the NASA CV-990 aircraft South of
Hawaii, I am only too well familiar with this return flow).

4.   The Nature of the Red Spot

a.   Comparisons with Earth – Among the most informative presentations of the
terrestrial Tropical Convergence Zones are the half-monthly and full-monthly photo-
graphic averages of the NASA-ATS records composited by the Department of Meteoro-
logy at the University of Wisconsin in Prof. V. Suomi's institute. The results for
1967 have been published by Kornfield and Hasler (1969). The Tropical Convergence
Zone is prominent over the vast Pacific and the narrower Atlantic. The asymmetry
of land vs. water for the Indian Ocean area appears to destroy the regularity of
the pattern there, as do the land masses of America and Australasia. Through the
courtesy of Dr. Suomi's group, we are able to reproduce in Figure 7a-d, the 120°
Pacific arcs (90°W to 150°E) of the four *seasonal averages*, typified by January,
March, June, and September 1967. In addition, Figures 8a -ƒ reproduce six *half-
monthly averages*, in Spring and Fall. The North American west coast is recognized,
as is the Gulf of California (114°W, 30°N). Hawaii is seen as a small cloud mass
(155°W, 20°N). Remarkably "clear" skies appear to prevail near Canton and Jarvis
Islands, 172° and 160°W, near the equator. (Canton Island was briefly explored in
1957 by L. Salanave as part of the AURA site survey, included on the basis of favo-
rable weather reports and the assumption that good day-time seeing is to be expected
on sites surrounded by water).

The North Tropical Convergence is well-marked and regular in these averages,
centered at about 6°N (with little seasonal variation; this appears due to the great
thermal inertia of the ocean). The South Tropical Convergence is weaker and broken,
with a latitude separation from the North Tropical Convergence of about 12°. More
prominent is a broad cloud belt from New Guinea ESE-ward through the Solomon Is-
lands, the New Hebrides, and the Fiji Islands (the two bright masses), constrained
by local topography and ocean currents.

On *individual* satellite records the Tropical Convergence Zone is usually
broken up into "cloud clusters". Such records are available in large numbers,
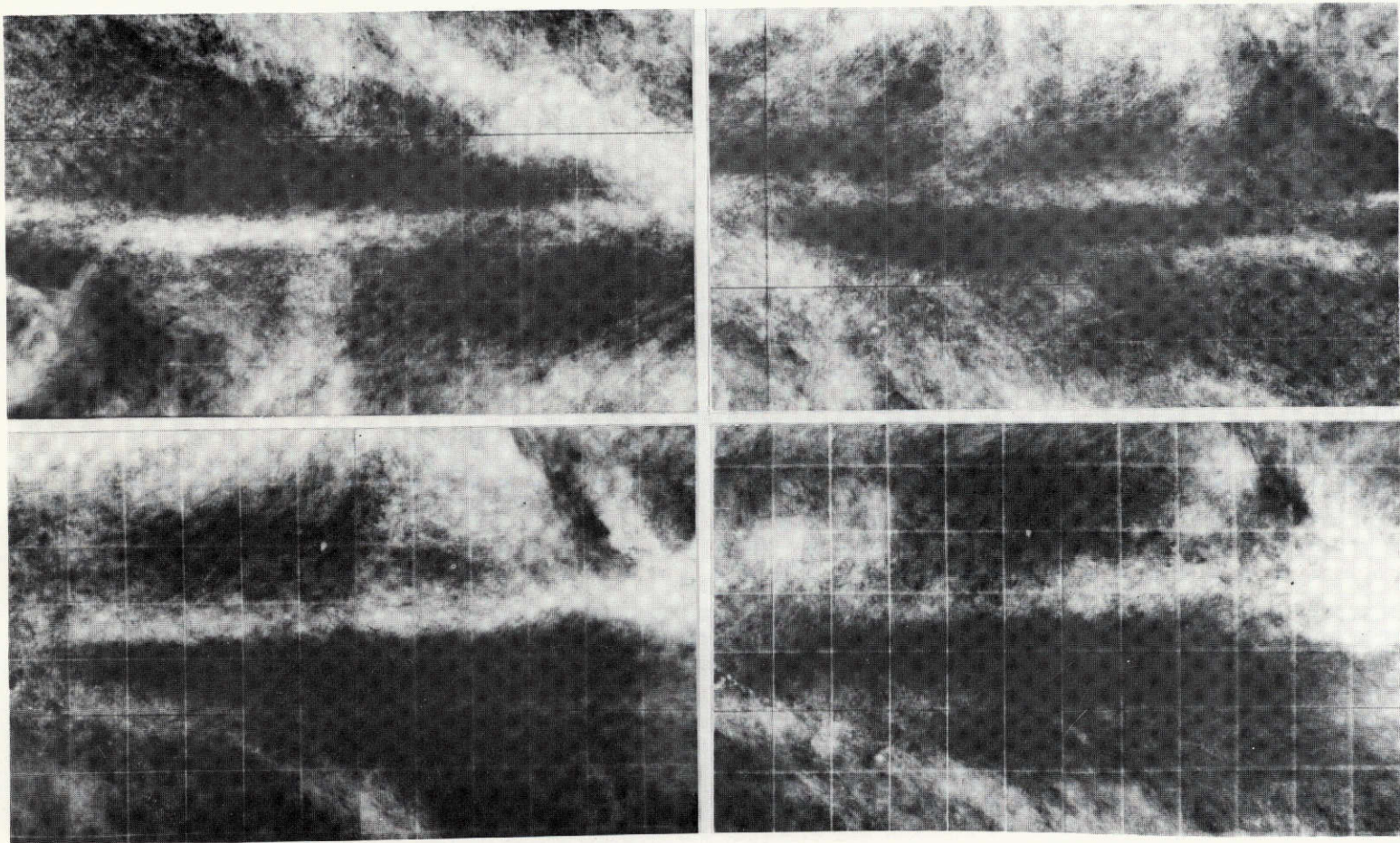
Fig. 7 Monthly averages of cloud cover over tropical Pacific (90°W to 150°E, 30°S to 40°N), Jan, Mar, Jun, Sept 1967 (courtesy Prof. V. Suomi)
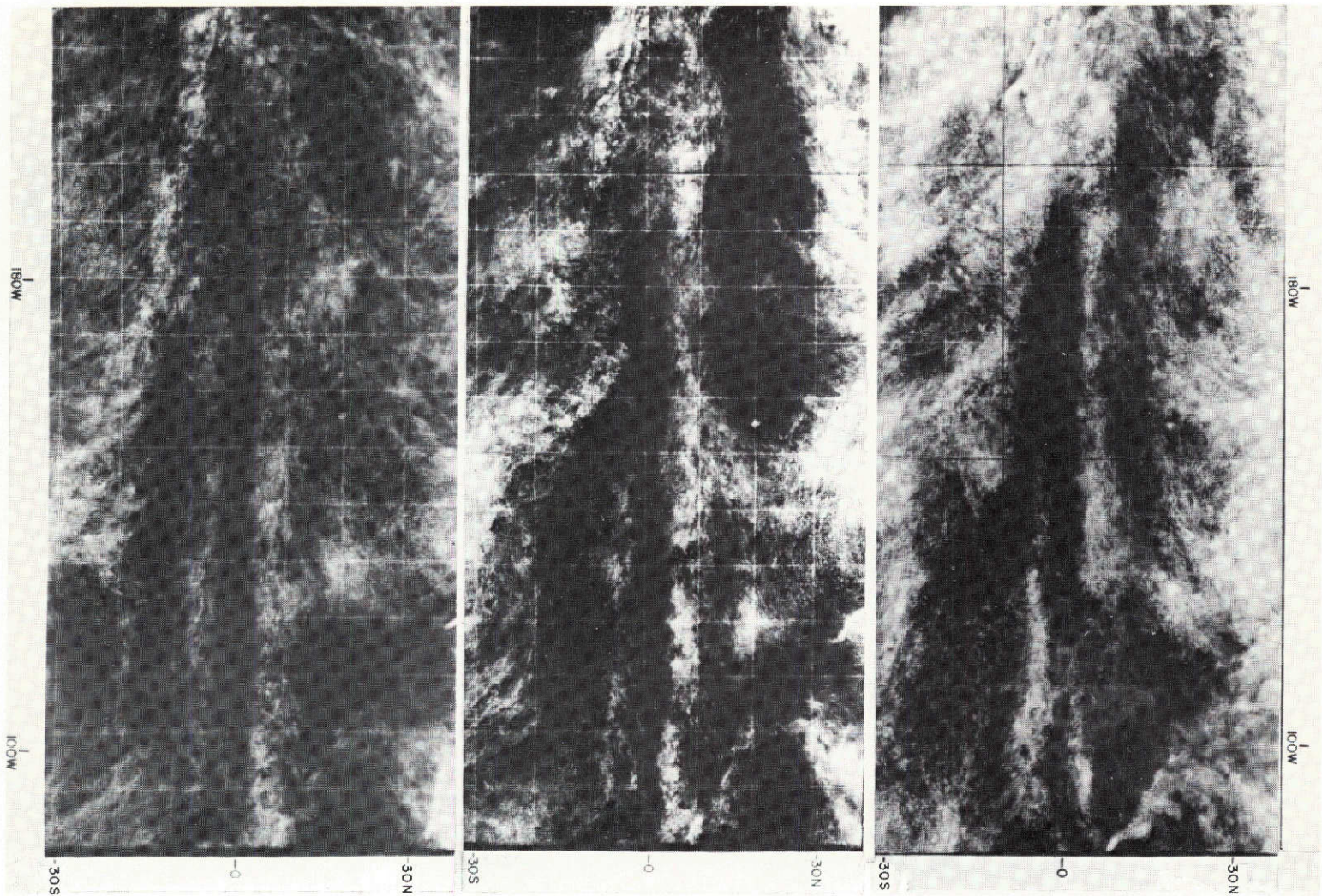
Fig. 8 Half-monthly averages of ATS photographs of tropical Pacific (80°W to 130°E, 30°S to 40°N): *a*. Mar 1 -15; *b*. Apr 16-30; *c*. May 1-15, 1967
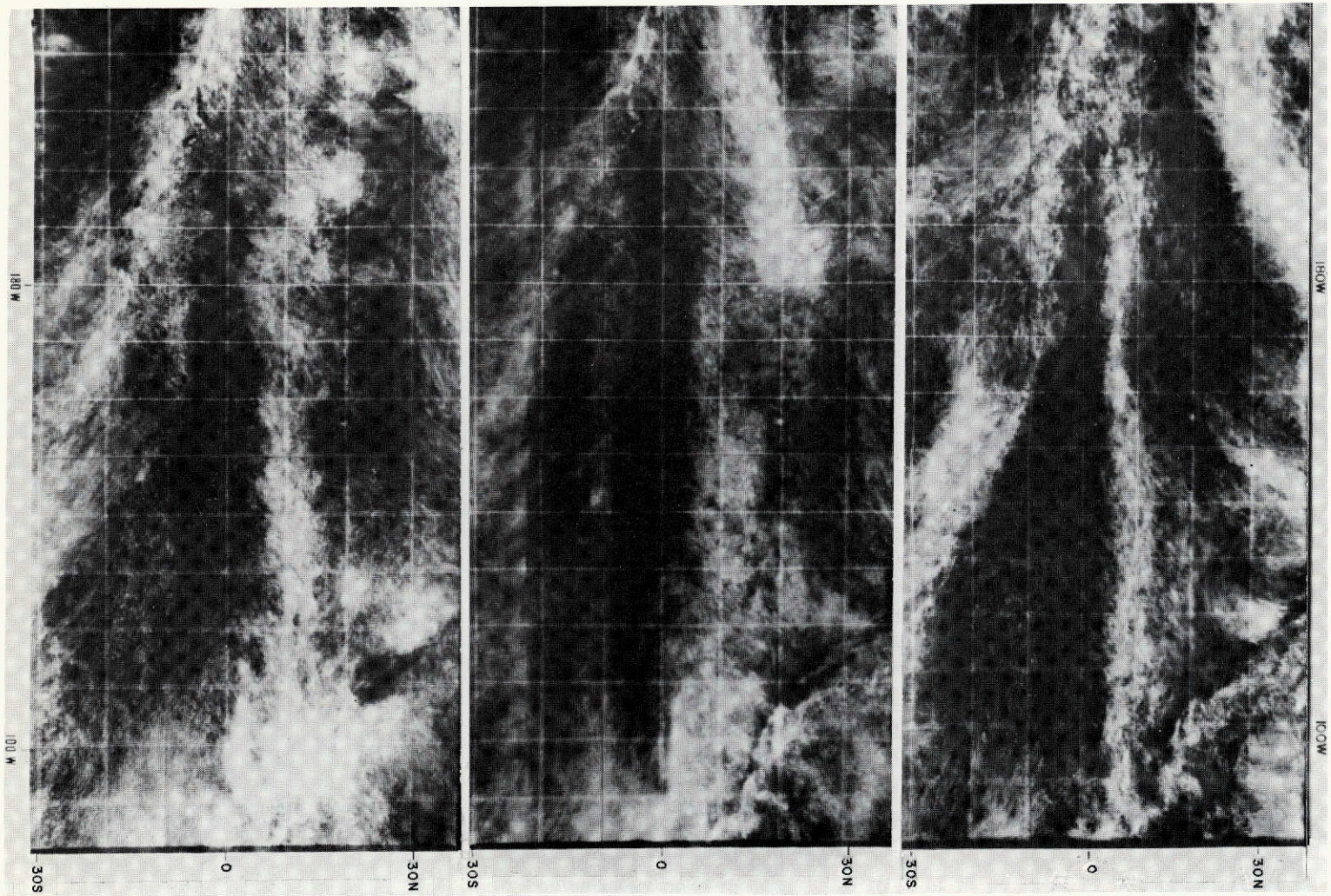
Fig. 8 (cont.) *d.* May 16-31; *e.* Sept 1-15; *f.* Sept 16-30, 1967 (courtesy Prof. V. Suomi)

starting 1967, from the beautiful reproductions in the 5-volume Catalogue of the ATS Meteorological Data. Some are readily available through the article by A. W. Johnson (1969). In Figure 9 we reproduce two representative records, centered on the equatorial Pacific (the Gulf of California is seen at the upper right). These records may be compared with Jupiter photographs. There is a striking contrast especially at the middle and high latitudes where the Earth shows powerful transzonal, often cyclonic, flow patterns.

It is of great interest that the "cloud clusters" in the Tropical Convergence Zones have, on the whole, a systematic Westward motion. Figure 10α shows a compilation of ESSA-5 records of the 5°-10°N Pacific zone published by Chang (1970) for 45 consecutive days, July 1-August 14, 1967. The clusters clearly have a tendency to propagate westward (phase velocity 9 m/sec) and often survive as organized masses across the entire Pacific. Chang's composite for the adjacent latitude belt, 10°-15°N, is similar in appearance and yields the same 9 m/sec systematic motion. The cloud centers are marked by heavy precipitation, strong ascent at middle levels, and strong upper-level divergence. The clusters represent concentrations of cyclonic vorticity at low levels and anticyclonic vorticity at 200 mb (Holten *et al.*, 1971). This is due to the strong divergence near the tops of the anvils, causing the upper flow-pattern to resemble that of a barometric high at ground level. Chang's studies were extended to all tropical longitudes and latitudes 20°N-20°S, in 5° strips, by Wallace (1970), for the entire year, Dec. 1966-Nov. 1967. We reproduce in Figure 10b one of the many Wallace composites covering the period June 1-Aug. 31, 1967, 0-5°N (thus adjacent to Figure 10α but extended for all longitudes). Figure 10b shows that some cloud masses may be traced from about 10°E Westward nearly around the globe, to 70° or 80°E or less, with a nearly-constant phase velocity. Wallace (1971, p. 594) published also a time-longitude section of cloud brightness at 10°N based on averages for 5° x 5° squares, for July 1-Oct. 1967, both for unsmoothed and longitudinally-smoothed values. He concludes (p. 595):

"1. There is a high degree of organization in the brightness pattern at this latitude, the major fluctuations being associated with long-lived synoptic-scale systems that propagate westward.
"2. Many of these systems retain their identity over a period of weeks, as they pass from one ocean to another.
"3. The phase speeds of these systems range from 5 to 10° of longitude per day. For a frequency of 0.2 cpd this corresponds to a range of wavelengths between 2500 and 5000 km."

Wallace remained uncertain about the cause of the Westward wave of tropical storms (Wallace, 1971, p. 600, 603 ff).

Holton (1971) states:

"Several studies indicate beyond reasonable doubt that westward propagating synoptic disturbances do exist in the tropical Pacific and that much of the precipitation in that area is associated with the cloud clusters which are embedded within these waves. At the same time it should be said that the observed average amplitude, period and wavelength of these disturbances vary from year to year, and that the structure of the disturbances also depends on the season and longitude. The range of periods reported in the above spectral studies is ~4-7 days while the reported zonal wavelengths range from 2000-10,000 km.
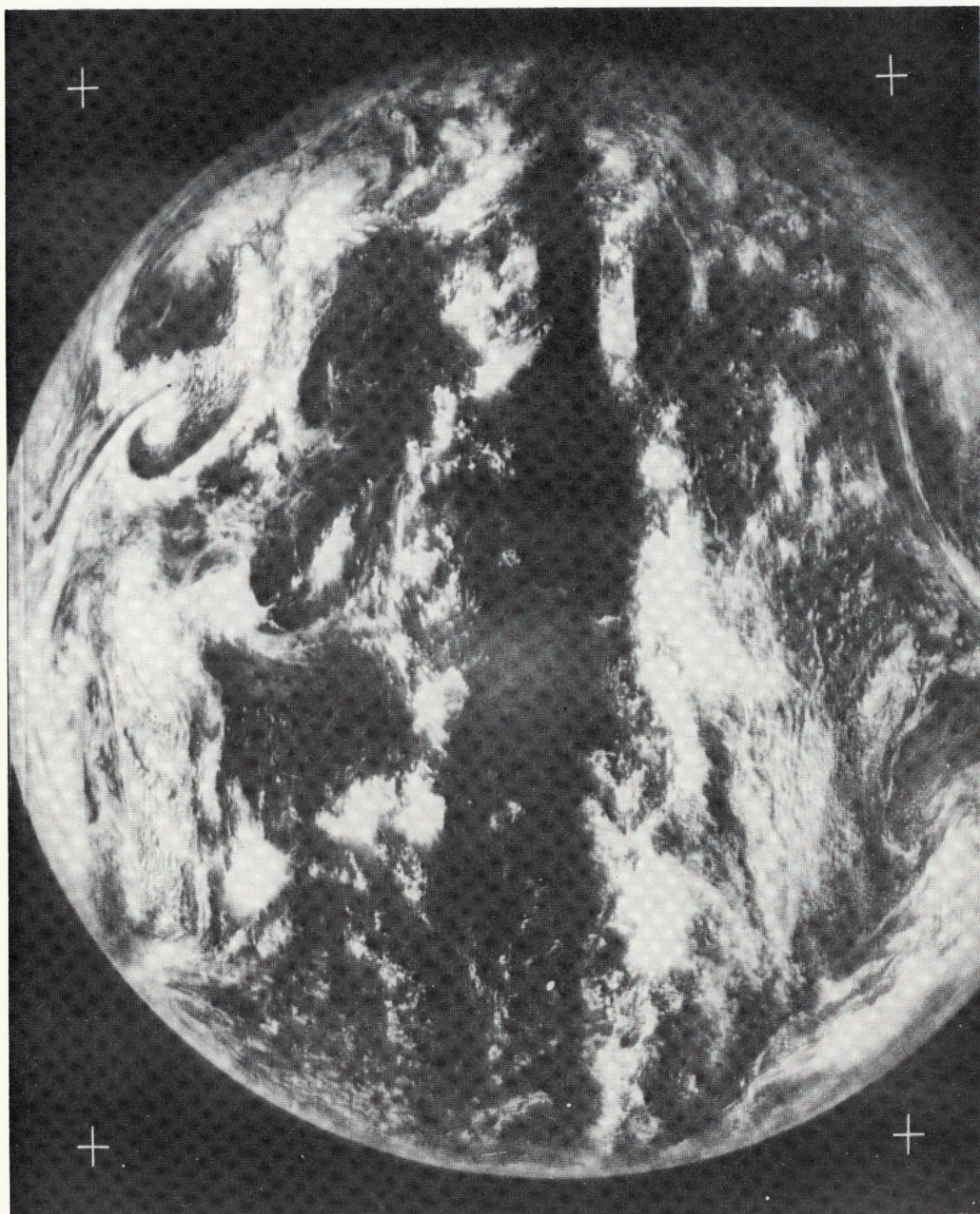
Fig. 9　The North and South Tropical Convergence zones across the Pacific
a. ATS-1　19 Feb 1969　$21^h21^m44^s$ GMT

Fig. 9 (cont.) b. ATS - 1 18 Mar 1969 $21^h45^m06^s$ GMT

"This wide range in zonal wavelengths is apparently due to the exis-
tence of two types of wave modes (Chang *et al.*, 1970). The first type
with wavelength range of 6000-10,000 km has its maximum amplitude in the
upper troposphere. The axes of waves of this mode generally have substantial
tilt with height. Nitta (1970) has suggested that this mode is the mixed
Rossby-gravity mode first observed in the stratospheric data by Yanai and
Maruyama (1966). This mode has been discussed theoretically by Lindzen and
Matsuno (1968). The second type of wave mode with a wavelength range of
2000-5000 km is most prominent in the lower troposphere at the western
Pacific stations. Holton (1970) has shown that this latter mode may be
theoretically interpreted as a forced equatorial Rossby wave.

"In summary, the observational evidence proves the existence of west-
ward propagating wave disturbances in the equatorial Pacific; however, a
number of questions remain concerning their origin, maintenance and structure".

An earlier study by Williams (1970),based on 1257 individual satellite-
observed cloud clusters just N. of the equator in the W. Pacific, appears to
lead to distinct empirical answers. Williams attributes the Westward drift
simply to the Trade Wind; but he does not review the compound wave-like periodi-
cities in longitude. His cloud clusters are mostly located between 4° and 10°N,
with some reaching 20°N and a few beyond. Since Williams' observations and de-
ductions have a clear relevance to future studies of the Red Spot and the White
Ovals of Jupiter, we quote his statements on the Dynamical Properties of the 1257
observed clusters (note that an Easterly wind or current moves Westward):

"Wind Field at Cloud Center

The typical trade wind cluster is embedded entirely in an easterly
current which extends through the depth of the troposphere. The zonal
wind is strongest in the lower layers, averaging 10 kts. At 200 mb,
the zonal flow is typically easterly but considerably weaker than the
low-level flow. This is primarily due to the variability of easterly
and westerly winds in the upper troposphere above the lower-level steady
trade winds. The meridional wind is observed to be weak, less than 3
kts, at all levels. The horizonal shears of the zonal wind primarily
determine the relative vorticity.

"Horizontal Shears and Relative Vorticity

In the low and middle troposphere, the trade flow is revealed to be
stronger north of the cloud center than to the south. These clusters
exist on the cyclonic shearing side of the trades. Table 1 shows values
of 950 mb shear of the zonal wind ($\Delta v/\Delta y$) from 4° north of the cluster
to 4° south. For the clusters, this shear averages about 10 kts. The
v shear taken east-west ($\Delta v/\Delta x$) is also cyclonic but very much weaker.

"To determine whether clusters are associated with easterly waves,
streamline analyses at several low tropospheric levels were made. Up-
wind from the clusters, the wind direction averages about 110°; downwind,
about 85°. There is indeed a weak amplitude wave in the streamline pat-
terns, but there is little contribution by this curvature to the com-
puted values of relative vorticity. Fully 75% of the relative vorticity
is contributed by shears in the zonal flow, i.e., $-\Delta u/\Delta y$. These clusters
appear to be associated, therefore, with a weak wave typified not so much
by curvature but by cyclonic shear of the trade flow.

Fig. 10α Cloud records for the 5°-10°N Pacific
zone for 45 consecutive days, July 1-Aug 14, 1967,
based on ESSA-5 data (Chang 1970)
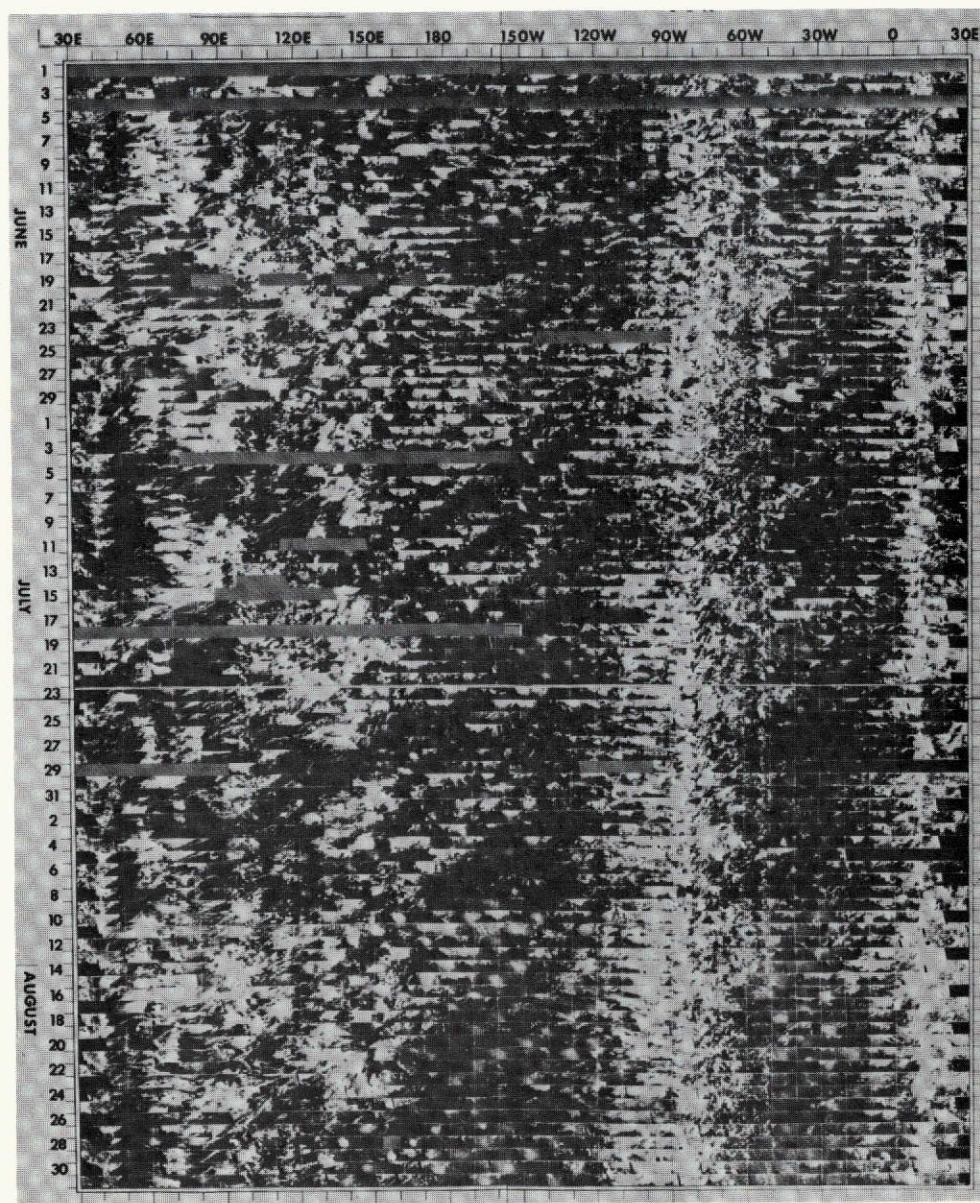
Fig. 10*b* Cloud records for period June 1-Aug 1967,
all longitudes, 0-5°N

"The relative vorticity profiles . . . are primarily determined by the horizontal wind shears. For most clusters, the relative vorticity is positive throughout the lower and middle troposphere. The pre-storm clusters possess by far the largest vorticity values; the non-conservative or developing-dying clusters, the smallest.

"It is thought that low-level horizontal shears are critically important to cloud cluster dynamics. Charney and Eliassen have proposed CISK (conditional instability of the second kind) as an instability mechanism by which mesoscale frictionally-forced convergence in the boundary layer in cooperation with the heating potential of cumulus convection combine to initiate development of tropical cyclones. This mechanism is viewed by the author as a plausible means of producing and maintaining tropical cloud clusters, some of which may later develop into tropical storms. Gray has previously shown a strong positive relationship between trade-wind cyclonic wind shear and disturbances which intensify into tropical storms. To maintain the cluster, low-level mass convergence and cumulus convection must be continually active.

"Divergence

Fig. A shows vertical profiles of divergence taken at the center of each cluster type. Convergence is typically maximum at cloud base and gradually decreases with height. A striking maximum of divergence is centered at 200 mb. This agrees very well with previous vertical divergence profiles determined from tropical storms.

"These vertical divergence profiles also show that the mass balance of a cloud cluster is achieved nicely by a two-layer model with inflow below 400 mb and outflow strongly concentrated from 250 to 150 mb (at 250 to 150 mb cumulonimbi updrafts rapidly lose their buoyancy). Because the surface pressure tendencies following a cloud cluster show very little change (<±2 mb per day), a rigid balance of the integrated divergence through the troposphere must take place. This requirement is obviously met. It should be noted that the inflow is by no means confined to the lowest layers. Middle-level convergence is probably the result of entrainment into the cumuli, which are developed by boundary-layer frictional convergence.

"These divergence profiles were obtained completely from the computer composites with no 'massaging' of the data. It was indeed surprising that these kinematic-determined divergence and vertical motion profiles should show such a remarkably close mass balance. This lends confidence to the other data computations.

"Moisture Convergence

A computation of moisture convergence for the conservative clusters reveals that although this convergence is a maximum in the lowest 100 mb layer, it is not confined to this layer. More than half the net moisture convergence into the cluster-centered 4°-square box occurs above 900 mb.

"A computation of P-E (where P = precipitation and E = evapo-
ration at the ground) was made from the advective term plus the
change in storage over 24 hours. The result is P-E = 2.0 cm/day,
with the advective term contributing more than 90%. If E is assumed
to be 0.5 cm/day, then the resulting 4°-square area-averaged preci-
pitation from a typical cloud cluster is 2.5 cm/day. Rainfall of
this magnitude requires the presence of cumulonimbi, and indeed the
bulk of the rainfall in this area comes from cumulonimbi which are
maintained by synoptic-scale cyclonic wind shears.

"Vertical Velocity

All cluster categories show maximum vertical motion at 400 to
300 mb. A typical vertical velocity (averaged over an area 4° on
a side) at this level is 170 mb/day or 3 cm/sec. The upward motion
becomes zero between 200 and 100 mb.

"Table 1. 950 mb horizontal shear in zonal wind (kts) taken over
a N-S distance of 8° latitude. A positive value denotes cyclonic shear.

	Pre-Storm	Devel-oping	Conser-vative	Dying	Dev.-Dying	All Clouds	Clear Areas
$\Delta u/\Delta y$	17.0	10.4	9.4	9.6	3.2	10.4	-6.8
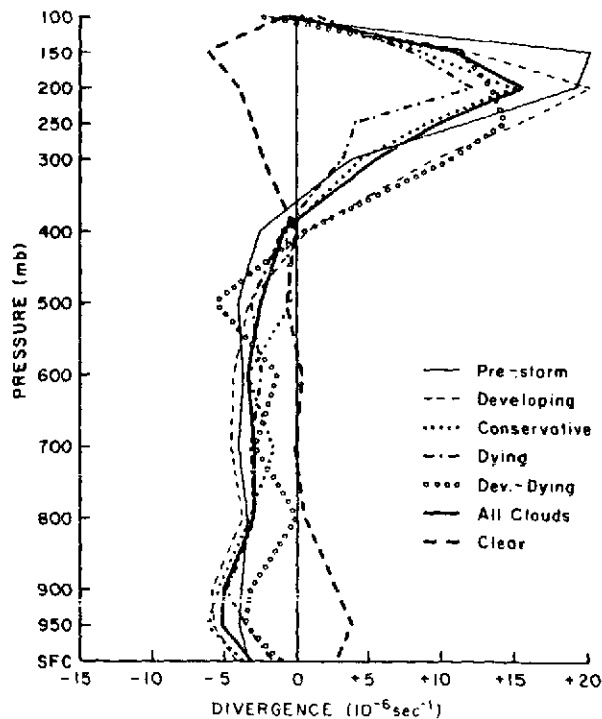
Fig. A. Vertical profiles of 4°-square area-average
divergence at cluster centers."

b. Red Spot Motions - The self-rotation of the visible Red Spot of Jupiter is also anticyclonic. This has been particularly well demonstrated by the recent observations of Reese and Smith (1968). *The Red Spot therefore behaves as a giant ascending column, flowing out at the observable level of the top.*

The westward motion within the Earth's North Tropical Convergence is due in part to the Trade Wind Easterlies feeding it but also to a propagation of cumulus column production; individual cumuli usually last only an hour or two. The average rate over the Atlantic is about 10 knots (5 m/sec) or 1% of the rotational velocity (Rosenthal, 1971); compared to the 9 m/sec for the Pacific (Chang, 1970). Chang notes that the Pacific storms (5°-10°N) pass a given longitude every four days or so (12 disturbances in 45 days). The "wavelengths" suggested by Figure 10 are of the order of 3000-6000 km, not unlike figures derived previously by other authors quoted by Chang. On Jupiter the two Tropical Zones rotate with periods that are surprisingly close to that of the solid surface, 1^S faster for the NTropZ, 6^S slower for the STropZ. The Red Spot, whose top is even somewhat higher than the STropZ, is 8^S slower on the average, or 2^S slower than the STropZ The period of the Red Spot has varied from $9^h55^m31^S$ or 32^S in 1831-32, 1872-73, and 1924, to $9^h55^m42^S$-44^S in 1891, 1896-1900, 1907±, 1937-40, 1943-48, etc. On the whole, the period was *short* 1831-1882, *long* 1882-1908, *short* 1908-1937, *long* 1937-1962, shorter thereafter. On the assumption that a longer period would at least in part be due to increased distance from the axis of planetary rotation, a relationship between *period* and *height*, and hence *color*, would be expected. This is indeed the case, as was noted by Peek (*op. cit.* p. 150), who found *maximum visibility* (dark color) associated with abrupt *lengthening* of the period. This important relation could be considered to confirm the concept of the *Red Spot as a rising column of variable activity.*

For a better grasp of the geometry of the Red Spot and the currents in which it is embedded, we show in Figure 11 the planet as seen from different latitudes. These photographs (unretouched) were produced by rephotographing a Jupiter image projected on a white-mat ellipsoid of proper oblateness produced by Mr. R. Turner.

c. Rotation of Jupiter's Belts and Zones - Poleward of each Jupiter Tropical Zone, one expects drops in the periods of rotation, caused by the "peeling off" of cirrus-like material flowing in the opposite sense to the invisible "Trade Winds" below. Movement from 22° to 24°, with conservation of rotational velocity, would shorten the rotational period by 9 min; this is the maximum effect since friction will decrease the amount. Actually, just south of the STropZ on the north edge of the South Temperate Belt, the average period of rotation is 2^m34^S shorter than in the Zone itself, with no major anomalies occurring farther South. The South Temperate Belt at -29° has $P = 9^h55^m20^S$, only a little below the surface value, indicating a slight poleward flow. From -31° to -45°, $P = 9^h55^m7^S$, indicating a slightly larger poleward flow; while South of -45° the period is precisely that of the surface, $9^h55^m30^S$, in accord with the near-absence of zonal structure in the polar region. Figure 12a is based on Peek's (1958) compilation. A more recent study, covering the period 1897-1966, is that of Chapman (1969). His composite Figure 3 resembles Figure 12a quite well except for S latitudes 15°-20° where a second positive peak occurred in the interval 1917-36. Chapman's composite for the five intervals studied by him (comprising 1, 1, 2, 2, 1 decades) is reproduced in Figure 12b for purposes of comparison. Clearly, *there is considerable variation in the Jupiter flow pattern* over the 70 years covered.

In the Northern hemisphere the picture is similar, though not identical. Northward of the North Tropical Zone again a major drop in the period occurs, the south edge of the North Temperate Belt (1°-2°N of the Zone), having an average period
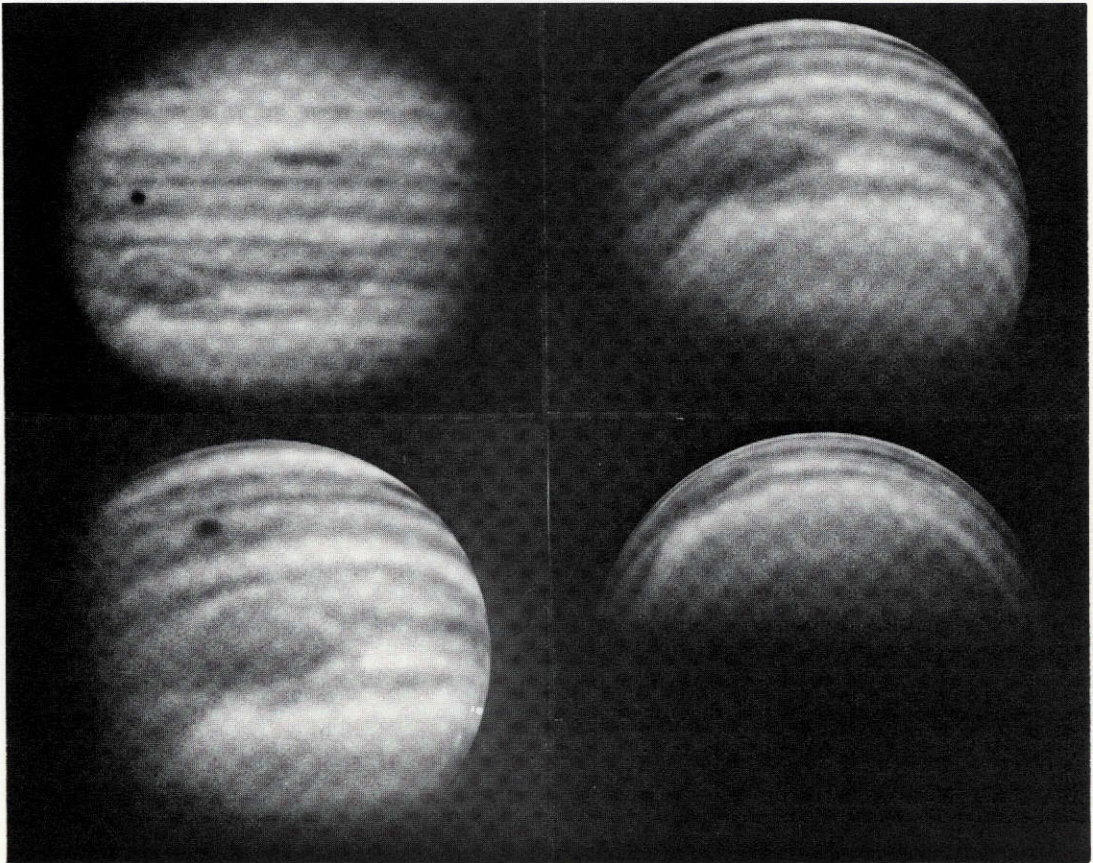
Fig. 11   Planet Jupiter with Red Spot, Zones and Belts,
shown from different latitudes
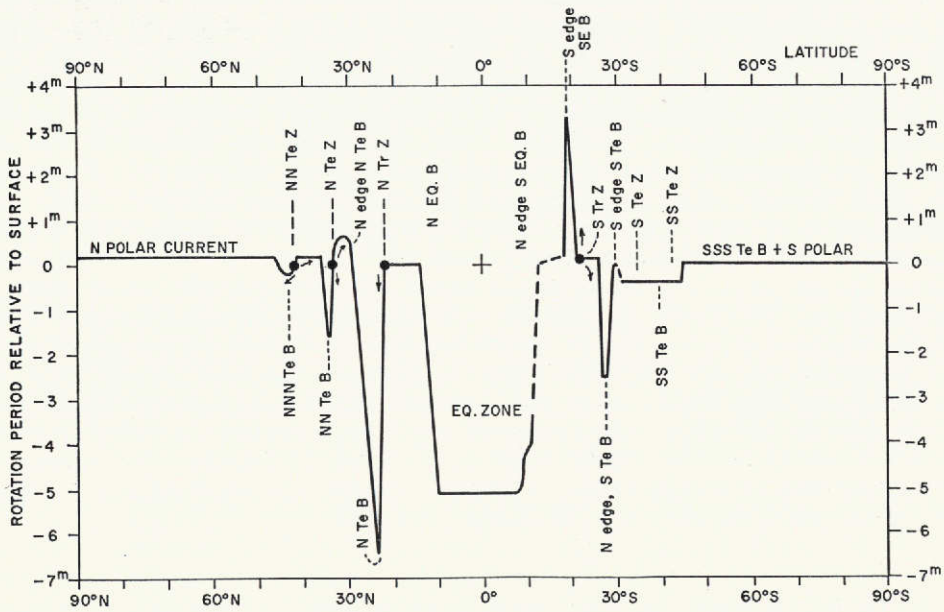
Fig. 12a Rotation periods of Jupiter Zones and Belts
(after Peek 1958)
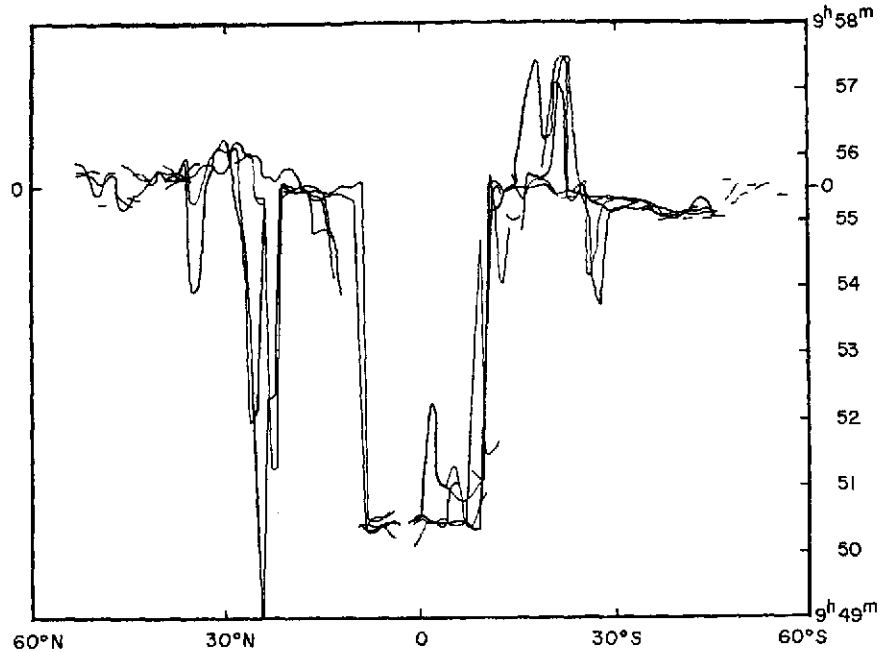
Fig. 12*b* Rotation periods of Jupiter Zones and Belts 1897-1966,
during 5 intervals (after Chapman 1969)

6^m22^s (6 apparitions) shorter than the Zone. At $+27°$, P has increased to
$9^h53^m17^s$ (N. Temp. Current B); at $+29°$ to $+33°$, to $9^h56^m5^s$ (N. Temp. Current A,
etc.). At $+35°$, $P = 9^h53^m55^s$; at $+36°-40°$, $9^h55^m42^s$; at $+43°$, $9^h55^m20^s$; and at
$47°-90°$, $9^h55^m42^s$. This pattern calls for a secondary "convergence" around 34°N
(between a high P value equatorward, a low P poleward). At least the 1970 records
show such a minor bright zone to exist (just above Io on Fig. 1*c*); it is the North
Temperate Zone. Poleward of 35°N no major transzonal currents appear to occur.
A minor Zone, the NN Temperature Zone, causes an expected ripple in the rotation
periods nearby. The fine structure on Figure 12 is somewhat variable, as shown by
Peek and Chapman.

The above description of the flow pattern accounts in a general way for the
rotational periods of the planet, with the exception of the Equatorial Zone. The
low period of this Zone,$9^h50^m24^s$, includes as well the two adjacent strips of the
neighboring Belts: the North Equatorial Belt ($9^h50^m24^s$) and the South Equatorial
Belt, North division ($9^h50^m26^s$). The total width of this rapid Zone is about 20°.
The higher atmosphere of the Earth presents an analogous phenomenon, though only
about half the time, when a 10 meter/sec Eastward current is found in the lower
stratosphere, around 50 millibars (20-km altitude). This means a period of rota-
tion 2% faster (12 min if it were Jupiter). Owen (then of LPL)and Staley (1963)
first called attention to this parallel; though admittedly the magnitudes of the
currents are very different. The significance of divergence above bright zones
as affecting the periods of rotation of adjacent strips was first discussed by Hess
and Panofsky (1951) based on studies at the Lowell Observatory. As to the Red Spot,
they considered it improbable that the variable period was due to variations in
solar radiation, though remarkably a correlation coefficient of 0.61 was derived
with the terrestrial zonal index.

d.   The Red Spot as a Region of Organized Cumulus Convection - Methane
photographs show the Red Spot to be the *highest cloud structure on the planet.*
This is the *opposite* of what a large suspended ice mass (see Appendix I) would
produce; it would impede the heat flow from below and cause the overlying cloud
cap to be lower than normal. On the contrary, the Red Spot must contain an
energy source, responsible for its exceptional height, its rising column, and *its*
outward flow on top (see above). Now, the thunderstorms along the Earth's Trop-
ical Convergence have these properties. The source is the latent heat of the
condensed water; they build up to the *full height* of the Tropical troposphere,
16-18 km, and produce enormous outflowing anvils near the tropopause so that,
when seen from above, they are about 100 times larger in area than the active
column nearer to sea level (cf. Fig. 13). If the height of the terrestrial
tropopause were not 2 scale heights, but 5-8, as for Jupiter, the vertical mag-
nification could be much greater.

Our tropical storms are among the long-lasting "severe storms" studied in-
tensively since World War II (*Meteor. Monogr.,* Vol. 5, No. 27, 1963). They are
also called "steady-state storms". The steady-state "giant thunderstorm is a
more highly organized phenomenon than its smaller air mass counterpart" (*op.cit.*
p. 33). *On Jupiter the steady-state storm is much more probable than on the Earth*:
(i) The thunderstorms over the Pacific lose the water they condense to the ocean
beneath; only a slow evaporation or transport of new moist air can keep the column
active. On Jupiter the water will fall into the hot lower atmosphere and promptly
evaporate. The "engine" can therefore go on indefinitely subject only to the
limitation of the heat flux; because, if the resulting upward flow of latent heat
exceeds that, the column will collapse. (ii) The absence of the day-night *variable*
heat supply to the lower atmosphere (which tends to limit the life time of terres-
trial thunderstorms). (iii) The stability of thunderstorms *increases with increas-
ing diameter* (Newton, 1963, p. 48).

On a scale larger than the individual cumulus cloud, the Convergence contains
"cloud clusters" (Figs. 9, 10). This empirical designation may be replaced by the
theoretical concept of *Regions of Organized Cumulus Convection,* signifying the
existence of a true physical association, not accidental proximity. This concept,
also called *collective, frictionally-controlled dynamics* (Ooyama, 1969, p. 4), was
theoretically developed during the last decade (Charney and Eliassen, 1964; Ooyama,
1969) and appears to offer a theoretical framework for an initial interpretation
also of the Red Spot and the White Ovals of Jupiter.

"Organized cumulus convection" involves a multitude of cumulus columns some
growing to full height and maturity, but each limited in duration (a few hours),
with new columns developing and old ones collapsing; all held together by a common
circulation system, often for several days. These are the *Tropical Cyclones,* called
Tropical Hurricanes after winds in excess of 75 mph develop. A typical cyclone
system will have a radius of 110-160 km for the array of active columns, while the
common cirrus cloud cover has a typical radius of 800 km (Dr. S. L. Rosenthal) or
some 6x that of the active array.

Ooyama's (1969) model study of tropical cyclones leads to the prediction of
an upper limit of the *Region of Organized Convection (op. cit.,* eq. 4.6):
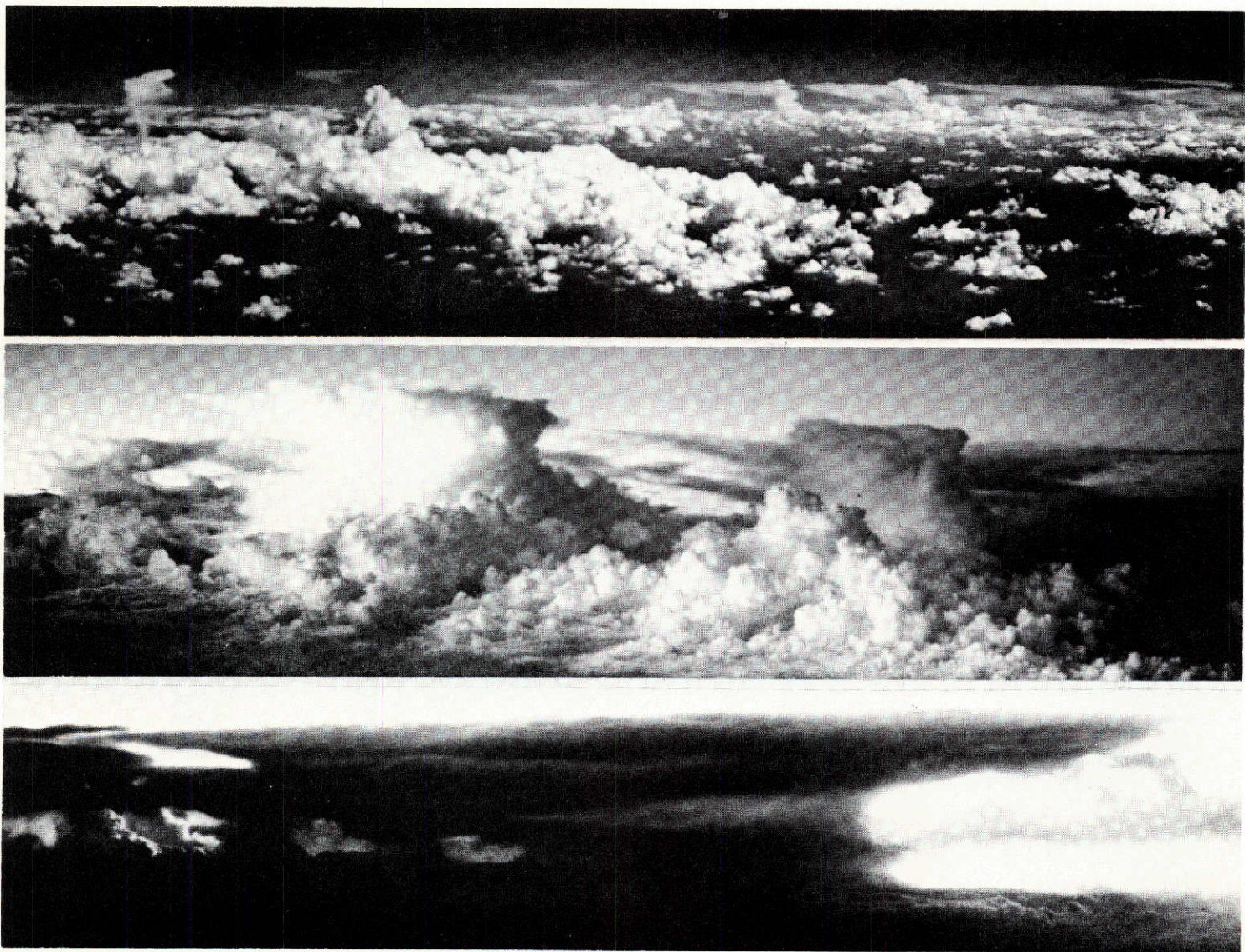
Fig. 13 Cumulus anvils: *a.* (Aug 2, 1968) from 100 miles N of San Francisco, looking toward Sierra Nevada (line of storms with anvils blown to N); *b.* anvils over Mt. Whitney area look-N (Aug 6, 1970); *c.* (Aug 15, 1970) over Atlantic
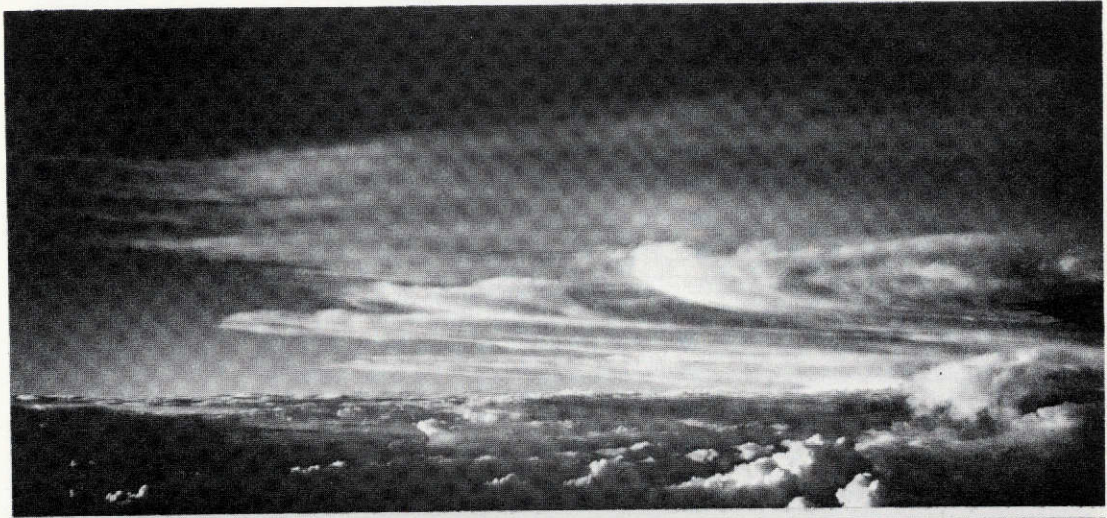
Fig. 13 (cont'd) *d*. and *e*.   (Aug 11, 1968) over Mt. Whitney
area, looking N, views beneath large anvil

$$R = (\sigma gh/2)^{\frac{1}{2}} f^{-1}, \qquad \ldots \ldots \qquad (1)$$

in which $\sigma = 1 - \rho_2/\rho_1$, $\rho_{1,2}$ the densities of the two atmospheric model layers; g the acceleration of gravity; h the mean thickness of the two layers; and f the Coriolis parameter ($2\Omega \sin \phi$; Ω is the angular velocity of rotation, ϕ the latitude). We may take $\phi = 22°$ for both Earth and Jupiter; then, with $g_J = 2.6g_E$, $f_J = 2.4f_E$; $\sigma_E \sim 1/2$, $\sigma_J \sim 0.9$, $h_J \sim 3h_E$, $R_J \sim 1.6 R_E$. Ooyama derives R_E to be about 1000 km; R_J would then be roughly 1600 km, or the diameter of the active column array 3200 km. If the diameter of the cirrus cover were indeed 6x that of active array (see above), it would be about 20,000 km, which is about that of the Red Spot. The White Ovals occur at 33.5° latitude and should therefore have an upper limit 0.68 of that of the Red Spot at 22°; the actual size ratio is somewhat less (the average Oval dimensions for 1970-71 were 13,400 by 8000 km - Reese). The theoretical framework needs refinement (more layers, etc.) but the Ooyama theory and the observed cirrus cap ratio of about 6, together, appear to account for the observed upper dimensions of the organized Jupiter cloud masses. High-latitude round or oval clouds should be no larger than about half the diameter of the White Ovals, which seems confirmed. Dr. S. L. Rosenthal points out that only order-of-magnitude representations could be expected from the present-day terrestrial models. The absence of long-lived oval clouds *close to the equator* indicates that Coriolis force is an active ingredient of the cloud dynamics elsewhere on the planet. Eq. (1) shows that there is no upper limit ($R = \infty$) to a storm system at the equator. Ooyama's theory also predicts the arresting effects due to friction on the growth of *small* disturbances, somewhat similar to the arresting effects on individual towers noted by Newton (1963).

Terrestrial cyclones or hurricanes usually move about; however, the cyclone motion is essentially that of *the air flow in which it is embedded.* Much meteorological discussion has centered on defining the "steering layer" responsible for the motion of the cyclone; typhoons may be entirely stationary for days, usually near latitudes 25°-30° (Riehl, 1951, p. 912). For Jupiter the zonal motion at the $T \cong 300°K$ level compared to the subsurface is expected to be small, so that the Red Spot columns would be nearly at rest. Also these columns, or "hot towers", will have *roots* unknown on Earth since the 300°K level is gaseous, not an ocean surface. These roots will further limit the migration of the Red Spot columns.

The terrestrial tropical hurricanes originate above the oceans at temperatures within 1°-2° of 27°C, or 300°K (Bergeron, 1954). The sensitivity of the hurricane life cycle to ocean temperature is explained by Ooyama's model studies (*op. cit.*, Sec. 13). Coincidentally, the $T \cong 300°K$ level can locally just be observed on Jupiter (Sec. 2a). Terrestrial tropical hurricanes produce up to 10^{22} ergs/sec (Dunn and Miller, 1960, p. 123; Dr. S. L. Rosenthal). With the heat flux of 10^4 ergs/cm² sec derived below, the heat transport through the Red Spot will be 10^{22}–10^{23} ergs/sec depending on whether the effective diameter of the heat supply area is about 10,000 or 35,000 km. (Cf. Sec. 4h).

It is expected that the Red Spot, a region of organized cumulus convection, will have associated with it *gravity waves* and *acoustic-gravity waves* that could possibly lead to observable phenomena. Dr. R. Krauss has informed me that for

the Earth gravity waves are seen emanating (as cloud waves) from storm centers, shown well on time-lapse photography based on ATS frames. If a single layer with depth h, caused, e.g., by a temperature inversion, ΔT, were responsible, the wave velocity would be given by $c^2 = (\Delta T/T)$ gh; and c might be $\geqslant$ 10 m/sec. However, a much more complex model may be required (cf. Dickinson, 1969).

    e. Confirmation of Red Spot Model - The model of the Red Spot, with a highly-active area some 3000 km in diameter beneath a thick cirrus cover some 6 times that size, makes understandable the remarkable properties of the several encounters of the South Tropical Disturbance with the Red Spot observed from 1902-1939 (Peek, 1958, Ch. 15). Peek describes the first of these as follows: "in June 1902 . . . its preceding end reached the following end of the Red Spot Hollow. . . . During the period of *at least six weeks*, which should have been required for the preceding end of the Disturbance to pass from one end of the Hollow to the other, and indeed during the whole of the conjunction *there was no sign whatever of any encroachment upon the region*; instead, within *a few days* of its arrival at the following end of the Hollow, a facsimile of the p. end of the Disturbance was seen by Molesworth to be forming at the other end of the Hollow, with the result that the Hollow itself, having become completely surrounded by the dusky shading, assumed the now familiar form of a light ellipse on a grey background, within which the Red Spot could be distinctly discerned . . . though it was very much fainter than the dusky region of the Disturbance. The new development at the p. end of the Hollow *proved to be a true p. end of the Disturbance* and it drew away from the Red Spot at approximately the same rate as that which it had shown when approaching it prior to conjunction. *Its rapid leap across the confines of the Red Spot* resulted in the addition of nearly the whole of the length of the Hollow to that of the Disturbance, which then totalled about 90°. The duration of this first conjuction was a little more than three months, the end occurring in 1902 September". Of the second encounter Peek (p. 139) writes: "We are led to the conclusion that its transference across the Hollow was practically instantaneous and similar to that which was observed in the case of the p.end in 1902". Of the third (p. 139): "Thus its passage through the longitudes occupied by the Red Spot region, which would have taken nearly *three months*, at its normal rate of progress, must have been accomplished in a matter of *fourteen days*". Of the ninth (p. 142): "At the beginning of the ninth the p. end of the Disturbance was seen to be appearing at the p.end of the Hollow within a few days of its arrival at the f. end!" - Apparently what is involved here, in the *arrest* before passage, the *leap* through the Red Spot, and the *slow departure* on the other side, are the visible ends of stream lines that would move much more uniformly some 50 km down, projected as shown in Figure 14. (During the nine close passages the Disturbance gradually slowed down and the Red Spot speeded up till the periods of rotation around the planet's axis became essentially equal, whereupon the Disturbance disintegrated). Peek's description may be interpreted as showing *EW asymmetry in the Red Spot*, with its array of towers left of center in Figure 14. (Asymmetric anvils are very common in terrestrial storms; cf. Fig. 13*a*).

    As noted above, the proposed model accounts in a general way also for the correlation between Red Spot's variable daily rotation period and its "visibility"; and for the observed anticyclonic surface rotation. The *numerical* aspects merit further study. A local barometric high will cause anticyclonic wind velocities, computed by balancing the outward pressure gradient with the inward Coriolis force (geostrophic approximation); or, one can add as a refinement the centrifugal force (the latter is often very important in cyclonic motion). In the Red
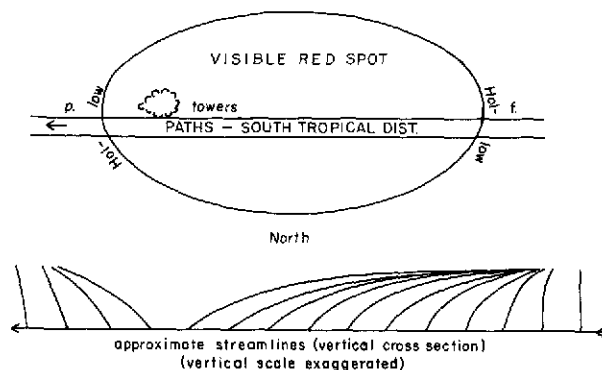
Fig. 14 Map of Red Spot with passing South Tropical Disturbance;
and vertical cross section showing typical stream lines at uniform
intervals along path of Disturbance

Spot model, however, the rate of ascent in the "hot towers" will set the rate of
outflow at the cirrus level. Thus, the horizontal pressure gradient is the re-
sult and not the cause of the wind flow. The rate of outflow will also determine
the frictional losses in the vorticity of the rising columns. If all vorticity
were lost, only the planetary rotational velocity (Coriolis effect) would remain
in the outflowing cirrus cover. This would spiral outward with a rotational
period $\sim P_J/\sin \phi$. Friction with the lower layers will lengthen this period. The
Red Spot model therefore will require an empirically-determined run of its rota-
tional motion with radius to establish both the remaining cyclonic vorticity at
the center and the frictional effects throughout. Ideally, this should be done
spectrographically along a meridian, with the Red Spot near the planet's limb -
a very difficult observation because of the sub-km velocities involved.

To make some estimate of these quantities, we assume that at $R = 6000$ km the
surface rotation period is 5 days. Then $v = 87$ m/sec; the Coriolis force $F = fv =
2v\Omega \sin \phi = 1.15$ dynes; the centrifugal force $v^2/R = 0.11$ dynes, or 10% of the
Coriolis force - rather typical of anticyclonic rotation. The radial pressure
gradient in the Spot must therefore balance $0.9F$:

$$\frac{dp}{dr} = -0.9\ F\rho; \quad \text{or} \quad \frac{1}{p}\frac{dp}{dr} = -0.9\frac{Fm}{RT} \simeq \frac{m}{RT} = 10^{-9.6}, \quad \ldots \quad (2)$$

where the mean molecular weight   is assumed to be 2.3, and $T = 120°K$. This means
that the fractional outward pressure drop would be only $10^{-9.6}$ per radial cm, or
1/5 or so for the entire inner half of the Spot. Because of the centrifugal force,
the velocity vector would deviate from the circular motion by 0.1 radian, so that
the outward velocity would be around 10 m/sec and the outward flow time for the
inner half around 8-10 days. For a *shorter period of rotation* v and F will in-
crease proportionally but v^2/R quadratically, so that the outward spiral of motion
is more open, and the pressure gradient larger (friction with the lower layers has
been neglected in these order-of-magnitude computations; its effect may be small
for a model such as shown in Fig. 14).

     The available data deal with small spots, blue or dark, seen to enter the
Red Spot from the borders of the STropZ, being swept through the Spot, then lost
or released. Figure 15 shows a bluish spot observed Jan 25, 1968, recorded dark
on red photographs. It will be described by Mr. S. M. Larson together with other
structural details observed in the Red Spot. The history of a series of five
spots which appeared Dec 1965-Feb 1967 was described by Reese and Smith (1968).
Spot A overtook the Red Spot, swung with it 1-1/2 periods of 9 days each. Spots
B and C were overtaken by the Red Spot; only a part of each participated in the
Red Spot motion for 1/2 period (P = 12 d). Spots D and E were also overtaken,
observed for 5 periods, of 12 days each. All motions were anticyclonic with res-
pect to the Red Spot center. Reese and Smith computed the anticyclonic velocities
to be 6100 km/day or 70 m/sec at the Red Spot rims North and South. This means a
total relative Doppler shift between the rims of 0.3 km/sec when the Spot is on
the limb for solar lines, and half that for the NH_3 and CH_4 lines. Conceivably,
the Red Spot itself might move faster (if the spots had roots extending below the
Red Spot cirrus cover).

     The interaction between the Red Spot and the South Tropical Disturbance, re-
ferred to above, was accompanied by period changes of the Red Spot itself, in the
sense that the periods of the two storm areas became more nearly equal. This *con-
firms the concept of both phenomena being atmospheric (meteorological) in nature.*
(A mountain or plateau would not be moved by a passing storm!).   According
to the record compiled by Peek (1958,Chapt. 15), the following stages can
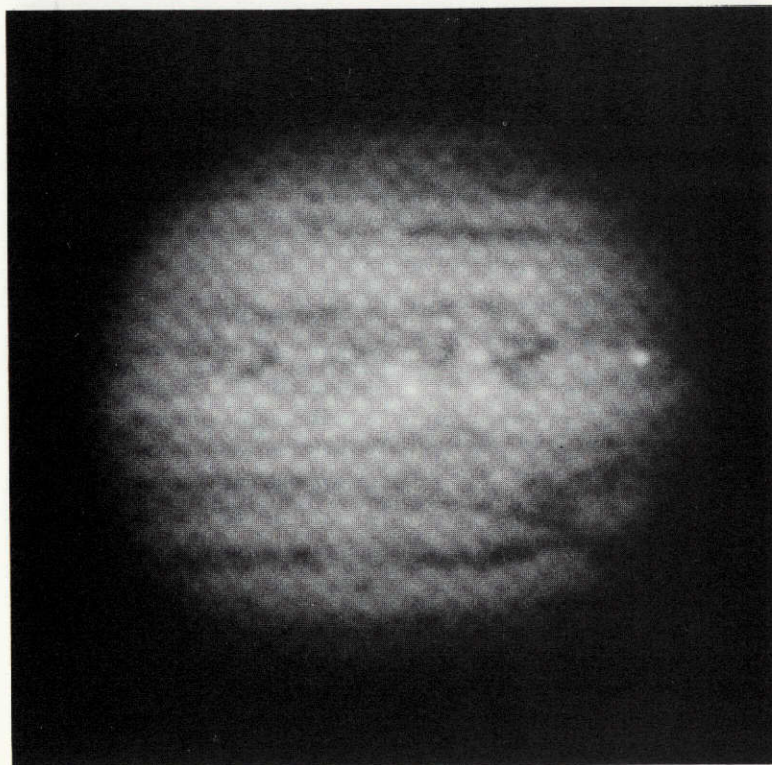
Fig. 15 Photograph of dark spot within con-
fines of Red Spot, 25 Jan 1968, $10^h01^m.3$ UT

be distinguished. The first four encounters occurred from 1901-1909. The Red
Spot was moving westward, the STropD moving eastward on the planet, with similar
speeds. The two storm areas just met and passed, each keeping its EW motion
essentially intact. During the next decade, comprising the 5th, 6th, and 7th
encounters, the Red Spot reduced its westward motion, the STropD reduced its
eastward motion which by the end of the decade had dropped to zero. During the
final two decades, 1920-39, encounters 8 and 9 occurred. The STropD was now
moving slowly westward, with its motion reaching equality with the westward
motion of the Red Spot toward the end of the period, while the Red Spot itself
still moved westward at the reduced speed of the 1910-1920 period. After the
1939 encounter the two storm areas apparently merged, whereupon the Red Spot
increased its westward motion on the planet. This timing suggests that *the
larger fluctuations in the westward motion of the Red Spot*,referred to in Sec.
4*b*,are also due to *meteorological effects*. These could be interactions with
smaller storm centers in the STropZ; or small shifts in latitude. The STropD
itself could have entered the Zone from slightly *lower latitudes*, explaining its
initial eastward motion and its eventual collision and merging with the Red Spot
tower area. Yet another meteorological effect on the Red Spot period would be
the *intensity* of the rising towers, as discussed in Sec. 4*b*.

   f. EW Asymmetry - The average daily period of rotation (around the planet's
axis) of the Red Spot is 8 sec longer than that of the denser layers beneath.
This could be viewed as due, at least in part, to the rapid rise of the columns
(cf. Sec. 4*b*); but, as in the terrestrial analogue, a true propagation of the Red
Spot along the STropZ must be involved as well. The columns will be topped with
a very extensive cirrus shield (the visible Red Spot). Since the shield has a
finite life time of possibly 40-60 days, as judged by the spots (cf. Sec 4*e*), due
to outflow at the center and subsidence or disintegration at the rim, the shield
is being continually renewed by the array of columns, and must therefore *appear
to move with the array*, though the *center of the Red Spot will be displaced* from
the center of the column array, as drawn schematically in Figure 14. A displace-
ment between the two centers is also suggested by Peek's account of the timing of
the jump of the STropD across the Red Spot (cf. Sec. 4*e*). Hopefully, other op-
portunities will occur to observe this type of passage.

   If it be assumed that the true daily rotation of the shield material itself
is 8 sec longer than that of the center of the Red Spot tower array, the displace-
ment may be computed. If T be the time taken by the Red Spot material to reach
the Spot's rim (and then be lost to view or be swept away horizontally), and the
8 sec excess be designated by ΔP, the displacement D will be:

$$D = \frac{\Delta P}{P} \cdot \frac{T}{P} \cdot 2 \pi R_J \cdot \cos \phi \quad \cdot \quad \cdot \quad \cdot \quad \cdot \quad \cdot \quad (3)$$

in which the factor following $\Delta P/P$ gives the total path travelled by the rotating
sub-surface during T. If $T \simeq 50$ days, $\Delta P \simeq 8$ sec, then $D \simeq 10,000$ km, the value
used in Figure 14. Clearly, these are merely plausible numbers.

   g. Propagation of Red Spot along Zone; Cycloidal Motions - If the Red Spot
period is indeed longer than that of the sub-surface in which the column array
is rooted (by 8 sec on the average, but by 1^S-14^S through the past century), then
the *array itself propagates along the STropZ*. The rate would be on the average of

2.5 meters/sec or 5 knots or 5 years for a complete 360° sweep. Such a motion
would be analogous to the movement of the organized cumulus convection centers
in the terrestrial Tropical Convergence (Figure 10). This motion along the
STropZ,does, however, not trigger the adjacent South Equatorial Belt disturbances
occurring every 5-10 years or so; because the longitudes of 10 major and 14 minor
disturbances are *not* correlated with the position of the Red Spot (Chapman and
Reese, 1968).

     The parallel with the terrestrial Tropical Cyclones may be further developed
by a comparative study of the *90-day oscillation of the Red Spot*, discovered by
Solberg (1968*a*, 1968*b*); and the cycloidal and looping motions of the terrestrial
centers. According to Dr. S. L. Rosenthal, the *cycloidal motions* have periods
around 12^h-24^h and are probably due to the internal structure of the vortex and
its interaction with the prevailing wind of the air mass in which the center is
embedded. The *looping motions* have periods of 1/2 day to several days; this effect
occurs in *stagnant air masses* and is due to the *vortex being asymmetrical*, provid-
ing thereby a steering effect through interactions with the ambient air mass. The
90-day oscillation on Jupiter has been traced back to 1963, and probably to 1946
by Solberg (1969); and carried forward to 1968 by Solberg (1969) and to the present
by Reese (1970, 1971*a*). Solberg (1969) found its semi-amplitude to average 0.8.
Figure 16 summarizes the New Mexico data on this important oscillation. (Figs 16*b*
and *c*, together with more recent material have been incorporated in a further
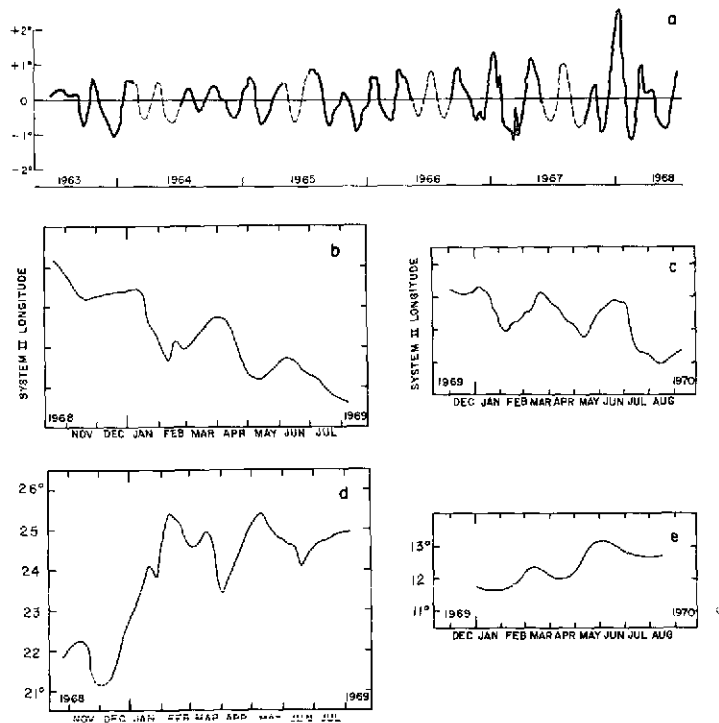
Fig. 16 The 90-day oscillation of Red Spot, based on New Mexico measures:
(a) oscillation in longitude after removal of secular drift (Solberg, 1969);
(b) same for 1968-1969 apparition, expressed in System II (Reese, 1970);
(c) as (b), for 1969-1970 (Reese, 1971*a*);   (d) length of Red Spot for 1968-
1969 (Reese, 1970); and (e) width of Red Spot, 1969-1970 (Reese, 1971*a*).
                    Vertical markers 1° apart

publication by Reese (1972), drawn on a scale similar to Fig. 16a). In addition, Solberg (1968b) suspected an 8-year oscillation of 10° amplitude since 1937, but after two cycles of 5-6 years no distinct period of this length has been found (Solberg, personal communication).

A 5-6 year period could be that of the complete sweep of the Red Spot along the STropZ. *The 90-day period is attributed to a rolling action of the asymmetrical vortex and a resultant displacement of the center.* The two periods involved, the hypothetical dimensions of the vortex area (Fig. 14), and the 1° amplitude, are consistent with this model. The trochoidal-type motion of terrestrial vortices was discussed by Yeh (1950, p. 110). Such a motion would probably be more enduring on Jupiter than on the Earth because of the near-absence on Jupiter of major trans-zonal disturbances; and the absence of oceans, continents, mountains, islands, and other local disturbances in the path. For the same reasons the Red Spot cirrus anvil may be a much more *regular structure* than the cirrus masses above terrestrial cyclones (some rather symmetrical cirrus caps are occasionally seen on photographs from terrestrial satellites). The 90-day oscillation would also be reflected in some measure in the *latitude* of the Red Spot and possibly its *dimensions*. The New Mexico measures indicate that such is the case, though not with complete regularity (Solberg, 1968a, Figs. 4-6; 1968b, Figs. 4, 6 and 7; Reese, 1970, Fig. 4; 1971a, Figs. 3, 4, and 5); and Figure 16.

The cycloidal paths of three terrestrial cyclones are shown in Figure 17. A summary of the first formation or detection of tropical cyclones for the period 1901-1963 and their paths is contained in the publication "Tropical Cyclones of the North Atlantic Ocean", Technical Report No. 55, U. S. Weather Bureau. While these data are of extraordinary interest in the context of this paper, the paths themselves have "been highly smoothed, being best-fit tracks, and hence the cycloidal motions are not discernible" (Rosenthal, personal communication). Case studies of eight cloud clusters of the Tropical Atlantic are presented by Martin and Suomi (1971). Evidently, these case histories are complicated by external factors such as atmospheric shearing or formation over Africa, South America, or the Island chains, with presumably no equivalents on Jupiter.

Comparison between Figures 16 and 17 may be confusing since the time scales in the abscissae in Figure 16 are arbitrary. In Figure 18 a plot of the longitudes is shown with respect to the solid surface (System III) of the same data of Figure 16c. The amplitude of the 90-day oscillation is now seen to be small in terms of the displacement of the Red Spot along the STropZ; in fact Figure 18 is not unlike Figure 17a.

On Jupiter not only the Red Spot shows *cyclic motions in longitude.*[*] Peek (1958, Ch. 19) deals with "The oscillating spots of 1940-41 and 1942". The periods are $P = 72^d$ and variable; the semi-amplitudes A both 5°; 24 and 31 observations. Solberg (1969) lists three other such spots, one of 1964-65, $P = 300^d$, $A = 4°$, 51 obs.; one of 1965-66, $P = 67^d$, $A = 1°$, 10 obs.; and 1967-68, $P = 66^d$, $A = 3°.4$, 20 obs. Further details of the last spot are given by Reese and Solberg (1969). Two additional such spots were observed since then (Solberg):

[*] Often spot positions are measured in longitude only since this is done more easily and since it defines the period of rotation.

GERARD P. KUIPER
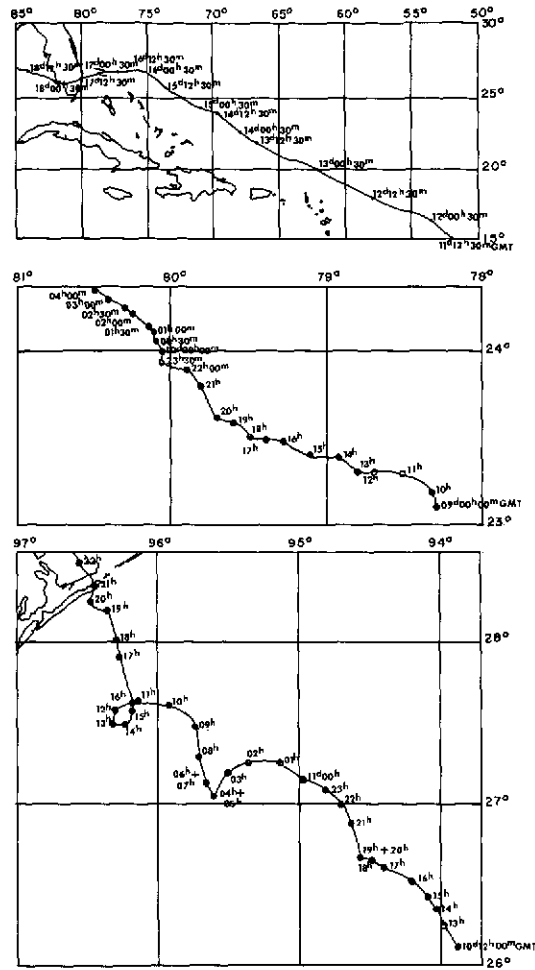
Fig. 17 Paths of three terrestrial cyclones: (a) Sept 11-20,
1957 (Yeh, 1950);   (b) Hurricane Donna, Sept 9-10, 1960; and
  (c) Hurricane Carla, Sept 10-12, 1961 (Neuman and Boyd, 1962)

Fig. 18 Longitude vs. time curve
for Red Spot, on System III;   same
data as in Fig. 16c. Shows ampli-
tude of 90-day oscillation to be
minor in scale of Red Spot dis-
    placement in STropZ
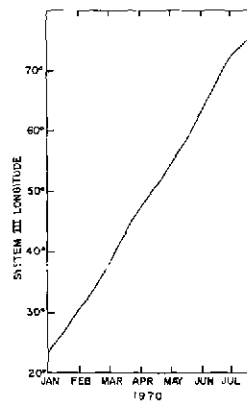
1968-69, $P = 75^d$, $A = 3°$, 18 obs.; 1969-70, $P = 64^d$, $A = 4°$, 9 obs. All but two of these spots were *dark* (the 1965-66, 1969-70 spots were *white*). The preference for cycles near 70 days is noteworthy. Probably numerous oscillating spots exist having still smaller amplitudes.

　　h. Life of Red Spot; Spin-off Cloud Masses - Another tentative conclusion may be drawn. If the Red Spot propagates along the STropZ in a cycle averaging 5 years (as indicated by the daily period of rotation around the planet's axis), this cycle may be due to the relaxation period discussed in Sec. 5: the *Red Spot triggers on its leading edge* the meteorological instability responsible for *the rapid growth of cumulus towers*. This type of propagation would not be uniform. It would explain why *the Red Spot motion is not precisely constant*; why there is only *one Red Spot in the Zone*; and why its period averages around $9^h55^m38^s$ (corresponding to a 5-year cycle, itself due to the meteorological relaxation period). The Red Spot, once having got into this resonance period, *could then continue to exist almost indefinitely*. Competing instabilities, set off "prematurely" before the next arrival of the Red Spot, may cause a STropD but they would necessarily be less effective in releasing latent heat, and could therefore be destroyed by the Red Spot during slow encounters. (The probability of an enduring large separation in longitude, given the inherent irregularities in motion for both storm centers, appears near zero).

　　The White Ovals move about $0°.8$/day faster than System II (Peek, p. 124) and thus have a period of about $9^h55^m10^s$, about the same as the STropZ in which they occur (Fig.12; 33°S). Since they have undergone such vast changes during the past 50 years, including a complete merging into a zone, it appears too early to speculate on their separate nature.

　　The latent heat released by the Red Spot must be less than that of the entire STropZ, since anticyclonic divergence has been observed over the entire zone (Fig. 12). The instability discussed in Sec. 5 must therefore pertain to one atmospheric layer only (perhaps the one between the H_2O and NH_3+H_2S condensation zones). This would require part of the planetary heat flux to continue to pass upward between successive passages of the Red Spot, presumably by radiative transfer. The total energy generated by the Red Spot could therefore be in excess of 10^{23} ergs/ sec (cf. Sec. 4*d*). It may also be necessary to reinterpret the observed relationship between the daily period of rotation (around the planetary axis) and visibility or color (Sec. 4*b*). *Strong color* correlated with *long period* would mean: more rapid advance of the Red Spot along the STropZ, thus increased release of latent heat per unit time, hence greater elevation.

　　At times the Red Spot produces long narrow clouds on its preceding edge (Pl. I*c*), well described by Reese (1970, p. 254). Since the Red Spot falls behind in its daily rotation with respect to the STropZ, the narrow cloud belts really are trailing in the westward motion of the Red Spot. The rate of separation is, however, much faster than corresponds to the 8 sec rotation difference and appears to stem from a slight poleward movement which brings the narrow belts into the S. rim of the STropZ (and the N. edge of the S. Temp. Belt), which tends toward the much more rapid rate of rotation shown in Figure 12*a*. Interestingly, on the best LPL blue photographs a fine line is also seen on the other (f) side of the Red Spot, stretching for 70°+ in longitude (Pl. I).   Conceivably, it stretches along the entire 360° arc; or else, it is located slightly closer to the equator (*P* longer, cf. Fig. 12), thus explaining how it also could stem from the Red Spot itself. These spin-off clouds are *brown* as is the envelope of the Red Spot (Pl. I); and dark in blue light.

The NTropZ, itself of variable brightness, has no Red Spot, but shows numerous smaller spots (Pl. I). The N. half of the Zone usually shows only *white* spots, sometimes brilliantly against the Zone. The Southern half shows dark spots and streaks, not unlike the adjacent North Equatorial Belt; the boundary between the Zone and the Belt varies considerably. Peek (pp. 95, 96) lists, for 47 annual apparitions of the planet, mean values of the daily rotation period derived from the measured spots, which numbered from 2 to 28 per year (13 years with 20 or more); the annual means run from $9^h55^m13^s$ to 41^s. Peek (p. 88) felt sure of one cloud mass having been identified for nearly 2 years, though he thought it likely that other such cases existed and he referred to two reported cases (with several spots present, identification across the annual observation gap is uncertain). Daytime observation in the near-infrared is indicated here. A narrow and faint grey line has at times been observed in the middle of the NTropZ (Peek, p. 83), apparently not unlike the line noted in the STropZ following the Red Spot. Nevertheless, some *asymmetry* between the two hemispheres is evident; cf. Sec. 6*c* and Pl. I.

i. Heat Balance in Jupiter Atmosphere - A convenient summary on the heat balance of the Earth's atmosphere is given by Byers (1954). One difference with the Earth will be the greatly increased greenhouse effect (H_2O, NH_3, H_2, as gases, plus condensation products), making for a much-reduced *net* outward thermal flux; but presumably a flux due to the hydrological *cycle* not greatly reduced compared to the Earth (the H_2O content is probably about 0.6%, the NH_3 content 0.2%, both by number (Lewis, 1969, Model B), not unlike our H_2O content). This will cause the transport by the latent heat flux to *dominate* in the Jupiter "weather zone". The latent heat flux will therefore be close to the *total* heat flux, which is readily computed from Dr. Low's effective temperature of the planet (with allowance for its solar radiation component): 10^4 ergs/cm^2 sec. (The predominance of the internal heat source over the absorbed solar flux is the *second* main difference with the heat balance of the Earth). Since 1 cm of precipitation requires a supply of latent heat of about 600 cal (depending on the temperature of the vapor) or $10^{10.4}$ ergs/cm^2, the average precip. rate will be about $10^{-6.4}$ cm/sec or 10^{-3} cm/hr. If the rain columns are 0.001 of the total surface area, the rainfall in the columns could be around 1 cm/hour (or more intense for smaller columns). The planet could therefore be covered with cumulus anvils 10^3 times the area of the precip. columns, on a more or less continuous basis, which appears meteorologically acceptable. The dominant internal heat flux will, of course, encourage a fairly complete *cloud cover.*

j. The Red Spot and Other Persistent Cloud Masses - In some respects the Red Spot is unique: its dimension, color, elevation above the general cloud level, and probably its longevity. Some representative LPL color photographs of the Red Spot and its Hollow are shown in Plate I.[*] At no time during the past six years was the Red Spot completely covered and white, though this has occurred around 1930 (Slipher, 1964, Plate 45, p. 91).

Among the regular, oval-shaped clouds, the three *White Ovals* follow the Red Spot in dimensions. Two are well shown on Plate I. Since their tops are lower than that of the Red Spot, they are more often obscured.

---

[*] Additional color reproductions are found on the covers of *Sky and Telescope,* May 1968 and Jan 1972; I*a* is the cover plate on M-30444 Columbia Masterworks, Mozart's Jupiter Symphony.

They appear to have been observed in the 1920's by Phillips (Fox, 1969); they merged as a zone in the 1930's (Peek, p. 123); were partly obscured again in the early 1960's, as reported by Fox; and again in part in 1968. At times the Ovals have dark borders, like the Red Spot, probably an outer edge in subsidence. In summary, there are strong parallels between the Red Spot and the White Ovals, though the latter are smaller, lower, whiter, and presumably have a shorter life time.

Still smaller cloud masses are seen on nearly all good Jupiter photographs, some of them resembling the White Ovals except for scale and life time. See Pl. I. Better definition than this record is obviously most desirable.

5. The SEB Major Eruptions; Atmospheric Instability

The year 1971 marked another major eruption in the South Equatorial Belt. This type of eruption was first observed in 1919-20, then 1928-29, and in great detail in 1943. The 1971 outbreak was spotted by Mr. Fox observing visually with our 61-inch telescope on June 21, 1971, as a small white cloud, and he at once recognized its significance. The outbreak was reported by Reese (1971*b*) and was found to have been first photographed by the NASA Planetary Patrol on June 18, 1971 (*Sky and Telescope*, Sept, 1971). A description of the LPL observations of the 1971 outbreak is given by Messrs. R. B. Minton and S. L. Larson in *LPL Comms. Nos. 178* and *179*).

In view of the absence of a correlation found by Chapman and Reese (1968) between the rotational periods of the SEB outbreaks and that of the Red Spot or the System III (solid-surface) rotation period, we examined whether purely meteorological processes could lead to a cyclic eruption process. Condensation in the water-vapor zone is expected to lead to a *temperature inversion* between the water and the NH_3, H_2S condensation layers, which, when gradually overcome by the heat flux build-up, could lead to almost explosive cumulus growth below the ammonia layer. Such an almost explosive growth following a period of stagnation is well-known in the terrestrial cumulus-formation process. Cf. Figure 13*a*, cloud in left margin, which is the first to break through the barrier layer.

Assume that the atmosphere on Jupiter *above* the level at which p = 5 atm -- at which the temperature is expected to be 290°K (Owen, 1969, Fig. 1)-- must on the average heat up 10°C to cause incipient instability. The atmospheric *mass* then corresponds to one that would cause p = 2 atm on the Earth, a mass equivalent of 20 meters of water. To heat this 10°C would take 2.10^4 cal/cm^2 or $10^{11.9}$ ergs/ cm^2. If hydrogen gas of the same mass is substituted for water, the needed energy will be $10^{12.45}$ ergs/cm^2; if the mean molecular weight is assumed to be 2.3, as deduced, the value becomes $10^{12.4}$. With the internal heat flux of Jupiter, this would take $10^{8.4}$ sec or 8 years to produce. Cyclic phenomena could therefore be produced by this process.

Since the above was written, Reese (1972) has re-examined the SEB outbreaks in a plot of time vs. the System III longitudes (based on the decametric radio rotation period of $9^h55^m30^s$). He now found that the outbreaks arranged themselves on *three* parallel lines, a possibility not examined by Chapman and Reese: (a) the three greatest disturbances ever observed, 1919, 1928, and 1971A; (b) five great disturbances (1943A, 1949, 1952, 1958, 1964), four of them with very active SEBZ branches; and (c) four secondary or less active disturbances (1943B, 1955, 1962,

1971B). Thus, *three discrete sources* appear to exist, defining the same rotation period, $9^h55^m30\overset{s}{.}11 \pm 0.03$. This is only $0\overset{s}{.}36$ longer than Carr's (1971) mean value for the decametric rotation period. In 1966.0 the longitudes in System III of the three SEB sources were about 50°, 225°, and 120°, respectively. By comparison, the much-more-frequently active 18 Mc radio sources A and B had λIII (reduced to $D_E = 0°$) of A ≃ 256° and B ≃ 145° (Carr *et al.*, 1970), some 25°-30° larger than SEB sources *b* and *c*. Clearly, the Reese (1972) results are of extraordinary importance; they suggest that *three vents exist in the Jupiter sub-surface* erupting with intervals of several years, with differing, but roughly repetitive, powers, *which trigger the enormous SEB outbreaks*. These eruptions will interact with the cyclic meteorological instabilities, described above, and together shape the intensity and extent of the observed disturbance. Another vent or at least a deep-seated storm center, nearly stationary in System III, is described by G. Solberg in *LPL Communication No. 180* and by R. B. Minton in *No. 182*.

The constant and equal rotation times derived from these vents indicate the presence of a *genuinely-solid crust* beneath the atmosphere. A supercritical fluid would not possess *fissures in fixed positions*, erupting every decade or so, with cycles not unlike, e.g., Mauna Loa. It further shows that the Red Spot, with all its motions described in Sec. 4, *could not possibly be related to any crustal feature*, which would have a constant rotation of $9^h55^m30^s$. Cf. also Appendix I, Sec. 2.

6. Other Topics

a. Planetary Cloud Patterns - The Earth's Tropical Convergence has a planetary cause and appearance (Figs. 6-9) in spite of the rather short life cycles of its component members - the cloud clusters or regions of Organized Cumulus Convection.

Likewise, the Jupiter Belts and Zones have persisted over at least a century, in spite of frequent major upheavals, which has made it appropriate to give them *names*. A separate discussion will be published on the Belts and Zones based on the LPL color photography and spectrophotometry.

b. Limb Brightening in the UV - Mr. J. Fountain photographed Jupiter with 37 narrow-band filters (λ/Δλ = 30) from 3000-9100Å. The 3000 and 3100Å images show the planet with *limb brightening*, evidently due to the increased molecular scattering near the limbs. Both polar caps are slightly enhanced on these pictures. Mr. Fountain is preparing a report (*LPL Comm. No. 175*).This limb brightening does not conflict with the near-absence of the secant effect reported above in the methane and ammonia distributions; because the 3000Å images see little more than the stratosphere which will contain no ammonia haze.

c. Asymmetry Between the Hemispheres - The marked asymmetry between the two Jupiter hemispheres has long been known, with the Red Spot and the White Ovals in the southern hemisphere, and no corresponding northern-hemisphere structures. The sources of the blue festoons are just North of the equator, with no corresponding sources South. The heat flux measurements at 5μ have shown hotter regions, around 300°K, than observed at the same southern latitudes, indicating a local absence of a high cloud cover just North of the equator. The polarization measures by Gehrels and his group (Fig. 4) also show a distinct asymmetry, as does the rotation curve of Figure 12. The asymmetry in the polarization has been observed also photographically, by J. Fountain, through polaroid filters, composited to show variations over the disk. The cloud belts on the planet are never strictly symmetrical.

The asymmetry between the two hemispheres may well be due to uneven energy release through the solid hydrogen surface; with presumably an above-average flux conducive to increased average storm activity. Indeed, *all three major gas vents* (Sec. 5)*appear to occur between 13° and 14° S* with their major eruptions every 3-6 years developing typically into three cloud masses, centered at 8°, 14°, and 19° S, respectively (Reese, 1972). Possibly the same latitude (14°S) is responsible for the additional two or three sources causing the 18-20 Mc radio bursts. Direct observation of the latitudes of these sources has not yet succeeded in spite of some remarkable interferometer tests with baselines up to nearly 1/2 million by Dulk (1970) and Carr *et al.* (1970) (summarized in the JPL report referred to), which indicate these sources to have *diameters* less than 400 km to 4000 km.

  d. Radio Frequency Emission by the Electrical Discharges - On the Earth they cause a very broad spectrum peaked at about 10 Kc but extending upward to 100 Mc. On Jupiter, because of the higher density of the water condensation zone, the discharges will be correspondingly shorter and the expected frequencies correspondingly higher, by about 1 decade.

  e. Concluding Remarks - Past discussions of Jupiter have often been confused by the fact that we observe only the uppermost layers of the Jupiter clouds, from *above*, while our familiar concepts are based on observations from the *ground*, on Earth. Figure 13e shows what this may mean. Similar problems exist in the interpretation of planetary polarization results; in fact, Dr. D. Coffeen has participated in using the NASA CV-990 for an infrared polarimetric study of terrestrial clouds below the aircraft. The circulation of the Jupiter atmosphere appears more confined than the Earth. In spite of enormous upheavals every 5-10 years or so, which temporarily destroy much of the familiar Belts and Zones near the equator, the planet returns to a pattern quite familiar from earlier years, so that the nomenclature system of the past still applies. This stability appears related to the low obliquity of Jupiter's equator, its high rate of rotation, the correspondingly-large Coriolis force, and thus the strict confinement to narrow belts in latitude, and long and narrow brown clouds. This paper focuses on the nature of the Red Spot, deferring a discussion of the wealth of information now available on the cloud belts, the bright zones, and numerous smaller features. Fortunately, ammonia makes more colorful compounds than water and makes wonderful tracers for cloud origins!

REFERENCES

Anderson, R. C., Pipes, J. G., Broadfoot, A. L., and Wallace, L. 1969, *J. Atm. Sci.*, *26*, 874.

Armstrong, R. L. and Welsh, H. L. 1960, *Spectrochimica Acta*, *16*, 840-852.

Armstrong, K. R., Harper, D. A., and Low, F. J. 1972, "Far-Infrared Brightness Temperatures of the Planets", *Ap. J.*, *178*, L89-L92.

Aumann, H. H., Gillespie, C. M., and Low, F. J. 1969, "The Internal Powers and Effective Temperatures of Jupiter and Saturn", *Ap. J.*, *157*, L69-L72.

Bergeron, T. 1954, "The Problem of Tropical Hurricanes", *Quart. J. Roy. Meteorol. Soc.*, *80*, 131-164.

Bishop, E. V. and de Marcus, W. 1970, "Thermal Histories of Jupiter Models", *Icarus*, *12*, 317-330.

Byers, H. R. 1954, "The Atmosphere up to 30 Kilometers", THE EARTH AS A PLANET, Vol. II of THE SOLAR SYSTEM (ed. G. P. Kuiper), Chapt. 7, 306-307 (Chicago: U. of Chicago Press).

Cadle, R. D. 1962, "The Photochemistry of the Upper Atmosphere of Jupiter", *J. Atm. Sc.*, *19*, No. 4, 281-285.

Carr, T. D. , Lunch, M. A., Paul, M. P., Brown, G. W., May, J., Six, N. F., Robinson, V. M., and Block, W. F. 1970, "Very Long Baseline Interferometry of Jupiter at 18 MHz", *Radio Sci.*, *5*, 1223.

Carr, T. D., Smith, A. G., Donivan, F. F., and Register, H. I. 1970, "The Twelve-year Periodicities of the Decametric Radiation of Jupiter", *Radio Sci.*, *5*, 495-503.

Carr, T. D. 1971, "Jupiter's Magnetospheric Rotation Period", *Astrophysical Letters*, *7*, 157-162.

Chang, C. P. 1970, "Westward Propagating Cloud Patterns in the Tropical Pacific as seen from Time-Composite Satellite Photographs", *J. Atm. Sci.*, *27*, 133-138.

Chapman, C. R. and Reese, E. J. 1968, "A test of the Uniformly Rotating Source Hypothesis for the South Equatorial Belt Disturbances on Jupiter", *Icarus*, *9*, 326-335.

Chapman, C. R. 1969, "Jupiter's Zonal Winds: Variation with Latitude", *J. Atm. Sci.*, *26*, 986-990.

Connes, J., Connes, P., and Maillard, J. P. 1969, NEAR INFRARED SPECTRA OF VENUS, MARS, JUPITER AND SATURN, Centre National de la Recherche Scientifique.

Cortright, E. M. 1968, EXPLORING SPACE WITH A CAMERA, Office of Technology Utilization, NASA, Washington, D. C., NASA SP-168.

Coulomb, J. and Jobert, G. 1963, THE PHYSICAL CONSTITUTION OF THE EARTH (New York: Hafner Publish. Co.), 244.

Curran, R. J., Conrath, B. J., Hanel, R. A., Kunde, V. G., Pearl, J. C. 1973, "Mars: Mariner 9 Spectroscopic Evidence for H_2O Ice Clouds", Goddard Space Flight Center Preprint X-651-73-156.

de Marcus, W. 1958, "The Constitution of Jupiter and Saturn", *A. J.*, *63*, 2-28.

Dickinson, R. E. 1969, "Propagators of Atmospheric Motions", *Rev. of Geophs.*, *7*, No. 3, 483-537.

Dopplick, T. G. 1972, "Radiative Heating of the Global Atmosphere", *J. Atm. Sci.*, *29*, 1278-1294.

Dulk, G. A. 1970, "Characteristics of Jupiter's Decametric Radio Source Measured with Arc-Second Resolution", *Ap. J.*, *159*, 671-684.

Duncan, R. A. 1971, "Jupiter's Rotation", *Planet. Space Sci.*, *19*, 391-398.

Dunham, T. 1952, "Spectroscopic Observations of the Planets at Mt. Wilson", THE ATMOSPHERES OF THE EARTH AND PLANETS, Chapt. XI, ed. G. P. Kuiper (Chicago: U. of Chicago Press), 286-303.

Dunn, G. E. and Miller, B. I. 1960, ATLANTIC HURRICANES (Louisiana State Univ. Press).

Fink, U., Dekkers, N. H., and Larson, H. P. 1973, "Infrared Spectra of the Galilean Satellites of Jupiter", *Ap. J.*, *179*, L155-L159.

Fox, W. E. 1969, "Report on the apparitions of 1966-67 and 1967-68", *Journ. British Astron. Assoc.*, *79*, 310-312.

Gallet, R. M. 1961, "Radio Observations of Jupiter II", PLANETS AND SATELLITES, Vol. III of THE SOLAR SYSTEM (eds. G. P. Kuiper and B. Middlehurst), Chapt. 14, 500-533, (Chicago, U. of Chicago Press).

Gehrels, T., Herman, B. M., and Owen, T. 1969, "Wavelength Dependence of Polarization XIV. Atmosphere of Jupiter", *A. J.*, *74*, 190-199.

Gehrels, T.,Suomi, V. E., and Krauss, R. J. 1972, in SPACE RESEARCH XII, ed. A. C. Stickland, (Berlin, Akad. Verlag).

Gillett, F. C., Low, F. J., and Stein, W. A. 1969, "The 2.8-14 Micron Spectrum of Jupiter", *Ap. J.*, *157*, 925-934.

Goody, R. 1969, "The Atmospheres of the Major Planets", *J. Atm. Sci.*, *26*, 997-1001.

Greenspan, J. and Owen, T. C. 1967, "Jupiter's Atmosphere: Its Structure and Composition", *Science*, 156, 1489-1493.

Hanel, R. A. and Conrath, B. J. 1970, "Thermal Emission Spectra of the Earth and Atmosphere from the Nimbus 4 Michelson Interferometer Experiment", *Nature*, *228*, 143-145.

Hanel, R. A., Conrath, B. J., Kinde, V. G., Prabhakara, C., Revah, I., Salomonson, V. V., and Wolford, G. 1972*a*,"The Nimbus 4 Infrared Spectroscopy Experiment. I. Calibrated Thermal Emission Spectra", *J. of Geophysical Research*, 77, 2629-2641.

Hanel, R. A., Schlachman, B., Breihan, E., Bywaters, R., Chapman, F., Rhodes, M., Rodger, D., and Vanous, D. 1972*b*,"Mariner 9 Michelson Interferometer", *Ap. Opt.*, *11*, 2625-2634.

Harper, D. A., Low, F. J., Rieke, G. H., and Armstrong, K. R. 1972, "Observations of Planets, Nebulae, and Galaxies at 350 Microns", *Ap. J.*, *177*, L21-L25.

Hess, S. L. and Panofsky, H. A. 1951, "The Atmospheres of the Outer Planets", *Compendium of Meteorology*, Amer. Meteor. Soc., Boston, Mass., 391-398.

Holton, J. R. 1971, "A Diagnostic Model for Equatorial Wave Disturbances: The Role of Vertical Shear of the Mean Zonal Wind", *J. Atm. Sci.*, *28*, 55-64.

Holton, J. R., Wallace, J. M., and Young, J. A. 1971, "A Note on Boundary Layer Dynamics and the ITCZ", *J. Atm. Sci.*, *28*, 275-280.

Hubbard, W. B. 1970, "Structure of Jupiter: Chemical Composition, Contraction, and Rotation", *Ap. J.*, *162*, 687-697.

Irvine, W. M., Simon, T., Menzel, D. H., Pikos, C., and Young, A. T. 1968, "Multicolor Photoelectric Photometry of the Brighter Planets. III Observations from Boyden Observatory", *A. J.* *73*, 826, Table XIV.

Johnson, A. W. 1969, "Weather Satellites", *Scientific American*, *220*, 52-68.

Johnson, H. L. 1970, "The Infrared Spectra of Jupiter and Saturn at 1.2-4.2 Microns", *Ap. J.* *159*, L1-L5.

Jolly, W. L. 1964, THE INORGANIC CHEMISTRY OF NITROGEN (New York: W. A. Benjamin).

Keay, C. S. L., Low, F. J., Rieke, G. H., and Minton, R. B.,"High-Resolution Maps of Jupiter at Five Microns", (in press).

Kornfield, J. and Hasler, A. F. 1969, "A Photographic Summary of the Earth's Cloud Cover for the Year 1967", *J. of Applied Meteorology*, *8*, No. 1, 687-700.

Kuiper, G. P. 1952, THE ATMOSPHERES OF THE EARTH AND PLANETS (Chicago: U. of Chicago Press).

Kuiper, G. P. 1957, "Infrared Observations of Planets and Satellites", abstract, *A. J.*, *62*, 245.

Kuiper, G. P. 1963, "Infrared Spectra of Planets and Cool Stars: Introductory Report", *Mémoires Soc. R. Sc. Liège*, Vol. IX, 365-391.

Lewis, J. S. 1969, "The Clouds of Jupiter and the NH_3-H_2O and NH_3-H_2S System", *Icarus*, *10*, 365-378; 393-409.

Lewis, J. S. and Prinn, R. G. 1970, "Jupiter's Clouds: Structure and Composition", *Science*, *169*, 472-473.

Low, F. J. and Davidson, S. W. 1965, "Lunar Observations at a Wavelength of 1 Millimeter", *Ap. J.*, *142*, 1278-1282.

Low, F. J. 1966, "Observations of Venus, Jupiter, and Saturn at λ20μ", *A. J.*, *71*, 391.

Low, F. J., Rieke, G. H., and Armstrong, K. R. 1973, "Ground-Based Observations at 34μ", *Ap. J. Letters*, (in press).

Martin, D. W. and Suomi, V. E. 1971, "A Satellite Study of Cloud Clusters Over the Tropical North Atlantic Ocean", Final Report on Contract E-127-69-(N), Space Science and Engineering Center, U. of Wisconsin, Madison.

Moroz, V. I. and Cruikshank, D. P. 1969, "Distribution of Ammonia on Jupiter", *J. Atm. Sci.*, *26*, 865-869.

Neuman, S. and Boyd, J. G. 1962, "Hurricane Movement and Variable Location of High Intensity Spot in Wall Cloud Radar Echo", *Monthly Weather Review*, *90*, 371-374.

Newburn, R. L. and Gulkis, S. 1971, "A Brief Survey of the Outer Planets, Jupiter, Saturn, Uranus, Neptune, Pluto, and their Satellites", JPL Tech. Report 32-1529.

Newton, C. W. 1963, "Dynamics of Severe Convective Storms", *Meteorological Monographs*, *5*, Amer. Meteor. Soc., 33-58.

Newton, C. W. 1967, "Severe Convective Storms", ADVANCES IN GEOPHYSICS, *12*, (Academic Press, New York).

Ooyama, K. 1969, "Numerical Simulation of the Life Cycle of Tropical Cyclones", *J. Atm. Sci.*, *26*, 3-40.

Owen, T. C. and Staley, D. O. 1963, "A Possible Jovian Analogy to the Terrestrial Equatorial Stratospheric Wind Reversal", *J. Atm. Sci.*, *20*, No. 4, 347-350.

Owen, T. C. 1965, "Comparison of Laboratory and Planetary Spectra. II. The Spectrum of Jupiter from 9700 to 11200A", *Ap. J.*, *141*, 444-456; and "III. The Spectrum of Jupiter from 7750 to 8800A", *Ap. J.*, *142*, 782-786.

Owen, T. C. and Walsh, T. E. 1965, "Radiation of Jupiter and Saturn", *Nature*, *208*, 477.

Owen T. C. 1967, "Comparisons of Laboratory and Planetary Spectra: IV. The Identification of the 7500Å Bands in the Spectra of Uranus and Neptune", *Icarus*, *6*, 108-113.

Owen, T. C. 1969, "The Spectra of Jupiter and Saturn in the Photographic Infrared", *Icarus*, *10*, 355-364.

Owen, T. C. 1970, "The Atmosphere of Jupiter", *Science*, *167*, 1675-1681.

Palmén, E. and Newton, C. W. 1969, "Tropical Cyclones, Hurricanes and Typhoons", ATMOSPHERIC CIRCULATION SYSTEMS (New York: Academic Press).

Peek, B. M. 1958, THE PLANET JUPITER (London: Faber and Faber).

Reese, E. J. and Smith, B. A. 1968, "Evidence of Vorticity in the Great Red Spot of Jupiter", *Icarus*, *9*, 474-486.

Reese, E. J. and Solberg, H. G. 1969, "Latitude and Longitude Measurements of Jovian Features in 1967-68", Rpt. TN-701-69-28, NASA grants, New Mexico State University.

Reese, E. J. 1970, "Jupiter's Red Spot in 1968-1969", *Icarus*, *12*, 249-257.

Reese, E. J. 1971*a*, "Jupiter: Its Red Spot and Other Features in 1969-1970", *Icarus*, *14*, 343-354.

Reese, E. J. 1971*b*, I. A. U. Circular 2338, July 2, 1971.

Reese, E. J. 1972, "Jupiter: Its Red Spot and Disturbances in 1970-1971", Rpt. TN-72-40, NASA grant, New Mexico State University.

Riehl, H. 1951, "Aerology of Tropical Storms", *Compendium of Meteorology*, Amer. Meteor. Soc., Boston, Mass., 902-913.

Rosenthal, S. L. 1971, National Hurricane Research Lab., Miami, Fla., personal communication.

Slipher, E. C. 1964, THE BRIGHTER PLANETS, Lowell Observatory.

Slipher, E. C., Shapiro, R., Giclas, H. L., Lorenz, E. N., and Hess, S. L. 1951, "The Project for the Study of Planetary Atmospheres", Rpt.No. 9, Lowell Observatory, Flagstaff, Arizona.

Smith, B. and Tombaugh, C. 1963, "Observations of the Red Spot on Jupiter", Rpt. TN-557-63-2, New Mexico State University.

Smoluchowski, R. 1971, "Metallic Interiors and Magnetic Fields of Jupiter and Saturn", *Ap. J., 166*, 435-439, and references given there.

Solberg, H. G. and Reese, E. J. 1966, "Recent Measures of the Latitude and Longitude of Jupiter's Red Spot, *Icarus, 5*, 266-273.

Solberg, H. G. 1968*a*, "Jupiter's Red Spot in 1965-1966", *Icarus, 8*, 82-89.

Solberg, H. G. 1968*b*, "Jupiter's Red Spot in 1966-1967", *Icarus, 9*, 212-216.

Solberg, H. G. 1969, "A 3-Month Oscillation in the Longitude of Jupiter's Red Spot", *Planet. Space Sci., 17*, 1573-1580.

Studier, M. H., Hayatsu, R., and Anders, E. 1968, "Origin of Organic Matter in Early Solar System - I. Hydrocarbons", *Geochim. et Cosmochim. Acta, 32*, 151-174.

Trafton, L. M. 1967, "Model Atmospheres of the Major Planets", *Ap. J., 147*, 765.

Ulmschneider, P. 1970, "On Frequency and Strength of Shock Waves in the Solar Atmosphere", SOLAR PHYSICS, (Dordrecht-Holland: Reidel Publish. Co.), pp. 403-415.

Ulmschneider, P. 1971, "On the Propagation of the Spectrum of Acoustic Waves in the Solar Atmosphere", *Astron. and Astrophys., 14*, 275-282.

Wallace, J. M. 1970, "Time-Longitude Sections of Tropical Cloudiness (Dec. 1966-Nov. 1967)", ESSA TECH. REPORT NESC 56, Washington, D. C., 37 pp.

Wallace, J. M. 1971, "Spectral Studies of the Tropospheric Wave Disturbances in the Tropical Western Pacific", *Rev. of Geophy. and Space Physics, 9*, 557-612.

Walsh, T. E. 1969, "Infrared Absorptance of Ammonia - 20 to 35 Microns", *J. Opt. Soc. Amer., 59*, 261-267.

Westphal, J. A. 1969, "Observations of Localized 5-Micron Radiation from Jupiter", *Ap. J., 157*, L63-L64.

Williams, K. 1970, "Characteristics of the Wind, Thermal, and Moisture Fields Surrounding the Satellite-Observed Mesoscale Trade Wind Cloud Clusters of the Western North Pacific", PROCEEDINGS SYMPOSIUM TROPICAL METEOROLOGY, American Geophysical Society, pp. D IV-1 to 7.

Yeh, T. C. 1950, "The Motion of Tropical Storms Under the Influence of a Superimposed Southerly Current", *J. of Meteorology, 7*, 108-113.

<center>APPENDIX I</center>

1. Planetary Energy Flux; Contraction Time Scale – During the second Lowell Observatory Conference on Planets, August 1951, much discussion ensued on the nature of the Jupiter and Saturn cloud covers. The spontaneous major eruptions and related phenomena indicated that the meterologies of these two planets differed greatly from that of the Earth and Mars; they appeared *internally driven* instead of *sundriven.*

In other words, the effects of the internal heat fluxes of Jupiter and Saturn appeared to exceed the effects of the absorbed solar radiation. Since for equal fluxes the effects on cloud formation of an internal source would be larger, the conclusion could *not* be reached that the fluxes of planetary origin were necessarily larger than the absorbed solar fluxes.

In THE ATMOSPHERES OF THE EARTH AND PLANETS (1952) I computed the total release of gravitational energy *after* the protoplanet stage, starting with $1.5R_J$. The result was that the average Jupiter emission will have been some 40 times the absorbed solar flux and the average surface temperature 250°K (*op. cit.* pp. 326-327). Since the present value was clearly much below that figure, "during Jupiter's early history, its surface temperature must have greatly exceeded 250°K and may well have corresponded to red heat". It was pointed out that the 8-14μ window did not

allow the measurement of the *present* flux ratio, planet/solar contribution, because of the double NH_3 band centered at 10-11μ which automatically gave $T \simeq 130°K$; but that this ratio might possibly be estimated from the observed cloud phenomena (*op. cit.* pp. 327, 376).

Öpik (1962) pursued the matter further, and derived from the cloud phenomena a provisional ratio of 1.6 ± 0.4.

As to the *time scale of the Jupiter contraction*, this was presented in the 1940's in my lectures at the University of Chicago along the following lines:

The empirical mass-luminosity relation for solar-type and smaller stars is $L \sim M^3$; the released gravitational energy for homologous stellar models, $E \sim M^2/R$; the Helmholtz-Kelvin contraction time scale therefore $E/L \sim M^{-1} R^{-1}$; or $\sim M^{-4/3}$ if ρ = constant. An extrapolation of the stellar data to Jupiter ($M_M = 10^{-3} M_{\odot}$) and Saturn would therefore make their time scales somewhat longer than the age of the solar system. Jupiter and Saturn in that sense, were considered small stars as well as planets. The planetary observations were considered a confirmation of this conclusion: "The Jovian atmospheres, at least those showing visible clouds (Jupiter and Saturn), are probably heated primarily from below. The spectacular cloud phenomena, sometimes altering the entire aspect of these giant planets, the motions of the clouds and their colors, do not appear to be governed by solar heating. It is quite likely that continued cooling and gravitational energy of contraction are still important in the heat budget of these bodies" (THE ATMOSPHERES, p. 376).

The first direct measures of Jupiter that indicated an excess of planetary radiation were made by Low (1966) who found that the energy emitted by the planet shortward of 25μ was already in excess of the absorbed solar radiation. He and his associates added data for the longer wavelength soon thereafter as described in the main text and illustrated in Figure 3*d*.

2. Earlier Red Spot Hypotheses - In the recent summary by Newburn and Gulkis (1971) the Red Spot is called "truly one of the great solar system puzzles". The Spot has been seen for 305 years since Cassini first described it (cf. *Sky and Telescope*, May 1968) but it may have existed before the telescope was invented. Its irregular motions had suggested that it was not attached to a large mountain; and its long life, that it was not a fluid-dynamic feature (a large eddy), but possibly instead a cloud cap about a large island floating in a highly compressed gaseous medium, as proposed by Wildt in 1939. Other authors have assumed that the solid surface might rotate irregularly after all, since the Earth exhibits minor fluctuations in its rotation, caused by variable interactions with the liquid core. They held that a "Taylor column" above a large plateau would fit the case.

Taylor (1923) used a fluid of very low viscosity; his "column" (being a quasi-cylindrical upward deflection of the flow) was produced by moving a strictly cylindrical box in a rotating liquid at right angles to the axis of rotation; and the "column" was observed only above the cylinder at a height comparable to that of the cylindrical box itself. While the application to the Jupiter Red Spot has been widely quoted, there are insurmountable difficulties with the application to the Red Spot of the phenomena observed by Taylor:

(a) The deeper atmosphere of Jupiter is *nearly stagnant* with respect to the solid surface; this was discussed on the basis of Figure 12.

(b)   The solid surface has a constant period of rotation, at $9^h55^m30^s$ (Sec. 5), not the *near-periodic motion*, both in longitude and latitude, with P $\cong$ 90 days, as shown in Figure 16; other *period changes* every 25-30 years causing overall departures from uniform motion by 1200° during the past 140 years; or even the departure of the average rotation period from that of the radio sources by 8 sec, indicating *a complete revolution* of the Red Spot with respect to the solid surface every 5 years or so.

(c)   Even if a current of *unexplained origin* in the dense, viscous H_2-He-H_2O-NH_3-CH_4 mixture (p > 10^5 atm) existed relative to the solid surface, the hypothesis further assumes that a protruding box-like cylindrical mesa of solid H_2 exists, some 11,000 km wide and 25,000 km long, with sharp vertical walls, as required for the upward flow to retain the cylindrical shape of the column. The *formation* of such a cylindrical box has no counterpart in geophysics and is inconceivable; nevertheless, if it once existed it would quickly *erode* by the hypothetical current itself, be rounded off on the upper rim, and thereupon cause the current to pass as a simple overflow.

(d)   The cylindrical mesa postulated under (c) would have to undergo *semiperiodic changes in length and width* with amplitudes 1000-4000 km over a period around 90 days (Fig. 16); and undergo *total changes in length* well in excess of 10,000 km. (The induced flow observed by Taylor (1923) had the diameter and shape of the moving cylinder below and was co-axial with it; the vertical dimensions of the Jupiter "atmosphere" are presumably below 1000 km).

(e)   The concept of a Taylor column of height some two orders of magnitude or more greater than that of the cylindrical mesa does not appear to have any *empirical* basis. Nor does the column as reported by Taylor just over the cylindrical box constitute a complete cylinder; it spans only some 300° of the periphery.

(f)   Such phenomena as the 9 passages of the South Tropical Disturbance between 1902 and 1939, first halting and then jumping beneath the Red Spot, would have no explanation on the basis of the Taylor column hypothesis, nor would it explain the anticyclonic surface rotation, the great altitude of the Red Spot, and other structural features cited in this paper; nor *the lasting changes in the daily rotation period of the Red Spot*, caused by passing meteorological structures (South Tropical Disturbance).

These problems and contradictions are all avoided by assuming that the Red Spot, the largest of the numerous oval-shaped clouds, has a *meteorological* explanation like the others. *The central location of the Red Spot within the South Tropical Zone* (one of the two symmetrical 22°-latitude high-level zones shown in Fig. 1) *re-enforces this conclusion.*- I am indebted to Mr. F. de Wiess for assistance with this summary.

After the above was written, Dr. R. Hide kindly called my attention to a joint quantitative experimental investigation by him and Dr. A. Ibbetson (Hide and Ibbetson, 1965; Hide and Ibbetson, 1966) designed to repeat and extend the original Taylor experiment. The result was that *already at a height of twice the cylinder thickness, the observed "column" was reduced to a minor disturbance in the flow pattern sweeping across the area above the cylinder*. This confirms the critique of the hypothesis made above as being entirely inapplicable to the Red Spot.

Further, Dr. A. Ibbetson has called our attention to a recent study, "Rotating Flow Over Shallow Topographies" by A. Vaziri and D. L. Boyer (1971). The authors state: "Since the time of Taylor's (1923) experiments, a great deal of effort has been expended in investigating the effects of bottom topography on flows in rotating frames of reference. Unfortunately, most of the theoretical studies are so restrictive as to make experimentation difficult, if not impossible, while for many of the experimental studies the theory is intractable. The present investigation is one for which both the range of applicability of the theory and the capabilities of the laboratory experiment coincide". They find the flow pattern over both conical and $\cos^2$ topographic features for height-to-width ratios of 0.0625, 0.125, 0.250, and 0.375. No "Taylor column" is present, only a perturbation in the flow pattern across the obstruction which at one point becomes a small (rotating) eddy.

De Marcus and Wildt (1966) showed that conceivably a "thermodynamic Cartesian diver" could exist in a "region where phase separation occurs under the condition that two distinct phases have the same density". Streett *et al.* (1971) examined this question further and found that some oscillations in the diver's rotation period, as observed for the Red Spot, would not be inconsistent with the model. In a second paper Streett (1971) estimates the "diver" to be about 800 km deep and the solid surface about 1600 km. Sagan (1963) objected to the floating-island concept on the grounds that it will tend to shift its latitude by the "pole-flight" force introduced into geophysics by Eötvös. If the island is truly floating, however, the density of the hydrogen ice must *equal* that of the hydrogen-helium compressed gas, with no "pole-flight" force acting on the island. In Sec. 4*d* a strong objection is given to the floating ice mass.

<div align="center">REFERENCES</div>

De Marcus, W. C. and Wildt, R. 1966, "Jupiter's Great Red Spot", *Nature, 209,* 62.

Hide, R. 1963, "On the Hydrodynamics of Jupiter's Atmosphere", *Mémoires Soc. R. Sc. Liège, Vol. VII,* 481-505.

Hide, R. 1971*a*, "Motions in Planetary Atmospheres: A Review", *Meteor. Magazine, 100,* 268-276.

Hide, R. 1971*b*, "On Geostrophic Motion of a Non-homogeneous Fluid", *J. Fluid Mech., 49,* 745-751.

Hide, R. and Ibbetson, A. 1965, "Taylor Columns", MAGNETISM AND THE COSMOS, 343-347.

Hide, R. and Ibbetson, A. 1966, "An Experimental Study of 'Taylor Column'", *Icarus, 5,* 279-290.

Kuiper, G. P. 1952, THE ATMOSPHERES OF THE EARTH AND PLANETS (Chicago: U. of Chicago Press).

Newburn, R. L. and Gulkis, S. 1971, "A Brief Survey of the Outer Planets, Jupiter, Saturn, Uranus, Neptune, Pluto, and their Satellites", JPL Tech. Rpt. 32-1529.

Öpik, E. J. 1962, "Jupiter: Chemical Composition, Structure, and Origin of a Giant Planet", *Icarus, 1,* 200.

Sagan, C. 1963, "On the Nature of the Jovian Red Spot", *Mémoires Soc. R. Sc. Liège, Vol. VII,* 506-515.

Streett, W. B. 1971, "Phase Behavior of Light Gas Mixtures at High Pressures", PLANETARY ATMOSPHERES (ed. Sagan), 363-370.

Streett, W. B., Ringermacher, H. I., and Veronis, G. 1971, "On the Structure and Motions of Jupiter's Red Spot", *Icarus, 14,* 319-342.

Taylor, G. I. 1923, *Proc. Roy. Soc. A., 104,* 213.

Vaziri, A. and Boyer, D. L. 1971, "Rotating Flow over Shallow Topographies", *J. Fluid Mech., 50,* Part 1, 79-95.

APPENDIX II

by S. M. Larson

Much discussion on cloud heights is based on the appearance of Jupiter on photographs taken with the "methane filter", an interference filter with pass-band 8850-9050Å (Fig. 19). (Actually, its pass-band is slightly displaced with respect to the CH_4 band which would optimally require 8820-9000Å). It will be shown that the gross features thus recorded are due to differential methane gas absorptions and not to intrinsic albedo differences. We here use photographs taken through three available interference filters, A, B, and C, around the $\lambda 8900$Å methane band, whose transmission curves are also shown in Figure 19.
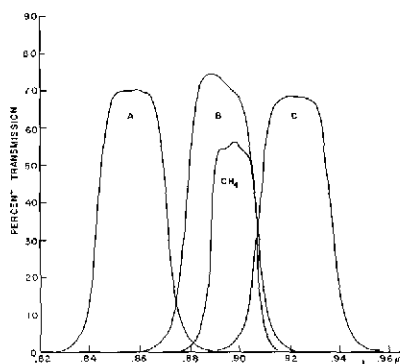
Fig. 19 Transmission curves for filters A, B, C, and the "methane filter" used in the Jupiter photography, Figure 1

The method used was that of photographic subtraction and is illustrated in Figure 20. To this end, gamma-one contrast positives were made from the original negatives taken on Kodak High-Speed Infrared film. We used a film whose response is nearly linear over a large range of densities (DuPont Commercial-S). While the originals and copies will not be entirely linear, the effects will not interfere with the detection of the strong contrasts produced by the methane absorption. The images were exposed on the straight-line portion of the characteristic curves, and the density difference between the planet's limb and the sky averaged 0.7; therefore, the largest departures from linearity are caused by "adjacency effects". These effects will be less serious on most methane-filter images because on them the differences between sky and limb are small. Since the $\lambda 8950$ methane band is deep and the film sensitivity there already low, the methane images require long exposures and inevitably are often on the toe of the characteristic curve. This non-linearity causes a lowering of contrast of images A+C' in Figure 20.

The features shown on the methane images result from differences in path lengths to the reflecting cloud layers. Since methane will not condense on Jupiter and is therefore representative of the equilibrium atmosphere, regions of less absorption must be higher. The features recorded since 1968 are consistent with those described by Owen (1969).

We find no clear correlation between cloud heights and brightness measured in the near-IR. In some frames of unusually high resolution, the bluish festoons can be recognized, and it is assumed that this is an albedo effect, caused by contamination due to the slight mismatch of the CH_4 filter.

GERARD P. KUIPER
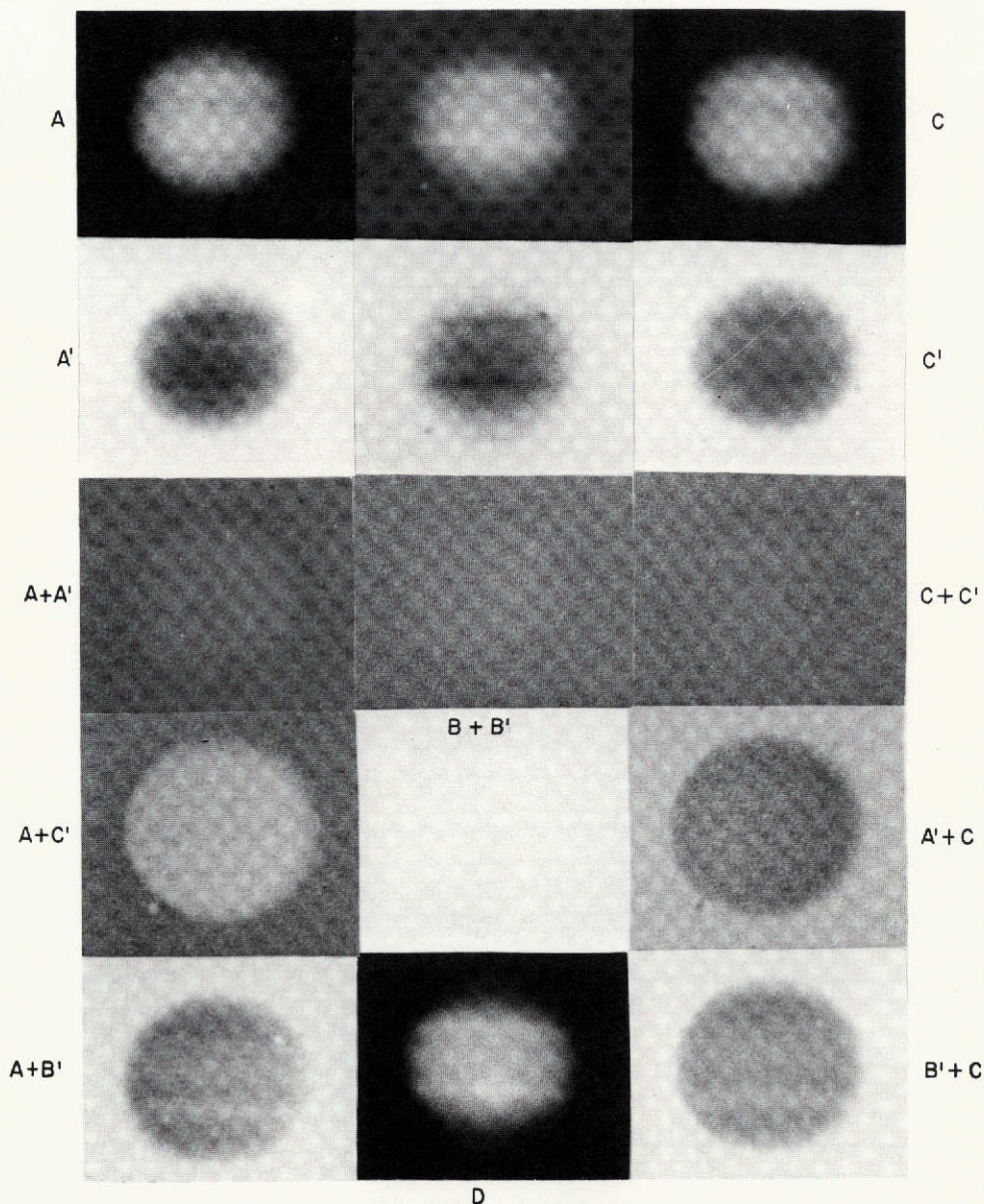
Fig. 20 - A, B, C,- Photographs taken on April 8, 1971, by J. Fountain with fil-
ters shown in Fig. 19. Exposure times 2 sec, 8 sec, and 120 sec.
A', B', C' - Gamma-one contrast copies of A, B, and C.
A+A', B+B', C+C' - Combinations showing that A', B', C' are actually
very close to having a contrast of one, and that registration errors
and photographic edge effects are minor.
A+C', C+A' - Combinations showing that intrinsic albedo differences
between wavelengths A and B are negligibly small.
A+B', C+B' - Showing the distribution of CH_4 absorption by subtract-
ing true albedo differences. Note that these two frames agree.
D - Taken about 2^h5 later (Red Spot has rotated into view), with re-
gular CH_4 interference filter used. Exposure 90 sec, seeing poorer.

Reference is made to a more extensive discussion of Jupiter filter photography by J. W. Fountain and S. M. Larson in *LPL Communications Nos. 174* and *175*.

Sensitometric and spectral regions data can be found in Kodak's PLATES AND FILM FOR SCIENCE AND INDUSTRY, p. 9, 1967, along with a good summary of photographic edge effects.   See also Dupont's GRAPHIC ARTS FILMS TECHNICAL DATA on the Commercial-S film A-30238, referred to above.

NO. 174 MULTICOLOR PHOTOGRAPHY OF JUPITER

by J. W. Fountain and S. M. Larson

September 1971

ABSTRACT

    Examples of wide-band filter photography of Jupiter between
1965 and 1970 are reviewed, describing the basic wavelength de-
pendence of the cloud features. The initial results of photography
in the 0.89μ methane band are discussed.

1. Introduction

    Direct photography of Jupiter provides much information on the nature and
circulation of cloud patterns. Because of the planet's large angular size, its
major features can be easily recorded and under the best conditions complex,
fine structure is seen. The changing nature of the clouds requires photography
at frequent intervals to follow their evolution. Most of the data on the ap-
pearance of Jupiter before this century are drawings by visual observers, but

with the application of photography, reliable, objective records provide the opportunity for systematic and quantitative studies of the visible clouds. It has been generally maintained that the visual observer can see more detail than the photograph can record, but this is only partly true. Under "average" seeing conditions the visual observer *might* be able to detect a small feature (given enough time to pick out moments of better seeing) not resolved on a photograph, but in the fraction of a second of the photographic exposure, a permanent, objective, geometrically and photometrically consistent record is obtained; and if many photographs are taken, a few may approach "visual" re- solution. Under excellent seeing conditions, the photography may show all the detail that the observer can see and may actually excel in resolving broad, low- contrast features because of the higher contrast detection capability of the emulsion. (The relative merits may be different for small telescopes).

In the early experiments of A. A. Common in 1879 and others, photographic emulsions were not very efficient; but with systematic programs that started about 1905, especially at Lowell Observatory (Slipher 1964), it was shown that the major changes could be followed successfully. Since then, Lyot (1943, 1953), Camichel (1946), and Humason (1961) have provided improved results with better techniques, emulsions and telescopes. More recently the New Mexico State Ob- servatory has achieved excellent resolution and coverage with modest aperture, and the NASA IPP has provided unprecedented patrol data.

A major milestone was reached in W. H. Wright's (1929) studies of the wave- length dependency of the clouds on Jupiter from 0.36-0.76μ. With the use of selected broadband glass filters,he produced the first objective records of the spatial distribution of the colors that at that time had been described only by visual observers.

2. The Program

In October 1965, Dr. Kuiper initiated a program of direct photography of the Moon and planets with the newly completed 154-cm telescope at the Catalina Observatory (32°4 N latitude, 2520m altitude). Every effort was made to opti- mize the optical performance of the telescope, and minimize local seeing effects. F/13.5 (10 arc-sec mm^{-1}), and f/45 (3 arc-sec mm^{-1}) Cassegrain secondaries are available. About one fourth of the telescope time has been used for lunar and planetary photography, with lunar photography having first priority during the period up to mid-1967 in preparation for the CONSOLIDATED LUNAR ATLAS (1967). Initially, D. Milon experimented with several black-and-white, and color emul- sions and scales to optimize results for the side conditions. The present authors became the principal observers in 1967 and initiated the use of filters and many more emulsions. In the continuing effort to refine our techniques, new emulsions are considered and adopted when the results are improved. Over the years we have been assisted by C. Campbell, D. McLean, J. Barrett, R. B. Minton, and others.

The primary objective of the program has been to obtain the highest pos- sible resolution; however, orientation trails and photometric calibration are applied routinely to make the data more useful for future studies. The expo- sure times are recorded on paper tape with 1 sec accuracy, and other pertinent data are recorded in a log.

For efficiency in storage, handling, and processing, and because of the diversity of available emulsions, 35mm roll films have been used almost exclusively. The camera is a Nikon F, which permits the image quality to be monitored in a reflex viewer; no exposures are made when the seeing is below average for the night. This greatly reduces the number of images which would not be used because of their low quality. Further improvements in image quality are realized with the use of a non-deviating, low-dispersion prism to compensate for atmospheric dispersion (allowing better coverage because observations may be extended to greater zenith angles) and sometimes by reducing the aperture in inferior seeing conditions with appropriate diaphragms either at the end of the telescope or at the secondary mirror.

Normally, 15-20 exposures are made within a short interval, to provide adequate material for compositing 2 to 10 images (Jupiter's rotation causes 0.2 arc-sec smear at the center of the disk during 45 sec). At our site a composite of selected high-quality images of short exposure is usually better than a single longer exposure on a slower, fine-grain emulsion. Only during the best seeing is the gain in quality negligible, for exposures up to several seconds. The result of compositing is an enlarged (to a constant scale) positive copy that can be further copied to adjust contrast or intensity gradients.

The selection of plate scale was determined primarily by the width of the passband filters and emulsions used. For wide effective passbands, large plate scales on fast emulsions were found preferable; thus f/45 to f/80 was most common. For narrow bands requiring long exposures, smaller plate scales, such as provided by the f/13.5 secondary, were necessary. Sometimes the image size was adjusted for the seeing; but since visual assessment of the (photographic) seeing is often unreliable, the optimum scale for average conditions was found most practical.

Processing of the black-and-white films is done manually or by the LPL's Itek Transflo automatic film processor. The exposure times for Jupiter at the f/45 focus are 1/30 to 1/15 sec for panchromatic film without filter; 1/8 to 1/4 sec, with broadband filters (1500Å); 1/2 to 1 sec for color films; and with the 8975Å interference filter at the f/13.5 focus, 60-90 sec.

This filter was obtained by Dr. Kuiper in October 1968. It passed a band 200Å wide centered on λ8975Å. The transmission curve is shown on page 311. It was obtained to cover the strong 200Å wide CH_4 band (e.g. Kuiper 1952, Plate 12), for the photography of the Jovian planets. The intensity of a portion of the planet in the photograph measures the methane absorption above it, and is thus interpreted as a measure of the height of that feature in the Jupiter atmosphere. Our records show that some of the bright belts, the Red Spot, and polar hoods, are higher than the other clouds. In 1970 an ammonia filter for λ6445Å (8Å wide) was used. The images appeared essentially the same as those taken through broadband red filters, apparently because the continuum between the rather sharp NH_3 lines dominated in the transmitted light.

3. Selection of Reproductions

We have selected representative records for the apparitions 1965-70. The black-and-white images shown are composites, produced as follows: the original telescopic negatives were composited on film (as positives), without photometric compensations (such as shading). Second negatives of appropriate scale on film
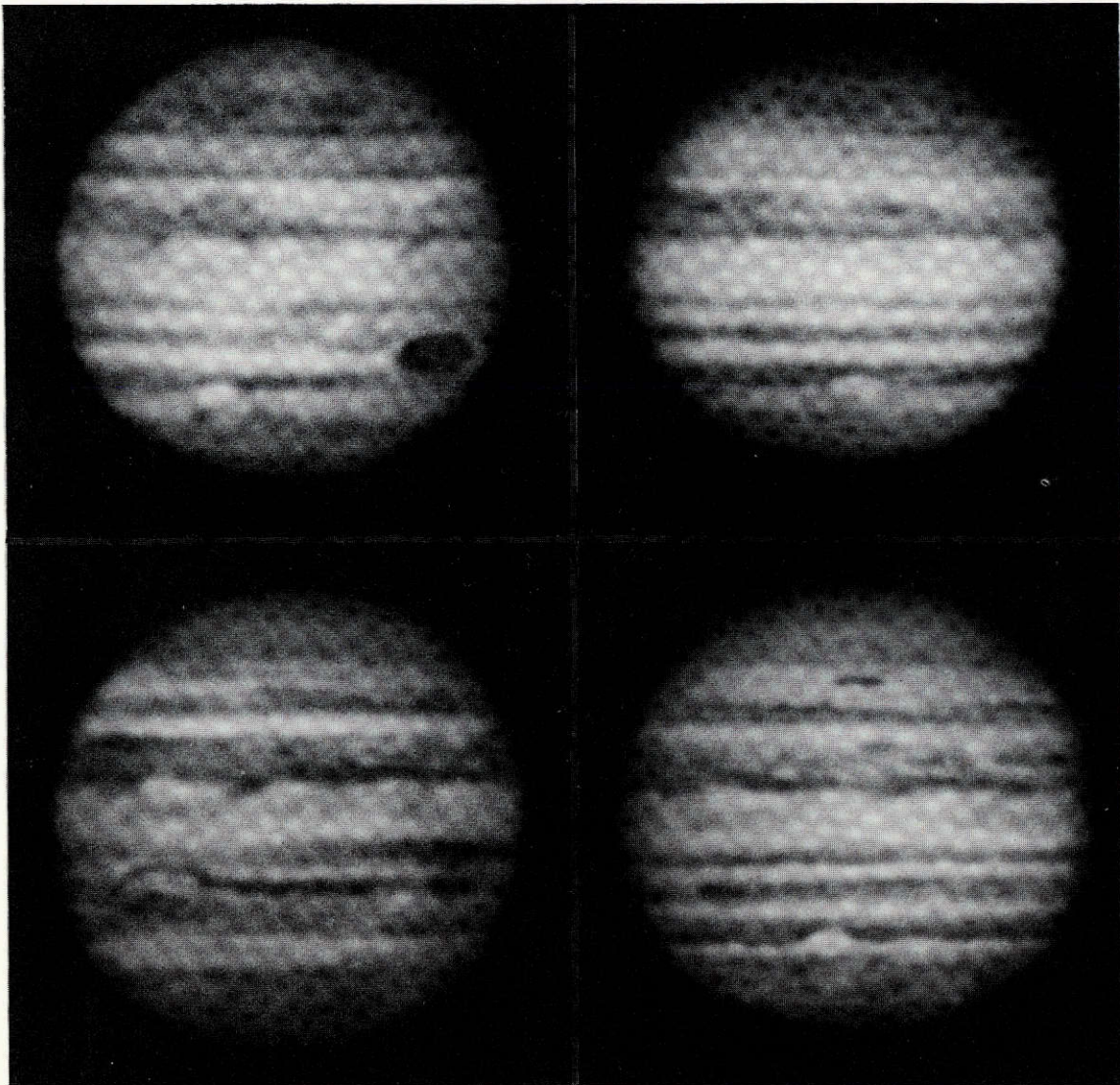
Fig. 1a. 1965 Oct 30, 08:35:07 UT. Panchromatic. RS prominent on limb. White oval visible South of STeB; smaller dark spots at high latitudes. Prominent festoons adjacent to NEB.
b. 1966 Feb 4, 05:39:45 UT. Panchromatic. Many small high-latitude spots visible, and mottling in belts. NTeB has faded since Oct 30; also diminishing festoon activity.
c. 1966 Dec 23, 08:35:22 UT. Panchromatic. All zones except NTrZ filled with darker material. Belts, e.g. NTeB and NEB, still prominent. SEBs is very dark and in vicinity of RS displaced toward equator. Size and shape of RS changed with appearance of light material between it and SEBs.
d. 1967 Jan 20, 05:52:37 UT. Panchromatic. Zones have lightened; many high-latitude spots and small detail in belts. On central meridian NTeZ is isolated dark bar. Note double nature of NTeB over most of its length and break near center of disk. Irregular belt edges.
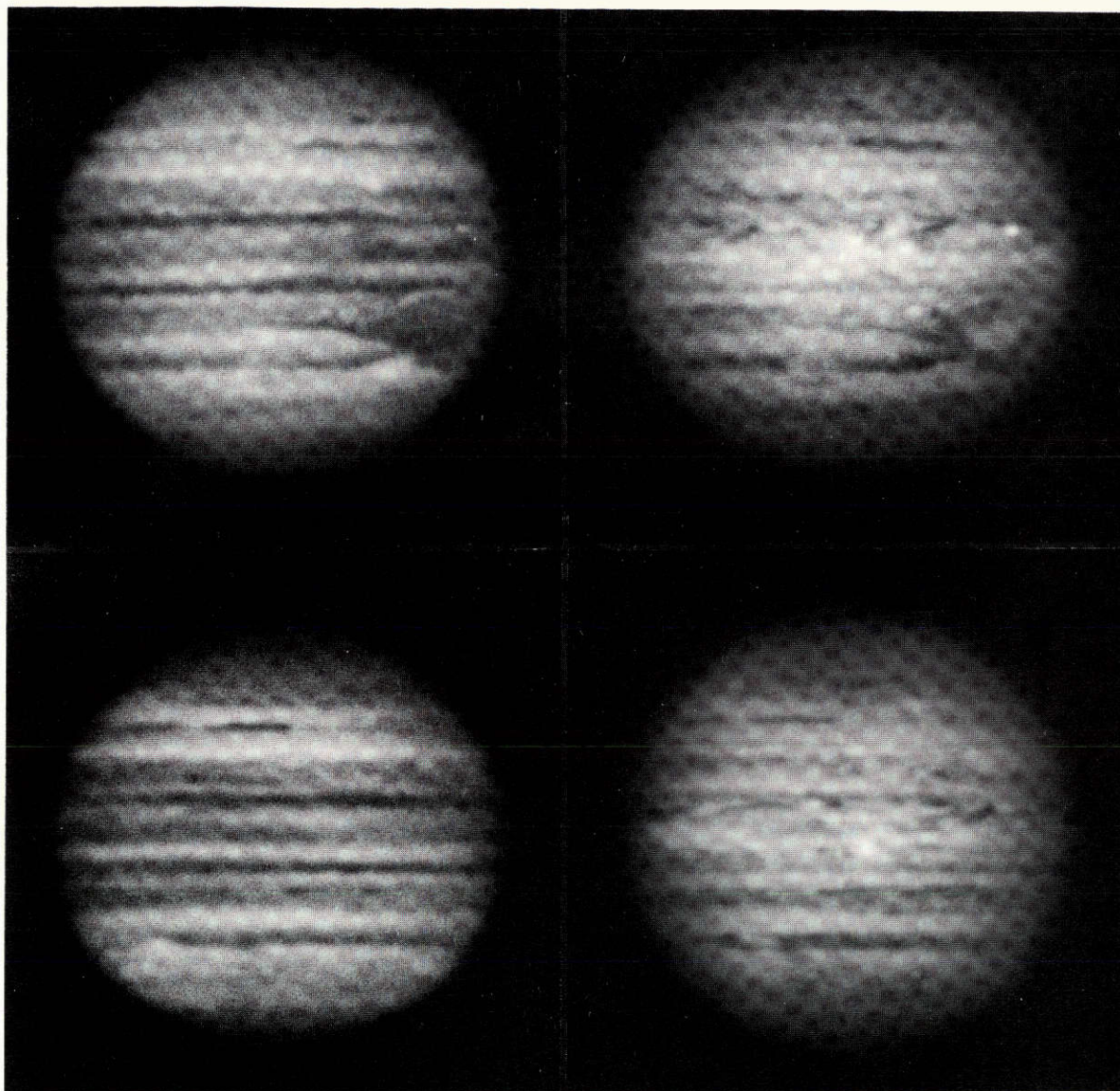
Fig. 2a. 1968 Jan 25, 10:09:57 UT, 0.35-0.48μ.
    b. 1968 Jan 25, 10:01:29 UT, 0.70-0.89μ.
a and b show typical differences between blue and red: greater prominence
of banded structure in blue and irregular structure in red. Sections of
NTeB indicate peculiar colorations. Broken-up appearance of SEBs immediately
following RS. Small spot within RS, darker in red and brighter in blue than
RS. Io near right side of disk, brighter in red; elongated appearance due
to lower albedo of poles.
    c. 1968 Jan 25, 11:46:52 UT, 0.35-0.48μ.
    d. 1968 Jan 25, 11:32:09 UT, 0.70-0.89μ.
Compare with a and b. Light spot near center of red image may be defect.

were produced from these positives, again without shading. Paper positives
were made by contact printing from the second negatives, with appropriate shad-
ing applied in order to bring out local contrasts to maximum advantage; in
general, that meant only a reduction of the limb darkening, but sometimes a
compensation for the Red Spot or an unusually dark belt showing detail on the
film copies (paper having a small dynamic range). The shading was never done
manually, but always with an appropriate mask placed between the negative and
the light source; and the resulting print was always carefully inspected against
the original film positive. This method was used, after much experimentation,
since it allowed maximum control and repeatability, and minimized spurious halos,
etc., introduced by some methods. For a given day the images have the same scale
(depending on the image quality); North is up.

The limb darkening has been reduced in the reproductions of the red-filter
images, which should be borne in mind in their use. Table I lists the relevant
observational data for each of the reproductions here included.

TABLE I

Figure	Date	Time (UT)	Film	Filter	Images in Composite	λ_I	λ_{II}	Comp. No.
1a	1965 Oct 30	08:35:07	TRI-X	NF*	12	250.9	64.5	1102
1b	1966 Feb 4	05:39:45	TRI-X	NF	1	355.3	143.7	1205
1c	1966 Dec 23	08:35:22	4-X	NF	8	145.7	356.3	1104
1d	1967 Jan 20	05:52:37	4-X	NF	8	151.5	149.3	1173
2a	1968 Jan 25	10:09:57	103-O	NF	3	15.9	69.3	214
2b	1968 Jan 25	10:01:29	HSIR	RG-5	4	10.7	64.2	210
2c	1968 Jan 25	11:46:52	103-O	NF	3	74.9	127.8	218
2d	1968 Jan 25	11:32:09	HSIR	RG-5	11	66.0	118.9	997
3a	1968 Dec 6	11:37:36	103-O	NF	8	251.2	53.0	381
3b	1968 Dec 6	12:00:41	HSIR	RG-5	7	265.3	66.9	385
3c	1968 Dec 6	12:14:07	HSIR	0.9μ	4	273.5	75.1	386
3d	1970 Apr 3	7:17:08	103-O	NF	8	13.3	91.2	1169
3e	1970 Apr 3	7:07:49	HSIR	RG-5	4	7.6	85.6	921
3f	1970 Apr 3	6:58:50	HSIR	0.9μ	3	2.2	80.1	916
4a	1969 May 30	4:00:19	103-O	NF	11	253.9	163.0	984
4b	1969 May 30	3:54:47	4-X	GG-14	9	250.6	159.6	982
4c	1969 May 30	3:48:27	HSIR	GG-14	12	246.7	155.8	983
5a	1968 Mar 22	5:58:44	103-O	UG-11	3	229.3	209.1	1092
5b	1968 Mar 22	5:53:01	103-O	NF	3	225.8	205.5	1093
5c	1970 May 16	7:25:27	103-O	UG-5	5	333.1	82.8	1028
5d	1970 May 16	7:21:55	103-O	NF	6	330.9	80.6	1031
6a	1970 May 16	7:31:04	4-X	GG-14	6	336.5	86.2	1033
6b	1970 May 16	7:34:40	HSIR	GG-14	9	338.7	88.4	1034
6c	1970 May 16	5:40:32	HSIR	RG-5	3	269.1	19.4	1112
6d	1970 May 16	5:50:07	HSIR	0.9μ	4	275.0	25.2	914
7a	1970 Jun 19	4:03:00	103-O	NF	10	178.1	29.7	1204
7b	1970 Jun 19	3:56:59	HSIR	GG-14	12	174.5	26.0	946

* NF = No filter
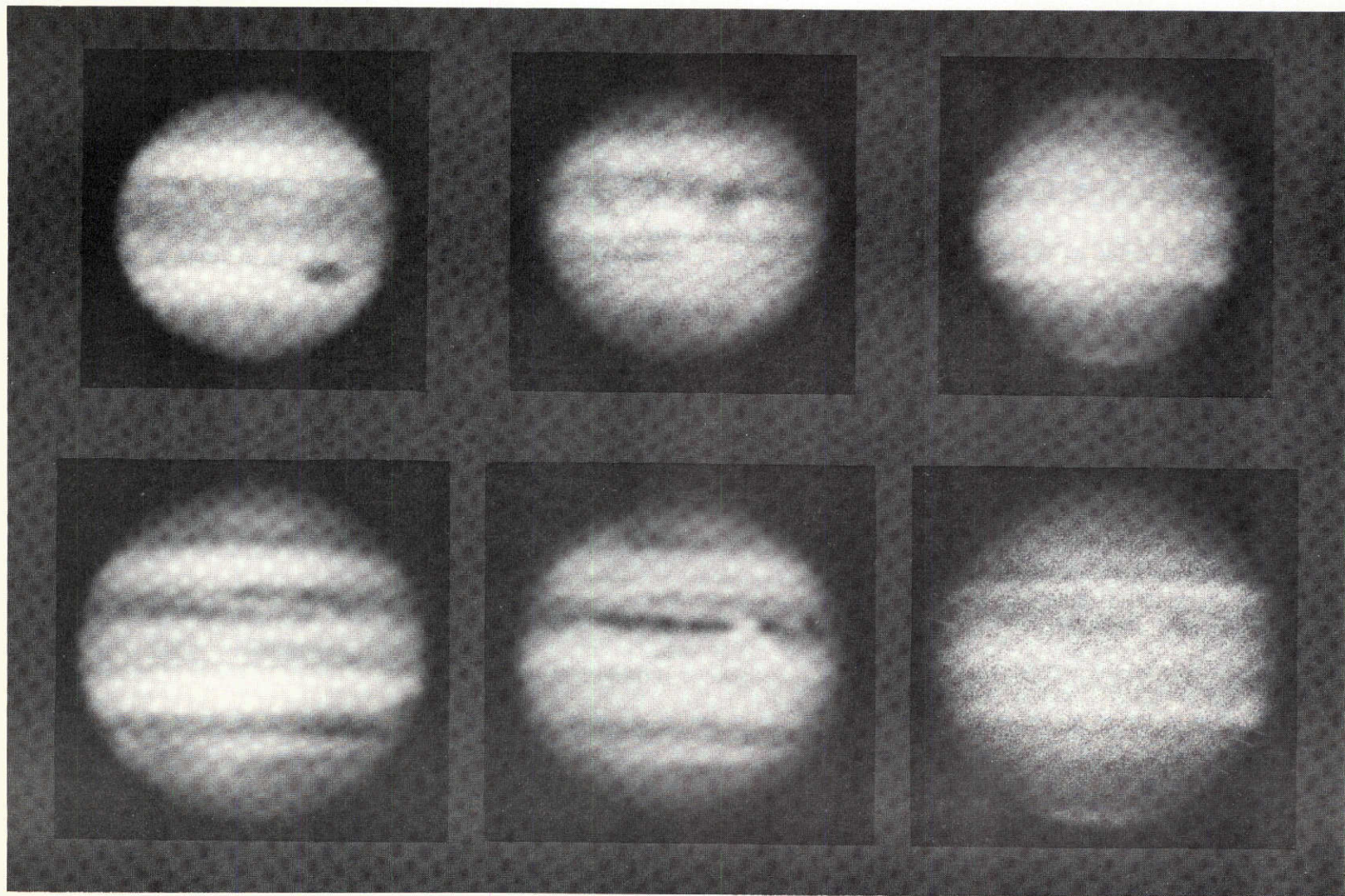
Fig. 3a. 1968 Dec 6, 11:37:36 UT; 0.35-0.48μ.
   b. 1968 Dec 6, 12:00:41 UT; 0.70-0.89μ.
   c. 1968 Dec 6, 12:14:07 UT; 0.90μ (CH$_4$). Light polar hoods,
    RS, EZ, and Tropical Zones; Io at right.
   d. 1970 Apr 3, 7:17:08 UT, 0.35-0.48μ.
   e. 1970 Apr 3, 7:07:49 UT, 0.70-0.89μ.
   f. 1970 Apr 3, 6:58:50 UT, 0.90μ (CH$_4$). Changes since 1968.

4. Discussion

    The nomenclature used herein is basically the same as adopted by the BAA,
but it should be noted that there are many difficulties in describing features
in different wavelengths. The qualitative manner in which some features are re-
ferred to is due to lack of standardization. With minor exceptions Jupiter's ap-
pearance from $0.3-0.5\mu$ is fairly constant, as it true longward of 0.5μ. Near
0.5μ the relative brightness of the belts and zones often changes considerably.
In blue light the banded structure of the planet is promiment, and the limb dark-
ening is small. In red light the appearance of the planet is less ordered and
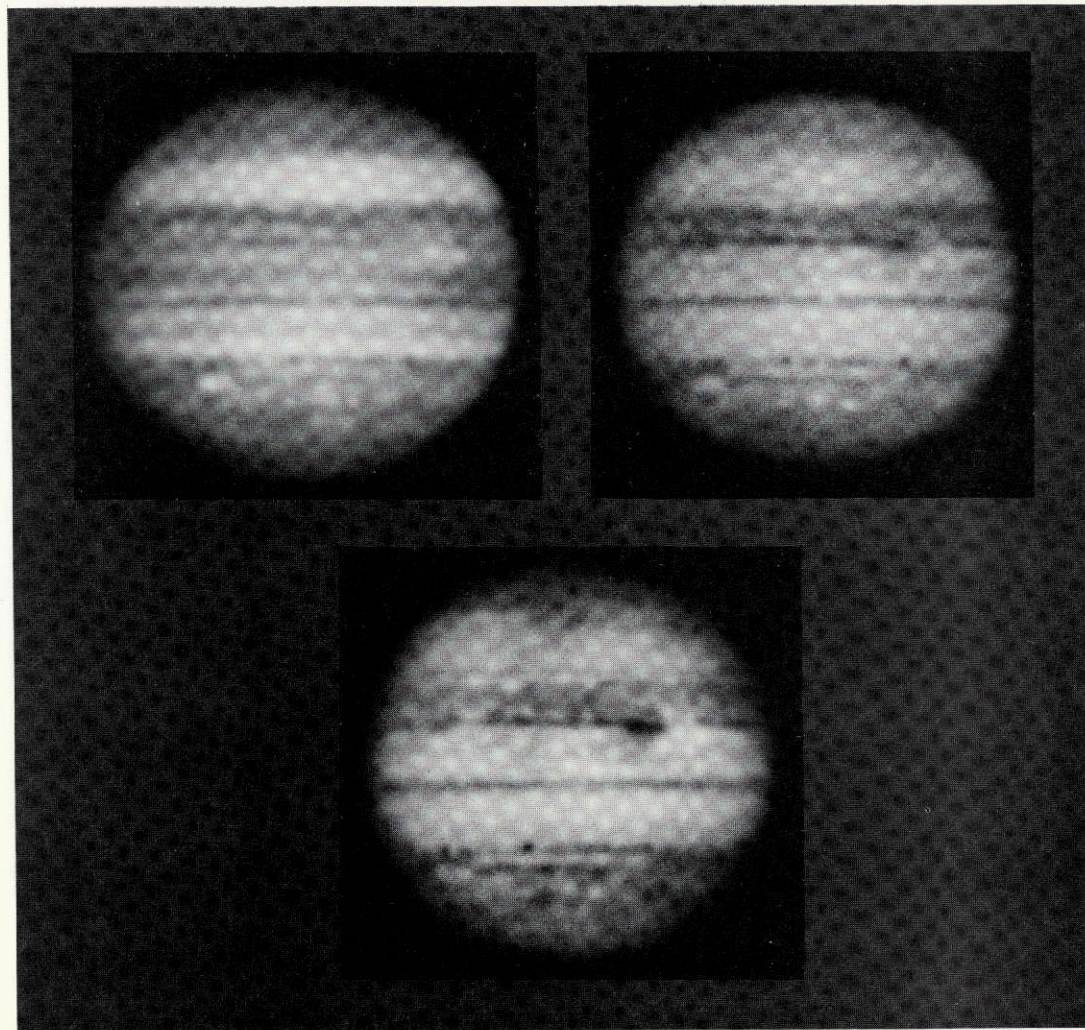
Fig. 4*a* 1969 May 30, 4:00:19 UT, $0.35-0.48\mu$.
    b 1969 May 30, 3:54:47 UT, $0.51-0.63\mu$.
    c 1969 May 30, 3:48:27 UT, $0.70-0.89\mu$.
An unusual number of spots: dark spots in STrZ, prominent in
all three wavelengths; white spots in NEB and SPR. Unusually
high-latitude festoons in Northern hemisphere of red image.

limb darkening is more severe, contrast between the belts and zones is reduced, and much of the visible structure no longer tends to be parallel to the equator. This is largely due to the intrinsic colors of the features, the belts often being somewhat reddish and the festoon-like features bluish. Green photographs of Jupiter are rarely taken since they contain contributions from these two distinctive appearances.
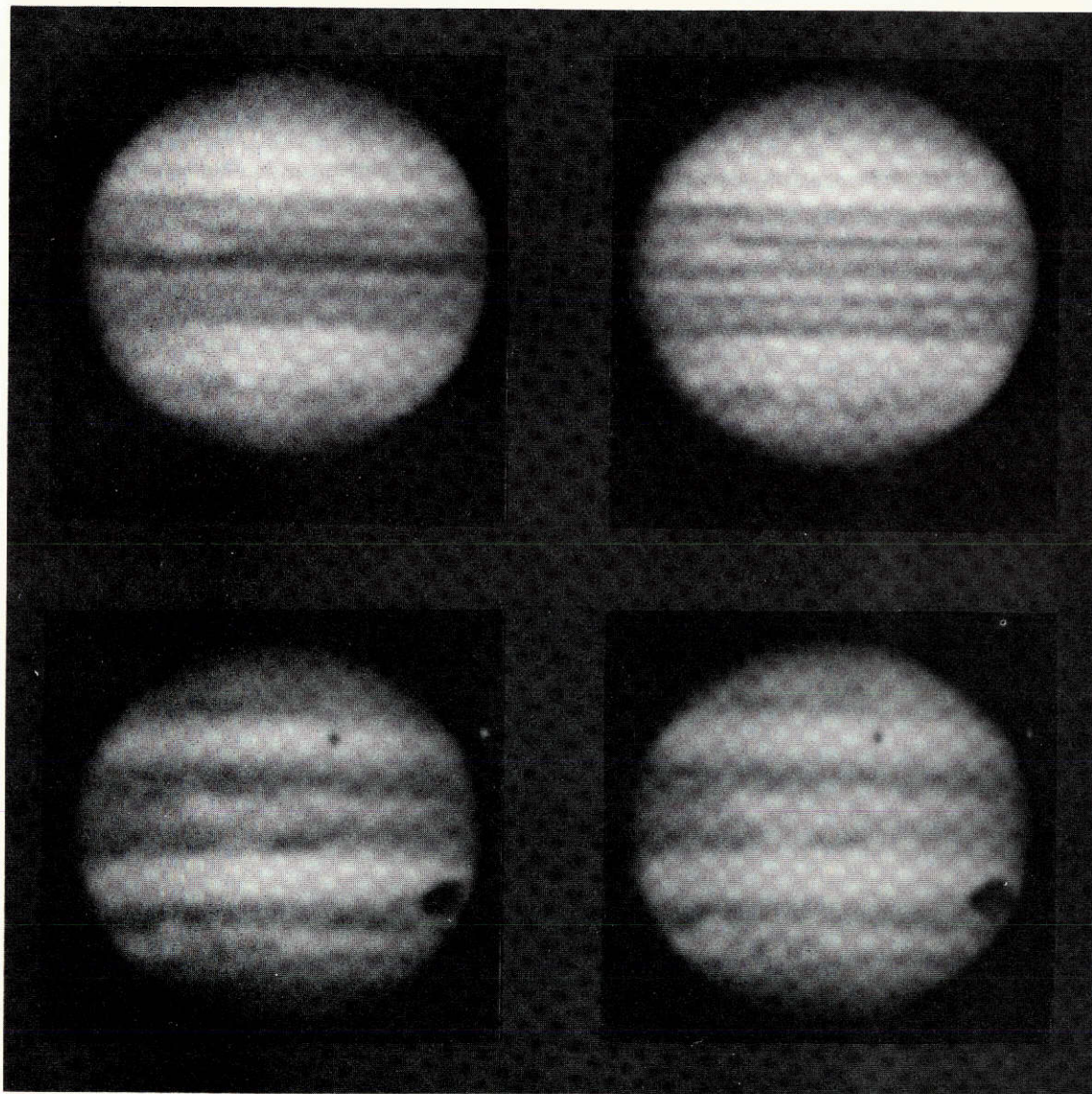
Fig. 5a 1968 Mar 22, 5:58:44 UT, 0.33-0.38μ.
     b 1968 Mar 22, 5:53:01 UT, 0.35-0.58μ.
     c 1970 May 16, 7:25:27 UT, 0.33-0.40μ.
     d 1970 May 16, 7:21:55 UT, 0.35-0.48μ.
Representing differences in UV and blue. In a, b, belt near equator is much darker in UV than in blue; the lower pair shows a more common difference - one of contrast.

The most dominant single feature on Jupiter is the Red Spot, and
since it shows color and boundary changes, it demands coverage in both blue
and red light. Because of its reddish color it appears dark on blue light
photographs and often shows interesting structure in red. When our photo-
graphy commenced in 1965, the RS was prominent (Fig. 1a) and had a darker
border. By late 1966 (Fig. 1c) the Northern edge was light, reducing its
overall prominence. In 1968 (Figs. 2a, b) it had returned to a more normal
appearance and remained so until 1970 when it had become very red (Fig. 7a).
At that time, the red images showed much interior detail.
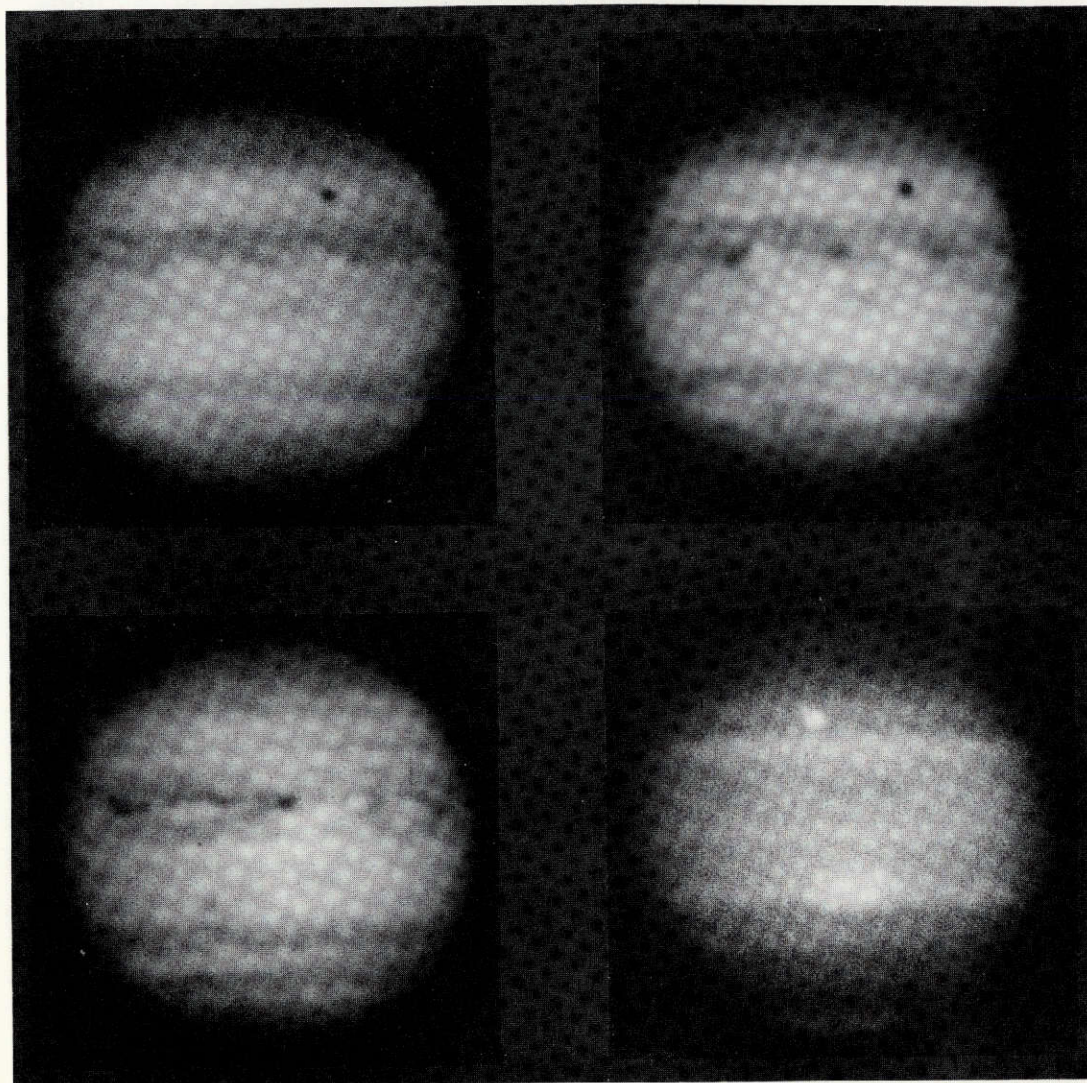
Fig. 6a 1970 May 16, 7:31:04 UT, 0.51-0.63μ.
     b 1970 May 16, 7:34:04 UT, 0.70-0.89μ.
     c 1970 May 16, 5:40:32 UT, 0.70-0.89μ.
     d 1970 May 16, 5:50:07 UT, 0.90μ (CH_4).
Compare with Fig. 5c, d, taken on same date. Europa's shadow on disk. Note
structure around and in RS in c, and strong Tropical Zones in d. Brightness
of Europa in d indicative of amount of methane absorption on planet.
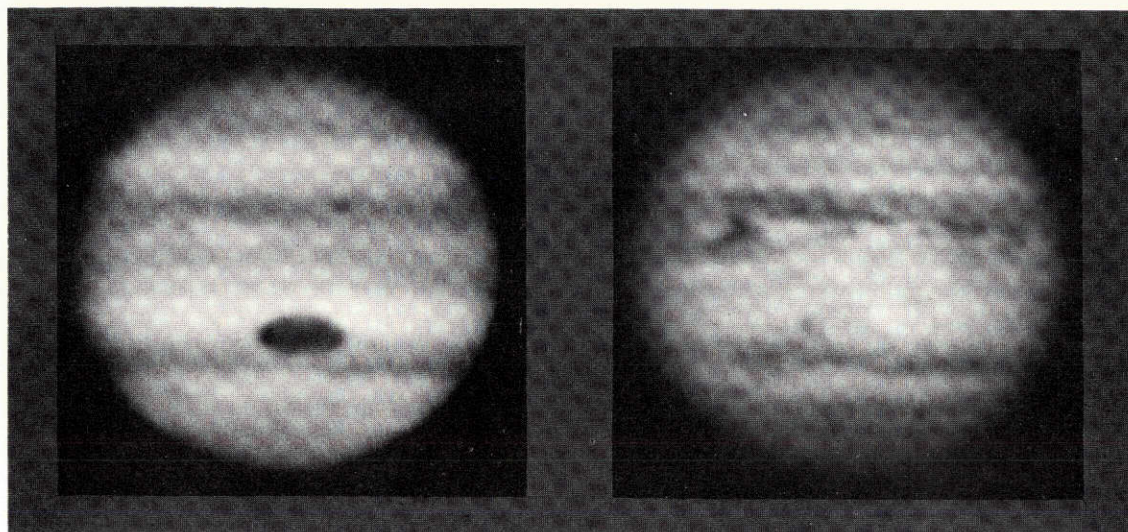
Fig. 7*a* 1970 June 19, 4:03:00 UT, 0.35-0.58μ.
    b 1970 June 19, 3:56:59 UT, 0.70-0.89μ.
Note prominence of RS in blue, and intricate structure
within RS in red.

There are many examples of belts that have changed their intensity, extent, and color in the interval 1965-70. E.g., the NTeB appeared orange in 1965, grey in 1966, broken in 1968, and hardly present in 1970.

North of the latitude of the RS, higher resolution photographs often show numerous light and dark spots whose lifetimes are on the order of weeks. From 1965 to 1970 the spots appear to have a higher frequency of appearance in the Southern hemisphere.

Photographs of Jupiter at 0.89μ show several distinctive characteristics attributed to differences in methane absorption above the clouds, since there are no important color changes on the planet in this part of the spectrum (*LPL Comm. No. 175*). The South pole shows a bright hood compared with the adjacent polar region, a much weaker hood is seen at the North pole, and the contrast of the bright zones against the rest of the planet is much greater than in the comparison images. We stress that the actual contrast between the bright and dark portions of the planet at 0.89μ is very great; it has been reduced here so that the full range of tones may be reproduced. Bright zones in the methane images are seen to correspond to bright zones in the comparison images; however, the relative brightnesses are not preserved. The North and South Tropical Zones are nearly always the most prominent zones in the methane images, and the Red Spot is the brightest feature. The limb darkening in the darker portions of the methane image appears to be greater than in the bright zones. In the higher-resolution methane images some of the dark festoons are resolved. It is uncertain whether their presence is a result of contamination by the continuum from the wings of the filter or if this accurately reflects the methane distribution. In the latter case the dark features must be lower than any other features observed in methane.

REFERENCES

Camichel, M. H. 1946, "Le Developpement de la Station Astronomique de l'Observa-toire du Pic du Midi", *l'Astronomie, 60*, 160.

Dollfus, A. 1961, "Visual and Photographic Studies of the Planets at the Pic du Midi", THE SOLAR SYSTEM (U. of Chicago Press), ed. G. P. Kuiper and B. Middle-hurst, Vol. III, Chap. 15, pp. 534-571.

Humason, M. L. 1961, "Photographs of Planets with the 200-inch Telescope", *Ibid,* Chap. 16, pp. 572-574.

Kuiper, G. P. 1952, THE ATMOSPHERES OF THE EARTH AND PLANETS, (U. of Chicago Press), Chap. 12, Plate 12.

Lyot, B. 1943, "Observations Planétaires au Pic du Midi, en 1941", *l'Astronomie, 57.*

Lyot, B. 1953, "Photographies de Jupiter en 1945", *l'Astronomie, 67*, Figs. 1-6, 21.

Owen, T. C. 1969, "The Spectra of Jupiter and Saturn in the Photographic Infra-red", *Icarus, 10*, 355-364.

Peek, B. M. 1958, THE PLANET JUPITER (London: Faber and Faber).

Reese, E. J. 1972, "Jupiter: Its Red Spot and Disturbances in 1970-1971", *Icarus, 17*, 57-72.

Slipher, E. C. 1964, A PHOTOGRAPHIC STUDY OF THE BRIGHTER PLANETS, (National Geo-graphic Society and Northland Press).

Wright, W. H. 1929, "Photographic Observations of Certain Jovian Phenomena Reported by Messrs. Hargreaves, Peek, and Phillips", *MN, 89*, 703-708.

NO. 175   NARROW-BAND PHOTOGRAPHY OF JUPITER AND SATURN

by John W. Fountain

August 16, 1972

ABSTRACT

Jupiter and Saturn were photographed with narrow-bandwidth interference filters ($\lambda/\Delta\lambda \sim 30$) from 3000 to 9200Å and in the 1-2μ region with an infrared-sensitive vidicon. Changes with wavelength are noted in the limb darkening and surface detail.

Photography of Jupiter and Saturn through wide-bandwidth filters (~1000Å) has been pursued with the 61-inch Catalina reflector for the past six years with gratifying results. The occasional use of narrower-bandwidth filters has sometimes yielded interesting features which remain unnoticed through broader filters. Three sets of wheel-mounted interference filters (14 per wheel) used for a 42-filter photometer were adapted for direct photography of the planets.

327

1. The Photography

The filters have effective wavelengths spacings of 100Å from 3000 to 4000Å, with bandwidths also of 100Å; from 4200 to 8000Å the spacing is 200Å and the bandwidth 200Å; while longward of 8000Å the spacing is 300Å and bandwidth 300Å. Not all of the filters were used since those with transmission above 9200Å would have required the use of an infrared emulsion with too-low sensitivity. The emulsions used are: Kodak Spectroscopic III-O for ultra-violet and blue light; Kodak High Contrast Copy, Type 5069, for visual light; and Kodak High Speed Infrared, Type 2481, for the infrared. The films were developed to gammas of approximately 3.5, 3.6, and 1.6, respectively.

Enlarged positive copies of the originals were made, composited with other frames whenever practical. Printing negatives were prepared from these positives and processed to a gamma which approximately equalized their effec-tive contrast. No attempt was made to correct for the variation in film gamma with wavelength. Contact prints were made on the same contrast-grade paper, with no dodging or shading applied, and processed identically. The images are reproduced here, North up, at a constant scale of about 1.0 arc sec per mm.

The filters, described by W. Wamsteker in *LPL Communication No. 167*, have a clear aperture of 12mm and could conveniently be mounted in a filter-wheel assembly which placed the film plane about 75mm from the filter. Although the image diameter of Jupiter on the film was only 4.2mm, the beam at the filter was 9.8mm, and required precise centering in the 12mm filter. For some frames a slight decentering has caused some vignetting: on the North limb of the Jupiter images 10-12, and on some images of the Rings of Saturn. In addition, variations in the thicknesses of the filters caused small displacements of the focal plane which could not easily be corrected, especially at the extreme wavelengths, so that some images are slightly out of focus. (The assembly is currently being modified and improved filters are being selected).

2. Infrared Vidicon Imagery

In order to record Jupiter and Saturn at still longer wavelengths, a Hamamatsu TV-Type 156/157 IR Vidicon was used. A Schott RG-1000 filter cut out wavelengths shortward of 1µ, making the response of the system nearly constant from 1.0 to 2.1µ and near zero elsewhere. The sensitivity of the vidicon was not completely constant over the field, which was detected by shifting the image between exposures. The TV imaging system introduced geometric distortion causing the planet image to appear stretched.   It was not practical to calibrate the picture intensities so that the contrast is somewhat uncertain.

3. Jupiter

Two nights were required to record the planet with all the filters. The results here presented are considered preliminary because of the low declination of the planet, 20°S. The rapid rotation of the planet resulted in noticeable displacement of features from frame to frame. It is therefore not possible from our data to compare features at a particular longitude for all wavelengths. How-ever, the change with wavelength in the general appearance may be seen, since aside from the persistent spots and equatorial fine structure, the planet on these dates had a rather similar appearance at all longitudes. Data for the Jupiter photographs are found in Table I. Two prints are included of the 3000Å image, the second one printed precisely as all following images; the first print with slightly enhanced contrast.

TABLE I

Jupiter Photographs

Frame	Date 1971	Time UT	Film	Å	No. images	Exp. Sec.	CM λ(I)	CM λ(II)
1	Apr 7	11:23:02	III-0	3000	1	330	74°.9	216°.0
2	"	11:23:02	III-0	3000	1	330	74.9	216.0
3	"	11:32:48	III-0	3090	3	60	80.9	221.9
4	"	11:36:13	III-0	3200	5	20	82.9	223.9
5	"	11:38:41	III-0	3325	5	15	84.5	225.5
6	"	11:41:09	III-0	3420	5	15	86.0	227.0
7	"	11:43:06	III-0	3530	6	7	87.2	228.2
8	"	11:44:33	III-0	3625	5	7	88.0	229.0
9	"	11:50:45	III-0	3720	4	5	91.9	232.8
10	"	11:51:41	III-0	3800	5	3	92.4	233.3
11	"	11:52:31	III-0	3940	5	2	92.9	233.8
12	"	11:53:31	III-0	4000	5	1.5	93.5	234.4
13	"	11:54:30	III-0	4260	5	1	94.1	235.0
14	"	11:54:59	III-0	4440	5	1	94.4	235.3
15	"	11:55:39	III-0	4600	3	1.5	94.8	235.7
16	"	10:27:27	HCC	5000	1	25	41.1	182.4
17	"	10:29:40	HCC	5200	1	6	42.4	183.8
18	"	10:31:35	HCC	5400	1	7	43.6	185.0
19	"	10:33:19	HCC	5600	1	7	44.6	186.0
20	"	10:46:27	HSIR	5800	4	1.5	52.7	193.9
21	"	10:47:13	HSIR	6060	5	1	53.1	194.3
22	"	10:47:51	HSIR	6200	5	1.5	53.5	194.7
23	"	10:48:55	HSIR	6400	5	1.5	54.2	195.4
24	"	10:49:47	HSIR	6620	5	1.5	54.7	195.9
25	"	10:50:30	HSIR	6775	5	1.5	55.1	196.3
26	Apr 7	9:40:34	HSIR	8964	3	90	12.4	154.0
27	Apr 8	9:28:39	HSIR	7000	1	1.5	163.2	250.6
28	"	9:13:44	HSIR	7200	5	2	154.1	288.2
29	"	9:13:01	HSIR	7400	4	2	153.7	287.8
30	"	9:04:22	HSIR	7600	3	2	148.4	282.6
31	"	9:03:24	HSIR	7800	2	1	147.8	282.0
32	"	9:03:00	HSIR	8000	3	1	147.6	281.8
33	"	9:02:30	HSIR	8300	3	1	147.3	281.5
34	"	9:01:48	HSIR	8600	3	2	147.0	281.1
35	"	9:00:32	HSIR	8900	5	8	146.0	280.3
36	Apr 8	8:56:14	HSIR	9200	2	120	143.4	277.6
37	Jan 21	3:06:00	IR Vidicon	1-2μ	8	1/4	10.7	14.4

It is seen that there are no major changes for λ<4600Å. From 4600 to 5000Å the change is rapid, with festoons and other fine structure becoming prominent. From 6000 to 9200Å, again little change is seen with the exception of the 8900Å frame which includes a strong methane band. The planet was also photographed through a filter with effective wavelength 8964Å, bandwidth 190Å, which has a transmission more nearly corresponding to the methane band and is less contaminated by the continuum (see *LPL Comm. No. 174*).
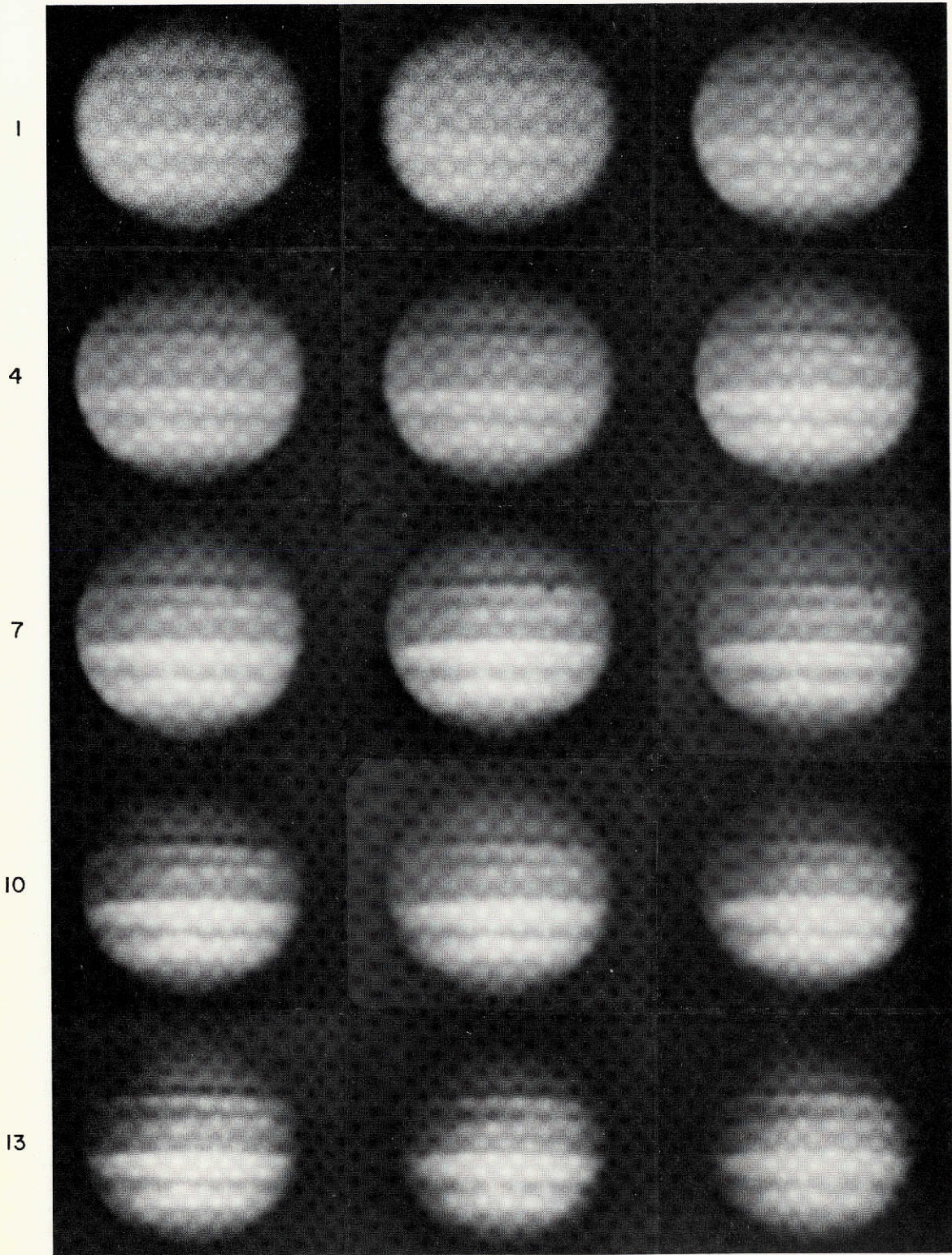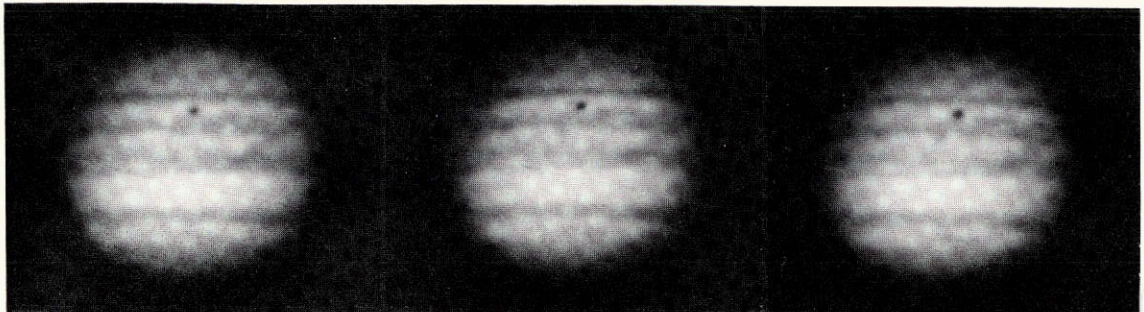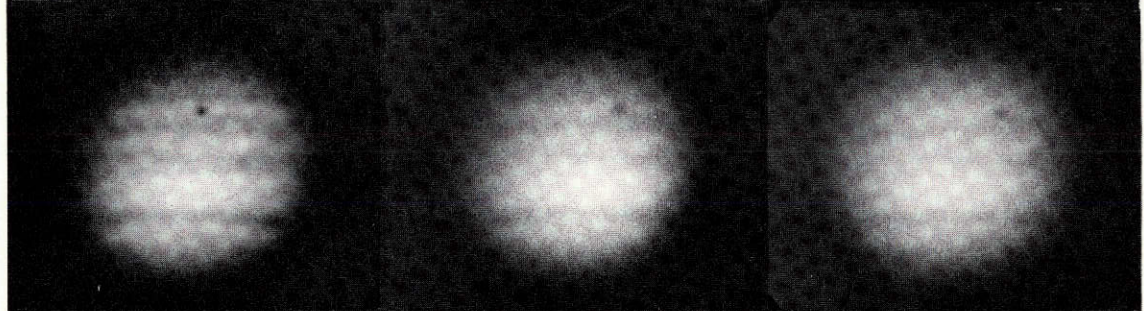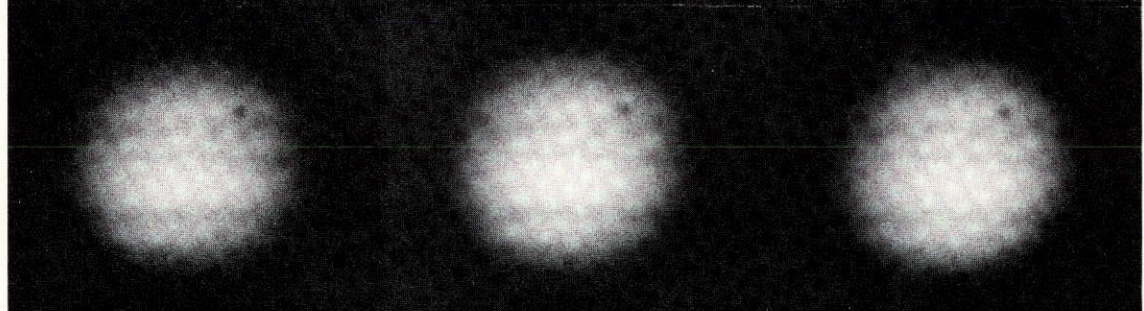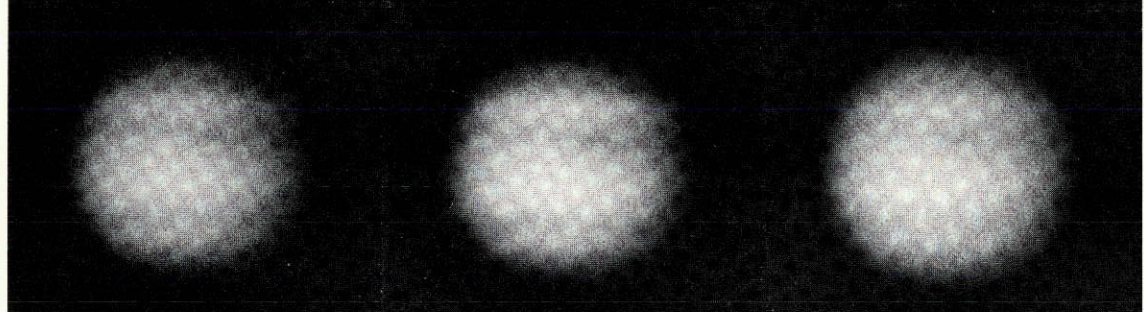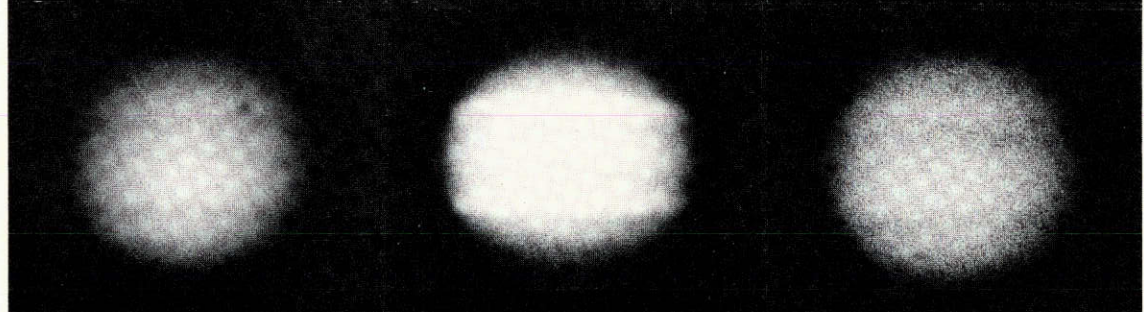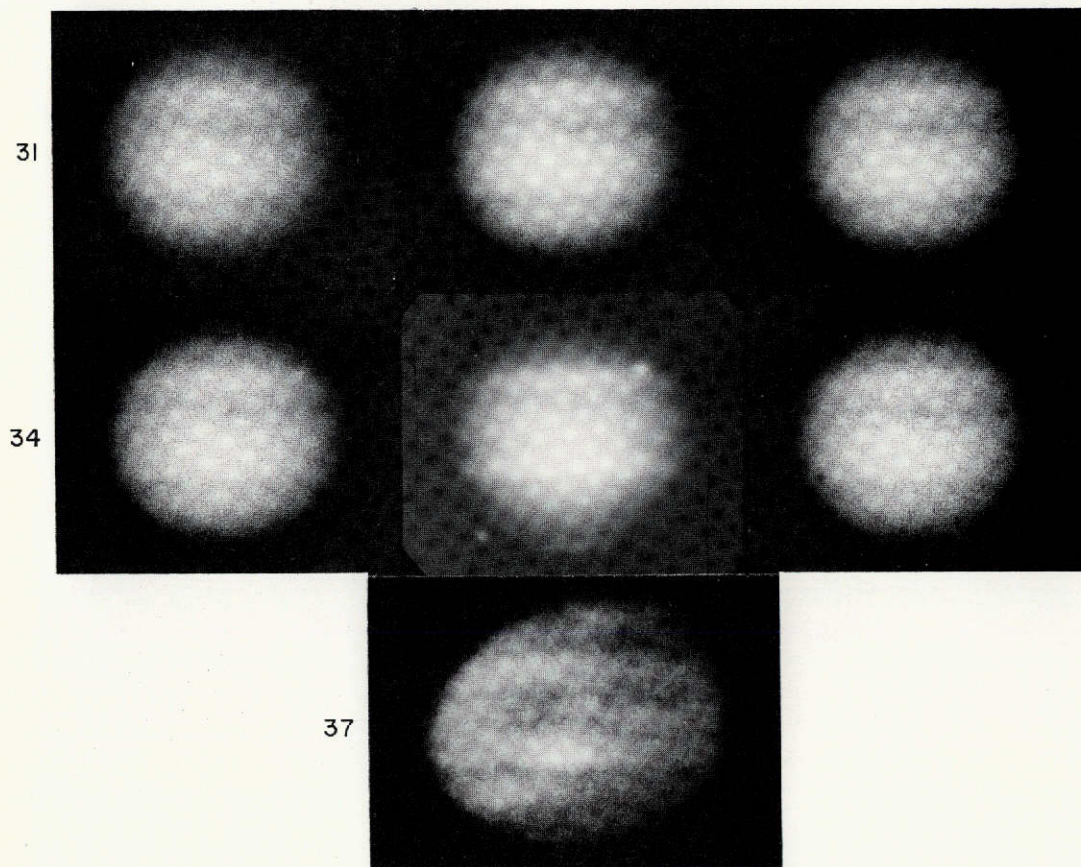
        On the images taken at 3000-3300A a *hood is seen over the South Pole* which
is somewhat lighter than the rest of the dark South Polar Region (SPR)[*]. The
North Polar Region (NPR) is darker than the SPR and only a slight hint of a cor-
responding hood is seen there. The South Temperate Belt (STeB),flanked by the
bright South Temperate Zone (STeZ) and the South Tropical Zone(STrZ), is clearly
seen. From the South edge of the North component of the South Equatorial Belt
(SEBn) to the North Temperate Belt (NTeB)there is an almost uniform appearance
except for light features near the equator. *Slight limb brightening* from Ray-
leigh scattering is seen, especially along the bright (East) limb. The North
Equatorial Belt (NEB) is dark. From 3400 to 4000Å the brightness of the STeZ
and the STrZ   increases, and the visibility of the Polar hood and limb bright-
ening decreases. *Limb darkening* is seen in the dark regions for $\lambda > 3600$Å.

        The contrast between belts and zones diminishes somewhat from 4200 to 4600Å,
and limb darkening becomes strong. The North Tropical Zone (NTrZ) and the
Equatorial Zone (EZ) become somewhat lighter. From 4800 to 5600Å the NTeB lightens

---

[*]   The nomenclature used here is explained on p. 352.

with respect to the STeB. Festoons and fine structure are seen in the EZ. The STeB,SEBn, and the NEB all have approximately the same brightness. From 5800 to 8600Å there is no substantial change in the appearance of the planet. The 7200Å image appears unaffected by the 7250Å methane band which does affect the Saturn image.

The 8900Å filter includes the strong methane absorption band, so the image is strongly influenced by the variation in the methane absorption over the planet. Strong limb darkening is seen in the belts. The NTeZ, EZ, and STrZ are very bright. The South Polar hood is much brighter than the adjacent SPR and extends to about the same latitude, -68°, as the Polar hood seen around 3000Å. A weaker hood is just visible at the North Pole. The negative planetocentric declination of the Earth may be responsible for the southern hood appearing stronger than the northern one. This hood has been interpreted as a haze of moderate density (Owen, 1969), since weak bands show little variation over the disk (Münch and Younkin, 1964). Polarization data (Gehrels *et al*, 1969) and the bright hoods in the deep ultraviolet also indicate conditions at the Jovian poles different from the remainder of the planet. The 9200Å image appears much the same as the 8600Å image, so that the singular appearance of the planet at 8900Å can safely be attributed to the methane distribution above the clouds. The belts tend to appear dark and the zones light on the methane image, but not in the same proportion as the visual image. Interestingly, the relation to the visual brightness is opposite for the Saturn belts and zones (p. 337).

The 1.0-2.1µ TV image shows characteristics of both the normal infrared and methane images. This region has strong ammonia and methane absorptions as well as islands that approach the continuum. A hint of the South Polar hood is visible and the STeB,NEB, and NTeB are dark. The centrally-placed Red Spot is the brightest feature on the planet. Because of inadequate sensitivity of the detector, it was not possible to image separately the spectral ranges corresponding to the ammonia, methane, and continuum, so this image is a composite of all of these and is not uniquely informative about any.

4. Saturn

Color differences on Saturn are far less apparent than on Jupiter; however, certain colors can be reliably observed with a large telescope. The color of the South Polar Region (SPR)[*] may vary from blue-green to grey; the Equatorial Zone (EZ) is often a deeper yellow than the South Temperate Zone (STZ), and the Rings appear a paler yellow than the ball; but since the greatest change in the appearance of the planet is from the blue to the ultraviolet, the most striking color differences escape visual detection.

Data for the Saturn images are found in Table II. The photographs taken from 3000 to 3200Å show the EZ dark, with the Equatorial Band (EB) somewhat lighter. The STZ is bright and the SPR is dark. *Limb brightening* is seen except within the SPR. From 3300 to 3500Å the EB fades, the contrast between the STZ and the SPR increases, and the South Temperate Belt (STB) and South South Temperate Belt (SSTB) become visible because of improved resolution. The contrast between the

---

[*] The system of nomenclature used here follows that of Alexander (1962).
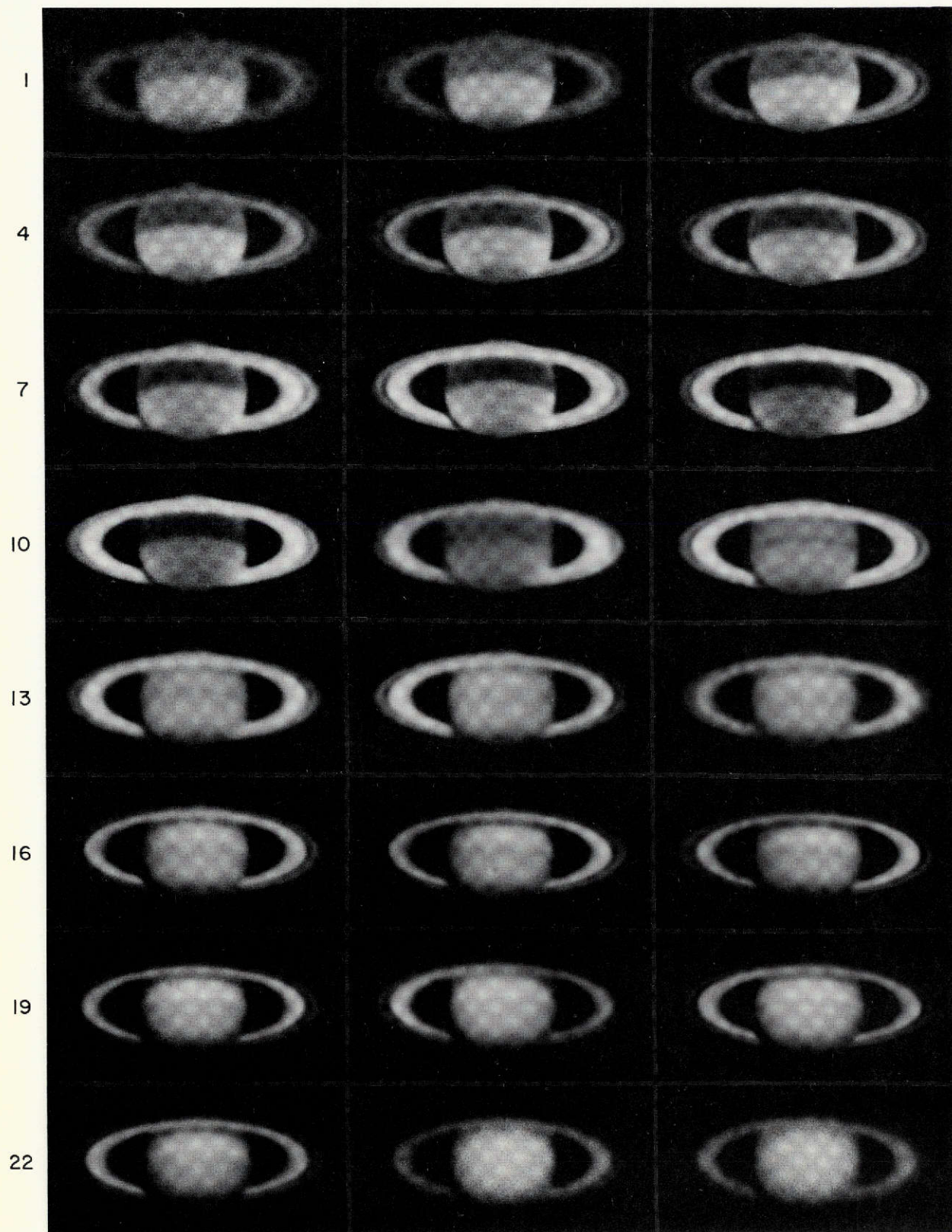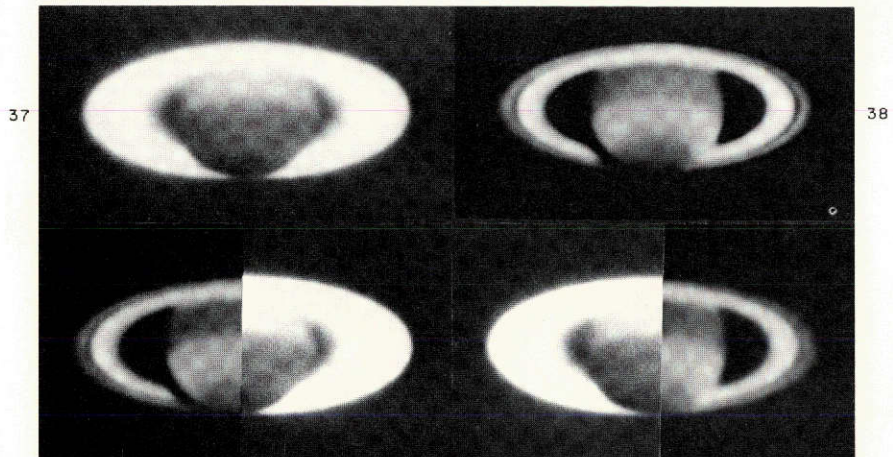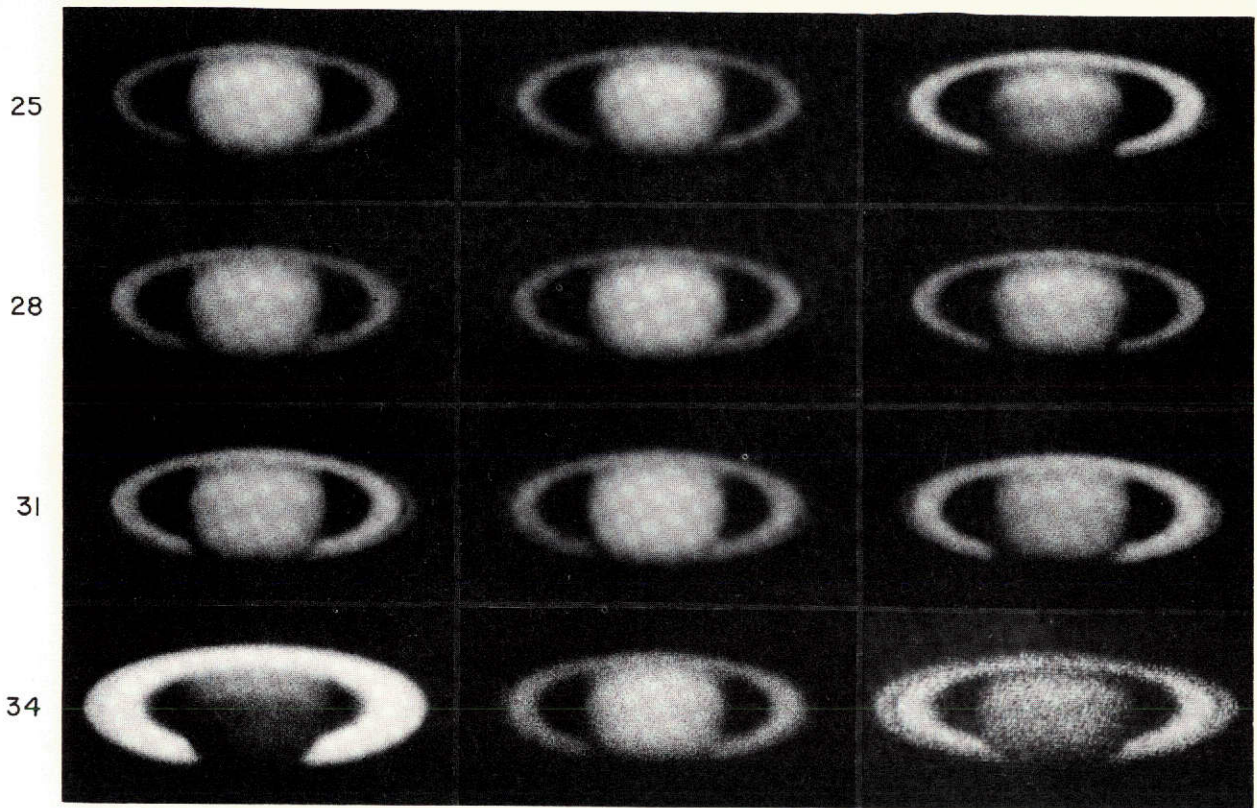
TABLE II

Saturn Photographs

Frame	Date	Time UT	Film	Å	No. images	Exp. Sec.
1	Dec 14 1970	5:04:30	III-O	3000	2	300
2	"	4:56:20	III-O	3090	5	60
3	"	4:48:13	III-O	3200	5	30
4	"	4:45:05	III-O	3325	5	30
5	"	4:42:02	III-O	3420	5	28
6	"	4:38:55	III-O	3530	5	20
7	"	4:36:52	III-O	3625	5	15
8	"	4:35:02	III-O	3720	5	15
9	"	4:32:09	III-O	3800	5	8
10	"	4:29:09	III-O	3940	5	8
11	"	5:25:30	HCC	4000	1	130
12	"	5:29:27	HCC	4260	1	45
13	"	5:31:19	HCC	4440	1	45
14	"	5:33:04	HCC	4600	1	45
15	"	3:52:40	HCC	4810	1	60
16	"	3:54:22	HCC	5000	1	45
17	"	3:57:55	HCC	5200	1	12
18	"	4:00:40	HCC	5400	1	20
19	"	4:02:07	HCC	5600	1	15
20	"	4:03:27	HCC	5800	1	15
21	"	4:05:36	HCC	6060	1	12
22	"	4:08:40	HCC	6200	1	60
23	"	6:08:13	HSIR	6400	5	4
24	"	6:09:29	HSIR	6620	5	4
25	"	6:10:20	HSIR	6775	5	3
26	"	6:17:14	HSIR	7000	5	3
27	"	6:25:31	HSIR	7200	5	4
28	"	6:26:12	HSIR	7400	5	4
29	"	6:27:04	HSIR	7600	5	3
30	"	6:27:43	HSIR	7800	5	3
31	"	6:30:52	HSIR	8000	4	2.5
32	"	6:34:17	HSIR	8300	5	2
33	"	6:34:58	HSIR	8600	5	4
34	"	6:35:57	HSIR	8900	2	24
35	"	6:42:52	HSIR	9200	2	240
36	Oct 21	6:48:00	Plus X	10,000-21,000	5	0.25
37	Jan 25 1972	2:51:44	HSIR	8964	12	90
38	"	3:31:24	103-O	4000	8	1

SPR and the lighter STZ diminishes between 3600 and 3900Å; and at 4000Å the EZ begins to lighten, especially at the North end, and the limb brightening diminishes. At 4200Å the EZ has lightened to equality with the STZ except for the extreme South edge which remains dark. Neither limb brightening nor darkening

is apparent here. Slight *limb darkening* is seen at 4400Å and the North part of
the STZ darkens, while the South part gets lighter. Between 4600 and 5200Å the
North part of the STZ forms a dark band consisting of two dark components separa-
ted by a lighter one; further, the EZ brightens, and the ball and the Rings
achieve approximate equality of brightness. From 5400 to 5600Å the SPR becomes
darker and limb darkening increases. The two dark components of the SEB become
brighter, and from 5800 to 6200Å they continue to brighten until they blend with
the light zone separating them, making the region between the SPR and the EZ
fairly uniform in brightness. Limb darkening increases and the SPR is seen to
be divided into an outer, lighter ring and the darker polar cap. At 7200Å the
EZ is very bright and the SEB is noticeably darker than the STZ. This is pro-
bably due to the 7250Å band of methane which lies within the bandpass of the
filter. In the 7400 to 8600Å region the SEB appears about the same brightness
as the STZ.

In the 8900Å image, which includes the strong methane band, the EZ is bright
and the rest of the planet quite dark, especially the SPR which is the darkest
part of the disk. Considerable limb darkening is seen overall. Frames 37 and
38 show recent 8964Å methane and UV images taken by S. M. Larson; Frames 39 and
40 show the match of the two. The methane picture is undodged. The STB, the
SSTB, and the northern edge of the SPR, as well as the prominent EZ, are light
in the methane image and dark at 4000Å, though the polar cap is dark on both.
Hence, the EZ reaches high altitude while the polar cap contains no high layer
of condensed material. Also, the STB, SSTB, and the North edge of the SPR may
be rather higher than other regions on the planet. Polar haze, present on Jupiter,
is absent on Saturn. The Saturn Rings are, of course, very bright in this image.
At 9200Å the appearance of the planet is similar to the 8600Å image, so no impor-
tant color change takes place around the methane band. The Saturn image taken
with the infrared vidicon in the 1-2μ region is similar in appearance to the 8600Å
image, with strong limb darkening, bright EZ, somewhat darker STZ, and dark SPR.

5. The Rings of Saturn

There is nothing in the images taken to indicate a change with wavelength
in the appearance of the Rings. Differences among these images may all be
attributed to vignetting by the small filters.

REFERENCES

Alexander, A. F. O'D. 1962, THE PLANET SATURN (London: Faber and Faber).
Fountain, J. W. and Larson, S. M. 1972, "Multicolor Photography of Jupiter",
   LPL Comm. No. 174.
Gehrels, T., Herman, B. M., and Owen, T. 1969, "Wavelength Dependence of Polari-
   zation XIV. Atmosphere of Jupiter", *Astron. J., 74,* 190-199.
Münch, G. and Younkin, R. L. 1964, "Molecular Absorptions and Color Distributions
   Over Jupiter's Disk", *Astron. J., 69,* 553.
Owen, T. C. 1969, "The Spectra of Jupiter and Saturn in the Photographic Infrared",
   Icarus, 10, 355.

NO. 176   LATITUDE MEASURES OF JUPITER IN THE 0.89μ METHANE BAND

by R. B. Minton

November 30, 1972

ABSTRACT

Jupiter has been photographed by the Lunar and Planetary Laboratory in the 0.89μ methane band since October 1968. A photometric evaluation of these photographs has not yet been carried out, but a visual study of this collection and a comparison with the color records has been made. This comparison, together with diameter and latitude measures of the methane records, shows that the albedos and latitudes of most features shown in 0.89μ vary with time and that there is no simple correlation between the visual color and/or intensity of a feature and its intensity in the methane band. The latitudes of the Red Spot and South Tropical Zone have remained unchanged, while those of the Equatorial Zone, North Tropical Zone,and South Polar Hood have changed. Measures of images taken near opposition show the polar diameter to be within 0.5% of the American Ephemeris value, but the equatorial diameter as 1.3% smaller. Measures near quadrature suggest a phase defect 3.5 times greater in value than the American Ephemeris value. The large phase defect and bright South Polar Hood contribute to the circular appearance of Jupiter in methane. Latitude variations of the North edge of the South Polar Hood support the 1964 Münch and Younkin hypothesis that this feature is composed of frozen methane.

Jupiter has been photographed in the 0.89μ methane band with the 154-cm reflector from October 1968 through 1972, and with the Cerro Tololo Inter-American Observatory 152-cm reflector in Chile in 1969. The images measured were obtained with both telescopes at f/13, at a scale of approximately 10"/mm, and with exposure times of 60-120 seconds on Kodak High-Speed Infrared (HSIR) film. In addition, photography in this band began with an RCA 6914 infrared image-converter tube in June 1971; but these images lack astrometric quality and continuity of the direct photographic images and have not been measured. The small scale and long exposures of the direct images cause a decrease in angular resolution as compared to more conventional photography. Other than the Red Spot (RS), bright and dark spots and similar small-scale markings are not recorded - only featureless belts and zones. There have been only two exceptions noted during these four apparitions. The South Equatorial Belt (SEB) disturbance white spot (WS) was photographed July 10, 1971; and the long-lived South Temperate Zone (STeZ) White Oval BC was barely recorded August 23, 1972. As part of the present study, the LPL color photographs have been carefully compared with the methane records.

TABLE I

Mean Latitudes and Standard Deviations

(0.888μ)

Feature	Apparition			
	1968-69	1969-70	1971	1972
n/SPH	$-67°.9 \pm 1°.3$	$-69°.4 \pm 1°.2$	$-70°.2 \pm 0°.7$	$-69°.0 \pm 1°.3$*
s/STeZ	--	-41.3 ± 1.2	--	--
n/STeZ	--	-35.1 ± 1.0	--	--
s/RS	--	-29.3 ± 0.6	-30.0 ± 0.4	-28.5 ± 0.2
s/STrZ	-26.5 ± 0.8	-27.0 ± 0.6	-27.1 ± 0.6	-26.2 ± 0.5
n/STrZ	-18.0 ± 0.8	-19.6 ± 0.8	-19.9 ± 1.4	-19.6 ± 0.5
n/RS	--	-16.7 ± 1.4	-15.4 ± 0.4	-17.2 ± 0.3
s/EZ	$- 5.7 \pm 0.5$	$- 8.5 \pm 0.8$	$- 7.0 \pm 0.8$	-10.5 ± 0.7
n/EZ	6.5 ± 0.8	1.8 ± 2.7	4.0 ± 1.3	8.4 ± 0.7
s/NTrZ	17.6 ± 1.0	16.9 ± 0.7	17.6 ± 0.7	19.0 ± 0.5
n/NTrZ	22.8 ± 0.8	23.3 ± 0.6	25.5 ± 0.6	24.9 ± 0.4
s/NTeZ	--	30.6 ± 0.5	--	--
c/NTeZ	--	--	--	34.8 ± 0.4**
n/NTeZ	--	34.9 ± 0.2	--	--
s/NNTeZ	--	--	38.9 ± 0.4	--
n/NNTeZ	--	--	44.3 ± 0.3	--

      n/: North edge
      s/: South edge
      c/: center
      *: -67.8 ± 0.9 with 0.886μ filter
     **: very faint, only center was measured

2. Method of Measurement

The latitude measures were made with the digitized Mann measuring machine, previously used by D. W. G. Arthur for selenodetic measures. Six digits of X and Y to 0.001 mm, plus seven digits of keyboard information, constitute one setting with a nineteen-digit field. The central meridian (CM) of the image is brought into coincidence with the Y crosshair and measures are made along the CM   at power 3x. Four settings each are required for a North and South determination; South limb, South edge of feature, North edge of feature, and North limb. The tape-to-card program punches one card containing four settings. Each image is measured at least three times for each feature. The latitude reduction program (JLAT) utilizes the LPL IBM 1130 computer, and calculates from four set-tings the North and South latitudes of the feature, the latitude of its center,
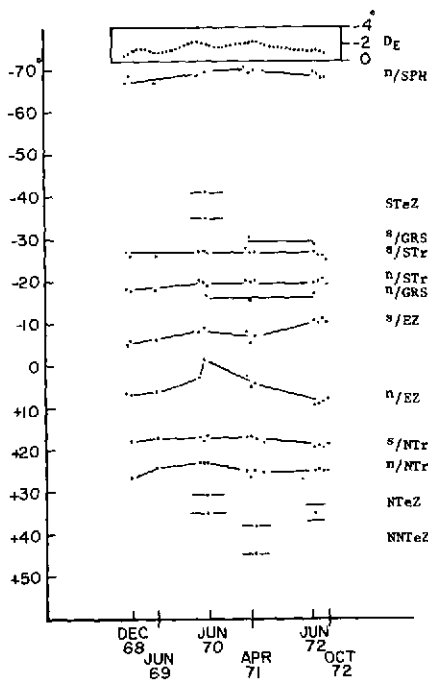
Fig. 1 Summary of latitude mea-
sures of features observed on
methane records. South is up.
Explanation of dots in Fig. 2.
D_E (insert on top) is on dif-
ferent scale
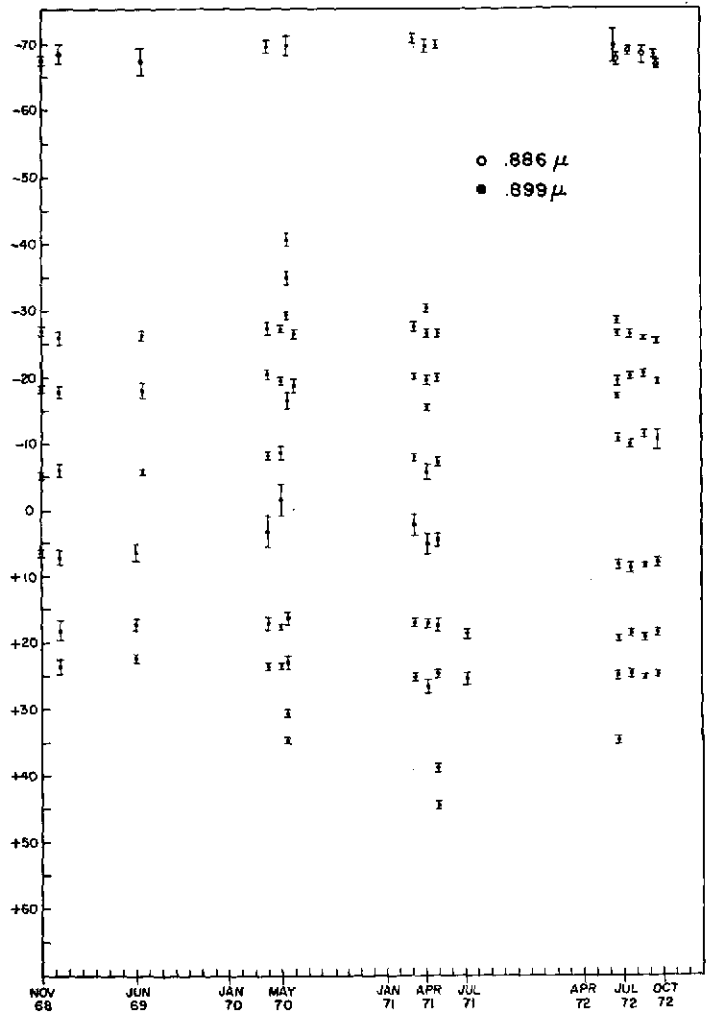
Fig. 2 Explanation of dots used in Fig. 1. Most points represent averages over 2-4 weeks; error bars are standard deviations for that period.

the width, and a ratio named AVG. R. This is the angular ratio of the measured
polar diameter to that of the American Ephemeris diameter. AVG. R. provides a
check of measuring consistency and possible scale changes. This has proven
valuable toward consistent measures of black-and-white and color original images
of varying density, contrast, and scale. If the scale is unknown, AVG. R. cannot
be found. In this event, an approximate value of the scale is calculated in JLAT
from the limb settings and latitudes are redetermined from this average scale
value. This procedure reduces the systematic and random errors in measures of
features at high latitudes. Finally, the cards are arranged by feature and de-
sired time interval, and run to calculate averages and standard deviations. The
large number of measures required for this type of program dictates the use of a
digitized Mann and computer reduction. The present study is based on 780 latitude
and 100 diameter measures.

3. Measurement Errors

In 1972 a new methane filter (0.886μ) was acquired. Figure 3 shows the trans-
mission of this filter, the older filter (0.899μ), the sensitivity curve of the
HSIR film, and of the SI image tube. It is seen that, used with the image tube,
the new filter is much superior to the old one; with the HSIR film, the contribu-
tion of μ>0.900 was not too serious. Fifty-four comparative measures of identi-
cal features on images taken nearly simultaneously with the two filters show that
the standard deviation (sd) of latitude measures of all features for the 0.899μ
filter is 0°.75 in latitude, and 0°.62 for the new 0.886μ filter, which gives higher
contrast.

The first test of accuracy was a measurement of the methane polar diameter
and a comparison with the American Ephemeris value. The oblateness of Jupiter in
methane light was in question because of the apparent circularity of many images.
If there was a difference, additional investigation and modification to JLAT would
be necessary. Toward this comparison, the author secured 38 methane images taken
within 35 hours of opposition. Seventeen of the best images taken on June 25.35,
1972 were measured.

	0.886μ	A.Eph.	O-C
P. Dia.	43".76 ± 0.25 (sd)	43".55	+0".21
Eq. Dia.	46".06 ± 0.34 (sd)	46".67	-0".61

There is no difference in the polar diameters greater than the standard deviation
of the measures. This difference is less than one part in 175 for 17 images. For
latitude measures of a single image, an AVG. R. of 0.9900 to 1.0100 is tolerated.

Investigation of a possible systematic error due to the bright South Polar
Hood (SPH) was made by comparative measures of the latitude of J1 (Io) in methane
light and blue light. These images were taken within a maximum time interval of
15 minutes and were secured with J1 near the CM. Forty-eight North and South
latitude measures of 3 methane images and 5 blue images yield:

|	0.899μ	0.430μ	Diff.
J1 Latitude	17°.31 ± 0°.49	16°.86 ± 0°.46	+0°.45 (N)
J1 Width	5°.32 ± 0°.52	3°.37 ± 0°.48	+1°.95
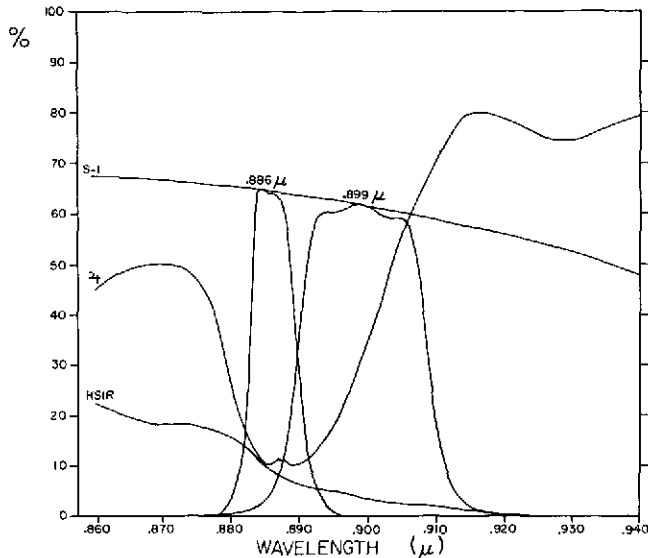
Fig. 3 Relative response of S-1 photo-emissive surface (RCA 6914), with
100% assumed at 0.370μ; Sun/Jupiter intensity ratio for EZ, from Carl
Pilcher (1971); relative sensitivity of Kodak HSIR film, with 100% assumed
at 0.400μ; and transmission of 0.899μ and 0.886μ filters

The latitude difference is less than 0°.5 or 1 part in 230 of Jupiter's diameter.
The blue sd is large because of the poor visibility of Jl at the CM in blue
light. In contrast, the brightness of Jl relative to Jupiter's disk in methane
results in an irradiation of 0°.98 at the North and South edges at -17° latitude.
This value should represent an upper limit, as all methane features have an albe-
do below that of Jl. The conclusion is that the methane polar diameter is in
agreement with the American Ephemeris, and that the bright SPH does not contri-
bute a systematic error greater than the random errors of measurement.

When the scale is defined, JLAT uses limb settings to determine the center
of the disk. Latitudes are calculated from the fractional distance of a feature
from the center of the polar diameter, using the Ephemeris value and the known
plate scale. There will be no error in the location of the measured center as
long as the errors in the polar limb measurements, depending on the density
of the images, are the same. If the plate scale was unknown, the polar radius
was determined from the polar limb settings. In that case the center of the disk
is still well determined, but the derived latitudes will be affected by systematic
errors in the limb settings.

Test measures of a computer-drawn (GLOBE) grid with scale unspecified in-
dicate that North and South limb settings, each $\frac{1}{2}$% of a polar diameter too
large,resulted in an O-C error of +1°.3 at -70° latitude, and +0°.1 at 0° latitude.
With a specified scale, these errors were reduced to zero for both latitudes.
Test measures with scale unspecified and with only the South limb 1% too large
gave errors of +2°.7 at -70° latitude, and +0°.8 at 0° latitude. With a specified
scale, these errors were reduced to 1°.6 and 0°.7,respectively.

The scale should be known to at least ±0.2% for latitude and longitude measures of Jupiter. Double-star photography in early 1972 with the Catalina telescope at f/13.5 allowed determination of the present scale to within this limit, and also showed that this limit is exceeded when the film plane moves more than 28 mm in either direction along the optical axis. Consequently, because of scale uncertainties, measures prior to 1972 have been run twice on the IBM 1130. The first run determined a scale for every four settings if scale was unknown. It was found that a minimum of four scale values was required for the four apparitions. The second run used the appropriate scales and also calculated average latitudes and their sds. The sd of all latitude measures arranged by year and telescope are: 1972 Catalina $0°.57$, 1971 Catalina $0°.67$, 1970 Catalina $0°.91$, 1969 Cerro Tololo $1°.00$, and 1968 Catalina $0°.79$.

The sds for 12 comparative measures of the SPH at $-70°$ latitude are $1°.26$ for the 0.899μ filter and $0°.75$ for the 0.886μ filter. There is a systematic error between the 0.889-0.886μ filter of $+1°.9$ latitude (N). This stems from the reduced intensity of the adjacent polar region which introduced some additional irradiation. The magnitude of this error is exaggerated by the high latitude of the feature. Measures of all other features were mutually consistent to $0°.3$ latitude and were averaged together with equal weight. Consolidated measures with both filters are listed as at 0.888μ.

4. Results

The measured equatorial diameter near opposition is 1.3% ± 0.7% (sd) less than the American Ephemeris value. This results from the large equatorial limb darkening. The equatorial diameter was measured again with Jupiter near evening quadrature on September 22.09, 1972, when the geometrical phase defect was $0''.36$ in angular width. Measures give an equatorial diameter $1''.51$ less than the American Ephemeris value of $38''.63$. The loss at each limb cannot be directly measured as there were no measurable features which would permit determination of the CM. The amount of recorded phase defect can be estimated by the measured limb loss at opposition compared to that at quadrature. The equatorial radius was measured to be reduced by 0.65% at each limb with no defect present. Subtracting this value from the total defect at quadrature would give an angular loss of $1''.26$ at the East limb. This is 3.5 times greater than the geometrical value and is defined as the "phase exaggeration". (Smith and Reese, 1968).

The measured latitudes of the RS and the South Tropical Zone (STrZ) are the most consistent with measures at 0.430μ; these features also varied by the least amount of latitude in methane light.

	1970			1971		
Feature	0.888μ	0.430μ	0.888-0.430μ	0.888μ	0.430μ	0.888-0.430μ
s/RS	$-29°.3$	$-28°.6$	$-0°.7$	$-30°.0$	$-28°.9$	$-1°.1$
n/RS	-16.7	-16.2	-0.5	-15.4	-16.2	+0.8
s/STrZ	-27.0	-24.8	-2.2	-27.1	-25.8	-1.3
n/STrZ	-19.6	-20.6	+1.0	-19.9	-20.0	+0.1

There is some tendency for measures at the North edges (n/) to be about $1/2°$ too high (N), and South edges (s/) about $1°$ too low (S). The measures of J1 show that some of this may be attributable to irradiation. The agreement in this comparison with external data (Reese, 1971, 1971a) exemplifies the measuring accuracy of other methane features.
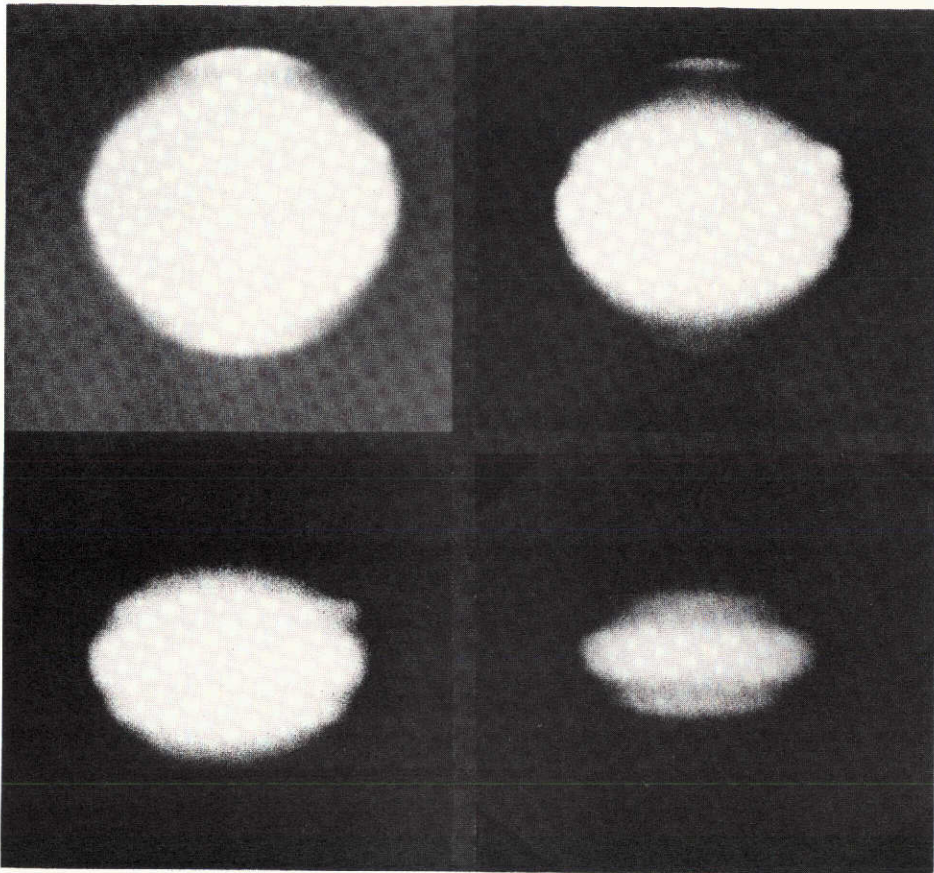
Fig. 4   1972 July 22, 04:11 UT, Jupiter at 0.886µ printed with high contrast at different densities to show relative densities in original image; no dodging
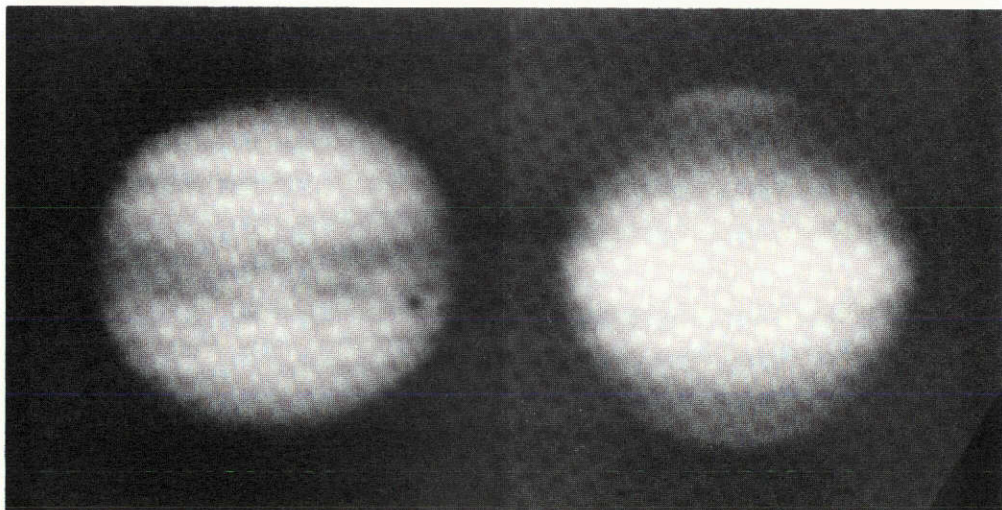

Fig. 5 *Left*: Panchromatic,1972 June 19, 07:28 UT, λ_2=136.4.   *Right*: 0.886µ,1972 June 21, 09:22 UT, λ_2=146.2; 3 min exposure at f/45 with RCA 6914 infrared image-converter tube

The greatest change in latitude during this interval was the decrease and subsequent increase in width of the Equatorial Zone (EZ). The ^{n}/EZ changed from $+7°.2$ in early December 1968 to $-1°.5$ in early May 1970, to $+9°$ throughout 1972. From late 1970 to early 1971, the ^{n}/EZ was castellated in longitude between the latitudes of $1°.5$ and $+2°.3$. The South edge moved irregularly from a minimum of $-5°.7$ in 1968-69 to $-10°.5$ in 1972. The greatest change in latitude of the South edge occurred between May 1971 and June 1972. Both edges were moving away from the equator at the highest observed rate during the 1971 apparition. The rapid increase in brightness of the EZ occurred between September 1971 and June 1972, but the Northward movement of the ^{n}/EZ was already in progress by March 1971.

The ^{n}/SPH varied in latitude by only $3°.2 \pm 1°.2$ (sd) during this interval. Because of this large uncertainty, a least-squares analysis of 43 measures from 1968-69 and 1970 was made and compared with a similar analysis of 29 measures from 1971 and 1972. No images taken with the 0.886µ filter were included. The first two apparitions give a slope of $-0°.78$/yr $\pm 0°.24$ (sd slope); and the last two, $+0°.85$/yr $\pm 0°.38$. During these time intervals, the slopes of the values of the declination of the Earth as seen from Jupiter (D_E) were $-0°.83$/yr and $+0°.73$/yr, respectively. The values of the declination of the Sun as seen from Jupiter (D_S) were $-0°.83$/yr and $+0°.80$/yr. Therefore, the latitudes of the ^{n}/SPH varied in the same direction as D_E and D_S, and within the sds of the slopes, by the same amount.

In 1971 the South edge of the North Tropical Zone (^{S}/NTrZ) moved about $4°.5$ South and the ^{n}/NTrZ about $1°$ South at visible wavelengths, but in methane light the South edge remained stationary and the North edge moved about $2°$ North. Figure 1 depicts these events, Figure 9 shows the rapid change in latitude of the NTrZ in blue light (0.430µ), and Figure 6 shows Jupiter at 0.430µ and 0.886µ near opposition, 1972. Throughout 1971 and 1972 the widened NTrZ in methane included both the NTrZ and North Temperate Belt (NTeB).

The STeZ, North Temperate Zone (NTeZ), and North North Temperate Zone (NNTeZ) were not consistently photographed. In some cases when these features were absent, the photographic resolution was judged to be better than those images taken at other dates showing the features. The latitudes of these three zones are in good agreement with values obtained at 0.430µ by myself and Reese (1970, 1971). The NTeZ was only measurable once during the 1972 apparition - that of June 21, 1972 near System II longitude (λ_2) = 75°. Methane photographs taken later that night show this zone becoming broader towards the North and indistinct near λ_2 = 140°. Figure 5 compares a color image and a methane image at nearly equal CM System II (ω_2) longitudes only two days apart.

5. Interpretation of the Methane Photographs

The surface intensity at 0.888µ is inversely correlated with the amount of overlying methane gas. This is the basis of the following interpretative remarks based on visual inspection. At this time it does not seem justified to undertake a time-consuming photographic photometry of the methane collection.

Visual inspection of the original methane images in our collection shows that from 1968-69 through 1972:
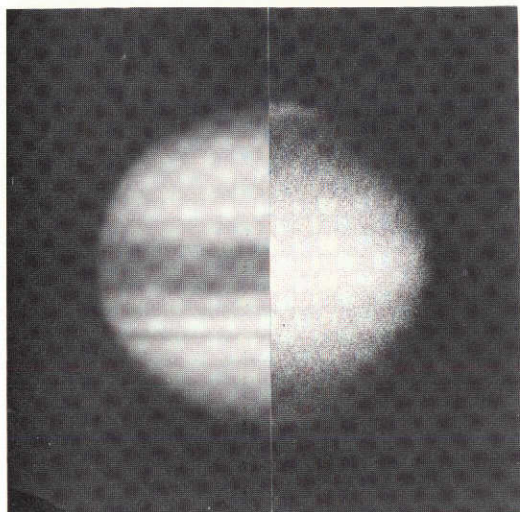
Fig. 6 *Left*, 0.430μ, 1972 July 21; *right*, 0.996μ, 1972 June 25
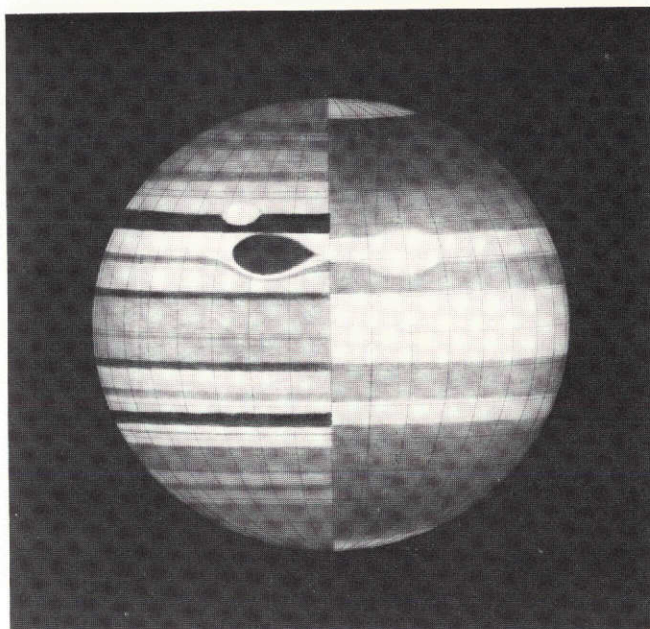
Fig. 7 Drawings from 0.430μ and 0.888μ latitude measures for opposition, 1972
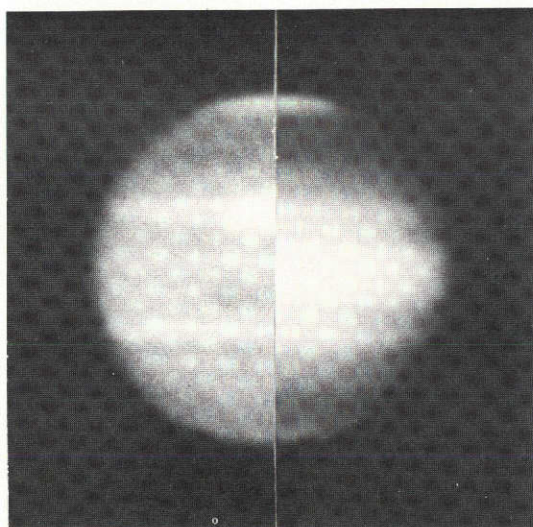
Fig. 8 *Left*, 0.899μ, 1970 May 16; *right*, 0.886μ, 1972 June 26; 90 sec exp at f/22 with RCA 6914
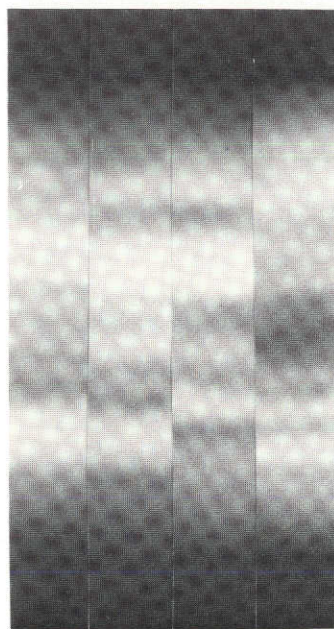

Fig. 9 Jupiter's belts and zones at 0.430μ for 1968-69 through 1972

(1)   Both polar regions appear somewhat darker than the rest of the
      disk, excluding obvious zones.
(2)   The South Polar Region (SPR) is slightly darker than the North
      Polar Region (NPR).
(3)   The RS is the brightest feature.
(4)   The STrZ is almost or equally bright as the RS.
(5)   Except in 1968-69, the NTrZ is equal in brightness to the STrZ.

A visual comparison of the color and methane collection for these four
apparitions (see Table II) reveals the following:

(1)   Throughout the four apparitions the RS was always yellow-red in
      color, and was always bright in methane.
(2)   Throughout the four apparitions the STrZ was always bright and
      nearly white, and was always bright in methane.
(3)   From 1971 through 1972 the NTeB was yellow-red in color, and was
      bright in methane. Prior to this it was split and faint, and also
      faint in methane.
(4)   In 1972 the EZ was yellow-red in color, and bright in methane.
(5)   In 1969-70 the EZ was dominated by cyan-colored festoons, and was
      dark in methane.
(6)   In 1969-70 when the NTrZ became light red in color, it also became
      bright in methane.
(7)   During the four apparitions the NNTeZ was most prominent in 1971.
      This was true in methane as well.
(8)   Throughout the four apparitions, the three long-lived STeZ White
      Ovals BC, DE, and FA, were frequently as bright as any zone, but
      they were nearly absent in methane.
(9)   In 1968-69 the NTrZ was one of the brightest zones, but was faint
      in methane.
(10) Throughout the four apparitions, the STeZ was quite prominent, but
      was faint in methane.
(11) In 1971 prior to the two SEB disturbances, the South Equatorial
      Belt Zone (SEBZ) was the brightest zone, but was dark in methane.

6. Discussion

The latitude of the ^{n}/SPH varied in the same direction and amount as the
value of D_E and D_S. The visible effect of this is that the apparent width of
the SPH remained unchanged. Because the sd of the slopes of the observations
is greater than the difference between the slopes of D_E and D_S, either or both
of these two parameters may have contributed to the observed latitude varia-
tions. A dependence on D_E would suggest that it is a diffuse feature and is
rendered more easily visible by the increased light path when viewed edge-on.
A dependence on D_S would suggest that insolation is responsible.

The latitude of the ^{n}/SPH is very close (< sd) to the latitude of the
South edge of the South Polar Belt (^{S}/SPB) measured by Reese at 0.430μ for
the same apparitions. His measures also show a latitude variation of the
^{S}/SPB very similar to that of the ^{n}/SPH (Reese 1970, 1971, 1971a). This and
the scarcity of features at these high latitudes is strong evidence that they

are a common edge of two features. At both wavelengths, Jupiter becomes brighter South of this latitude. The North Polar Hood (NPH) was consistently weaker in appearance than the SPH and could not be measured.

The rapid brightening of the EZ appears to be a result of the June and July, 1971 SEB disturbances. The WS reported on p. 340 did move from the SEBZ into the Southern component of the EZ over a period of five weeks. Additional material may have been transported along this path, or the increased activity in the EZ evident at visible wavelengths was effective in mixing the higher gaseous atmosphere with the lower reflective cloud particles. In either case, the optical depth of the EZ at 0.888μ would be reduced.

The expansion of the EZ may coincide with these two disturbances. However, the Northward motion appears to have started within the interval three to twelve months prior to this. The Southward motion coincided with the disturbance more closely, but a longer coverage is needed before a relationship of these latitude variations can be suggested.

TABLE II

Visual Estimates of Colors and Intensities in
Visible Light vs. Methane Light
(explanations, p. 350)

Feature	1968-69			1969-70			1971			1972		
	Color/I		CH_4	Color/I		CH_4	Color/I		CH_4	Color/I		CH_4
SPR	G	4	0	G	4	0	G	4	0	G	4	0
SPB[a]	C[f]	3	4	C	3	4	Lt C	3	4	C	3	4
SSTeZ	--[e]			W	5		--			--		
SSTeB	G	4		G	3		G	4		G	4	
STeZ	W	6	0	W	6	2	W	6	2	W	6[g]	2
BC,DE,FA	W	6		W	6		W	6		W	6	
STeB	G[d]	3	G	G[d]	3		G[d]	3[h]		Br	3[h]	
STrZ	Lt C	7	6	W	7	6	W	7[g]	6	W	6	6
RS	Y+R	3	6	Y+R	3	6	Y+R	3	6	Y+R	3	6
SEBs	Lt R	5		G	4		G4/G3[j]			Lt R	5	
SEBZ	W	6		W	7[g]		W8[g]/k	5		Lt R	6	
SEBn	Br	4		Lt C	5		Br4/k	4		Lt R	5	
EZs	Br	4	6	Lt C	5	2	Br	4	2	Br	4	6
EZ[b]	Lt Y	5	6	Lt Y	5	2	Br5/k	4	2	Y+R	5	6
EB[c]	Y+R	4		C[i]	4		G4/k	4		--		
EZn	Br+C[i]	4		C[i]	4		Br+C[i]	4		Br	4	6
Festoons	C	4		C	3		C	4		C[n]	4	
NEBs	Br	3[h]		Br+R	3[h]		Br	3[h]		G	3	
NEBZ	Br	4		Br+R	4		--			G	4	
NEBn	Br	3		Br+R	3[h]		Br	3[h]		G	3	
NTrZ	W	7[g]	4	Lt R	7	6	W5/W7		6	W	6	6
NTeBs	--			--			Y+R[m]	4	6	Y+R[m]	4	6
NTeBn	--			--			Y+R[m]	4	6	Y+R[m]	4	6
NTeZ	W	7	2	W	6	2	--		2	W	6	2
NNTeB	--			--			--/G3			--		
NNTeZ	--			--			--/W5		2	--		
NPR	G	4	0	G	4	0	G[d]	4	0	G	4	0

Explanations of Table II

The colors are the apparition average, unless otherwise noted. They were determined by visual comparison with Kodak Color Compensating (CC) filters of similar density. The intensity estimates of color images are in accordance with the Association of Lunar and Planetary Observers Jupiter Handbook (1964) by Reese. The methane intensity estimates use four steps of intensity: 0 = dark, 2 = faint, 4 = average, and 6 = bright.

Superscripts:

a. SPB for visual light, SPH for methane light
b. $\pm 7°$ latitude, excluding EB, darker markings, and festoons
c. Near 0° latitude
d. Grey color, also warm in tone
e. Absent or faint
f. Underlined colors are vivid
g. Brightest feature(s) on disk
h. Darkest feature(s) on disk
i. Festoons contributing color to that feature
j. Before/after the SEB disturbances
k. Much turmoil, colors include cyan, yellow, and red; colors vary with longitude
m. Joined into one belt, the NTeB
n. Very few in number

There may be a tendency for yellow-red belts to appear bright in methane, but this cannot be said for spots except the Red Spot. Many of these were noted during this interval, especially in the EZ, yet were not prominent or visible in the methane photographs. However, the lower resolution of the methane photographs will hinder detection of small colored features. The EZ was near maximum darkness when the cyan-colored festoons were most numerous and colorful. The absence of high clouds in methane at this time would suggest that festoons normally occur at lower levels. This is consistent with infrared observations at 5μ of a dark feature by Westphal (1969). LPL color photographs show this feature to be a cyan-colored festoon. The color may be indicative of locally greater amounts of Rayleigh scattering and absorption of the red by the atmospheric methane. LPL results since 1969 abundantly confirm this correlation of blue color with deep penetration (cf. p. 221 and refs. there given).

The sudden appearance of the yellow-red colored NTeB in 1971 appears to be responsible for the [n]/NTrZ moving North in latitude and including this belt in its expanse. Curiously, the [S]/NTrZ moved North by about 4° one year after the [n]/NTrZ moved North by the same amount.

The scarcity of long-lived zones poleward of the tropical zones, and the somewhat greater darkness of the polar regions in methane light, suggest an increased depth of the denser haze layer as one approaches the polar areas, no doubt owing to lower tropospheric temperatures. The meteorology of Jupiter within 100 to 200 km of the visible cloud deck has

been suggested to be internally-driven (Kuiper, 1972), and the largest escaping
flux appears to be within the boundaries of the tropical zones (Keay, Low, Rieke,
1972). A relatively stagnant SPR is consistent with the suggestion by Peek (1958)
that spots at latitudes South of -45° have almost a uniform rotation period.
The suggestion was made by Münch and Younkin (1964) that the bright Polar Cap
observed with their spectrophotometer might consist of frozen methane. A tempera-
ture and pressure range of from 91°K at 1 atm to 64°K at 0.05 atm would permit
methane to exist in a solid phase for a comparatively long time. If the equili-
brium of the two phases was at a critical temperature and pressure, a small change
in temperature resulting from a small change of D_s might produce a large shift in
equilibrium. The Münch and Younkin hypothesis is consistent with the latitude
variation of the North edge of the SPH.

This study illustrates the need for extensive time coverage in the study of
Jupiter. One cannot catagorize the various types of telescopic features (belts
vs. zones) by differing amounts of methane absorption based on a few observations
only.

Acknowledgments.   I am indebted to Steven Kutoroff for converting American
Ephemeris data from magnetic tape to punch cards, and to Richard Poppen for his
interest in writing the GLOBE Jupiter computer program. This work was supported
by the NASA Grant NGL-03-002-002.

REFERENCES

Keay, C. S. L, Low, F. J., and Rieke, G. H. 1972, "Infrared Maps of Jupiter",
    Sky and Telescope, *44*, No. 5, 296-297.
Kuiper, G. P. 1972, *Sky and Telescope*, Jan-Feb issues; and *LPL Communication
    No. 173.*
Münch, G. and Younkin, R. L. 1964, *Astron. J., 69*, 553.
Peek, B. M. 1958, THE PLANET JUPITER, Faber and Faber, London.
Pilcher, C. B. 1971, private communication.
Reese, E. J. 1970, "Photographic Observations of Jupiter in 1968-69", N.M.S.U.
    TN-701-70-32.
Reese, E. J. 1971, "Photographic Observations of Jupiter in 1969-70", N.M.S.U.
    TN-71-38.
Reese, E. J. 1971*a*, "Photographic Observations of Jupiter in 1970-71", N.M.S.U.
    TN-72-41.
Smith, B. A. and Reese, E. J. 1968, "Observations of Io at Inferior Geocentric
    Conjunction", Contributions of the Observatory, *1*, No. 2, N.M.S.U.
Westphal, J. A. 1969, "Observations of Localized 5-Micron Radiation from Jupiter",
    Ap. J., 157, L63-L64.

ADDENDUM

Recommended Abbreviations (BAA system, with minor modifications)
used in this and subsequent papers

A. Features, Locations, Directions

B	Belt	CM	Central Meridian
Z	Zone	Tr	Tropical
R	Region	Te	Temperate
H	Hood	n	North component of Belt or Zone
P	Polar	s	South component of Belt or Zone
E	Equatorial	p	preceding edge
N	North	f	following edge
S	South	c/	center
RS	Red Spot	s/	South edge
WO	White Oval	n/	North edge

B. Colors

G	grey	R	red
Cy	cyan (blue-green)	Br	brown
W	white	Lt	light
Y	yellow		

NO. 177 PHOTOGRAPHIC OBSERVATIONS OF THE OCCULTATION

OF BETA SCORPII BY JUPITER

by Stephen M. Larson

April 1972

ABSTRACT

The occultation of the multiple star Beta Scorpii by Jupiter was observed visually and photographically from the Bosscha Observatory in Lembang (Java), Indonesia, on May 13, 1971. The photographs recorded the dimming of the stars as the light was differentially refracted by the Jovian atmosphere, and gave support to a scale height much greater than 8 and more nearly 30 km (Fig. 7). In addition, during the ingress of Beta Scorpii, *flashes* up to 1 second long were observed visually (while guiding, in the reflex device of the camera) that occurred at irregular intervals, spaced by 2-8 seconds, over a total period of 7 minutes. Measurements of the position of the brightest component of Beta Scoprii during ingress shows refraction of approximately 1".4 before becoming unobservable.

1. Introduction

An observing run was made at the Bosscha Observatory in Lembang (Java), Indonesia, during the month of May 1971 (Larson 1971) in preparation for an extensive stay in the summer to observe Mars during its favorable opposition. The project involved the observation of Jupiter, Mars, and Mercury as a part of the continuing program of planetary photography which is carried out by this Laboratory (Kuiper 1972*a*, 1972*b*, Fountain and Larson 1972).

Taylor (1970) calculated the occultation of Beta Scorpii to occur at about 18[h] UT on 13 May 1971, predicting that the best observations could be made from the region of the Indian Ocean. We had made no plans to observe the occultation since we understood that the Director of the Observatory, Dr. Bambang Hidajat, had planned to make visual timings of ingress and egress for Dr. W. B. Hubbard's program at the University of Texas. However, as soon as our equipment was adapted to the twin 60-cm refractor, it became evident that a program of photography would not interfere with Hidajat's visual timings and would, in fact, supply additional data. As there was no time to test for optimum image size and exposure times, the scale that was used (3.75 arc sec mm^{-1}; f/76) was chosen so that the exposures ($\frac{1}{2}$, 1 sec) would be minimized to give the best records of the instantaneous brightness of the star. This proved to be a good choice since the light from the "flashes" might not have been recorded otherwise.

2. Observations

The configurations of the objects observed during occultation are shown in Figure 1. Beta Scorpii is a B0.5V spectroscopic binary of visual magnitude 2.63 and has a companion of magnitude 9 at a distance of 0.5 (P.A. = 132°) (Hubbard, et al. 1972) which, under the observing conditions, could not be detected. Another star, SAO 159683, of visual magnitude 4.92, type B2V, and 13.64, North of Beta Scorpii (P.A. = 24°) (Hubbard, op. cit.) was also occulted. At the time, Jupiter was 10 days before opposition and was moving Westward by its equatorial diameter of 45.04, in about 2.5 hours.

The photographs were taken with the double 60-cm Zeiss refractor which has one objective corrected for blue light and one for yellow (Voûte 1933). The ingress of both stars was recorded with the visual refractor on Kodak 4X Panchromatic film with a Schott GG-14 yellow filter, and the egress of both stars was recorded on unfiltered Kodak 103-0 spectroscopic emulsion with the photographic telescope (Fig. 2). All black-and-white films were processed at the Observatory in Kodak D-19 for 6 minutes at 68°F.

Although the rainy season on Java is usually over by April, it lingered well into May, greatly reducing the anticipated observing time. Most of the night of May 13 was cloudy, but occasional clearing of the clouds allowed observation of the first ingress, while only incomplete coverage of the other events was obtained. As SAO 159683 disappeared, photographs were taken at a rate which was estimated to include the whole event on one 36-exposure roll, since changing film or cameras would take too much time. Between exposures, the occultation was observed visually through the reflex sight of the camera whose ground glass was replaced by clear glass with a reference cross-scratch. The star dimmed as expected with no peculiarities; the first ingress having a duration of only 60 seconds because of its location near Jupiter's equator. This series (Fig. 3) was the only event not hampered by clouds.

Because of the clouds, the ingress of Beta Scorpii (Fig. 4) was first observed after it had already begun to dim; after about two minutes of the expected dimming, we noticed that it reappeared intermittently, with these reappearances lasting less than a second and occurring irregularly every 2-8 seconds. The first suspicion was that variation in the seeing was responsible for the flashes but after careful observation, it was obvious there was no correlation. The flashes continued to be observed for almost 7 minutes, bring-
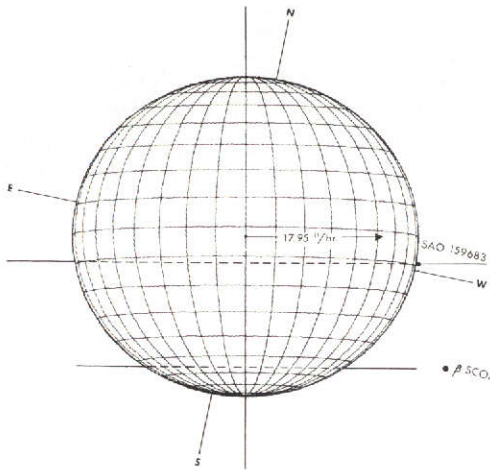
Fig. 1 Configuration of the occul-
tation of ingress of SAO 159683

Fig. 2 (upper) Jupiter in yellow
light near ingress of SAO 159683
($17^h44^m17^s$ UT); (lower) Jupiter in
blue light after egress of Beta
   Scorpii ($19^h49^m39^s$ UT)
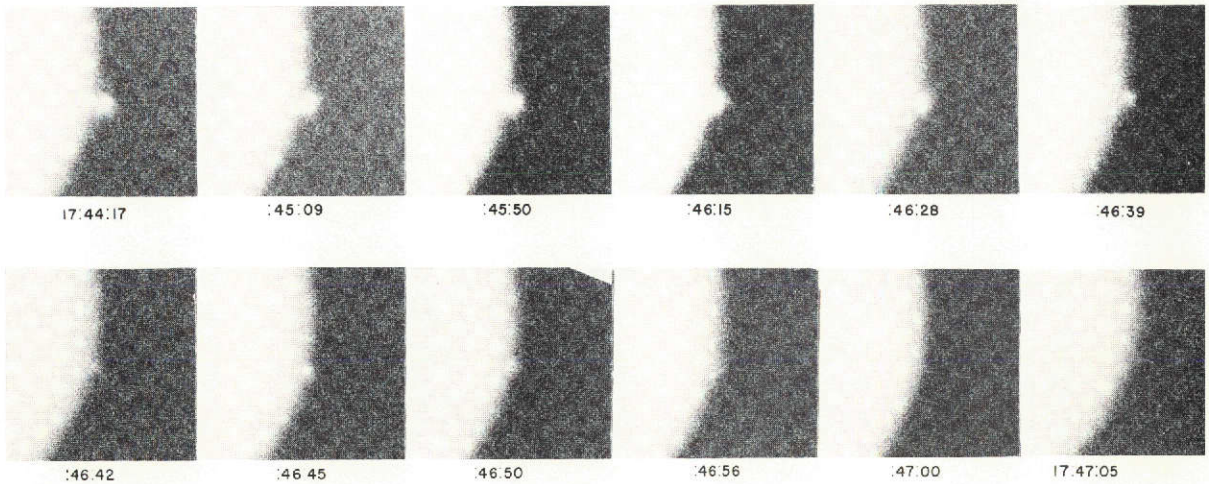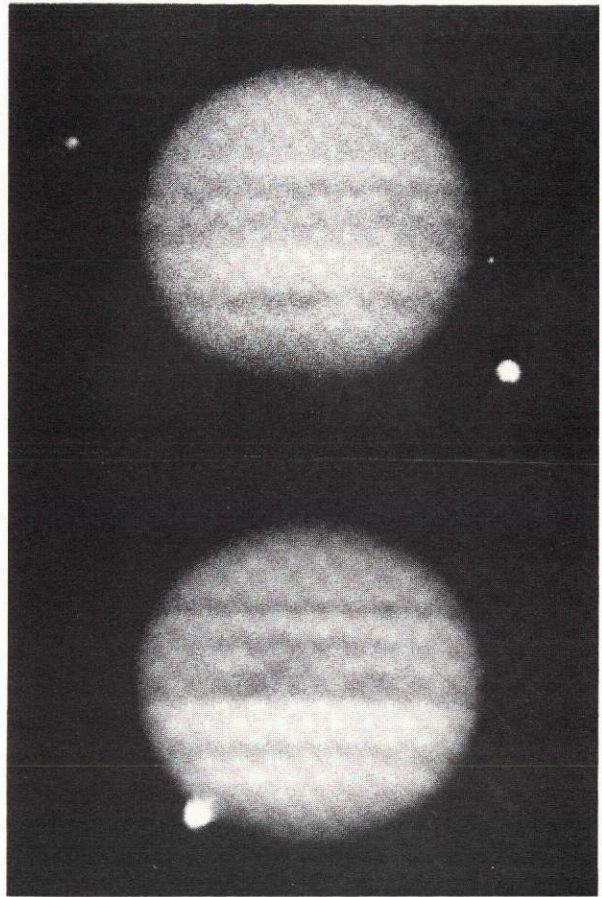
Fig. 3 Ingress of SAO 159683; times in UT

18:24:09   :28:54   :29:28   :29:54   :27:18

:30:34   :30:45   :31:20   :32:21   18:33:02
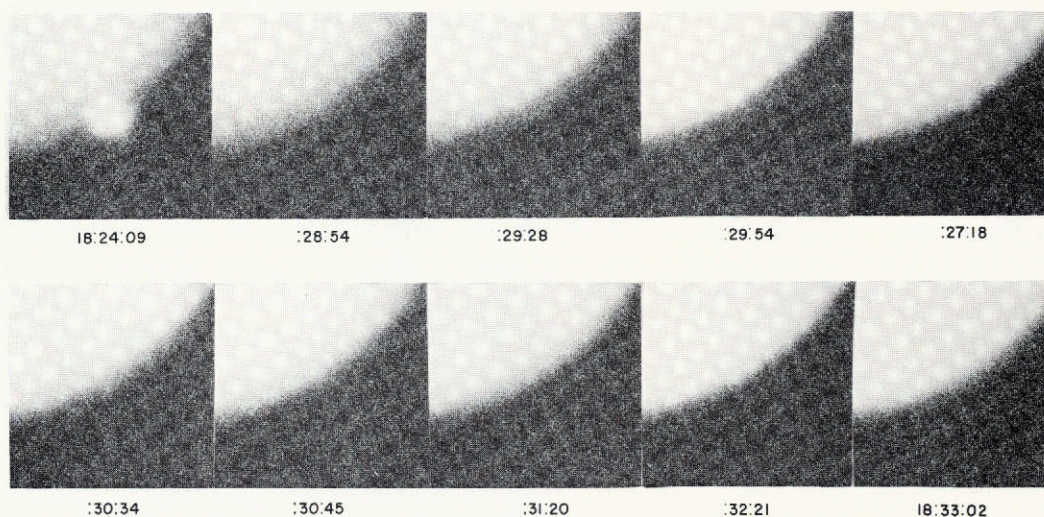
Fig. 4   Ingress of Beta Scorpii

ing the total time of ingress to nearly 8 minutes. No color could be observed
during the flashes since the image was viewed through the yellow filter.

   Although the egress of Beta Scorpii was underway when the clouds parted
again (Fig. 5, upper), it took nearly 5 minutes to return to normal brightness.
The clouds also prevented us from securing a good series of photographs of the
egress of SAO 159683 (Fig. 5, lower). Table I summarizes the timing of egress
and ingress along with the measured position angles.

19:46:27   :46:50   :46:58   :47:27   :47:40   19:49:12

20:07:21   :07:44   :07:57   20:08:19
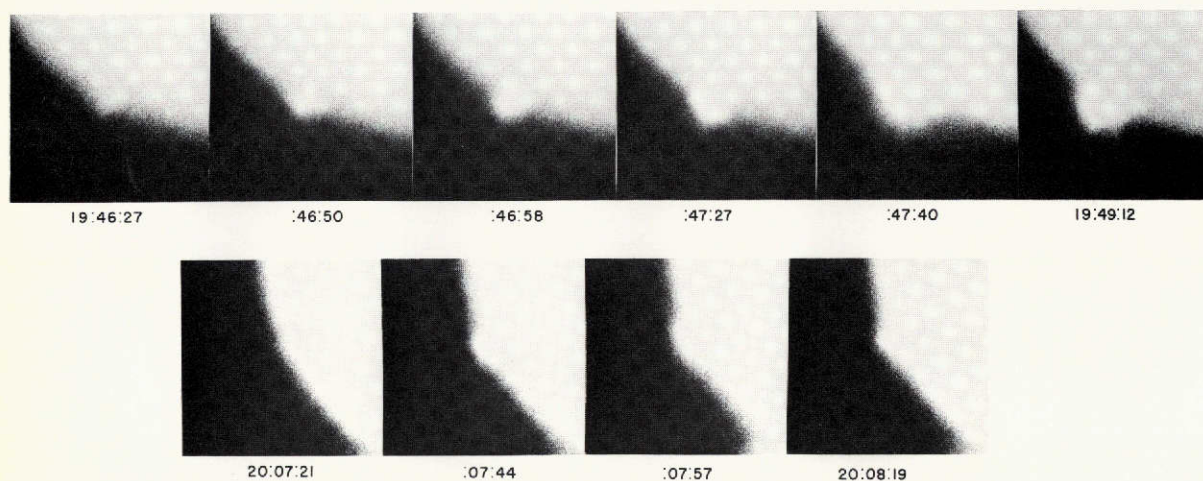
Fig. 5 (upper) egress of Beta Scorpii;   (lower) egress of SAO 159683

TABLE I

Timings of Ingress and Egress (UT)

Sequence	SAO 159683	P. A.	Beta Scorpii	P. A.
Start dimming	$17^h46^m15^s$	$271°.5$	$18^h24^m34^{s*}$	$229°.6$
Ingress	17 47 04		18 32 21 +	
Egress	20 07 21		#	
End of brightening	20 08 07	$111°.1$	19 47 40	$153°.0$

* Clouds prevented accurate determination
+ Last flash photographed
\# Brightening underway at first observation

3. Measurements

The images were later measured both by projection onto a computer-drawn Zenographic grid that had been carefully positioned with the edge of the film and orientation trails for reference and, independently, in a projection comparator (described in *LPL Comm. No. 179*). Both methods gave the same results, i.e., as Beta Scorpii dimmed or brightened, it appeared to move along the limb of Jupiter by refraction (Fig. 6). The maximum displacement of Beta Scorpii after ingress measured $1''.4$. Because of the geometry, the effect for SAO 159683 was too small to be measured.

An estimated light curve (Fig. 7) was constructed, based on the diameter of the star images approximately normalized for contrast, density, and the
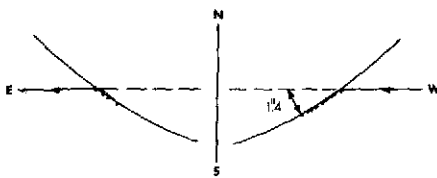


Fig. 6 Displacement of
Beta Scorpii
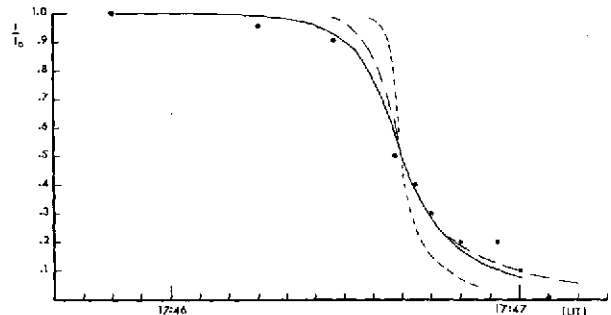
Fig. 7 Estimated light curve of ingress of
SAO 159683 and Beta Scorpii with theoretical
curves for atmosphere with scale heights of
12 km(short dashes) and 32 km (long dashes)

effect of the limb of Jupiter. The curve is not precise due to the variables mentioned above, especially the photographic edge effects introduced by Jupiter's limb. It is, however, sufficient to support higher values of the scale height than those obtained by Baum and Code (1953). The theoretical light curves were calculated assuming that extinction is negligible compared to atmospheric dispersion so that

$$vt/H = (I_o/I - 2) + \log_e (I_o/I - 1)$$

where

v = apparent velocity of the star normal to the limb,
t = time,
I_o = normal brightness of the star,

and

I = observed brightness of the star,

(Baum and Code, *op.cit.*). The much larger scale height, of about 30 km, implies a lower mean molecular weight and/or a higher temperature, since

$$H = RT/\mu g,$$

where R = gas constant, T = absolute temperature, μ = molecular weight, and g = surface gravity.

The above article was written before the results by Hubbard *et al.* (1972) were known. Dr. Hubbard later pointed out to the writer that the present results are in general accord with his.

4. Summary

It is obvious from the scatter in the light curves of SAO 159683 that departures from an isothermal atmosphere are present. Despite the lack of photometric accuracy compared to others (Hubbard, *op. cit.*), the presence of light variations (flashes) in the toe of the light curve was recorded. The complicated atmospheric density profile shown by Hubbard is present in the form of layering, perhaps with areas of turbulent mixing affecting the light curve in the same manner as scintillation. The greater scale height supports both the high temperatures observed, especially in the equatorial region, and a lower mean molecular weight.

REFERENCES

Baum, W. A. and Code, A. D. 1953, "A Photometric Observation of the Occultation of σ Arietis by Jupiter", *A. J.*, *58*, 108.

Fountain, J. W. and Larson, S. M. 1972, *LPL Comm. Nos. 174 and 175*.

Hubbard, W. B., Nather, R., Evans, D. S., Tull, R. G., Wells, D. C., van Citters, G. W., Warner, B., van den Boot, D. 1972, "The Occultation of Beta Scorpii by Jupiter and Io. I. Jupiter", *A. J.*, *77*, 41.

Kuiper, G. P. 1972*a*, "Lunar and Planetary Laboratory Studies of Jupiter", *Sky and Telescope*, *43*, 4, 75.

Kuiper, G. P. 1972*b*, *LPL Comm. Nos. 172 and 173*.

Larson, S. M. 1971, "The Bosscha Observatory in Indonesia", *Sky and Telescope*, *42*, 70.

Taylor, G. E. 1971, "Occultation of Beta Scorpii by Jupiter", *IAU Circular No. 2279, Sept. 29*.

Voûte, J. 1933, *Bosscha Obs. Ann.*, *1*, Pt. 1.

Westphal, J. A. 1969, "Observations of Localized 5-micron Radiation from Jupiter", *Ap. J.*, *157*, 1636.

NO. 178   INITIAL DEVELOPMENT OF THE JUNE 1971 SOUTH EQUATORIAL BELT DISTURBANCE ON JUPITER

by R. B. Minton

November 26, 1971

ABSTRACT

Photographs taken with the Catalina 61-inch reflector from June 21 through July 10, 1971 have enabled the author to study and measure the early developments of a major South Equatorial Belt (SEB) disturbance. High-resolution photographs of the disturbance were obtained on seven nights during the 19-day interval. Our first photograph at 04:38 UT on June 21 recorded the initial outbreak at $79°.5$ longitude (System II), and $-14°$ Zenographic latitude. From this point, dark spots moved along the SEBs towards increasing longitude, and white spots a short distance along the SEBn towards decreasing longitude. The preceding white spot in Figure 18 had an initial period of $9^h54^m32^s.5 \pm 3^s.5$, and retrograding dark spots on the SEBs a mean period of $9^h58^m30^s.5 \pm 7^s$. The feature from which all the spots emerged had a rotation period of $9^h55^m29^s \pm 2^s.5$, and is close to the System III radio period of $9^h55^m29^s.73 \pm 0^s.04$ derived by Carr.

1. Introduction

Major South Equatorial Belt (SEB) disturbances have been recorded about a dozen times beginning in 1919 (Chapman and Reese, 1968). They are recognized by their common characteristics. Initially, a small white or dark spot, or a faint wisp is seen within the SEB Zone (SEBZ). From this point, the seat of the disturbance, dark spots move along the S component of the SEB (SEBs) towards increasing longitude in System II. These are known as the "retrograding dark spots". Also, white and dark spots leave the seat of the disturbance and move along the SEBn towards decreasing longitudes. The SEBn is in System I, but during a disturbance, the change in longitude is usually expressed relative to System II. The SEBZ becomes filled with many spots, wisps, columns, and loses its conspicuousness when the retrograding dark spots reach its vicinity. The June 1971 disturbance was a major one with above-average activity, although the Red Spot has failed to fade.

2. Observations

Mr. W. E. Fox, Director of the Jupiter Section of the B.A.A. was probably the first person to see and recognize the importance of a small white spot located in the SEBZ of Jupiter, June 21, 1971. (E. J. Reese discovered a second disturbance on July 18, 1971 near $\lambda_2 = 144°$). As a guest and consultant of the Lunar and Planetary Laboratory, using the Catalina 61-inch telescope, Fox estimated the time of Central Meridian (CM) passage of the spot, made a sketch, and alerted the photographic team to its nature and importance. Previous photographs, taken with the 24-inch reflector on Mauna Kea on June 18, indicate that a white spot was present then near the limit of visibility in blue light, but invisible in red light (Baum, 1971). Our 61-inch photos of June 16 fail to show anything unusual near the longitude of the outbreak.

At Catalina Observatory on June 21, 04:38 UT, the white spot was seen and photographed at longitude 79°.5 (System II) and latitude -14°. When near the CM it was the brightest feature on the disk at all observed wavelengths (3100-8800Å). However, its contrast against the SEBZ became less as it approached the preceding limb. It was faintly recorded June 21, 06:00 UT in blue light, and just barely at 06:10 UT in infrared. There were no "irradiating" spots (Peek, 1958) photographed during the interval of June 21 to July 10, 1971.

On June 28 and July 10, Jupiter was photographed with the 61-inch in the 8860Å methane band. The white spots preceding the center of the disturbance were much brighter on the methane photo than on the infrared photo, 6550-8800Å (10% passband limits). This indicated they were relatively high in the Jovian atmosphere, but the lack of irradiation suggests they were not extremely high. Examination of color and black-and-white photographs consistently revealed the SEBZ spots preceding the center of the disturbance as *white*, the oblique column bridging the SEBn and SEBs as *red*, the seat of the disturbance as *red*, and the retrograding dark spots as *blue*.

Table I lists the observational records for the 17 composites here shown, including the number of images combined in each composite. These composites were prepared and measured by the author. The increase in contrast permitted recognition and measurement of features barely seen on original negatives. The summer rains prevented observations much beyond the 19 days here covered.

TABLE I

Observational Data on Photographs

| Fig.	Date 1971	UT	Color	Film	Filter	Roll #	Compos.	No.
1	21 June	04:50:30	B	103-0	NF	1399	1286	7
2	21 June	05:01:34	IR	HSIR	GG-14	1400	1305	10
3	23 June	05:43:34	IR	HSIR	RG-5	1407	1306	6
4	23 June	05:49:03	B	103-0	NF	1408	1287	4
5	26 June	05:08:00	UV-B	103-0	NF/UG-5	1418	1288	3
6	28 June	05:10:44	IR	HSIR	GG-14	1423	1289	4
7	28 June	05:16:39	UV	103-0	UG-5	1424	1290	4
8	6 July	03:45:51	B	103a-0	NF	1442	1292	5
9	6 July	04:01:08	IR	HSIR	GG-14	1443	1291	5
10	7 July	07:00:43	UV-B	103-0	NF/UG-5	1453	1285	12
11	7 July	07:06:26	IR	HSIR	RG-5	1454	1293	7
12	10 July	04:16:21	B	103-0	NF	1457	1294	6
13	10 July	04:24:39	IR	HSIR	RG-5	1458	1295	6
14	10 July	04:38	8990Å	HSIR	8900Å	1459	1301	3
15	10 July	05:14:39	G	Plus-X	GG-14	1462	1297	6
16	10 July	06:05:42	IR	HSIR	GG-14	1467	1298	5
17	10 July	06:27:24	UV-B	103-0	NF/UG-5	1469	1299	5

3. The Measures

The longitude measures were made on 65-mm diameter composites using a milimeter scale, aligned parallel to the equator, and with estimates to the nearest 0.2 mm. Measures of the same features on different composites were generally consistent to within 1° near the CM and 3° near the limb. A least-squares analysis of all longitude measures indicates that the mean standard deviation of a longitude determination is $0°.9$. Latitudes were similarly determined, but only near the CM. Measures were reduced by an IBM 1130 computer with a program written by H. Gordon Solberg. His measures of a few of the more prominent features on a digitized Mann measuring machine provided a check.

Figure 18 shows a drift chart of the features measured. On June 26 they were so near the limb that only their separations were measured. Their absolute longitudes were located by a visual best fit. The Red Spot was measured near the CM and drawn with its following end at System II (λ_2) longitude 20° for the entire interval. No interaction with the disturbance was noted.

Of the two major and other minor preceding white spots in the SEBZ, the brightest (marked WS in Fig. 18) was also the longest lived, and can be identified as the June 21 white spot representing the initial outbreak. From June 21 to July 7 it remained near -14° latitude, with a period of $9^h54^m32^s.5 \pm 3^s.5$. On July 10, however, its latitude was -12°, placing it in apparent contact with
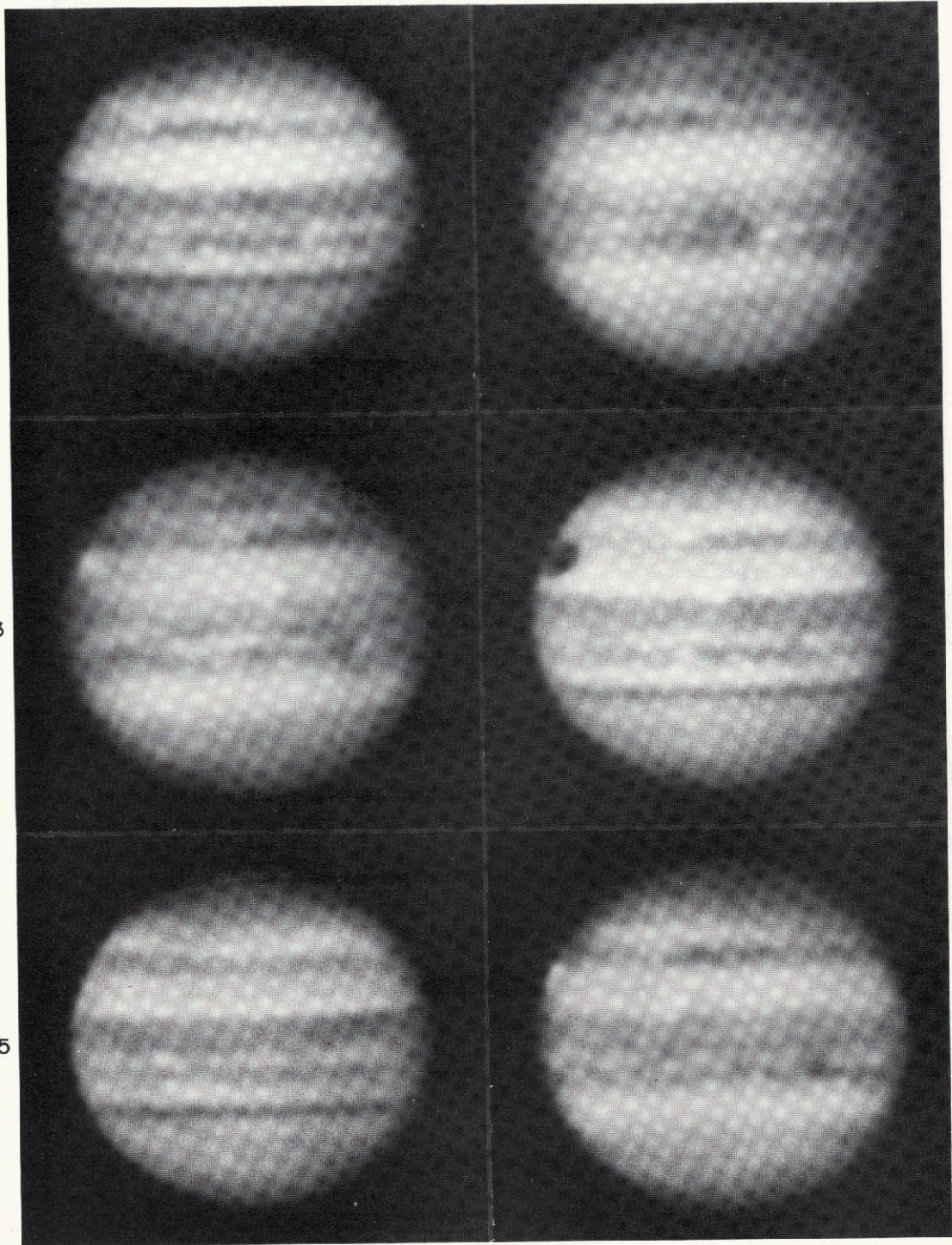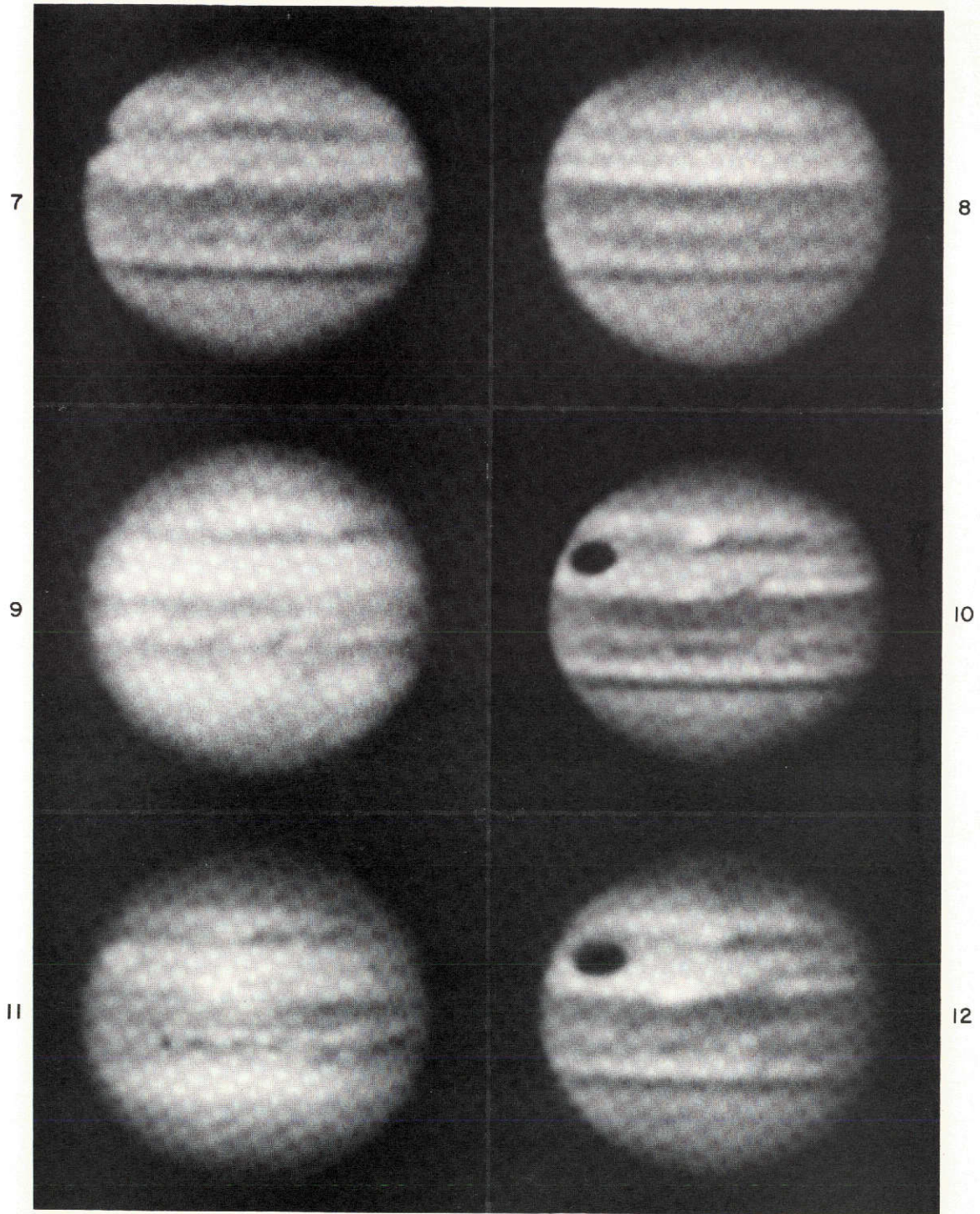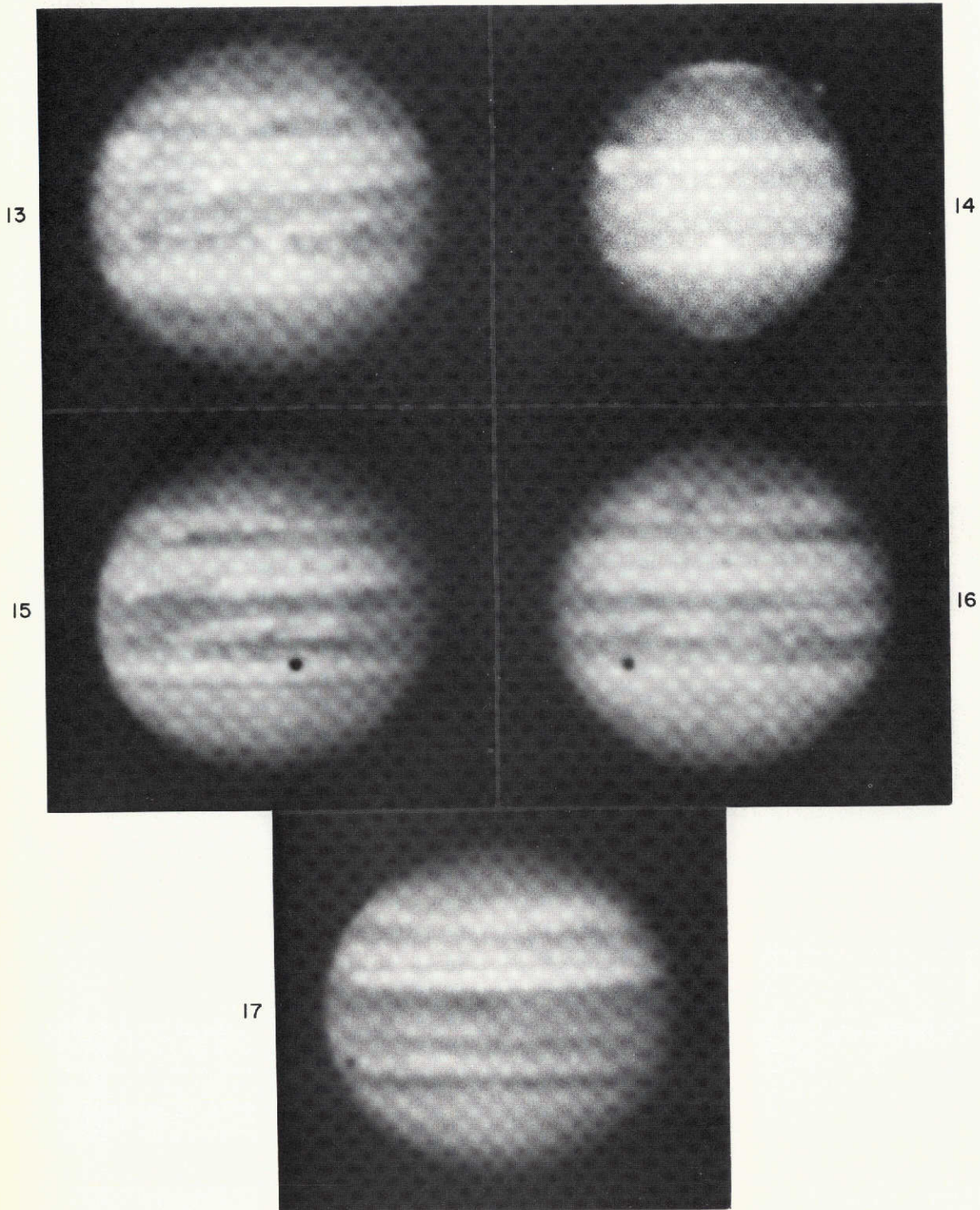
the SEBn, which was rotating close to that of System I. Its longitude increased by 6° in this 3-day interval over what was projected, yielding an approximate period of $9^h54^m19^s$. This rapid decrease in period, as the SEBn is approached, is well illustrated by the increasing curvature of the dark (in blue light) column joining the SEBn and SEBs, as time progresses. The other minor SEBZ white spots were evidently torn into invisibility upon reaching the SEBn, as none were photographed proceeding toward decreasing longitudes. Three factors indicate that the long-lived WS was higher in the Jovian atmosphere than any other SEBZ white spots. First, the others were swept into invisibility upon reaching the SEBn. Second, WS is the more prominent one shown in the July 10 methane photograph (Fig. 14). Third, and most important, shortly after July 10, WS crossed *over* the SEBn into the Equatorial Zone (Reese, personal communication). This suggests that this cloud, some 5,000 km in diameter, was not attached to the visible cloud deck. The fact that WS accelerated toward decreasing longitudes upon reaching the latitude of the SEBn, suggests the presence of an atmospheric current above the SEBn cloud deck rotating in the same direction, but with a longer period. Scarcity of observations prevents more quantitative interpretation. In past disburbances, dark spots advanced along the SEBn by 4-9° per day, and white spots"retrograded"along the SEBs 3-5° per day (Peek, 1958), which may be compared with the drift rates found in Table II.
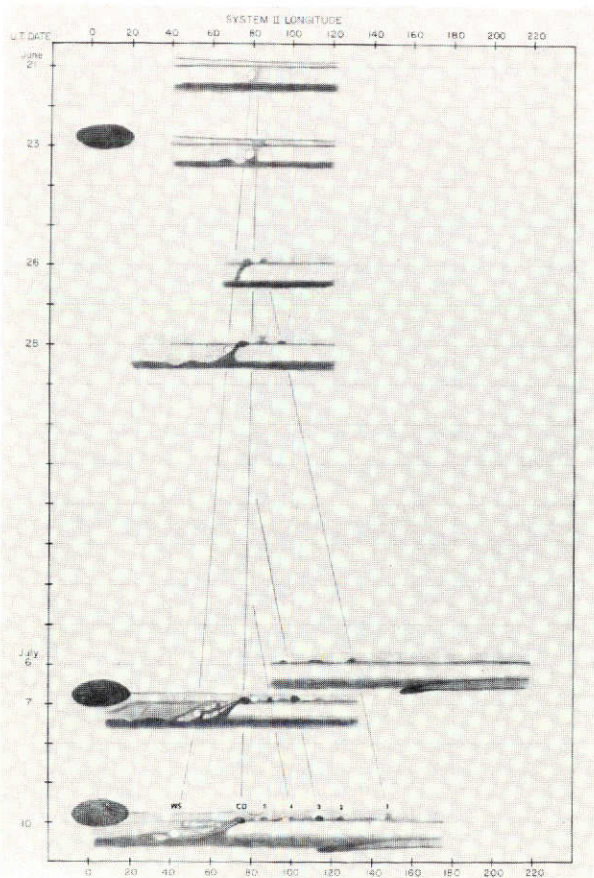

Fig. 18 Drift chart of June 1971 SEB disturbance from June 21 to July 10. Each day tick mark also represents -18° Zenographic latitude in the sketches, with their vertical scale 2° per small square in both coordinates

The most interesting result of the measures is that the seat of the distur-
bance had a period of $9^h55^m29^s \pm 2^s.5$ between June 21 and July 10, 1971. This
period is quite close to the System III radio period of $9^h55^m29^s.73 \pm 0^s.04$ (Carr,
1970). In 1953, Reese suggested that the observed longitudes of the *initial* out-
breaks of SEB disturbances might be consistent with one or two Jovian surface
features rotating with one *uniform* period (Reese, 1953). It had also been ob-
served by Reese and others that in the course of a disturbance, spots appear to
erupt from a point rotating closely with that of System II ($9^h55^m40^s.643$). The
seat of the June 1971 disturbance rotating at nearly that of System III streng-
thens the 1953 Reese hypothesis. Very recently, Reese has plotted the outbreaks
of the twelve disturbances in System III, and has found an even closer fit than
the 1968 determination (Chapman and Reese, 1968; Reese 1972). Of the three in-
dicated source longitudes, the outbreak of June 18, 1971 was less than 1 degree
from the longitude of the primary source. The longitude of this source is given
by $\lambda_2 = 353^\circ.1-0^\circ.25627$ (JD - 2435839.5).

By July 10, five dark spots were retrograding along the SEBs. The first had
the longest period, consistent with some past disturbances. Its period was
$9^h58^m46^s \pm 2^s$. Spot No. 3, the darkest, had a period of $9^h58^m18^s \pm 10^s$; and
No. 4 a period of $9^h58^m18^s \pm 10^s$. Spots Nos. 2 and 5, which were only measured
once, were assumed to rotate with the period of Nos. 3 or 4 in order to estimate
their dates of formation. This date of formation was determined by a least-
squares analysis of the longitude of the spot versus the longitude of the seat
of the disturbance. The mean interval between formations was 2.8 days. This
regular spacing of SEBs spots is well illustrated in Slipher (1964, p. 97, lower
left). By July 10, 1971, each dark spot had one or more white spots associated
with it. In some cases their Northerly latitude produced apparent breaks in the
SEBs, or at least a reduction in its width. The dark SEBs spots retrograded at
a maximum of 135° per 30 days. At this rate of drift, it was calculated that the
first spot would be N of the preceding edge of the Red Spot near August 24, 1971.
Photographs at Catalina Observatory at this longitude and date were not obtained,
but subsequent photographs show the SEBs curving to the N, avoiding the Red Spot.
As of October 14, 1971 our photographs show the Red Spot as prominent as ever
during the 1970-71 apparition.

TABLE II: Bright SEBZ and Dark SEBS Spots

Spot	Period	Drift per day	Nm	Np	Dates Measured	Date Formed	Formation Interval
WS	$9^h54^m32^s.5 \pm 3^s.5$	$-1^\circ.67$	4	4	Jun 21-Jul 7	--	--
WS	9 54 19 ±4	-3.7	2	2	Jul 7-10	--	--
1	9 58 46 ±2	+4.5	3	4	Jun 28-Jul 10	Jun 24.6	--
2	9 58 43*	+4.4*	1	2	Jul 10	Jun 28.1	$3^d.5$
3	9 58 43 ±10	+4.4	3	3	Jul 6-10	Jul 1.8	1.7
4	9 58 18 ±10	+3.8	2	2	Jul 7-10	Jul 4.6	2.8
5	9 58 18*	+3.8*	1	1	Jul 10	Jul 7.7	3.1

Nm: Dates measured; Np: Dates photographed; *Assumed, not calculated

5. Conclusions

The basic 1953 Reese hypothesis, of *constant* rotation period of the SEB sources, together with his 1972 revised source rotation period, is strengthened by two facts. The longitude of the initial outbreak was 1 degree from the predicted longitude of the primary source, and the seat of the disturbance drifted $-8.23° \pm 2.2°$ per 30 days or moved nearly with System III. The Kuiper hypothesis of the recurrent nature of the SEB disturbances is that because the meteorology of Jupiter is internally driven, a temperature inversion builds up and eventually breaks through the visible cloud deck (Kuiper, 1972). The period of this meteorological relaxation time is calculated to be about 8 years. Both hypotheses are satisfied if one assumes that a surface feature *triggers* the outbreak near the longitude of this feature. The simultaneous display of two SEB disturbances would seem to favor the meteorological explanation; otherwise one is faced with the improbability of two nearly simultaneous volcanic-type eruptive processes occurring some 120° of longitude apart. However, an eruptive process is not vital to the validity of the Reese hypothesis. On the other hand, the properties of WS suggest a violent ejection and transport in the higher atmosphere. Kuiper (1972) points out that a deep solid surface of Jupiter probably exists. The three source longitudes determined by Reese have remained fixed and retained their identities for 52 years.

A thorough search of observational material may show whether prior disturbances rotated closely with that of System III. This period may have existed for a fraction of the lifetime of the 1928 SEB disturbance. According to observations by the Jupiter Section of the B.A.A., the seat of eruption "showed accelerated motion in the direction of diminishing longitude", and over a 17-day interval, had a drift of -19° per 30 days (Phillips, 1935). In addition, the center of eruption of the 1958 disburbance had a period of $9^h55^m33^s$ from April 19 to 30, 1958 (Reese, personal communication). The need exists for additional investigations by Jupiter observers and meteorologists.

REFERENCES

Baum, W. A. 1971, "Observations of New Major Disturbances on Jupiter", *Sky and Telescope, 42*, 176-180.

Carr, T. D. 1970, "The Twelve-Year Periodicities of the Decametric Radiation of Jupiter", *Radio Science, 5*, 495-503.

Chapman, C. R. and Reese, E. J. 1968, "A Test of the Uniformly-Rotating Source Hypothesis for the South Equatorial Belt Disturbances on Jupiter", *Icarus, 9*, 326-335.

Kuiper, G. P. 1972, *Sky and Telescope*, Jan,,Feb issues; *LPL Comm. No. 173.*

Peek, B. M. 1958, THE PLANET JUPITER (London: Faber and Faber).

Phillips, T. E. R. 1935, "Twenty-Seventh Report of the Section for the Observation of Jupiter", *Mem. of the B. A. A., 30,*213.

Reese, E. J. 1953, "A Possible Clue to the Rotation Period of the Solid Nucleus of Jupiter", *J. Brit. Astron. Assoc., 63*, 219-221.

Reese, E. J. 1972, "Jupiter: Its Red Spot and Disturbances in 1970-71", New Mexico State University Observatory TN-72-40.

Slipher, E. C. 1964, A PHOTOGRAPHIC STUDY OF THE BRIGHTER PLANETS (Lowell Obs. and NGS).

NO. 179 OBSERVATIONS OF THE SOUTH EQUATORIAL BELT

DISTURBANCE ON JUPITER IN 1971

by Stephen M. Larson

March 1972

ABSTRACT

Some aspects of the major South Equatorial Belt disturbance of
1971 are described from photographic observations obtained at the
Catalina and Bosscha Observatories. The motions of several spots
produced by the disturbance during the first two months of activity
were measured. The projection comparator used for measurement is
also described.

1. Introduction

Starting in late June 1971 the appearance of Jupiter was remarkable for the
great amount of activity associated with the recurrence of a major disturbance
in the South Equatorial Belt (SEB). These major disturbances are marked

by violent meteorological activity that changes the appearance of a large area
in a relatively short time. The extent of activity in each disturbance was
varied. The most active one occurred in 1928, followed by one in 1943 (Reese
and Chapman 1968), and the present one. The sequential development of a "typical"
SEB disturbance has been documented (Peek 1958, Reese and Chapman 1968), and
the 1971 disturbance was fairly typical. Because the SEB disturbance affected
some 20° of latitude in the Southern Hemisphere, the SEB region has been divided
into three sections or "branches": the SEBs (-19°), the SEBZ (-14°), and the
SEBn (-8° Zenographic latitude) (Reese 1972). The spread of activity in longitude
of the disturbance was due in part to differential rotation of these branches.

2. The Observations

The routine program of planetary photography was in progress at the 154-cm
reflector of the Catalina Observatory on June 21, 1971 when Visiting Astronomer
W. E. Fox, Director, Jupiter Section, B. A. A., noted *a small white spot in the
bright SEBZ*. The other observers were alerted to the possibility of the impor-
tance of this object, and the photographs obtained by R. B. Minton on that night
recorded the spot (Minton 1972). The outbreak was later announced by Reese in
IAU Circular 2338 and the small spot was found on photographs in the ultraviolet
reported by Baum (1971) as part of the NASA Planetary Patrol on June 18, 1971.

Thereafter, with increased emphasis on Jupiter photography, high-resolution
coverage was obtained of the early development until the rainy season severely
limited coverage in mid-July. At about this time, J. W. Fountain was starting
an observing run at the Bosscha Observatory in Lembang (Java), Indonesia, (Larson
1971) for direct photography of Mars during the very favorable opposition. While
in Java, he obtained over 3,000 images of Jupiter in several wavelength bands
with the twin 60-cm refractor.

Together, the data obtained at the Catalina and Bosscha Observatories provide
enough coverage to study the motions of several features produced by the distur-
bance. Figures 1-4 show 22 photographs of the planet (all composites) selected
from both observatory collections, to illustrate the Disturbance during the period
July 14-October 4, 1971. Reference is made to R. B. Minton's *LPL Comm. No. 178* for
illustrations during the first 19 days following the eruption (these were all ob-
tained at the Catalina Observatory). Table I lists the times and emulsion data for
the 22 photos in Figures 1-4.

Measurements on individual features of the disturbance are shown graphically
in Figure 5, expressed in System II. They cover the period June 21-August 20, 1971.
The measurements were made with the comparator shown in Figures 7 and 8, below.

The relative velocities of the features in a particular latitude region have
been shown to vary with time (Chapman 1969), making the determination of rotation
as a function of latitude difficult. In addition, the developmental changes in
the shape of a feature can introduce irregularities in the apparent motion. Still,
events producing features whose identities are certain for several weeks, such as
the SEB disturbances, presently offer the best opportunity for studying currents
in the Jovian atmosphere. Figure 6 shows the average rotation period of several
observed features belonging to the 3 latitude regions of the disturbance.
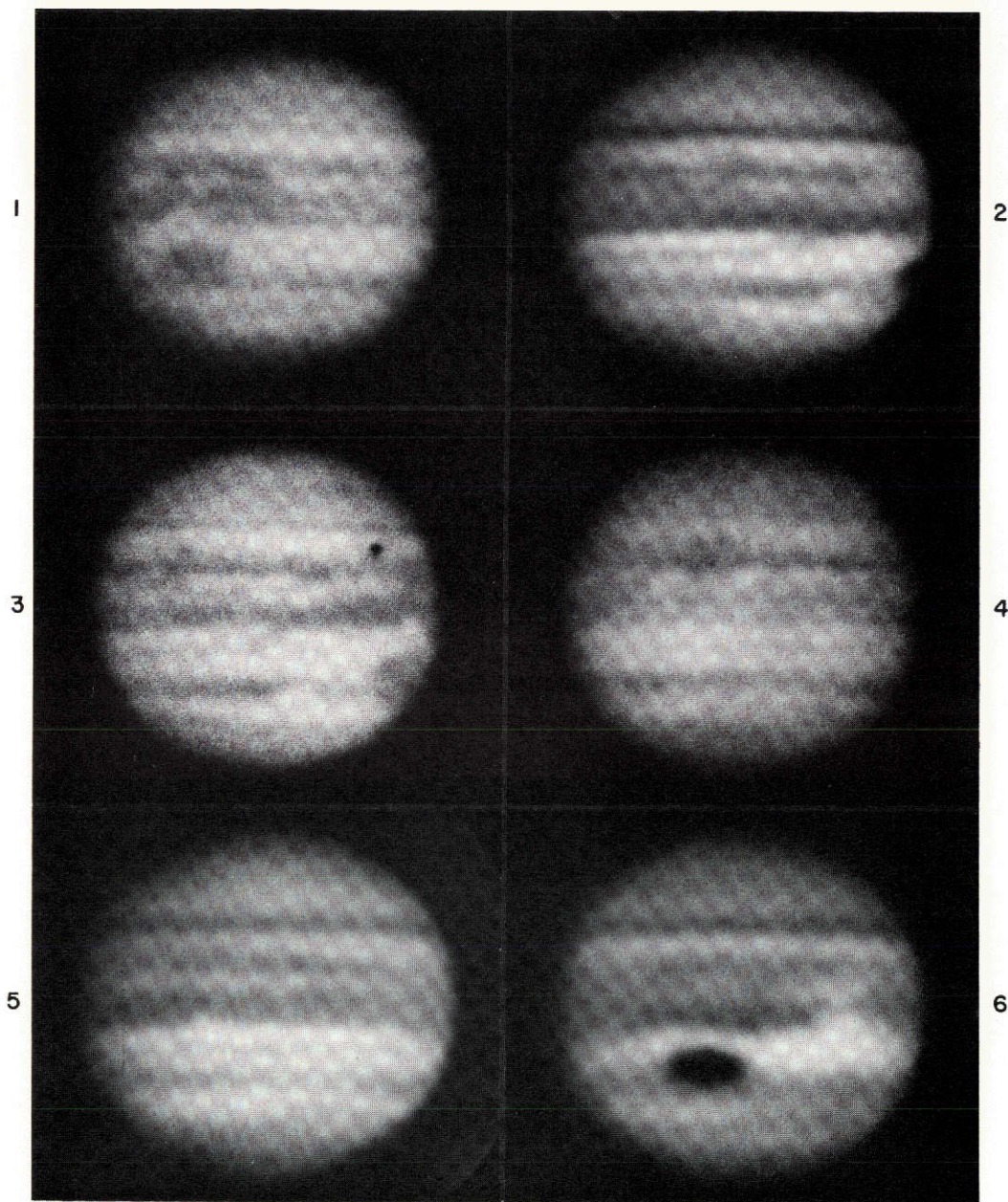
Fig. 1   Image No. 1:   July 14, red.   Large bay N of RS (Feature A in Fig. 5).
No. 2:   July 15, blue.   Dark spots in SEBs not as distinct. SEBs appearing
more continuous than in No. 3.   No. 3:   July 15, red. Spot A (Fig. 5) is N
of RS.   Dark spots in SEBs.   No. 4:   July 18, red.   Outbreak of second dis-
turbance seen as small white spot in SEBZ after being overtaken by leading
edge of SEBs spot.   No. 5:   July 20, blue.   Column joining SEBs and SEBn
shown adjacent to second disturbance.   No. 6:   July 24, blue.   Activity
        spreads in SEBn as leading white spot A moving away from RS.
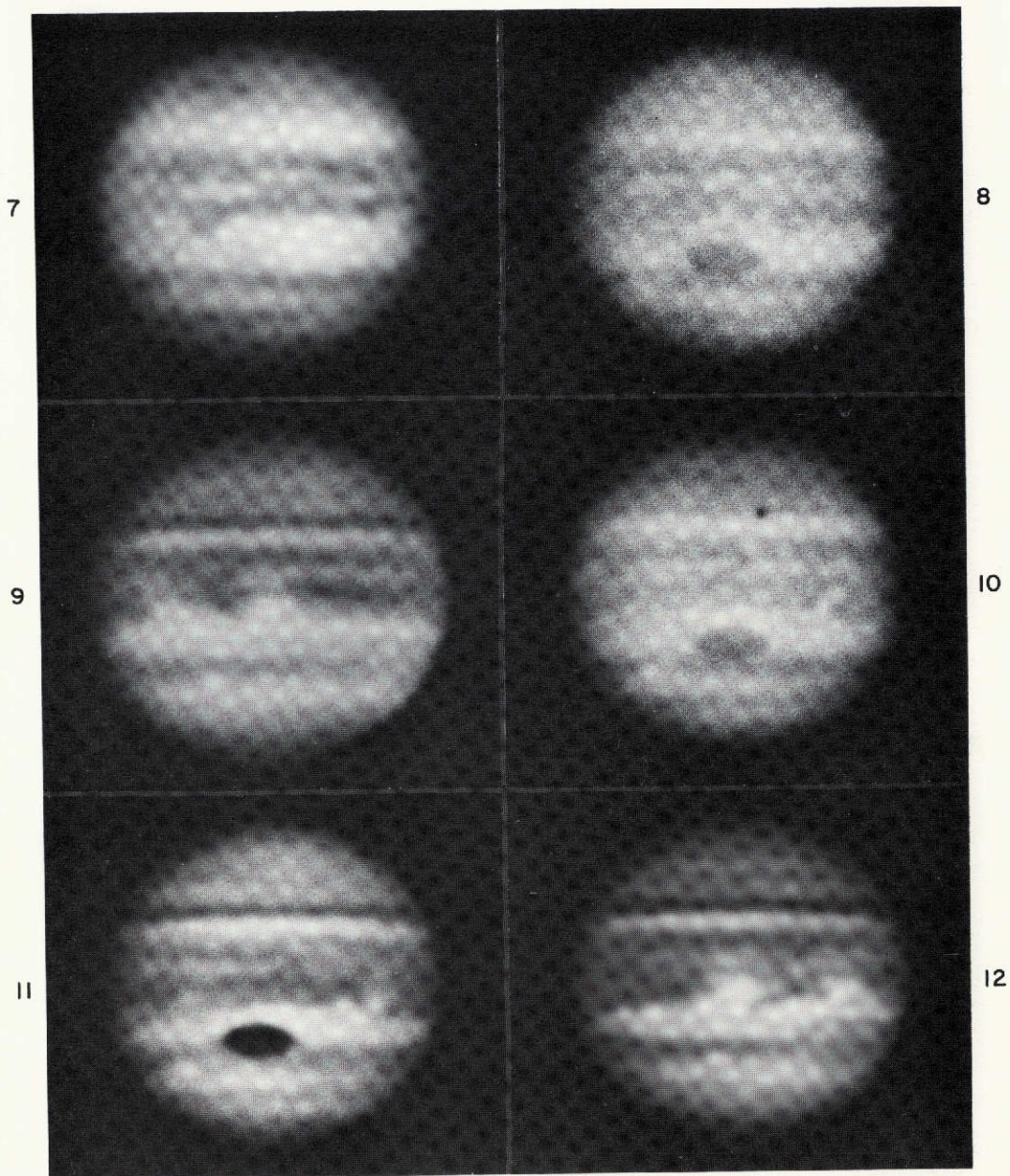
Fig. 2 Image No. 7: July 24, near-IR. RS is nearly invisible in near-IR; compare with No. 6. No. 8: July 29, red. Spectacular wisps from N of RS in SEBs. No. 9: Aug 2, blue. Large white spots A and C (Fig. 5) disrupt appearance of SEBn. No. 10: Aug 3, red. Object B of Fig. 5 extends deep in SEBn. No. 11: Aug 5, blue. Compare with No. 10, similar longitude. No. 12: Aug 7, blue. Comparison between this image (and 12a) and No. 13 (plus 13a) indicates large differences.
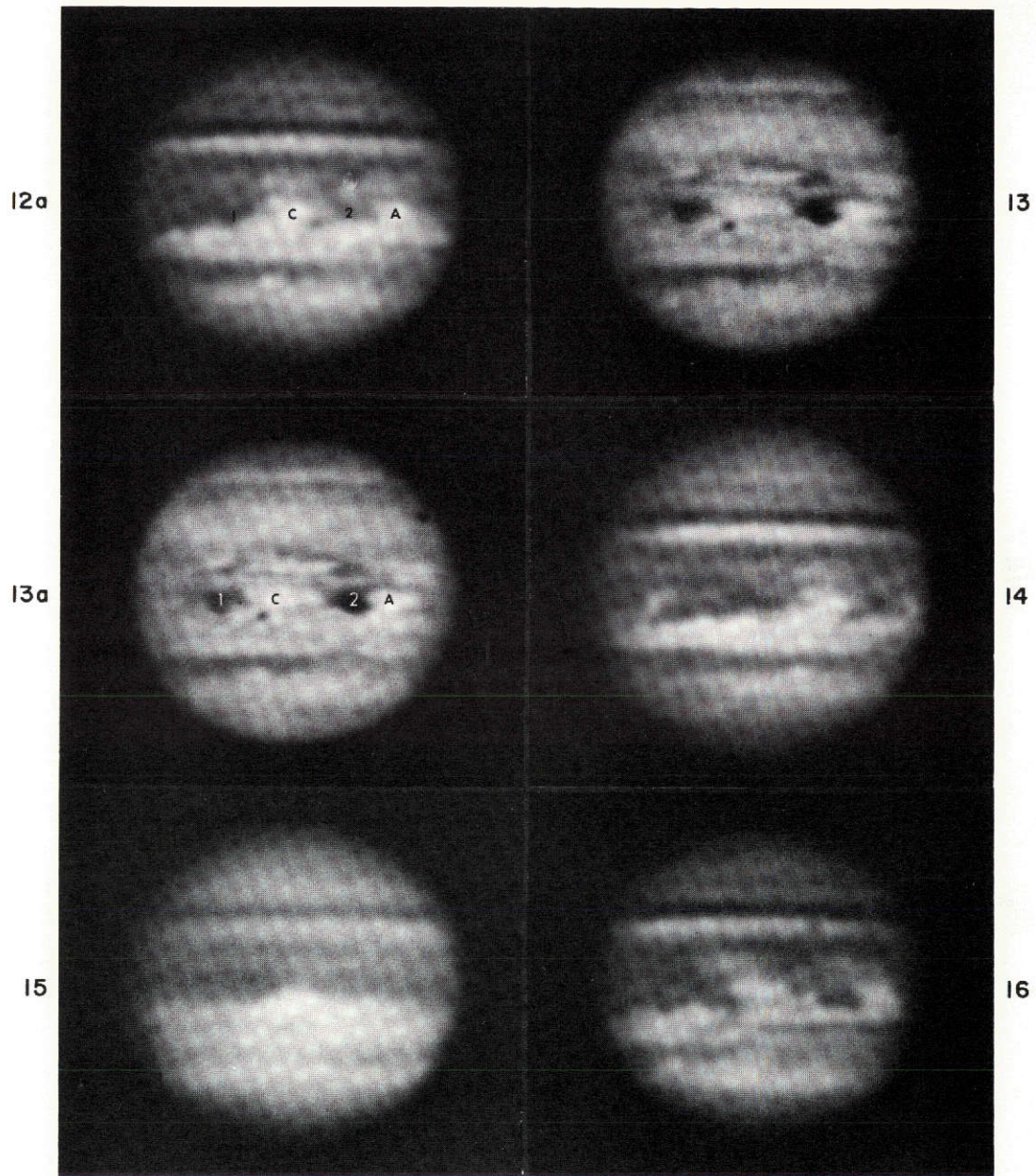
Fig. 3   Image No. 12α: Aug 7, blue (same as No. 12).   Features labelled A
and C, shown in Fig. 5, are identified. (Features 1 and 2 not shown in Fig.
5 but used in comparison with No. 13α).   No. 13: Aug 7, near-IR.   Repeated
with identifications in 13α.   Blue features 1 and 2 very dark in near-IR;
their blue color is shown on simultaneous color records. No. 14: Aug 7,
blue.   Spots A and C of No. 12α have moved 1 cm to right; similar spot,
called B in Fig. 5, has appeared 1 cm from left limb.   No. 15: Aug 8, blue.
Spot D (of Fig. 5) prominent on CM in SEBn.   No. 16: Aug 14, blue. Longitude
similar to No. 12α, with Spots A and C shown (modified).
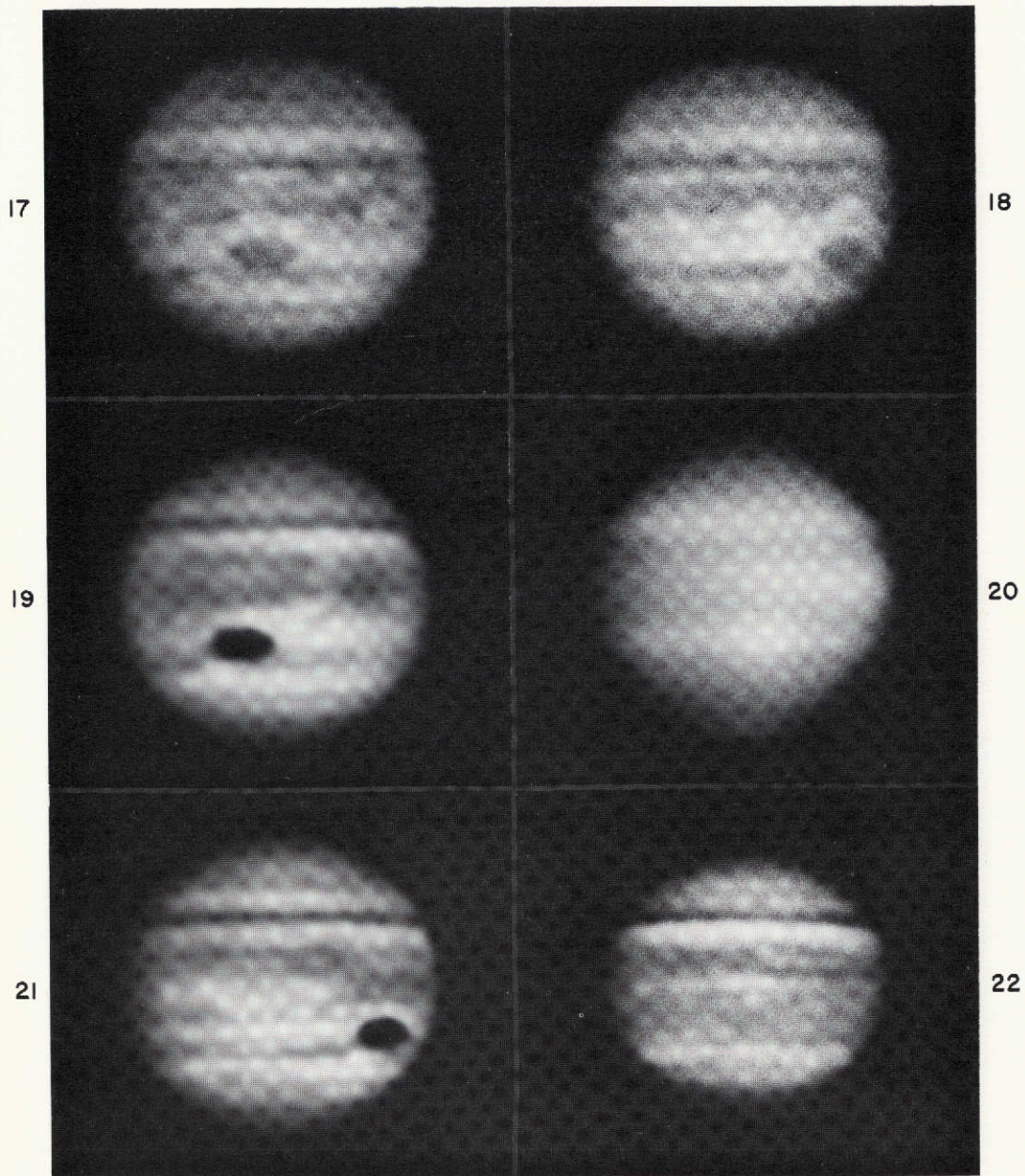
Fig. 4 Image 17: Aug 15, red. Taken 12 days after No. 10, with equatorial
detail enhanced. No. 18: Aug 20, red. Note bright bay in SEBn. No. 19:
Sept 3, blue. RS still prominent, contrary to case histories of other major
eruptions. No. 20: Sept 3, methane filter. RS appearance normal but EW
gradient across equatorial region. No. 21: Sept 6, blue. RS still prominent
despite train of small dark spots in SEBs having by then drifted past RS.
No. 22: Oct 4, blue. Disturbance in equatorial region diminished. NTrZ un-
                              usually bright.

TABLE I

Observational Data on Photographs

Fig.	Date 1971		Time(UT)	Film	Filter	CM II	Obsy.[*]	Compos. No.	No. Images
1	July	14	15:40.7	4-X	OG-5	347°.1	Bo	1370	4
2	July	15	14: 8.5	103-O	BG-3	81.2	Bo	1374	3
3	July	15	13:33.2	4-X	OG-5	60.0	Bo	1373	6
4	July	18	12:54.8	4-X	OG-5	127.6	Bo	1379	6
5	July	20	14:22.9	103-O	BG-3	121.3	Bo	1381	6
6	July	24	4:20.5	103-O		357.9	Ca	1501	5
7	July	24	4:46.2	HSIR	GG-14	13.4	Ca	1502	5
8	July	29	13:40.7	4-X	OG-5	8.5	Bo	1389	4
9	Aug	2	3:46.5	103a-O		249.0	Ca	1545	2
10	Aug	3	12:51.7	4-X	OG-5	8.9	Bo	1391	4
11	Aug	5	4:27.9	103a-O		4.6	Ca	1503	3
12	Aug	7	3: 9.7	III-O		257.6	Ca	1505	6
12α	Aug	7	3: 9.7	III-O		257.6	Ca	1505	6
13	Aug	7	3: 3.3	HSIR	RG-5	253.6	Ca	1504	5
13α	Aug	7	3: 3.3	HSIR	RG-5	253.6	Ca	1504	5
14	Aug	7	3:48.7	III-O		280.9	Ca	1506	4
15	Aug	8	14:15.5	103-O	BG-3	90.5	Bo	1393	4
16	Aug	14	3: 4.6	III-O		225.6	Ca	1507	4
17	Aug	15	12:38.9	4-X	OG-5	2.8	Bo	1403	6
18	Aug	20	13: 6.7	4-X	OG-5	50.3	Bo	1420	3
19	Sept	3	3:21.2	III-O		357.2	Ca	1511	5
20	Sept	3	3:56.9	HSIR	CH$_4$	19.2	Ca	1510	5
21	Sept	6	2:19.9	III-O		50.9	Ca	1512	4
22	Oct	4	1:45.5	103-O		271.6	Ca	1514	6

[*]
  Ca = Catalina; Bo - Bosscha

3. Description of the Disturbance

    Before the outbreak, the Red Spot (RS) was very prominent and the SEB Zone (SEBZ) was very bright and free of detail. The SEBs was very weak, appearing only as a poorly defined grey line in the best photographs. Because of the faintness of the SEBs, the SEBZ and the South Tropical Zone (STrZ) combined to form the brightest region on the planet. As stated, the actual outbreak started as a small white spot that later developed a darker border and a small grey column on a side of increasing longitude, connecting the SEBn with the SEBs. White spots later appeared near the position of the first spot and accumulated until being caught in the current of the SEBn. The point where the dark column connected with the SEBs emitted dark spots that travelled along the SEBs in the direction of increas-

ing longitude. These so-called retrograding[*] dark spots spread out in longitude
so that in a few weeks the whole S equatorial region was a confusing mass of
spots and other detail. Just less than a month after the first outbreak, the
second disturbance appeared as another spot and column at a longitude just over-
taken by the SEBs dark spots. A second disturbance source was also observed
during the 1943 disturbance. By the middle of August, virtually the whole
planet between the equator and -20° was affected, producing a very unsettled
appearance.

4. The SEBZ

The outbreak appeared in the SEBZ near -14° (Zenogr.)and 79° System II
longitude. The activity in the SEBZ was confined to the formation of white
spots that generally drifted towards the SEBn, and dark columns bridging the
SEBs and SEBn. The first white spot (A in Fig. 5) appeared and drifted slowly
in longitude (0.9°/day) and latitude, until about July 6. The influence of the
SEBn current took hold and the spot accelerated, attaining a new drift rate of
5.3°/day with respect to System II. Later, apparent changes in this period
seemed to result in a small latitude change, partly due to the fact that as the
spot grew its boundary became less distinct. The average period of these white
spots was $9^h52^m27^s$.

One notable spot (C in Fig. 5) formed very rapidly between July 24 and 26
in front of spot A, illustrating the extent of the unstable meteorological con-
ditions brought about by the disturbance.

The dark columns appeared grey at first, but as they developed took on the
yellow-brown color of the SEBn, as though material in the SEBn was being trans-
ported across the SEBZ into the SEBs where it may have developed into the SEBs
spots. The change in the shape of the first column was due in part to the shear
produced by the change in rotation period over the latitude it spanned. The
curved shape of the column on July 7 represents the drift since June 23, when
nearly the whole column was at the same longitude. The second disturbance had
also formed a column (cf. Figs. 4, 7, 10, and 12 of *LPL Comm. No. 178*) by July
20, only two days after the outbreak. At times other column-like features crossed
the SEBZ, but they were not associated with any disturbance-related spots.

After the disturbance was well developed,several dark spots and wisps, gen-
erally poorly defined and difficult to follow, appeared in the SEBZ.

5. The SEBn

The SEBn became a complicated mass of detail as a result of the white spots.
The most dramatic aspect, however, may have been the distribution of colors.
Strong blue and orange colors existed in unusual profusion. The uneven distri-
tion is also evident in the 8900Å methane band (Fig. 4, No. 20) where the ab-
sorption varies from E to W to a much greater extent than from the usual expected
phase exaggeration produced by limb darkening.

---

[*] Although they are "retrograding" with respect to the arbitrary System II period,
they of course rotate in the same direction as all other features on the planet.
A"Westward drift" would be more descriptive.

As the disturbance progressed, spots in the SEBn protruded Northwards to the equator, and it became evident that much of the energy released in the Jovian atmosphere by the disturbance was directed to this region. As the activity of the disturbance died down, the scale of the detail diminished and became more uniform over the whole SEB.

6. The SEBs

When the column in the SEBZ reached the latitude of the SEBs, the current (slow with respect to System II) appeared to tear off pieces of the column producing dark spots. Most of the time the SEBs appeared more continuous in blue light than in red where the individual spots were well-defined. The spots varied in size but because of the lack of consistent resolution, it is impossible to tell if there was a size-lifetime correlation. The larger spots protruded to the S of the SEBs, their Northern edges always being close to -19° Zenographic latitude. The average period of SEBs spots was $9^h58^m24^s$, but those appearing before July 20 had average periods of $9^h58^m45^s$, while those appearing after July 20, $9^h57^m47^s$.

It was probably coincidental that the leading spots at the time had just passed the longitude of the second disturbance when it broke out. Spots produced by the second disturbance could not be identified as such because of the presence of spots produced by the primary disturbance. Reese (1971) predicted that by late August, the spots would reach the longitude of the RS and that as in the earlier major disturbances, the RS would fade. Although it could be seen that the spots were deflected Northwards by the RS hollow, the visibility of the RS did not diminish, and at this writing is still quite prominent.

7. Discussion

The appearance of the SEB disturbances seems to indicate a nearly cyclic release of energy built up in the lower levels of the Jovian atmosphere. With the internal heat providing the source from which the internally driven meteorology can take place (Kuiper 1972), it is likely that there exists unstable regional energy stores built up under a temperature inversion in the H_2O region that are released periodically. Reese (1972) has shown a correlation between (a) the longitudes of the three possible sources rotating close to the dekametric radio period and (b) the level of activity of the disturbances. The systematic location of the disturbance sources lends strong evidence that "sources" act as triggers for the release of energy to the upper atmosphere. The images taken in the 8900Å methane band (Minton 1972) show the region of the outbreak as being either high, or at least free, of the methane gas that generally exists at the higher atmospheric levels. This can be caused by high local vertical velocities, and the varied distribution of colored material in the disturbed region probably represents vertical mixing and possible chemical reactions of different ammonium polysulfides normally present at various layers in the upper atmosphere.

8. The Projection Comparator

A simple instrument was constructed that allows easy measurements of planetary features by projecting a photograph of the planet coincident with an image of a coordinate grid of the appropriate parameters plotted by computer (Fig. 7). Basically, it is a comparator combining two optical systems with control for orientation, position, scale, and intensity differences. The main design constraint was that it accommodate the five-image strips of 35-mm film resulting from the planetary photography program, and that it be as compact and easy to construct as possible.
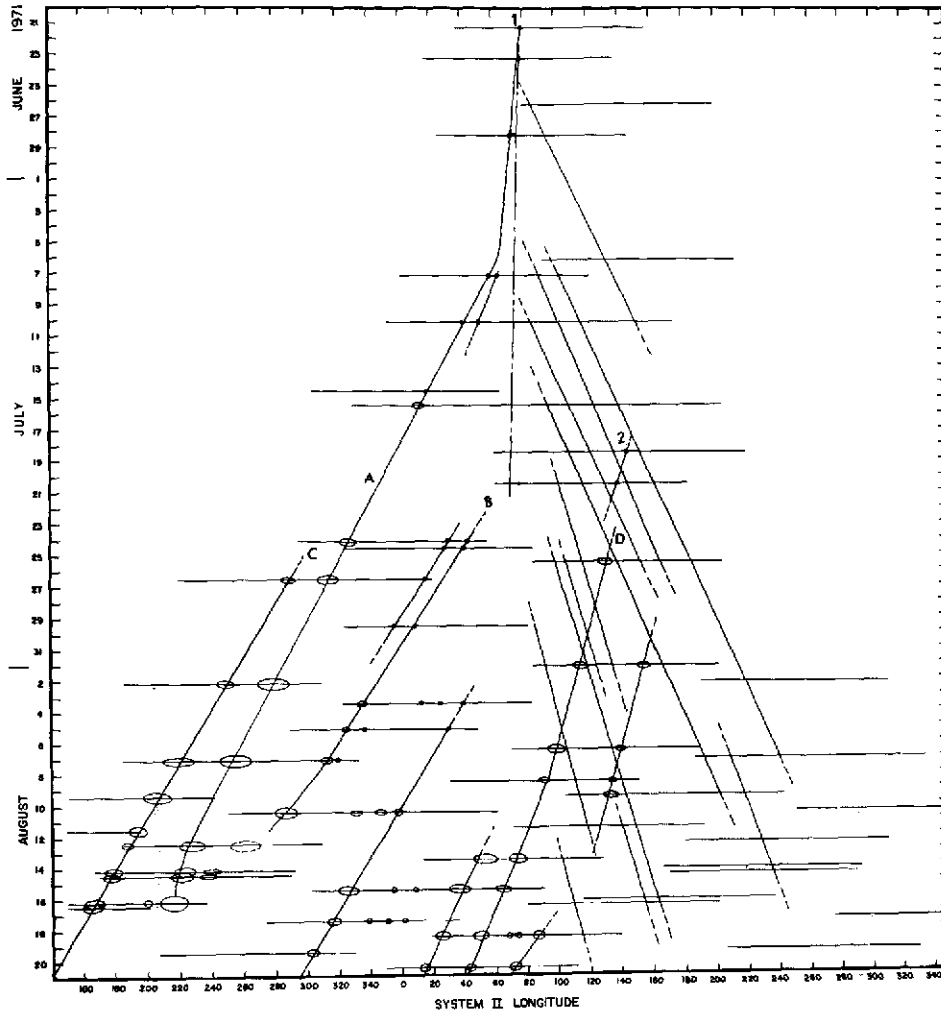
Fig. 5 Drift of features produced by SEB disturbance in System II $(9^h55^m42^s)$. Positive slopes indicate motions in SEBn branch, usually by white spots. Dark spots in SEBs have longer periods, thus negative slopes. Beginning of primary disturbance indicated by 1, of second by 2.   Nearly-vertical line would re-present System III period $(9^h55^m30^s)$, close to that of primary source. Small ellipses are observed dimensions of white spot (in x, y). Horizontal lines show longitude intervals observed.
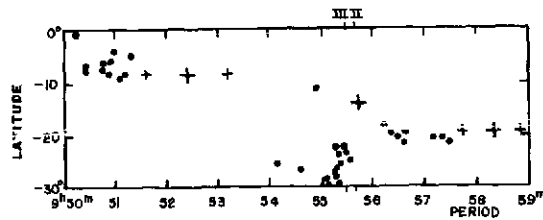

Fig. 6 Rotation period vs. Zenographic latitude determined from 1917-66 and 1971. Heavy crosses are average values and smaller crosses, extreme values, for 1971 disturbance. Dots are values given greatest weight from 1917 to 1966 by Chap-man (1969). System II and III periods are marked in margin.

Figure 7 shows the viewing screen that displays the combined images en-larged to about 60 mm. The controls for image and grid brightness can be seen, as well as the film holder and y-coordinate adjustment screw on the side. X-coordinate adjustments are made by sliding the film holder in its guides.

The optical components can be seen in Figure 8. The projector lens for the planet has a variable focal length (4 to 6 inches) to produce an image the same scale as the grid. The scale variation over the field introduced by the optical aberrations were found to be negligible within the 2-inch radius used. A well-corrected enlarger lens projects the grid.

The grids are photographed from a computer-plotted grid on high-contrast litho film on a dimensionally-stable base to a standard size, and either aligned in the holder such that a right ascension reference trail can be lined up with reference lines on either side of the grid, or rotated on the grid holder a pre-computed amount by means of a circle graduated in degrees. The grids are com-puted in either centric, graphic, or eccentric form by an IBM 1130 computer with a 1627 plotter, with latitude and longitude circles drawn every 10°.

The image is aligned with the grid by movement in the appropriate x-, y-directions and enlarged to fit the grid either by eye or by means of some scale reference such as a double star. In the most common case of the planet showing a phase, the limb not affected by a terminator is used for alignment with the grid to minimize phase error. The greatest source of error is in aligning images of Jupiter when the limb-darkening prevents a well-defined limb, or in less than optimum exposure of images such that photographic effects minimize or exaggerate the limb.

In practice, it was found that measures of well-defined features on Jupiter were repeated to within ±1° in longitude within 30° of the center, and ±2° out to 60°, although these values vary considerably depending upon their visibility (contrast) and extent of the object. Consequently, with their different limb darkening, images taken in the short wavelengths are easier to position and give better results, than images taken in long wavelengths.

The ability to vary the intensity of the images independently optimizes the visibility of the features. Since the grid is light with no background, it does not cover up features. Even if the feature has very low contrast, the operator can turn off the grid, set a pointer such as a pencil on the screen at the position of the feature, and then turn on the grid to read the position. Al-though this arrangement works best for positive images, original negatives can also be used.

In addition, the comparator is well-suited for measuring Venus UV markings, clouds on Mars, and markings on Jupiter and Saturn where great accuracy is not required, and usually with a minimum of computer time devoted to such programs.
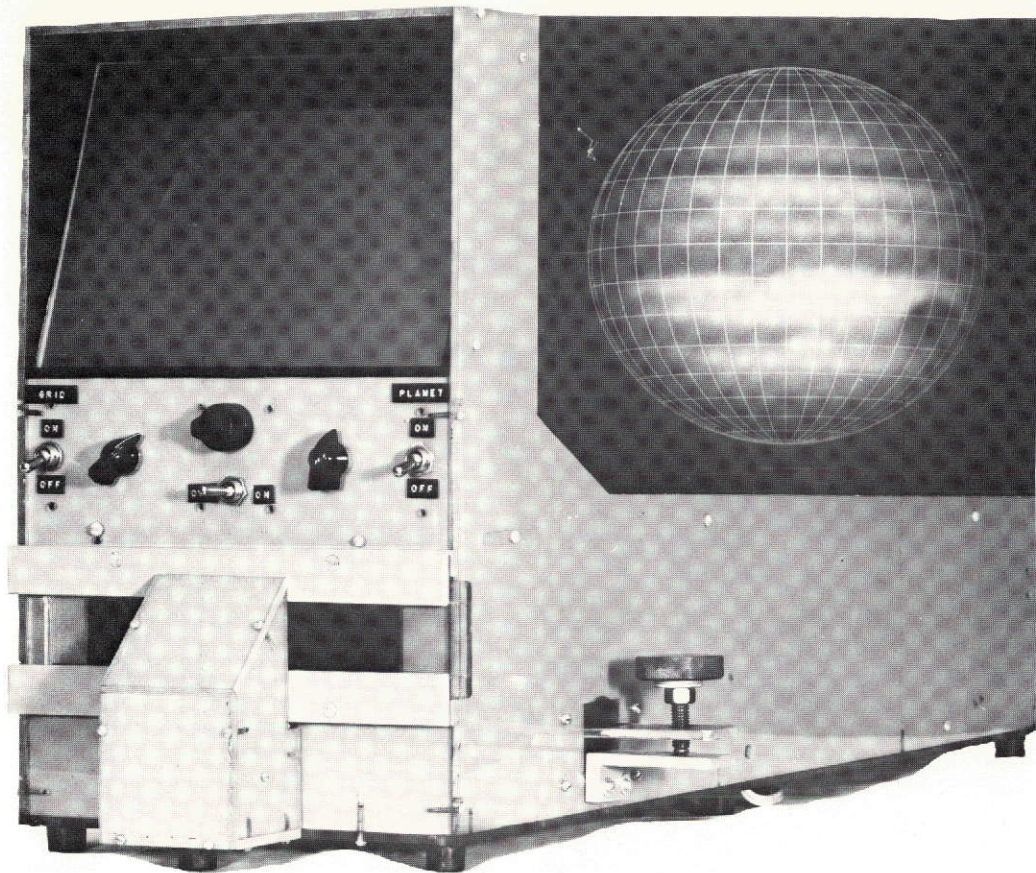
Fig. 7 The projection comparator controls and viewing screen, with the image of Jupiter and grid as seen on the viewing screen
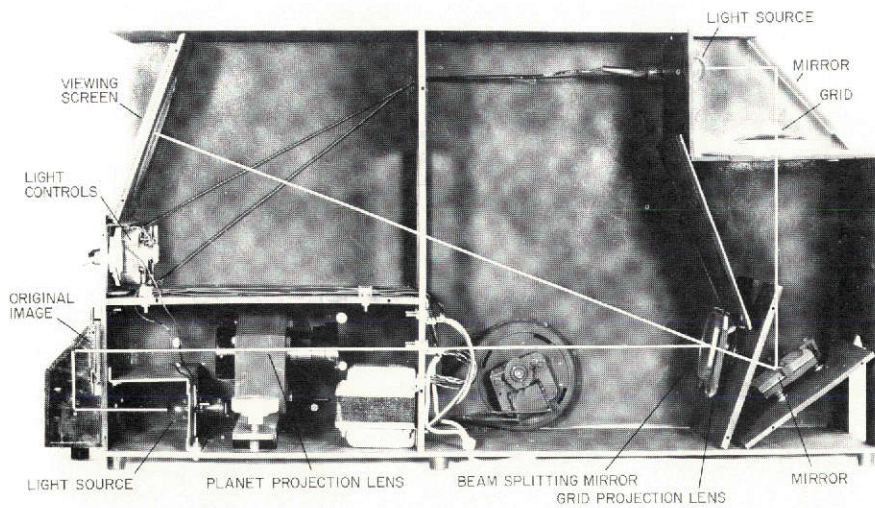

Fig. 8 The interior configuration of the projection comparator

REFERENCES

Baum, W. A. and Reese, E. J. 1971, "Observations of New Major Disturbances on Jupiter", Observers Page, *Sky and Telescope, 42*, 176-180.

Chapman, C. R. 1969, "Jupiter's Zonal Winds: Variation with Latitude", *Journal of Atmospheric Sciences, 26*, 198.

Kuiper, G. P. 1972, "Planetary Studies at LPL: Jupiter", *Sky and Telescope, 42*, Jan and Feb, and *LPL Comm. No. 173*.

Larson, S. M. 1971, "The Bosscha Observatory in Indonesia", *Sky and Telescope, 42*, 70-72.

Minton, R. B. 1972, "Initial Development of the June 1971 SEB Disturbance on Jupiter", *LPL Comm. No. 178*.

Peek, B. M. 1958, THE PLANET JUPITER, London (Faber and Faber).

Reese, E. S. 1972, "Jupiter: Its Red Spot and Disturbance in 1970-71", *Icarus, 17*, 57-72.

Reese, E. S., Chapman, C. R. 1968, "A Test of the Uniformly Rotating Source Hypothesis for the Southern Equatorial Belt Disturbance on Jupiter", *Icarus, 9*, 326-335.

NO. 180   ROTATION PERIOD FOR A SUBSURFACE SOURCE

IN THE NNTeB OF JUPITER

by Gordon Solberg

January 30, 1972

ABSTRACT

During two consecutive apparitions of Jupiter, 1968-69 and
1969-70, 12 and 9 spots were observed by Reese (1970) in the
NNTeB (latitude about 35°N). His drift curves are here extended
on the basis of LPL Jupiter photographs. It is shown that the
two source areas for these groups of spots are probably the same,
and define a rotation period of the common subsurface source very
close to that of System III.

The North North Temperature Current B, occurring at Zenographic latitude
+35° and having a rotation period of about 9^h54^m, is occasionally observed
when dark spots form on the South edge of the NNTeB and move rapidly in the
direction of decreasing longitude. This current was first observed by Har-
greaves in 1929-30, was next seen during five consecutive apparitions from
1940 to 1945 (Peek 1958), and was not seen again until 1965 (Reese and Sol-
berg 1969).

A summary of recent NNTeB activity is found in the following table:

Apparition	No. of spots observed	Mean Period
1965-66	2	$9^h53^m52^s$
1966-67	-	-
1967-68	1	9 53 45
1968-69	12	9 53 50
1969-70	9	9 53 50
1970-71	Faint	-

This paper deals with the 21 spots observed in 1968-69 and 1969-70.

The twelve spots of 1968-69 were all first observed near longitude (II) 60° (Fig. 1a), and Reese (1970) suggested their origin to be a subsurface source rotating with a period nearly the same as that of System II. This activity continued into the next apparition. The observed spots again had a non-random distribution, this time forming near longitude (II) 0° (Reese 1971); cf. Figure 1b. Only a few faint diffuse spots were observed the next year (1970-71),and it was not possible to obtain drifts for them.

The position of the hypothetical subsurface source proposed by Reese can be inferred from the longitudes at which the NNTeB spots were first observed. Since the spots drifted rapidly in longitude at the rate of $-2.7°$ per day and since the area of formation was not continuously observed, the position of the source is somewhat uncertain, though its longitude should be equal to or greater than the longitude at which the NNTeB spots were first observed. Furthermore, since there are many photographs showing longitudes where NNTeB spots do *not* exist, it seems reasonable to assume that the area of highest probability for the source would extend about 20° in longitude immediately following the area where the NNTeB spots were first seen.

The position of the subsurface source would be more accurately known if the NNTeB spots were observed immediately after they formed. To get a better idea of the longitudes of formation, I used the LPL collection of Jupiter photographs to extend back in time Reese's original observations.

The longitude at which each NNTeB spot was first observed was then plotted against time (Fig. 1c); a least-squares line through these points gives a rotation of $9^h55^m33^s9 \pm 0^s8$ (s.d.). A reasonable drift for the subsurface source was inferred from the indivual spots; it has a period of about $9^h55^m32^s$.

It is interesting to note that the hypothetical subsurface source had a rotation period close to that of System III ($9^h55^m29^s7$). The prominent NNTeB activity did not continue for a third apparition.
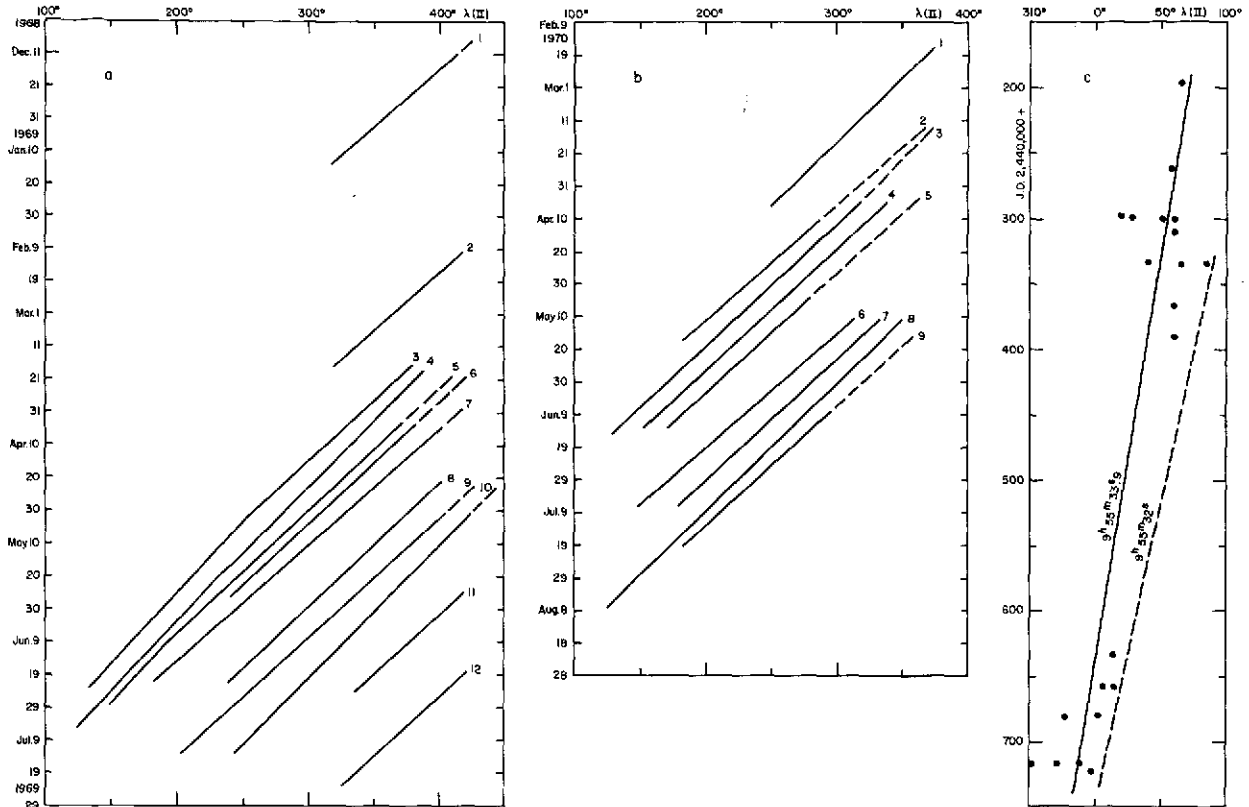
Figure 1*a*   S/NNTeB drifts observed during 1968-69. Solid lines: drifts observed
by E. J. Reese at NMSU; dashes: extensions using LPL photographs.

1*b*   S/NNTeB drifts observed during 1969-70. Solid lines: drifts observed
by Reese at NMSU; dashes: using LPL photographs.

1*c*   Longitudes at which NNTeB spots were first observed vs Julian date.
Solid lines: least-squares solution; dashed line: inferred drift
of subsurface source.

REFERENCES

Peek, B. M. 1958, THE PLANET JUPITER, New York - MacMillan.

Reese, E. J. 1970, "Photographic Observations of Jupiter in 1968-69", New Mexico
State University Observatory, TN-701-70-32.

Reese, E. J. 1971, "Photographic Observations of Jupiter in 1969-70", New Mexico
State University Observatory, TN-71-38.

Reese, E. J. and Solberg, H. G. 1969, "Latitude and Longitude Measurements of
Jovian Features in 1967-68", New Mexico State University Observatory,
TN-701-69-28.

NO. 181   A CORRELATION BETWEEN COLORS OF JOVIAN CLOUDS

AND THEIR 5μ TEMPERATURES

by R. B. Minton

March 8, 1973

ABSTRACT

Observations of Jupiter at 5μ by Keay, Low, and Rieke were
compared with color photographs by Minton and Kutoroff taken near
the same epoch. A strong correlation is evident between the 5μ
temperature distribution on the Jupiter disk and the cloud colors.
Further comparison is made with photographs in the .888μ CH_4 ab-
sorption band. Strong correlations exist for features in System
II latitudes at all three wavelegths but not for those that move
with System I. This is attributed to more intensive convection
in the Equatorial Zone. Owen's suggestion that colors may re-
sult from at least two mechanisms appears valid; a third appears
responsible for blue features only.

1. Introduction

Observations of Jupiter at 5μ by Keay, *et al*. (1973) with the 61-inch tele-
scope, in May 1972, revealed a considerable amount of thermal structure. Earlier
observations, in April 1972, (Keay, *et al*. 1972) had been at lower resolution. A
port diameter of 5.5 arc sec. was used for the April observations, reduced to 3
arc sec. for the May runs. In addition, the smaller port also defined the coor-
dinates of recorded features with greater accuracy. Observations on May 20-22,
1972, at many Jovian longitudes, enabled these investigators to construct a cylin-
drical equal-area map of the entire planet. The reductions also disclosed the
variation with distance from the Central Meridian (CM) of the heat flux.

2. Color Comparisons

Attempts by Dr. Keay and the author to correlate the 5μ features observed
in April with features evident at photographic wavelengths were not success-
ful. Photographs taken in blue, infrared, and methane-light were used for this
comparison. However, attempts by Drs. Keay and Rieke to correlate the 5μ fea-
tures observed in May with blue-light photographs met with some success. There
is positional agreement between a 5μ depression and the Red Spot (RS), a group
of 5μ sources and the South Temperate Belt (STeB); and between some 5μ depres-
sions and light features in the Equatorial Zone (EZ). There was no obvious
correlation between the 5μ features and their albedo in blue or infrared
light.

However, when I compared the equal-area map with the 61-inch color photographs
and with previous measures of features, a correlation between the Jovian colors
and their 5μ brightness temperature (T_5) became evident. The RS and the NTeB are
both orange-red (1972) and agree well in position with thermal depressions. Blue
festoons in the EZ and two blue spots in the North Tropical Zone (NTrZ) agree well
in position with areas of the greatest amount of 5μ radiation.

3. Position Measures and Map

The initial correlation warranted latitude and longitude measures of all
visible features on our May 23 color photographs. Measures were made of these
features on previous and subsequent dates, and drift rates were calculated. The
positions of all features were reduced to the epoch of the 5μ observations and
were plotted on the equal-area map. These measures ensured an objective analysis.
An accurate comparison within the latitudes of +10° to -10° was only possible for
features at System I longitudes of 170° to 330°. This region was photographed
with the Catalina 61-inch reflector on May 23, 1972, at 0908 UT and 1047 UT by
Mr. S. Kutoroff and the author. The remaining System I longitudes were photo-
graphed at dates found to be too distant in time for a comparison. This require-
ment was relaxed for features outside these latitudes for two reasons. The
majority of belts and zones have few features, but those spots that were photo-
graphed drifted with a longer period and at a more predictable rate.

A table was prepared for each feature representing the area of that feature,
its color, and the associated 5μ temperatures. If the feature lacked a distin-
guishable color, it was classified as either white or grey. This table depicts
a temperature distribution for each visible-light feature.

4. Results

The areas of enhanced 5μ radiation are all associated with dark-brown or blue features. From +10° to - 10° latitude, some of the strongest 5μ sources coincide with blue sections of the North and South components of the EZ (EZn and EZs). The remaining strong sources almost invariably coincide with dark-brown sections of the EZn and EZs. At remaining latitudes, the two strong 5μ sources found near 130° and 170° longitude (System II) coincide closely in latitude and longitude with two distinct blue spots near the center of the NTrZ. Other sources were located along the STeB and near the NNTeB, with the stronger sources coinciding with the darker-brown regions of these belts.

The areas of weak 5μ radiation (depressions) tend to cluster in latitude. The thermal depression near +20° to +35° latitude has the greatest continuous extent in longitude. This area is occupied by the NTeB and the NTeZ, with the NTeB in better positional agreement at more longitudes than the NTeZ. The NTeB is orange-red in color. A thermal depression is evident from −18° to −24° latitude, and 357° to 8° longitude (System II) This may be compared with visible-light measures (reduced to May 21) of the RS, whose boundaries are −17°.5 to −28°.0 latitude, and 352° to 12° longitude. It is significant that the 5μ dimensions are distinctly smaller. The RS was orange-red in color. The thermal depressions within −10° to −25° are almost totally within the expanse of the North and South components of the South Equatorial Belt (SEBn and SEBs). These normally dark components are presently bright, and this entire region(−10°.0 to −20°.3) is light-salmon in color. From +10° to −10° latitude, the thermal depressions tend to coincide with irregularly-shaped yellow features. Figure 1 shows the relation between color and temperature measures at 5μ.
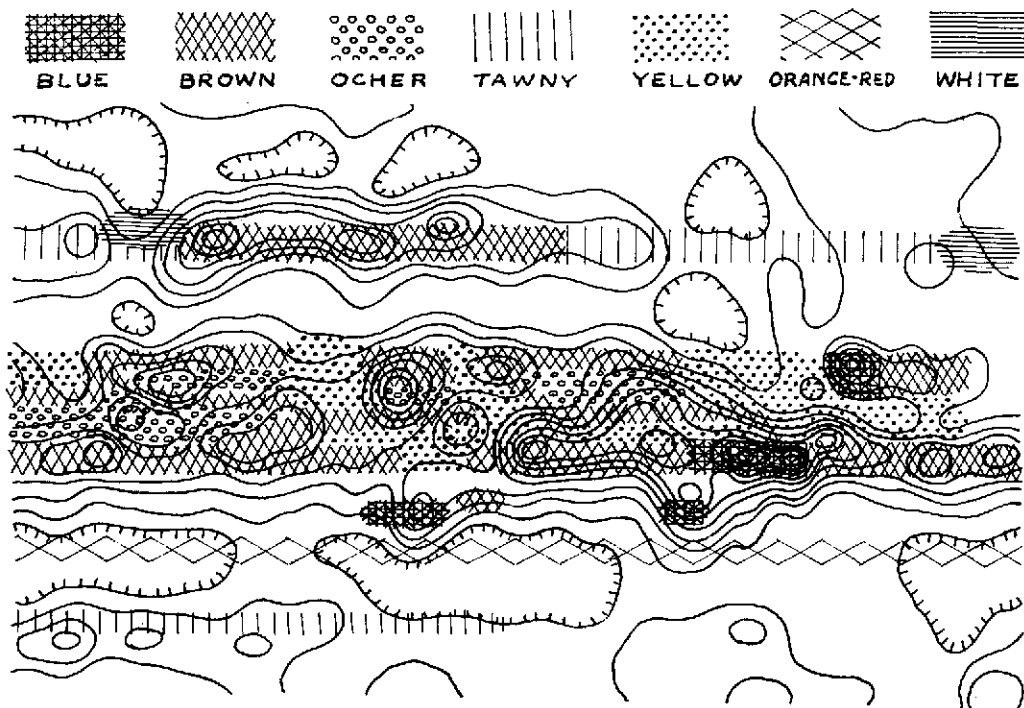

Fig. 1 Visible colors from color photos of May 23, 1972 vs. surface
distribution of 5μ temperatures obtained May 20-22

The regions of Jupiter which lack both prominent 5µ sources and thermal depressions tend to be either *white zones* (or spots) or *grey regions*. Grey regions include both dusky zones and faint belts. No obvious difference exists between white and grey features with respect to their 5µ temperatures. Nor is a close correlation evident between the type of feature (spot, belt, or zone) and its T_5.

However, a relation does exist between all distinguishable Jovian colored features and their associated values of T_5. This is shown in Figure 2 which depicts the percentage of area (within the area surveyed) of each color as a function of T_5. For reasons mentioned previously, different types of features were consolidated by color, and white and grey features were combined. As T_5 increases, there is a progressive change in the associated color of that feature from yellow or orange-red to blue. Figure 2 also shows that as T_5 increases, the transition in color becomes more abrupt. That part of the graph for System I applies to areas within +10° to -10° Zenographic latitude and 170° to 330° longitude, and represents 7% of the Jovian surface. The part for System II applies to all remaining latitudes and longitudes, and represents 85% of the Jovian surface.

5. Interpretation

Although these relations are based on May 1972 observations only, those found for System II may be more generally representative. The area surveyed is large and not presently (1972) unusual in appearance. However, the characteristics of features within the domain of System I have recently changed. Following the outbreak of two SEB disturbances in 1971, the EZ has become considerably more reddish-yellow in color; and brighter in methane-light photographs (Minton 1973*a*). This unusual circumstance and the smaller area surveyed, suggest that this relation may not be representative of the long-term aspect. However, the dark, wedge-shaped area, reported by Westphal (1969) to produce the highest flux recorded, was identified on LPL color films of May 14, 1969, as a *blue festoon*.

Danielson and Tomasko (1969) propose a two-layer model of Jupiter to reconcile spectrographic and bolometric temperature observations. In this model, there exists an upper cloud deck at a temperature of 145°K which has a transmission of about 0.5. The lower deck would be near 219°K and have a large optical depth. Based on much spectroscopic evidence, they suggest that the upper cloud is composed of NH_3 ice, and, following the analysis of Lewis (1969), they suggest that the lower clouds are
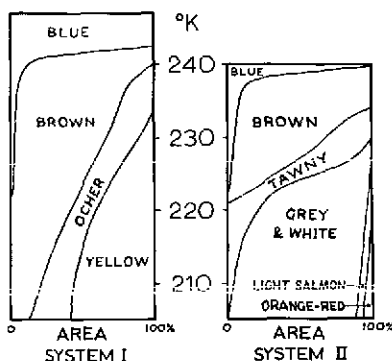

Fig. 2 Color distribution vs. 5µ temperatures by
area, separately for System I and II regions

composed of NH_4HS and H_2O ice. In the two-layer model, light returned from the
upper deck would give Jupiter characteristics of a reflecting model; and from
the lower deck, that of a scattering model. Lewis and Prinn (1970) propose that
in the lower deck, H_2S may be responsible for the observed colors. Brought up
from unobservable depths, this gas would dissociate into H and HS by solar UV
(.220-.270μ), penetrating through breaks in clouds and, to some extent, through
the upper NH_3 cirrus deck. Lewis and Prinn indicate that .220-.270μ radiation
is not absorbed by H_2, He, and CH_4, somewhat by NH_3 and considerably by H_2S.
They determine the amount of Rayleigh scattering at these wavelengths based on a
cloud-free, molecular (H_2, He) atmosphere. They show that recombination of H and
HS would produce hydrogen polysulfides, ammonium polysulfides, and sulfur. These
are yellow, orange, and brown in color. Owen and Mason (1969) suggest that sulfur
compounds may be responsible for only part of the observed cloud colors, and that
organic polymers may play a major role. Since the Lewis-Prinn theory applies to
the Jovian colors at the lowest observable levels, Owen and Westphal (1972) sug-
gest that solar UV may be responsible for the color of the highest features.
Therefore, we have two somewhat discordant hypotheses that ultraviolet light is
ultimately responsible for the observed colors of the highest *and* lowest Jovian
features. Direct observation of cloud altitudes is therefore important.

I have compared the appearance of Jupiter in the .888μ CH_4 band with the
colors and intensities of features at coincident positions from 1968-69 through
1972 (Minton 1973a). I find no simple correlation between the colors of all the
features and their intensity in this band (color vs. CH_4), nor one between the
intensities at visible wavelengths and their intensity in this band (V vs. CH_4).
The intensity in the CH_4 band should be a fair approximation of relative alti-
tudes, if only for a limited vertical range.   Scattering at .888μ is not as
strong as it is at shorter wavelengths. Belts and zones show considerably more
contrast at this wavelength than in the UV near 0.32μ, and there is no evi-
dence of limb brightening near quadrature as there is at UV and blue wavelengths.
In view of the good correlation between the color of a feature and its associated
5μ temperature (color vs. T_5), it is surprising that there is not an equally good
correlation between the color of a feature and its intensity in the .888μ CH_4
band, since there is overwhelming evidence that temperatures increase with depth.
However, when features within the domain of System I boundaries (+10° to -10°)
are omitted in these comparisons, a good color vs. CH_4 correlation is obtained
for the abovementioned four apparitions, while there is still no obvious V vs. CH_4
correlation. Evidence for the good color-vs.-CH_4 correlation is based on the
following observations. During this period, the RS was always orange-red in
color and always bright in methane light. From 1971 through 1972, the NTeB was
orange-red in color and bright in methane light. Prior to this, it was split
and faint; and was also faint in methane light. In 1969-70 when the NTrZ became
light red in color, it became bright in methane light. Prior to this, it was
white; but not exceptionally prominent in methane light. No exceptions in this
trend were evident in System II. The lack of a marked blue vs. dark-in-CH_4 trend
is related to the lack of blue features in the area of System II, and the great
strength (small penetration) of the CH_4 band. It is provisionally concluded that
the positive correlation between orange-red color and elevation in the System II
areas is related to the greater stability there, giving time for the solar UV
exposures discussed by Lewis and Prinn to run their course. In the Equatorial
(System I) Zone the time scales of the clouds observed are on the whole shorter,
possibly inadequate for the photochemical processes to reach near-equilibrium.
The Lewis-Prinn computations indicate that the critical period dividing the two
regions may be of the order of some weeks.

Although there appears to be no general correlation between the visual in-
tensity of a zone and its intensity in the CH_4 band, the latitudes of the bright
CH_4 zones do coincide with the latitudes of some visible-light zones or orange-
red features. The only exceptions are features within the System I area and the
South Polar Hood. However, UV photographs of the SPH suggest that it has scatter-
ing properties unlike the surrounding South Polar Region (Owen and Mason 1969).
The latitude of the North edge of the SPH varies in accord with the amount of in-
solation, which suggests that this haze cap is more volatile than the intermediate
latitude zones (Minton 1973).

Owen (1972), in summarizing much spectroscopic evidence, points out that there
appears to be no increase in the effective absorbing path in NH_3 and CH_4 over the
dark areas emitting strongly at 5μ. This needs verification with high spatial re-
solution. The 5μ sources predominantly occur in the System I area. Molecular
absorption differences are found within System II latitudes (Gehrels, *et al*. 1969),
(Owen, Mason 1969), (Moroz, Cruikshank 1969). Gaseous NH_3, CH_4, H_2 and He are
nearly transparent at 5μ, leaving the opaque clouds as the principal sources of
radiation. Westphal (1969) suggests that the hot sources may coincide with either
partially-transparent regions or breaks in the cloud deck. Danielson and Tomasko
(1969) based their model on the first possibility. Keay *et al*. (1972) suggest that
if the sources could be identified with visible features, the latter interpretation
would be greatly supported. It is significant that in 1969 and 1972, *no* 5μ sources
were found to be coincident with white, grey, orange-red, or light-red features.
Features with these colors move predominantly in System II. This is strong evidence
that these cloud layers block 5μ radiation from the hotter layers beneath.

The characteristics of Jupiter at the various latitudes (thermal outflux, ro-
tation periods, molecular absorptions, periodic disturbances, feature longevity)
suggest that large features within the System I area have more nearly equal altitudes
than those in System II. This may be due to greater vertical mixing in System I
caused by the greater thermal outflux there. In System II, thermal sources are
generally coincident with breaks in a higher cloud cover; in System I there is more
of a mixture of hot and cold features. Kuiper (1972) attributes periodic distur-
bances (SEB, STrZ), and long-enduring spots (RS, STeZ white ovals) to the sudden
or gradual relaxation of low-altitude inversions. He cites the lack of long-lived
oval clouds close to the equator as an indication that Coriolis force is an active
ingredient of cloud dynamics at other latitudes. An additional factor may be that
in System I the greater outflux produces more vertical convection which prevents
establishment of an inversion. As stated above, this more intensive convection
near the equator will also shorten the time scales of UV exposures and thereby
affect the cloud colors.

It is important to differentiate between the two classes of "warm" colors
observed in System II. Features with light-red to orange-red colors appear to be
cool at 5μ, and bright in methane-light photographs. Features of tawny (light-
brown) to brown-red colors tend to be 5μ sources of varying temperatures, and are
dark in CH_4. This second group would include those colors Lewis and Prinn attri-
bute to sulfur and its complex forms. The greater longevity of most System II
features would favor any UV-induced color change, assuming other conditions (al-
titude, composition) were met.

The blue features observed in 1969 and 1972 to be among the *strongest 5μ sources* were festoons and two NTrZ spots. Their 5μ temperatures were greater than or equal to the boiling point of NH$_3$ at 1 atm. of pressure. It is tempting to attribute the blue color to Rayleigh scattering in a predominantly gaseous cloud. The motions of blue festoons are not well documented in the literature, but are being investigated. The motions of blue spots in System II suggest that they are discrete spots, i.e., opaque clouds - not vents or holes in a lower deck. This interpretation obviously contradicts the proposal that sources coincide with cloud breaks in System II, but it should be emphasized that the remaining System II sources (STeB, NNTeB) are much longer-enduring features. In all probability, they are in closer thermal equilibrium with the surrounding atmosphere.

The lifetimes of blue spots in System II appear to be significantly longer than those (festoons) in System I. The two NTrZ blue spots were evident for the entire 1972 apparition. This is fairly typical for other blue spots in System II at previous apparitions. *The lifetimes of the two festoons* in Figure 2 were one and two months. This appears to be a typical lifetime for a festoon. Prior to being blue, these two areas were dark-brown sections of the EZn and EZs. They reverted to their former color with the disappearance of the blue color.

The 5μ temperatures determined for the remaining strong sources appear to be high enough for most proposed cloud constituents to exist in liquid phase or liquid solutions. The influence of this on the Lewis and Prinn hypothesis for colors observed in the lower deck is uncertain. The proposed vertical mixing in System I may not allow the required time scale for a slow color-producing mechanism. The observed color changes of the highest features suggests depletion of ultraviolet light already at the highest altitudes. *White zones and spots with long lifetimes,* and at presumably intermediate altitudes (System II latitudes) *have not turned light-red or orange-red.* This would indicate that other effects are operative at the deeper layers to produce orange colors.

The temperatures of the coldest features are significantly higher than those determined spectrographically, 210°K vs. 145°K. It will be important in the future to obtain accurate temperature measures of the coldest regions, even at the expense of resolution since values near 200°K are close to the limit of sensitivity at 5μ. Except for blue features, the interpretations here presented are not based on absolute values of temperatures. The hottest and coldest regions are well identified, and relative temperatures are well determined. These observations indicate that regardless of the composition of the hottest features, their observed colors are temperature-dependent.

REFERENCES

Danielson, R. E. and Tomasko, M. G. 1969, "A Two-Layer Model of the Jovian Clouds", *J. Atmos. Sci., 26,* 889-897.
Gehrels, T., Herman, B. M., and Owen, T. 1969, "Wavelength Dependence of Polarization. XIV. Atmosphere of Jupiter", *Astron. J., 74,* No. 2, 190-199.
Keay, C. S. L., Low, F. J., and Rieke, G. H. 1972, "Infrared Maps of Jupiter", *Sky and Telescope, 44,* No. 5, 296-297.

Keay, C. S. L., Low, F. J., Rieke, G. H., and Minton, R. B. 1973, "High-Resolution Maps of Jupiter at Five Microns", *Ap. J.*, (in press).

Kuiper, G. P. 1972, "Planetary Studies at LPL: Jupiter", *Sky and Telescope*, *42*, Jan and Feb, and *LPL Comm. No. 173*.

Lewis, J. S. 1969, "The Clouds of Jupiter and the NH_3-H_2O and NH_3-H_2S Systems", *Icarus*, *10*, 393.

Lewis, J. S. and Prinn, R. G. 1970, "Jupiter's Clouds: Structure and Composition", *Science*, *169*, 472-473.

Minton, R. B. 1973, "Initial Development of the June 1971 South Equatorial Belt Disturbance on Jupiter", *LPL Comm. No. 178*.

Minton, R. B. 1973*a*, "Latitude Measures of Jupiter in the 0.89μ Methane Band", *LPL Comm. No. 176*.

Moroz, V. I. and Cruikshank, D. P. 1969, "Distribution of Ammonia on Jupiter", *J. Atmos. Sci.*, *26*, 865-869.

Owen, T. and Mason, H. P. 1969, "New Studies of Jupiter's Atmosphere", *J. Atmos. Sci.*, *26*, 870-873.

Owen, T. and Westphal, J. A. 1972, "The Clouds of Jupiter: Observational Characteristics", *Icarus*, *16*, *392-396*.

Westphal, J. A. 1969, "Observations of Localized 5-Micron Radiation from Jupiter", *Ap. J. (Letters)*, *157*, L63.

NO. 182 RECENT OBSERVATIONS OF JUPITER'S NORTH NORTH
TEMPERATE BELT CURRENT B

by R. B. Minton

January 19, 1973

ABSTRACT

An outbreak of thirteen spots in Jupiter's North North Temperate Belt Current B was observed in 1972. These have been measured and compared with measures of the two most previous outbreaks. The drift in longitude of a hypothetical source supports both Reese's original hypothesis of a subsurface source, and Solberg's observation that its period is close to that of System III. There is some evidence that long-enduring atmospheric features exist at lower, unobservable depths.

1. Introduction

The North North Temperate Belt (NNTeB) Current A is a frequently-observed current at the latitude of the NNTeB. This current is evident by dark sections, dark spots, and light gaps in the NNTeB. Prior to 1929-30, dark spots were not observed on the South edge, ($^S/$), of this belt (Peek 1958). Subsequently, spots

397

have been observed on the ^{S}/NNTeB during eleven (of forty) apparitions. These
spots have characteristically short periods (9^h54^m), compared to normal Current
A spots ($9^h55^m42^S$); and this is designated as Current B. Table I summarizes
these apparitions.

TABLE I

Apparition	No. of Spots	Mean Period	Source
1929–30	7	$9^h53^m54^S$	Peek 1958
1940–41	3	54 02	"
1941–42	6	53 55	"
1942–43	6	53 52	"
1943–44	1	53 53	"
1944–45	1	53 51	"
1965–66	2	53 52	Solberg 1972
1967–68	1	53 45	Reese 1969
1968–69	12	53 50	Solberg 1972 Reese 1970
1969–70	9	53 50	Solberg 1972 Reese 1971
1972	13	54 34	Minton 1972

2. Observations, Measures, and Results

Following the 1968–69 outbreak near 60°, Reese (1970) suggested that a sub-
surface source might be responsible for the non-random distribution in the longi-
tudes at which these spots first appeared. He suggested a period near that of
System II. Following the 1969–70 outbreak near 0°, Solberg (1972) observed that
this drift was closer to the period of System III. By measuring LPL photographs
for these two apparitions, he redetermined these formation longitudes for about
half the spots. A least-squares analysis of these measures gives a period of
$9^h55^m33^S9 \pm 0^S8$ (s.d.). He inferred a period of $9^h55^m32^S$ from those spots with
the greatest longitudes.

There was no outbreak of spots in 1970–71, but in 1972 thirteen spots were
identified and measured. Figure 1 shows these dark spots and a light feature at
which they apparently disappeared. This was observed directly only for Spots 3
and 13. For the other spots the relation is inferred only. Gaps in the coverage
prevented direct verification; however, no spots were seen passed the Dislocation.
There was a marked tendency for the earliest spots to drift toward decreasing
longitudes faster than the later spots. This is shown in Figure 4. This acce-
leration towards increasing longitude was $0^{\circ}0124/day^2 \pm 0^{\circ}0028$. Table II sum-
marizes these measures. Although the periods of these spots averaged some 40^S
longer than that of Current B, their period was still 70^S shorter than Current A.
These outbreaks occurred very close to the longitude predicted from Solberg's
least-square analysis of the two previous outbreaks. A least-square analysis of
these three outbreaks gives a period of $9^h55^m34^S3 \pm 0^S3$ for this hypothetical
subsurface source.
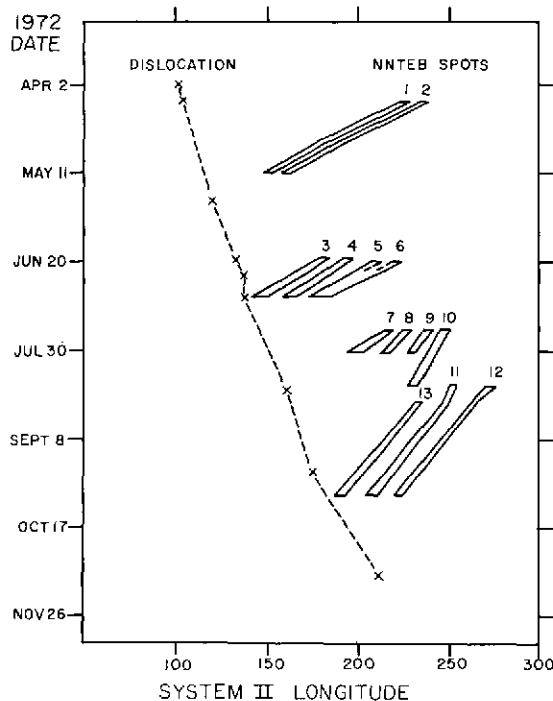
Fig. 1 Drift curves for 13 dark spots
in NNTeB and of Dislocation

The longitudes at which the 1972 spots faded from view coincided with an abupt *dislocation in latitude of the NNTeB*. This dislocation is shown in Figure 2. The aspect appears very similar to that described for 1942-43 (Peek 1946). The dates of these aspects are not tabulated by Peek (1958), who finds them to occur when part of the belt is strong (dark), and part of it faint. It appears to be the rule, rather than the exception, that outbreaks occur when the NNTeB is dark at some longitudes and faint at others. The more common reported aspects of this belt are "double", "conspicuous", and "faint".

TABLE II

| Spot No.	Limiting Dates	No. of dates	Limiting Longs.	Drift per day	Period (9^h+)
1	Apr 10 - May 11	3	$226.6 - 151.8$	-2.42	$54^m 01^s$
2	Apr 10 - May 11	3	$237.6 - 160.7$	-2.49	53 58
3	Jun 19 - Jul 6	3	$184.3 - 147.6$	-2.17	54 11
4	Jun 19 - Jul 6	3	$196.1 - 162.7$	-1.98	54 20
5P/	Jun 20 - Jul 6	2	$208.9 - 174.1$	-2.16	54 12
6f/	Jun 20 - Jul 6	2	$224.3 - 186.7$	-2.34	54 05
7	Jul 21 - Jul 31	2	$218.7 - 198.9$	-2.00	54 19
8	Jul 21 - Jul 31	2	$227.6 - 216.5$	-1.12	54 55
9	Jul 21 - Jul 31	2	$240.0 - 236.7$	-0.94	55 02
10	Jul 21 - Aug 15	3	$249.4 - 231.7$	-0.71	55 11
11	Aug 14 - Oct 2	3	$254.0 - 208.5$	-0.95	55 20
12	Aug 15 - Oct 2	3	$277.0 - 222.8$	-1.13	54 54
13	Aug 22 - Oct 2	2	$234.5 - 190.4$	-1.08	54 56
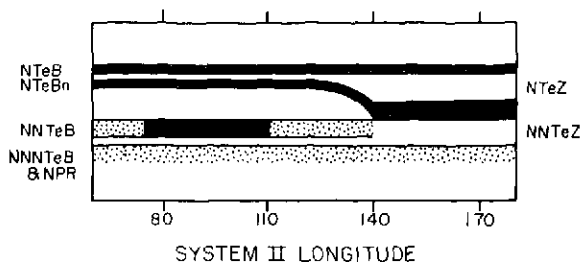
Fig. 2 Aspect of Dislocation as of
June 26, 1972

A least-square analysis of the *drift of this dislocation* shows that it was $173°.0 \pm 7°.9$ per year during the 1972 apparition, corresponding to a period of $9^h 56^m 00^s.1 \pm 0^s.9$. This long period has been found near the latitude of the NNTeB only once before. In 1934 an "anomalous" spot had a period of $9^h 56^m 03^s$ (Peek 1958).

The drift of the 1972 NNTeB spots was somewhat analogous to the drifts of SEBs spots during the June 1971 SEB disturbance. In both cases, the earliest spots drifted with the largest rate.

3. Interpretation

The latitude dislocation of the NNTeB was observed for seven months during 1972, but not previously. Because of its long life, influence in the spots' disappearance, and slow rotation relative to System II (once every two years), its observed drift was projected back through the previous two well-observed outbreaks. Figure 3 shows the formation (dot) and disappearance (cross) longitudes of these NNTeB spots, a least-squares lines representing the drift of the hypothetical source, and the projected drift (180°/yr) of the dislocation (dotted line).

A relation appears to exist between the location of the spot disappearances and the extrapolated position of the dislocation. One could perhaps interpret this as the spots fading near 210° (±50°) System II longitude, with the relation resulting from the commensurate periods of the dislocation and System II. The well-observed disappearances in 1972 support a direct positional relationship between dislocation and spot disappearance. In fact, no spots were seen in 1971 when the dislocation was in conjunction with the source.

These phenomena could be interpreted as the removal of an inversion by two processes. The first is similar to that proposed earlier (Minton 1972, Kuiper 1972) for SEB disturbances, wherein a surface feature or surface event triggers a rapid break-through of an inversion with subsequent spot formation. The second is similar to that proposed by Kuiper (1972) to explain the longevity of oval features. As they propagate slowly through System II longitudes, they remove the inversion. The proposed longevity of the dislocation implies that long-enduring atmospheric features exist at lower, unobservable depths.
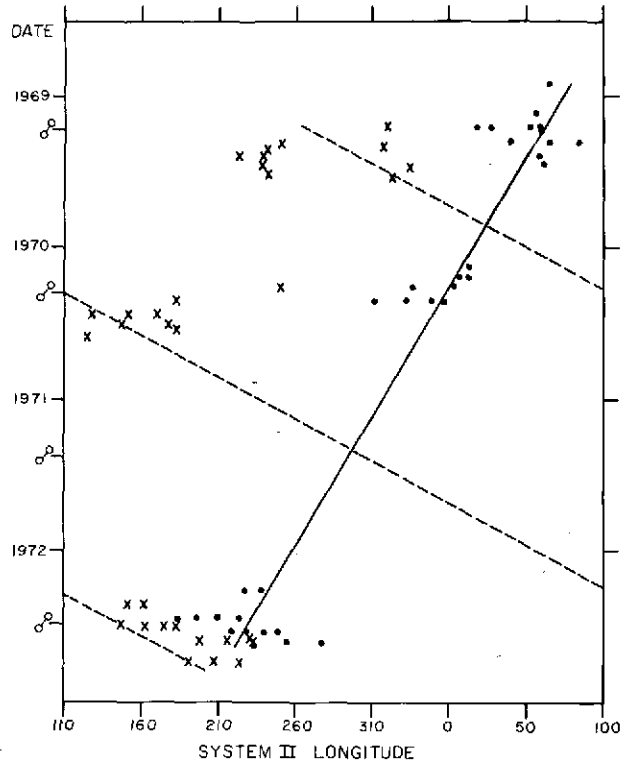
Fig. 3 *Dots:* longitude and date of formation of NNTeB
dark spots; *crosses:* disappearances of same. *Solid
line:* drift of hypothetical subsurface source; *dashed
lines:* measured (1972) or estimated (1969-71) drift of
Dislocation, invisible but assumed present before 1972.
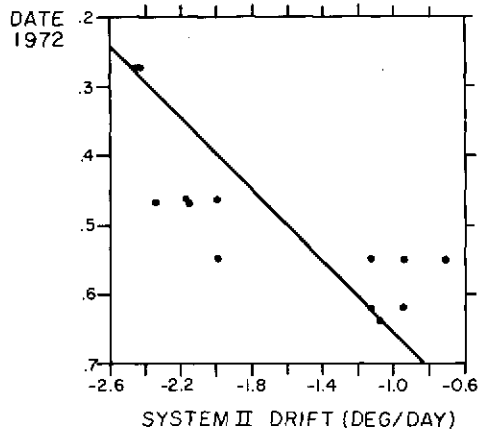
Fig. 4 Change in drift rates
of the 13 dark spots

R. B. MINTON

REFERENCES

Kuiper, G. P. 1972, "Planetary Studies at LPL: Jupiter", *Sky and Telescope, 42,* Jan and Feb, and *LPL Comm. No. 173.*

Minton, R. B. 1972, "Initial Development of the June 1971 South Equatorial Belt Disturbance on Jupiter", *LPL Comm. No. 178.*

Peek, B. M. 1946, THIRTY-THIRD REPORT OF THE JUPITER SECTION, APPARITION OF 1942-43, *Mem. B. A. A., 35,* Part 4.

Peek, B. M. 1958, THE PLANET JUPITER, London: Faber and Faber.

Reese, E. J. 1969, "Latitude and Longitude Measurements of Jovian Features in 1967-68", N.M.S.U. Observatory, TN-701-69-28.

Reese, E. J. 1970, "Photographic Observations of Jupiter in 1968-1969", N.M.S.U. Observatory TN-701-70-32.

Reese, E. J. 1971, "Photographic Observations of Jupiter in 1969-1970", N.M.S.U. Observatory TN-71-38.

Solberg, H. G. 1972, "Rotation Period for a Subsurface Source in the NNTeB of Jupiter", *LPL Comm. No. 180.*

NO. 183   DISCOURSE

Following Award of Kepler Gold Medal at A.A.A.S. Meeting,

Franklin Institute, Philadelphia

by   Gerard P. Kuiper

December 28, 1971

Kepler's work caused a revolution in thought and science. It marked the transition in Planetary Astronomy from concepts held for 15 centuries, to the Newtonian and Laplacian period of universal law and order. Kepler's was the period of great discoveries of regularities, partial solutions, break-throughs, and of hopes of still greater things to come. He recognized the immense implications of his work and upon discovery of his third law, full of emotion, thanked God for having given him insights that had been withheld from humanity for 6,000 years.

Our modern times resemble more those of Kepler than those of Newton and Laplace. It is true that Einstein was a modern Newton; but most of the current work in scientific exploration deals with advances and new insights in one of the dozens of sub-disciplines in which Science has divided. Victor Starr has eloquently shown that Meteorology is in the Kepler era. Much the same can be said for Planetary Physics. It is a time full of excitement and often very hard work, in part directed by large and competent teams comprising numerous

specialists and supported by major government programs. No doubt Kepler would be bewildered could he attend a planning session defining the mission profile for exploring life on Mars, the planet he loved so much; but he would be pleased to find that the spacecraft would (during the cruising modes) obey his laws of planetary motion.

This is a period of transition, turmoil, and frequent reassessment of priorities, in Science as in Society. Dr. Fred Singer suggested to me that I might review some of the more *continuing* trends in planetary research. Since it has been my privilege to work on the planets both in a university setting (Chicago, Texas) for one or two decades and during the Space Age, such comments may have a broader interest.

Astronomy before the Space Age had already gone through a period of rapid growth. The development of powerful telescopes on selected mountain sites around the turn of the century, plus the dramatic growth of Physics – atomic, molecular, nuclear – soon thereafter, combined to completely reset the priorities in Astronomy. Astrophysics absorbed all available manpower and research interests in most universities. Planetary research drew little attention, with the exception of traditional positional work at the Naval Observatories and studies in Celestial Mechanics which became more powerful and exciting after large computers were developed. The observation of the physical phenomena on the planets was mostly left to amateur astronomers in Britain, France, and elsewhere.

One might therefore wonder how a double-star astronomer, also involved with discoveries of white-dwarf stars, was deflected to planetary studies. The actual sequence was different. At the beginning of my career I was asked to review a book on the origin of the Solar System. The analytical part of this book impressed me greatly. The second, synthetic, part was entirely disappointing. After the review was written, I continued for many months to struggle with this problem and had to conclude that the state of Astronomy did not permit its solution. I was nevertheless fascinated by it, and had become aware of at least part of the extensive and difficult literature written in search for solutions. I then determined to find a closely-related problem, that with finite effort would probably lend itself to a solution. This, I thought, was the problem of the origin of double stars.

Some years later I felt that I had come to understand the problem of double-star origin, at least in outline; that it was identical to the general process of star formation, from slightly-turbulent prestellar clouds upon contraction, with conservation of angular momentum. It followed that the Solar System was no more than an "unsuccessful" double star with the companion mass spread out radially into a disk that in time developed the planets. The contraction process of a set of randomly-selected clouds would normally lead to a certain distribution function of semi-major axes for the new-born double stars – which appeared consistent with observation. The *mass partition* between the two components would be by random mass fractions of the total, a result I had derived empirically from a statistical study of double-star mass ratios. Thus, planetary systems clearly had to originate as the low-mass extremity of the almost universal process of double-star formation. Indeed, the median separation in double stars was just of the dimension of the system of the massive Jovian planets, around 10 A.U. A basis had thus been found for estimating the *frequency* of planetary systems in our galaxy.

Before this result was obtained it had been assumed by Chamberlin and
Moulton, and later by Jeans and Jeffreys, that planetary systems must be ex-
tremely rare (about 1 in 10^{12} stars), being the result of stellar collisions.
Thus Chamberlin, in his THE TWO SOLAR FAMILIES (1928), could write that the
Earth was of "noble birth". I concluded that the frequency was at least 1 in
10^3 (the mass fraction of the planets). I announced this result on 4 September
1949 at a regular Sunday broadcast of the University of Chicago Roundtable. I
still remember the skepticism of my astronomical colleagues; so strong was
astronomical tradition. A year or two later I estimated the fraction to be at
least 1 in 100 (the mass fraction of protoplanets).

Another item of personal history was my participation during World War II
in the ALSOS Mission, the Overseas Branch of the Manhattan District. I learned
about the great advances, made by both sides, in infrared detection and instru-
mentation. Upon returning to the University of Chicago I determined to use the
lead-sulfide cell in a stellar spectrometer on the 82-inch telescope. This in
1947 led to the discovery of CO_2 on Mars, H_2O ice on the Rings of Saturn, follow-
ing the earlier result of Titan as a satellite with a very substantial atmos-
phere. These and other reasons led me to the organization of a Conference on
the Earth and Planets in 1947, at the 50th Anniversary of the Yerkes Observatory
of the University of Chicago (such conferences became more frequent after 1957).
The results were published in THE ATMOSPHERES OF THE EARTH AND PLANETS, the
Second Revised Edition of which appeared in 1952. This was followed by two much
larger editorial projects, the 4-Volume SOLAR SYSTEM series and the 9-Volume STARS
AND STELLAR SYSTEM series, both published at the University of Chicago Press.

A third early item refers to the *small planets* in the Solar System, inciden-
tally the source of the meteorites. In spite of enormous efforts, observational
and computational, astronomers had no *statistics* that could assist in building
further our concepts on the origin of the Solar System. In 1949 I started a
7-year program (the Yerkes-McDonald asteroid survey) providing reliable statis-
tics down to magnitude 16.5; and in 1960 organized a second survey with the 48-
inch Palomar Schmidt to extend this to 20.5 magnitude. In addition, a concen-
trated program of asteroid *light curves* was started, also in 1949, after 1960
continued by Dr. Gehrels. These light curves provided the first information on
the periods of rotation of the asteroids, the orientation of their axes, and
the approximate shapes of these bodies. Curiously, nearly all of them show
to have marked deviations from sphericity, attributed in part to the collisional
history that also produced the known meteorites. These three large asteroid
programs have provided a much-needed basis for the understanding of the role
of these hundreds of thousands of bodies in the larger framework. My associates,
the van Houtens, have graciously taken the initiative with the I.A.U. for naming
Asteroid 1776 in recognition of these efforts.

A very exciting era began with the organization of the National Aeronautics
and Space Administration in 1958. Participation in the NASA programs became a
dream to which any planetary astronomer would aspire. I had the privilege of
being Principal Investigator on NASA's Ranger Program, 1960-1966, which led to
the first close-range investigation of the moon, many surface studies, and the
recognition of the NASA Space Program by naming the mare on which Ranger VII
impacted, Mare Cognitum. This I proposed at the 1964 Hamburg meeting of the
I.A.U. The 5-Volume Atlas of Ranger Photographs, comprising 1000 prints,
11" x 14", was produced under the personal direction of Mr. Ewen Whitaker and

myself, in Tucson. Earlier our Lunar and Planetary Laboratory, started in 1960, had produced through a major Catalogue of 4500 coordinated base points and the ORTHOGRAPHIC ATLAS OF THE MOON, using the best available photography, the lunar coordinate system that is still in use on all lunar charts.

The Surveyor, Orbiter, and Apollo programs followed and supplied a storehouse of data about our satellite - and indirectly the Earth - that will take much more time to fully assess. It was naturally a personal satisfaction that our ideas developed through telescopic observation in the 1950's were in broad outline confirmed. I refer here to the nature of the maria, the craters, faults, graben, wrinkle ridges, etc.

Reference must be made to the parallel and in a sense competitive program developed in the U.S.S.R. The origins of the Russian program stemmed from the personal actions and inspirations of two great men, Tsiolkovsky in the 1890's, and Korolev beginning 1930 (not 1957!). The Great Designer, as Korolev was referred to anonymously till his death in January 1966, had unforeseen effects on world history and on the competition between two great nations. It is pleasant to contemplate that individual intellects can on occasion be so influential.

The modern developments in the Planetary Sciences have often paralleled those in Geophysics. Yet the astronomical setting remains. With the one exception - the recent lunar surface exploration and the collection of lunar samples - all studies of the planets from spacecraft have been made by astronomical methods, through imagery, spectroscopy, photometry, polarimetry, radio astronomy, and celestial mechanics. It is true that fly-bys make these methods much more effective, but the techniques of remote investigation remain.

I would like to conclude with a reference to some recent work on the planet Jupiter. It will illustrate the close interdependence of the Planetary Sciences and Geophysics, appropriate at this meeting of the A.A.A.S. At LPL we have made an effort to photograph Jupiter in color as well as through filters, into the infrared. Slide 1, taken in the heavy methane absorption band at $\lambda 8900$Å, shows that, especially in 1970 and 1971, the North and South Tropical Zones, at 22° latitude N and S, are high in the atmosphere, with the famous Red Spot even higher. The identification is based on Slide 2, also showing the planet in red light. The Red Spot shows *anticyclonic rotation* and therefore flows outward on the top. Its visibility varies, with maximum visibility associated with the longest period of rotation around the planet's axis. Clearly, the Red Spot contains a *source of energy*, which must be the latent heat of condensation (H_2O, NH_3, + H_2S). A close study of the Red Spot, being published elsewhere, shows it to be a large cirrus anvil or shield over a 3,000 km diameter cumulus-type storm array, not unlike the Regions of Organized Cumulus Convection in the Earth's Tropical Convergence (Slides 3, 4). Typical terrestrial anvils of single cumulus towers are shown in Slide 5. The motion of the terrestrial "cloud clusters" or, better, "Regions of Organized Convection" within the Tropical Convergence are illustrated in Slide 6. The model of the Red Spot emerging is shown in Slide 7, both in plan view and vertical section. The detailed paper shows that the theory of Ooyama (1969) for terrestrial tropical cyclones accounts in a general way for the dimensions of the Red Spot (Slides 8, 9). The White Ovals (Slides 9, 11) are the next largest organized and persistent storm areas on

Jupiter, smaller because of the higher latitude (33° vs. 22°) and the stronger Coriolis force. Slide 12 shows a blue spot *inside* the Red Spot. Pre-mission planning may be done on the basis of reprojected photographs such as Slide 13, with rotation periods found at the various latitudes on the planet shown on Slide 14, readily interpretable except for the 20°-wide Equatorial Zone.

This summary is, of course, merely a glimpse of what may be expected in the decade of the 1970's, from the various missions planned by NASA and, presumably, the U.S.S.R.; supported by a vigorous ground-based program to keep track of - and interpret - the everchanging planetary atmospheres and cloud systems.

(The concluding remarks of the Discourse and my expressions of appreciation for the A.A.A.S. honor were made extemporaneously, and were not recorded or part of the prepared manuscript herewith reproduced. The slides here referred to are all found in *LPL COMMUNICATION NO. 173*).

Erratum: On p. 214, Fig. 18, No. 5 (Jupiter, blue) the UT is 07:00:43.

TABLE OF CONTENTS